

Minimising Infection Risk of Implantable Titanium

Savannah Jane Britton

A thesis submitted in partial fulfilment of the requirements of the University of the West of England,
Bristol for the degree of Doctor of Philosophy.

Centre for Research in Biosciences, Department of Applied Sciences,
Faculty of Health and Applied Sciences, University of the West of England, Bristol

Word Count: 43,492

November 2023

Author's Declaration

This copy has been supplied on the understanding that it is copyright material and no quotation from the thesis may be published without proper acknowledgement.

Abstract

The use of antibacterial coatings on bone biomaterial has attracted interest from various fields such as orthopaedics, dentistry and veterinary medicine. However, the process of attaching suitable compounds to biomaterial surfaces in a stable manner presents a significant challenge. One pragmatic approach is to utilise approved antibiotics that have been shown to remain effective when immobilised. One such antibiotic is teicoplanin (Teic), a glycopeptide that was discovered in the 1990s to be useful as a chiral selector in chromatographic enantiomeric separations. Importantly, Teic works at the level of the bacterial cell wall making it a potential candidate for biomaterial functionalisations. Initial investigations attempted to functionalise titanium (Ti) with polydopamine and use this platform to capture Teic. However, Teic was found to have a natural affinity for the oxide layer of Ti. Whilst Teic demonstrated a robust adsorption to Ti, it was found that the presence of phosphate compromised this interaction, resulting in the antibiotic eluting from the oxide. Before attempting to covalently attach the Teic to Ti, a commercially available Teic stationary phase was exposed to *S. aureus* to evaluate its antibacterial capabilities. Unfortunately, it was found that the Teic stationary phase had no impact on the viability of *S. aureus*, despite its ability to bind to N-Acetyl-L-Lys-D-Ala-D-Ala, indicating that covalent attachment of the glycopeptide antibiotic to a biomaterial surface does not result in the generation of an antibacterial surface. Yet, as expected, Teic has consistently displayed great antibacterial activity and was also able to enhance the maturation of osteoblasts and so work moved toward controlling the elution of Teic by encapsulating the antibiotic in a composite hydrogel made from chitosan and gelatin and crosslinking with genipin. This composite hydrogel scaffold demonstrated a sustained release of Teic over the course of a week and the same observations were made when the hydrogel was injected into a cancellous bone model, demonstrating the potential of this composite scaffold in reducing the incidence of periprosthetic joint infection (PJI). Overall, this thesis has demonstrated the potential of using Teic in orthopaedic applications but has also highlighted the difficulty in generating a stable, Teic-coated Ti surface finish.

Acknowledgements

Wow, I have a lot of people I want to thank! To say this journey has been difficult, would be an understatement. This has been one of the biggest obstacles I have gone through, from both a personal and professional standpoint. I don't think I would have seen this PhD to the end if it wasn't for the immense support and guidance from colleagues, friends and family. Firstly, I want to give my endless gratitude to Dr. Jason Mansell for not only providing me the opportunity to undertake this research but for the unlimited support, motivation and for giving me a metaphorical kick up the butt when I needed it most. I would also like to thank you for being a great "lab dad" (yes, I have referred to you as such, please forgive me). You have helped me to expand my discipline beyond microbiology and into an interdisciplinary scientist. I would also like to thank the rest of the supervisory team, Dr. Wayne Nishio Ayre and Dr. Tim Craig for providing me with their perspectives on how to approach my research and for the invaluable insight and support whenever needed. I also can't forget the incredible support I have received from the microbiology academics along with a belly full of laughs, thank you so much Dr. Gareth Robinson, Dr. Shona Nelson and Dr. Lynne Lawrance, I wouldn't have gotten this far without you!

I also want to give a huge thanks to the Microbiology Technical Team, Dr. Richard Thompson and James Dawson, for putting up with me invading your office, crying over failed experiments and knicking your chocolates, but most importantly, you provided me good banter, great laughs and "character development" which I am sure I will not see the end of and will gain even more character development down the line. In particular, I would like to thank Dr. Lee Graham, you have become a dear friend and have been such a huge support throughout all this, I am so very thankful to have you as a friend, thank you for everything.

During this PhD journey, I have had the privilege of forming life-long friendships with some incredible people like Dan, Eva, Buffy, Marina, Alex, Angeliki, and especially my brotha from anotha motha, Josh and my forever Glossier gal, Mog! It has been an absolute pleasure being on this doctoral adventure

alongside you all and I am forever grateful for all of the endless love and support you provided me over the years, I cannot wait to celebrate by drinking some good ale and having some delicious food! Last but not least, I would like to give my upmost gratitude to my ride or die, fellow braincell sharer and pedicure pal, Mary. I love ya and cannot thank you enough for the pep talks, cocktail nights and spooky gaming that has kept me sane. I got a friend for life in you!!

I would also like to thank a little online community that has become a huge piece of my heart, Old Dogs! You have helped me through this PhD and I cannot thank you enough for all the pewpew feet tapping, party games, anime nights and ghost hunting! Deshan, I am so endlessly grateful to have you in my life. During this past year you have been my rock, my biggest cheerleader and believed in me when I didn't believe in myself. I love you so very much. Also, thank you for providing me with herbal teas and being my matcha vendor. Finally, I want to thank my family, for the endless love and support and for reminding me to always be myself, I wouldn't be the person I am today without you all.

Table of Contents

Authors Declaration	iii
Abstract.....	iv
Acknowledgements.....	v
List of Figures.....	xi
List of Tables.....	xiii
Abbreviations	xiv
Chapter 1 Introduction and Literature Review	1
1.1 Overview.....	1
1.2 TJA.....	2
1.3 Implant Structure and Function.....	3
1.4 Implant Placement and Maintenance	6
1.5 PJI.....	10
1.5.1 Overview	10
1.5.2 Epidemiology and Economic Impact.....	12
1.5.3 Pathogenesis of PJI.....	13
1.5 Current Research to Prevent PJI	28
1.5.1 Overview	28
1.5.2 Immobilisation Strategies	29
1.6 Teicoplanin	33
1.6.1 Structure of Teicoplanin and Mode of Action.....	33
1.6.2 Use of Teic in Chromatography Applications.....	36
1.7 Objectives.....	37
Chapter 2 Polydopamine-modified Titanium for the Immobilisation of Teic.....	39
2.1 Introduction.....	39
2.2 Origin and Basic Characteristics of PDA	39
2.3 Materials and Methods.....	44
2.3.1 Bacterial Strains and Culture Preparation	44
2.3.2 Maintenance and Treatment of Human (MG63) Osteoblasts.....	44
2.3.3 Reagents and Ti Disk Preparation	45
2.3.4 Influence of Teic on Human Osteoblast Maturation	45
2.3.5 Attachment and Growth of <i>S. aureus</i> on Teic-Sepharose.....	46

2.3.6 PDA Optimisation.....	47
2.3.7 Attachment of <i>S. aureus</i> on PDA-modified Ti.....	49
2.3.8 Attachment of <i>S. aureus</i> on Teic-PDA-modified Ti.....	50
2.3.9 Statistical Analysis.....	50
2.4 Results	51
2.4.1 Influence of Teic on a Model of Human Osteoblast Maturation.....	51
2.4.2 <i>S. aureus</i> viability on Teic-Sepharose.....	53
2.4.3 PDA Optimisation.....	55
2.4.4. Attachment of <i>S. aureus</i> to PDA-modified Ti.....	63
2.4.5. Attachment of <i>S. aureus</i> to Teic-PDA-modified Ti.....	66
2.5 Discussion	68
2.6 Conclusions	73
Chapter 3. Assessing the Interaction Between Teic and TiO₂	74
3.1 Introduction	74
3.2 Materials and Methods	76
3.2.1 Bacterial Culture Preparation.....	76
3.2.2 Reagents and Ti Disc Preparation.....	76
3.2.3 Bacterial Attachment to Teic-modified Ti.....	76
3.2.4 X-Ray Photoelectron Spectroscopy (XPS) of Teic-Ti.....	77
3.2.5 Adsorption of Teic onto Ti.....	77
3.2.6 Impact of Phosphate on the Binding of Teic to TiO ₂	79
3.2.7 The Effect of Phosphate on the Detachment of Teic from TiO ₂	80
3.2.8 Elution Assessment of Teic from Ti.....	80
3.2.9 Bacterial Viability and Elution studies of Teic-modified Iron Oxide Nanoparticles (IONPs).....	81
3.2.10 The Binding of N-Acetyl-L-Lys-D-Ala-D-Ala to a Teic Stationary Phase (TSP).....	82
3.2.11 Bacterial viability to TSP.....	83
3.3 Results	84
3.3.1 Bacterial viability to Teic-Ti.....	84
3.3.2 XPS of Teic-Ti.....	86
3.3.3 Adsorption of Teic onto Ti.....	88
3.3.4 Elution Assessment of Teic from Ti Discs.....	100
3.3.5 Bacterial Viability and Elution Studies of Teic-IONPs.....	102
3.3.6 Binding of N-Acetyl-L-Lys-D-Ala-D-Ala to the TSP.....	106
3.3.7 Viability of <i>S. aureus</i> to the TSP.....	108
3.4 Discussion	110

3.5 Conclusions.....	116
Chapter 4 A Teic-Chitosan-Gelatin Hydrogel Composite for Antibacterial Applications: Proof-of-Concept	117
4.1 Overview.....	117
4.2 Gelatin Hydrogels.....	118
4.3 Chitosan Hydrogels.....	119
4.4 Composite Hydrogels	120
4.5 Chemical Crosslinkers.....	121
4.6 Materials and Methods.....	125
4.6.1 Bacterial Strains and Culture Preparation	125
4.6.2 Reagents & Mock Bone Preparation.....	125
4.6.3 Fabrication of Teic-Gel and Gel Hydrogels.....	125
4.6.4 Effect of Crosslinker Concentration on Teic Elution	126
4.6.5 Trypsin Digestion of Teic-Gel Hydrogels	127
4.6.6. Fabrication of Teic-CS-Gel and CS-Gel Composite Hydrogels.....	127
4.6.7 Antibacterial Synergy Assessment of CS and Teic.....	128
4.6.8 Characterisation of the Crosslinked Composite Hydrogels loaded with Teic using FT-IR .	129
4.6.9 <i>In vitro</i> release of Teic from Composite Hydrogels – HPLC Analysis.....	129
4.6.10 <i>In vitro</i> release of Teic from Composite Hydrogel – Disk Diffusion Assay	130
4.6.11 Statistical Analysis.....	130
4.7 Results	131
4.7.1 Effect of the Crosslinker Concentration on Teic Elution from Gel Hydrogels.....	131
4.7.2 Antibacterial Synergy of CS and Teic.....	137
4.7.3 FT-IR Analysis of Composite Hydrogels.....	139
4.7.4. <i>In vitro</i> release of Teic from Composite Hydrogel Pucks	141
4.7.5. <i>In vitro</i> release of Teic from Composite Hydrogels in a Mock Bone Model	145
4.8 Discussion	149
4.9 Conclusions.....	156
Chapter 5 Discussion & Future Work	157
5.1 General Discussion	157
5.2 Concluding Remarks.....	164
5.3 Future Work.....	165
References.....	169
Appendix I Published Material.....	202

Appendix II Supplementary Material 215

List of Figures

Figure 1.1 Total Hip Arthroplasty.....	5
Figure 1.2 Total Knee Arthroplasty.....	9
Figure 1.3 Schematic of Implant Osseointegration.....	16
Figure 1.4 Stages of Biofilm Formation	19
Figure 1.5 Chemical Structure of Teic.....	35
Figure 2.1 Polydopamine Film Formation.. ..	41
Figure 2.2 Influence of Teic on a Model of Human Osteoblast Maturation.. ..	52
Figure 2.3 Antimicrobial assessment of Teic-Sepharose beads on <i>S. aureus</i>	54
Figure 2.4 Bactericidal activity of Teic-Sepharose beads on <i>S. aureus</i>	54
Figure 2.5 Effect of Incubation Time on PDA Formation.	56
Figure 2.6 LIVE/DEAD assessment of <i>S. aureus</i> attachment on PDA-modified TCP	57
Figure 2.7 Influence of Buffer Type on PDA Formation	59
Figure 2.8 LIVE/DEAD assessment of buffer choice on attachment of <i>S. aureus</i> to Teic-PDA-Ti.	60
Figure 2.9 Effect of temperature on PDA Formation.. ..	62
Figure 2.10 Attachment of <i>S. aureus</i> on PDA-modified Ti.	64
Figure 2.11 LIVE/DEAD assessment of <i>S. aureus</i> attachment on PDA-modified Ti.....	65
Figure 2.12 Attachment of <i>S. aureus</i> on Teic-PDA-modified Ti	67
Figure 3.1 Antibacterial efficacy of Teic-modified Ti.	85
Figure 3.2 Detection of Teic coating on the Ti surface.....	87
Figure 3.3 Influence of HEPES on Teic adsorption to TiO ₂	89
Figure 3.4 Durability of Teic-TiO ₂ to Washing.	91
Figure 3.5 Thermal stability of Teic immobilised on the surface of TiO ₂ using Thermal Gravimetric Analysis (TGA).....	93
Figure 3.6 Short Term Stability of Teic-TiO ₂ under Neutral Conditions	95

Figure 3.7 Influence of phosphate on Teic adsorption to TiO ₂	97
Figure 3.8 Influence of phosphate on Teic detachment from TiO ₂	99
Figure 3.9 Antibacterial activity of Teic-Ti after culture conditioning.....	101
Figure 3.10 Antibacterial activity of Teic-IONP.	103
Figure 3.11 Antibacterial activity of Teic-IONP after culture conditioning.....	105
Figure 3.12 The tripeptide N-Acetyl-L-Lys-D-Ala-D-Ala binds avidly to a TSP.....	107
Figure 3.13 Immobilised Teic does not display any antibacterial activity towards <i>S. aureus</i>	109
Figure 4.1 Origin of Genipin	123
Figure 4.2 Effect of Glut Concentration of the Elution of Teic from Gel Hydrogels	132
Figure 4.3 Evidence of Teic Recovery from Trypsinised Hydrogels	134
Figure 4.4 Effect of Gen concentration on the elution of Teic from Gel Hydrogels.....	136
Figure 4.5 Characterisation of the composite hydrogels using FTIR.	140
Figure 4.6 <i>In vitro</i> release of Teic from Composite Hydrogel Pucks – Disk Diffusion Assessment..	142
Figure 4.7 <i>In vitro</i> release of Teic from Composite Hydrogel Pucks – HPLC Analysis	144
Figure 4.8 <i>In vitro</i> release of Teic from Composite Hydrogel in a Mock Bone Model – Disk Diffusion Assessment.....	146
Figure 4.9 <i>In vitro</i> release of Teic from Composite Hydrogel in a Mock Bone Model – HPLC Analysis.	148

List of Tables

Table 3.1 Elemental composition of control and Teic-functionalised Ti	87
Table 4.1 Synergistic Activity of Teic and CS.	138

Abbreviations

Abbreviations	Definition
ALP	Alkaline Phosphotase
AMA	Antimicrobial agent
AMP	Antimicrobial peptide
AMR	Antimicrobial Reistance
APTES	(3-Aminopropyl)triethoxysilane
BCA	Bicinchononic acid
BHIA	Brain heart infusion agar
BHIB	Brain heart infusion broth
CFU	Colony forming units
CNBr	Cyanogen bromide
CNS	Coagulase negative staphylococci
CS	Chitosan
CSP	Chiral stationary phase
CVD	Chemical vapour deposition
DAIR	Debridement, antibioitcs and implant retention
DHC	Dopamine hydrochloride
DHI	5, 6-dihydroxyindole
DMEM	Dulbeccos Modified Eagle medium
DOPA	3, 4-dihydroxy-L-phenylalanine
ECDC	European Centre for Disease Prevention and Control
EDC	1-Ethyl-3-(3-dimethylaminopropyl)carbodiimide
EPS	Extracellular polymeric substances
FHBP	(3S) 1-fluoro-3-hydroxy-4-(oleoyloxy)butyl-1-phosphonate
FIC	Fractional inhibitory concentration
FICI	Fractional inhibitory concentration Index
FT-IR	Fourier-Transform Infrared
Gel	Gelatin
Genipin	Gen
Gent	Gentamicin

HA	Hydroxyapatite
HEPES	4-(2-hydroxyethyl)-1-piperazineethanesulfonic acid
IONP	Iron oxide nanoparticle
LPA	Lysophosphatidic acid
MBEC	Minimum biofilm eradication concentration
MES	2-(N-morpholino)ethanesulfonic acid
MGW	Molecular Grade Water
MIC	Minimum inhibitory concentration
MRD	Maximum recovery diluent
MRSA	Methicillin resistant <i>Staphylococcus aureus</i>
NCTC	National Culture Type Collection
NHS	National Health Service
NJR	National Joint Registry
OA	Osteoarthritis
OC	Osteoclasts
OD	Optical Density
PBS	Phosphate buffered saline
PDA	Polydopamine
PIA	Polysaccharide intracellular adhesion
PJI	Periprosthetic joint infection
PMMA	Poly(methyl methacrylate)
p-NP	para-nitrophenol
p-NPP	para-nitrophenylphosphate
QCM	Quartz Crystal Microbalance
ROM	Range of Movement
RPM	Revolutions per minute
SAM	Self assembled monolayer
SCV	Small colony variants
SD	Standard deviation
SFCM	Serum free culture medium
SSI	Surgical site infection
TCP	Tissue culture plastic

Teic	Teicoplanin
TGA	Thermogravimetric Analysis
TJA	Total joint Arthroplasty
TSP	Teicoplanon Stationary Phase
Vanc	Vancomycin
XPS	X-ray Photoelectron Spectroscopy

Chapter 1 Introduction and Literature Review

This thesis explores the development of an antibacterial titanium surface to help minimise total joint arthroplasty (TJA) infections. A leading cause of TJA is osteoarthritis (OA) and whilst prosthetic knee and hip joints have very successful outcomes, approximately 1-2% get infected and will need replacing. Coating titanium with suitable antibiotics could be one way of realising an antibacterial technology to help minimise infection risk. The following introduction provides a comprehensive account of TJA, periprosthetic joint infection (PJI), current research to prevent PJI and the glycopeptide antibiotic, teicoplanin. A potential route towards the development of an antibacterial titanium coating is also presented.

1.1 Overview

TJA is a surgical procedure that removes and replaces parts of arthritic or damaged joints with a prosthesis made of a biocompatible material. It is one of the most successful and cost-effective orthopaedic procedures for alleviating pain and disability associated with advanced joint disease and the number of primary TJAs being performed, per annum in the UK is currently rising and is predicted to increase by as much as 40% (~268,107) by 2060 (Matharu *et al.*, 2021). Historically, TJAs have been reliable orthopaedic interventions for end-stage joint disease and improving quality of life, with a \geq 90% implant survival at 13 years. Although the implant integrates well into the host tissue, approximately 10% fail over the lifetime of the patient. Around 30% of these TJA failures are due to a process known as aseptic loosening and a further 1-2% of failures are attributed to periprosthetic joint infection (PJI) with the most common aetiological agent being *Staphylococcus aureus* followed by coagulase-negative staphylococci (Arcioloa *et al.*, 2018; National Joint Registry, 2022). In England and Wales alone, the NHS carries out approximately 200,000 TJAs per annum with prosthesis costs ranging between £400 and £1,200. It is estimated that PJI-related revisions cost the NHS around £1.5 billion

yearly (Hamish & Simpson, 2022). Therefore, reducing PJI risk for TJA is of great importance for both the patient and the provider.

1.2 Total Joint Arthroplasty

Arthroplasty is defined as the essential surgical replacement of a joint, with an artificially produced material, such as metal, plastic, or ceramic, that is fixed in the bone (Bleb & Kip, 2018). In the UK, TJA is one of the most common elective surgical procedures. The annual incidence of total joint replacements grew steadily throughout the 1990s and has continued to rise since the year 2000. According to the National Joint Registry (NJR), around 241,467 and 237,924 primary hip and knee replacement procedures were performed, respectively, between 2019 and 2021 (NJR 19th Annual Report, 2022). In 2021 alone, 84,998 and 77,830 primary hip and knee replacement procedures, respectively, were performed in the UK. This number is predicted to increase drastically due to ageing as well as the growing prevalence of risk factors, such as obesity (Liddle *et al.*, 2014)

Hip and knee arthroplasties are the most frequently performed replacement surgeries, however arthroplasty can also be performed on other joints, such as the ankle, wrist, shoulder, and elbow (Bleb & Kip, 2018). The most common reason for arthroplasty is joint surface destruction from the wear and tear of the cartilage lining due to advanced joint diseases, such as OA, fractures and other changes in bone and connective tissue structures. These degenerative diseases could lead to permanent loss of function, pain, and impaired mobility of the affected joint, as well as a decrease in the quality of life (Seidlitz & Kip, 2018). If non-surgical treatments, like medications, physical therapy and activity modifications do not relieve the symptoms, then arthroplasty is the necessary option to avoid secondary complications and to sufficiently restore the patient's quality of life.

1.3 Implant Structure and Function

Biomaterials are employed to restore the function of compromised joints. They were first defined as non-viable materials used in a medical device, with the intention to interact with biological systems (Katti, 2004). Further, Black (2005) defined the term biomaterials as materials of natural or manmade origin that are used to direct, supplement, or replace the functions of living tissues.

Material scientists have investigated a variety of materials such as metals, ceramics, polymers, and composites as biomaterials for total joint replacements. The main criterion for a material's selection of bone implant materials are:

- It is biocompatible and does not cause an immunological or cytotoxic response beyond an acceptable level.
- It has appropriate mechanical properties that are close to bone.
- Manufacturing and processing methods are viable, economically.

Ideally, a bone implant, such as a hip prosthesis, should exhibit an identical response to loading as real bone. The average load on a hip joint is estimated to be up to three times body weight and the peak load can be as high as ten times, when doing strenuous activities, such as jumping (Katti, 2004). The bone biomaterial must also be surface and mechanically compatible, as well as display osteocompatibility. Historically, a hip replacement, for instance, aims to simulate the articulation of the hip joint with the use of two components, a cup and long femoral type element. The head of the femoral element fits inside the cup to enable sufficient articulation of the human joint (Fig. 1.1). These two parts of the implant have been made using a variety of materials such as the ones mentioned above. Currently, the main materials used in joint arthroplasty procedures are titanium, cobalt-chromium, polyethylene, and ceramics (Hu and Yoon, 2018). Titanium and its alloys (such as Ti6Al4V) have been the most commonly used metals for stem and acetabular components of hip implants due to its low density, high mechanical strength, great corrosion resistance and biocompatibility with the

bone (Hu and Yoon, 2018; Head *et al.*, 1995). However, during the last two decades, vanadium free titanium alloys, like Ti6AlNb, have been employed in hip implants, with improved biocompatibility in comparison to Ti6Al4V, by incorporating biocompatible elements such as niobium (Mindroiu *et al.*, 2014; Miura *et al.*, 2011). This is due to the potential toxicity of vanadium within the Ti alloy. Other replacement procedures, such knee arthroplasties, also use titanium, however cobalt chromium alloys are more common for this type of replacement (Kim *et al.*, 2021). A major limitation of using titanium is that it does not directly bond to the bone, and this could result in loosening of the implant. In order to achieve effective osseointegration with the bone prosthesis and reduce the risk of loosening, porous metals and coatings have been developed. In particular, hydroxyapatite (HA) and polymethylmethacrylate (PMMA) has been successfully employed as a coating for titanium implants and has greatly improved osseointegration of the implant (Landor *et al.*, 2007; Gibon *et al.*, 2017).

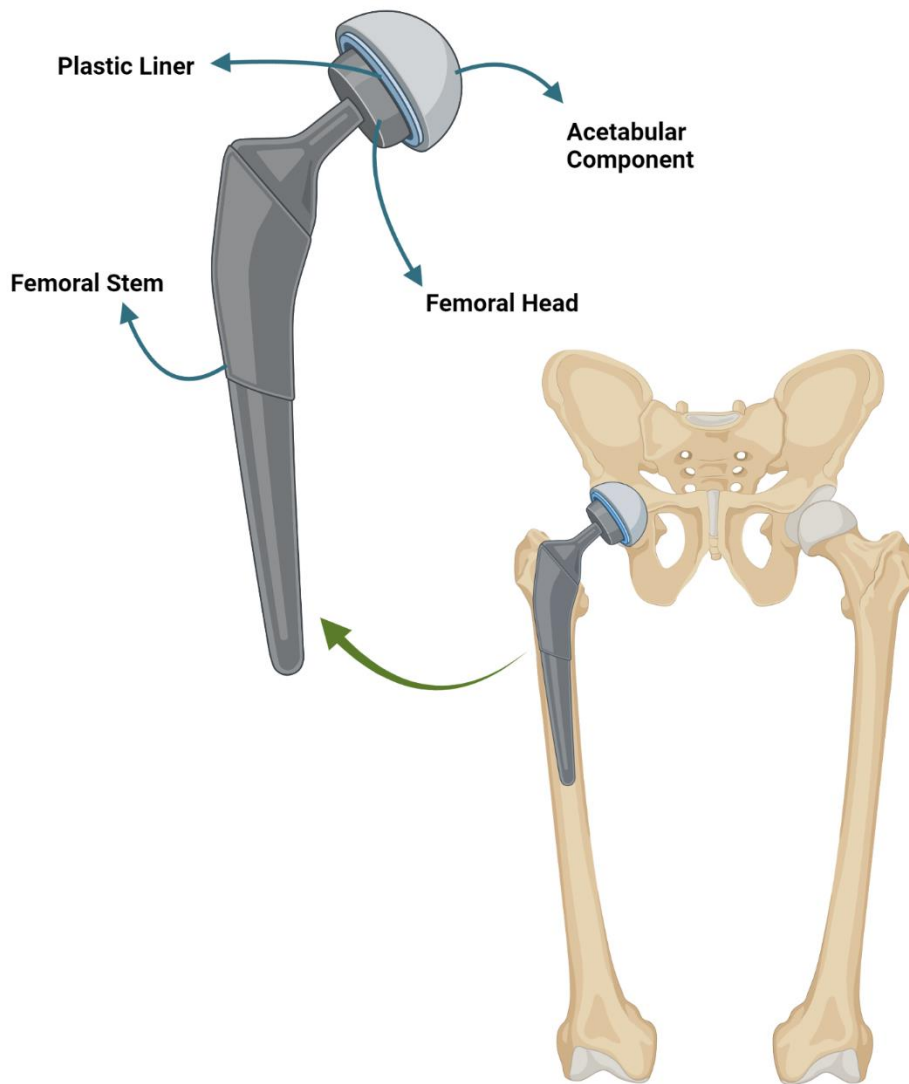


Figure 1.1 Total Hip Arthroplasty. A hip joint prosthesis (right) that typically consists of an acetabular component and a femoral stem (left). The head of the femoral element fits inside of the acetabular component to allow sufficient articulation of the human joint. These two parts of the implant have been made using a variety of materials such as the ones mentioned in 1.3. Created with Biorender.com.

1.4 Implant Placement and Maintenance

The rise in primary hip and knee arthroplasties has important implications for healthcare costs as well as capacity. As such, it is important that the patients are carefully selected and that the procedures are well timed in order to achieve the best possible outcomes and reduce the risk of a revision procedure, reducing future costs and worse outcomes (Gademan *et al.*, 2016). The placement of a bone joint prosthesis begins with a diagnosis which helps the clinician in choosing the most appropriate treatment option for the patient. According to Pivec *et al.* (2012) and the National Joint Registry (2022) the primary reason for an elective total joint procedure is due to OA, which accounts for over ~93% of all total hip and knee replacement procedures. Surgical indications for TJA are usually guided by severity of pain, functional impairment, physical examination, and radiographic findings. However, conservative therapy should always be attempted with analgesia, steroid injections, activity modification, ambulatory aids, and weight loss prior to surgical consideration (Hunter and Lo, 2008; Pivec *et al.*, 2012). If conventional treatment options fail to alleviate pain or the disease is significantly impacting the patient's day-to-day life, then surgical intervention is necessary.

Prior to surgery, patients are provided with comprehensive preoperative instructions to ensure they are prepared mentally and physically. Once the preoperative assessment is complete, the patient is then taken to the operating room and is provided with an anaesthetic. The most common option provided is a spinal anaesthetic, however, the patient can also be given an epidural or be put under general anaesthetic. Once the patient has been provided the appropriate anaesthetic, the surgical team carefully turn the patient from a supine position (laying horizontally, face up) to either an anterior (front), lateral (side) or posterior (back) position, depending on the type of surgical approach being performed (John Hopkins Medicine, 2022; NHS, 2019; Branson and Goldstein, 2003). For total hip arthroplasty, there are a variety of surgical approaches that might be used, such as posterior, lateral (Hardinge), direct anterior and supercapsular percutaneous assisted total hip (superPATH) (Palan & Manktelow, 2018). Posterior and Hardinge are the most common surgical approaches,

accounting for ~73% and ~26% of all primary hip arthroplasties performed in 2021, respectively (NJR 19th Annual Report, 2022). However, despite the Hardinge technique being the second most commonly used surgical approach, it has been found to be associated with worse outcomes, including more deaths and revisions, in comparison to the posterior technique. It has been suggested that the posterior technique be the standard approach used in total hip arthroplasties (Blom *et al.*, 2020).

After the incision has been made, the surgeon opens the hip capsule to expose the femoral head. The femoral head is dislocated, and an osteotomy is performed on the femoral head to remove it. Femoral instrumentation, such as broaches and reams, are used to hollow out the femoral canal and prepare it for the artificial stem. Once the femur has been prepared for stem implantation, the surgeon inspects the acetabulum (the socket component of the joint), clears the area of any soft tissue and osteophytes (bony spurs) and proceeds to remove the damaged cartilage in order to restore its original centre (John Hopkins Medicine, 2022; Branson and Goldstein, 2003). The surgeon places a shell into the acetabular cavity, followed by a liner made with either polyethylene, ceramic, or metal. The artificial stem is then placed into the femoral canal with or without cement and the femoral head is placed onto the stem, completing the femoral implant insertion. The surgeon will bend and move the leg to ensure that it functions appropriately and will then close the incision.

For total knee arthroplasty, the surgical approaches used are either medial parapatellar, midvastus or subvastus (Varacello *et al.*, 2022). The most used approach is the medial parapatellar, accounting for ~95% of all total knee arthroplasties performed in 2021 (NJR 19th Annual Report, 2022). However, it has been noted that other surgical approaches, such as the midvastus approach, could provide significant benefits in short term pain and range of movement (ROM) when compared to parapatellar technique and the subvastus approach provided better outcomes for short-term ROM and earlier straight leg raise in comparison to the parapatellar technique (Liu *et al.*, 2014). Yet, there are no differences in long-term clinical outcomes between these surgical techniques. After incision, the damaged ends of the femur (thigh bone) and tibia (shin bone) are cut away. The ends of the femur

and tibia are then carefully measured and shaped to fit the replacement prosthetic (NHS 2022; Williams *et al.*, 2010). Prior to fitting the final prosthetic, a mock joint is positioned to ensure that the joint is working properly. Once the final adjustments are made, the ends of the tibia and femur are cleaned, and the final prosthesis is fitted and is usually fixed into place with cement (NHS 2022). Generally, the prosthetic is comprised of three components, the tibial component, to resurface the top of the tibia, the femoral (thigh) component, which resurfaces the end of the femur, and the patellar component, to resurface the bottom of the kneecap (John Hopkins Medicine, 2022) (Fig. 1.2).

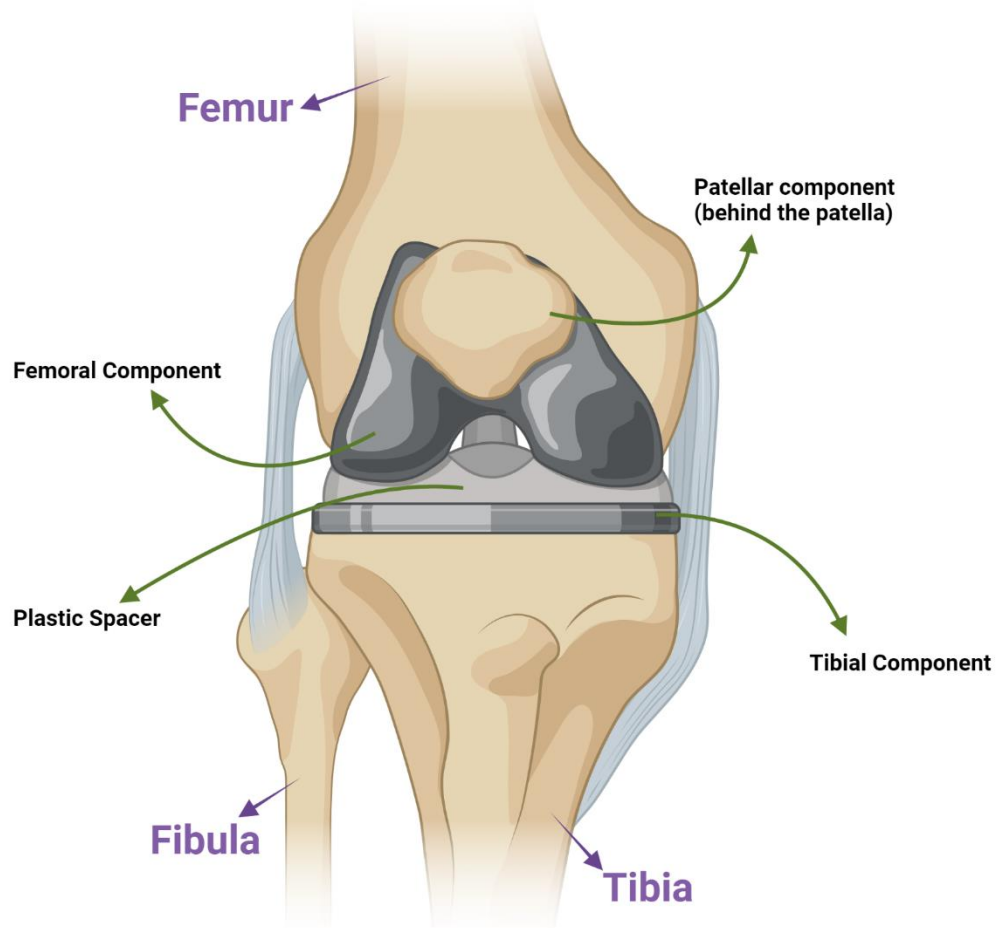


Figure 1.2 Total Knee Arthroplasty. Damaged bone is removed and resurfaced with metal implants on the femur and tibia, as described in 1.3. A plastic spacer is placed in between then implants. The patellar component is not shown for clarity. Created with Biorender.com

After total joint replacement procedures have been performed, patients are in hospital for around 3-5 days, depending on the progression made and the type of joint replacement. However, movement of the newly replaced joint is often encouraged within 12-24 hours post-surgery (NHS, 2022). Physical therapy is usually prescribed after arthroplasty in order to reduce the risk of post-operative complications or dislocation of the new joint. It has been found that physical therapy can promote early ambulation and can decrease the patients' stay at the hospital. Moreover, it can even improve the range of movement (ROM) and function of the new joint in the short term (< 1 year). However, these beneficial outcomes have not been assessed long term (Pivec *et al.*, 2012; Chen *et al.*, 2012; Liebs *et al.*, 2012; NHS, 2022). In the UK, care for patients with total hip and knee arthroplasty is often provided with long-term follow up appointments in order to ensure the joint has not failed. According to the British Orthopaedic Association Guidelines (2012), it is recommended that patients have a follow-up at one and seven years, post-implantation. Recently however, many hospitals face pressure to reduce outpatient appointments due to longer waiting lists for orthopaedic treatment and a reduction in follow-up services (Smith *et al.*, 2022). This could potentially impact on patient safety and increase the risk of revision arthroplasty if no follow-up is provided. Despite the post-operative care issues mentioned above, TJA of the hip and knee, when managed sufficiently, has a > 95% and > 80% survivorship at 10- and 25-years, respectively (Pivec *et al.*, 2012).

1.5 PJI

1.5.1 Overview

Although the implant integrates well into the host tissue approximately 10% of implants fail, and the patient will need additional surgery at some point over the lifetime of the implant (Arciola *et al.*, 2018; Tande & Patel, 2014). A TJA can fail for a variety of reasons including, aseptic loosening at the bone-cement interface, periprosthetic fracture, fracture of the prosthesis material itself, malposition, instability, material fatigue or PJI (Tande & Patel, 2014; Kapadia *et al.*, 2015). Despite the incidence of

PJI being lower than aseptic loosening (which accounts for around a third of all implant failures), it is a serious and more complex problem following arthroplasty (Li *et al.*, 2018).

A majority of PJIs are speculated to occur during implantation and are usually attributed to endogenous skin microbes or external sources from the operating theatre. Usually, PJIs that develop within three months after the procedure are classified as early postoperative infections. The other classifications are delayed (or subacute) infections, which develop around 3-24 months after surgery and finally, late infections, which occur more than 24 months after post operatively (Arciola *et al.*, 2018). This highlights that PJI could happen at any time during the patient's life post-surgery (Li *et al.*, 2018). Further to needing additional procedures, patients who have developed PJI often require extended antibiotic therapy. However, the advancement of antimicrobial resistance (AMR) is a concern, especially since the development of new antimicrobials has slowed down over the last few decades, which has subsequently restricted the options in combatting resistant organisms (Kapadia *et al.*, 2015; Finley *et al.*, 2013; Arciola *et al.*, 2018). Despite therapeutic intervention, eradication of established PJIs can fail and although rare, PJIs can result in severe pain, poor quality of life and death (Kunutsor *et al.*, 2016; Hickok & Shapiro, 2012; Jose *et al.*, 2005; Arcioloa *et al.*, 2018).

In orthopaedic implant-associated infections, the most common aetiological agent isolated are Gram-positive cocci, such as *Staphylococcus aureus*, coagulase-negative staphylococci (CNS) and enterococci. However, more recently there has been a notable increase in the isolation of methicillin-resistant *Staphylococcus aureus* (MRSA) and methicillin-resistant CNS, with around 46.7% of *S. aureus* strains and 85.7% CNS strains being resistant in the US, conversely, only around 6% of *S. aureus* strains that are isolated, are methicillin resistant in the UK (European Centre for Disease Prevention and Control (ECDC), 2022; Kapadia *et al.*, 2015). Despite this discrepancy, the clarity between west-to-east gradients remains unclear for Gram-positive infections and underlines the need for concerted action to combat antimicrobial resistance throughout the European Union (ECDC, 2022). Overall, the emergence of these resistant organisms is alarming and highlights the need for new drugs with novel

mechanisms of action, as these PJIs can result in increased morbidity and mortality for patients with joint arthroplasties (Parvizi *et al.*, 2010; Kapadia *et al.*, 2015).

1.5.2 Epidemiology and Economic Impact

PJI is estimated to occur in ~1% of hip arthroplasty failures and ~2% for knee, annually (Dale *et al.*, 2009; Kurtz *et al.*, 2010; Kapadia *et al.*, 2016). Nevertheless, findings from an analysis of individuals who underwent initial hip or knee arthroplasty procedures from 2006 to 2009 revealed that the rates of PJI may be greater than what was previously documented. (Kapadia *et al.*, 2016; Yokoe *et al.*, 2013). Interestingly, infection is the most likely reason that a joint is revised after the first year however, after ~7 years or more, infection is less likely in comparison to other reasons such as aseptic loosening or periprosthetic fracture (Kapadia *et al.*, 2015). Furthermore, PJI in the UK is more prevalent in a second revision than in a first revision, with ~14% of hip and ~24% of knee re-revisions resulting from infection (NJR 19th Annual Report, 2022; Kapada *et al.*, 2015). This highlights the increased risk of instability and infection following the first revision of a hip or knee replacement compared to that of a primary hip or knee arthroplasty.

Interestingly, the incidence of a revision procedure due to infection is higher in the elbow region, with infection frequencies ranging from around 2-10% (Li *et al.*, 2018). It is suggested that the reason for this higher incidence of infection is due to the more frequent occurrence of rheumatic disorders, trauma or multiple constructive procedures, when compared to hip and knee arthroplasty (Li *et al.*, 2018; Achermann *et al.*, 2011). However, shoulder revisions due to infection, carry infection rates similar to that of hip and knee arthroplasty (Tande & Patel, 2014).

The economic impact of PJI is serious. In the US, the overall cost to the US healthcare to treat PJI was \$566 million in 2009 alone, and it is projected to increase to as much as \$1.85 billion by 2030 (Tande & Patel, 2014; Premkumar *et al.*, 2021). Revision procedures continue to inflict substantial economic burdens in the European Union, with revision projected to be as high as €80,000 per case (Pavizi *et al.*, 2010). The costs for treating individual PJI cases depends on the treatment option used. The cost

of a single revision procedure for PJI is significantly higher than for non-infectious reasons and is estimated to be as high as £71,000 per case. One study even noted a cost of up to £84,000 per PJI case, which is five times higher than the cost of a primary arthroplasty (Parvizi *et al.*, 2010; Kapadia *et al.*, 2014; Kapadia *et al.*, 2016). These higher costs have been attributed to longer procedure durations, increased blood loss, longer rehabilitation time, extended use of antibiotics and analgesics, and increased complications (Vanhegan *et al.*, 2012; Tande & Patel, 2014).

1.5.3 Pathogenesis of PJI

1.5.3.1 Initiation of Infection

Most PJIs that occur within one year of implantation usually begin through the introduction of microorganisms at the time of surgery. They can either be through direct contact or aerosolised contamination of the prosthesis or periprosthetic tissue. Once the microorganisms come into contact with the implant surface, they start to colonise it. A significant factor during the initiation of the infection is the inoculum size. For instance, in a rabbit model study it was found that fewer than 10^2 CFU of *S. aureus* was needed to establish an infection if inoculated at the time of an arthroplasty in a rabbit model, in comparison to a 10^4 CFU inoculum when no prosthesis was implanted (Southwood *et al.*, 1985; Tande & Patel, 2014). The second mechanism which contributes to the initiation of infection is the spread of infection from an adjacent site to the prosthesis. Shortly after the procedure, a surgical site infection (SSI) could progress to involve the implanted prosthetic, due to incomplete healing of the incision area. However, the spread of infection from adjacent surfaces could also occur later on if the normal tissue is impacted through trauma or surgery at a location next to the implant. Erosion of the implant through a damaged soft tissue envelope may also put patients at an increased risk of late-onset infection (Tande & Patel, 2014). A third mechanism which contributes towards PJI, is haematogenous seeding (bacteria which are carried to the implant site through the blood). However, PJI resulting from haematogenous seeding is uncommon. In a study by Uckay *et al.* (2009) it was found that out of 553 remote infections which occurred in 6,101 arthroplasties, only 7 resulted in PJI. Despite

this, the overall proportion of haematogenous PJI accounts for approximately 20-35% of all PJI infections. The number of PJI with haematogenous origins are likely to be underestimated as most reports do not specify the route of infections and if it involves highly virulent organisms, the incidence of haematogenous PJI maybe even higher (Rakow *et al.*, 2019). For instance, from a cohort of patients with *S. aureus* PJI, over 70% had PJI which were of a haematogenous origin (Sendi *et al.*, 2011). This risk, in comparison to the 3-10% risk of *S. aureus* infection in native joints, highlights the importance of the implant material in haematogenous PJI.

1.5.3.2 Propagation of Infection

A useful way of observing the progression of PJI infection, is through animal models. A study conducted by Belmatoug *et al.* (1996) observed the progression of PJI by infecting a rabbit model with *S. aureus* and assessed the evolution of the infection microbiologically, histologically, by magnetic resonance imaging (MRI) and radiological analysis. The model is comparable to PJI seen in humans, although the inoculum density is higher in the animal model. It was found that the infection was initially confined within the joint. Between weeks one to eight, histological analysis demonstrated large granuloma formation, filled with neutrophils, abscess formation and the presence of Gram-positive cocci in the bone tissue. Over time, the infection spreads both proximally (close) and distally (far) to the neck of the metaphysis after three weeks of infection. The infection, if left untreated, can eventually involve the entire metaphysis and part of the bone shaft (diaphysis), leading to progressive osteomyelitis in the tibia and femur. Yet, it is uncertain if this process is the same as haematogenous PJI. It is thought that haematogenous osteomyelitis initiates at the metaphysis and can progress to a diffuse osteomyelitis, however the organism does not usually reach the bone by a haematogenous route (Cremlieux & Carbon, 1997). Moreover, it is difficult to design experimental models that simulate haematogenous infection, as the few studies that have tried to simulate haematogenous seeding resulted in excessive mortality rates and lower infection rates (Gatin *et al.*, 2015).

1.5.3.3 Race to the Surface Theory

Recently, the concept of “race to the surface” has been introduced to describe the competition between host cells and the contaminating organisms to occupy the implant surface. If the race is won by host cells, the implant is coated by tissue and less vulnerable to bacterial colonisation. Whereas if the bacteria win, the implant will become rapidly covered in a biofilm. As a result, the tissue cell functions are hampered by bacterial virulence factors and toxins. Therefore, quick integration of the implant into the host tissues is paramount for the success of implantation (Arciola *et al.*, 2018; Subbiahdoss *et al.*, 2009; Gristina & Myrvik, 1988).

In orthopaedics, bone tissue healing around the implant results in appositional bone growth and integration of the prosthesis into the bone tissue. This process is known as osseointegration (Fig. 1.3). However, *in vitro* observations with osteosarcoma cells have found that pre-colonising bacteria can drastically impact osseointegration of the implant, compromising host cell adhesion to the biomaterial surface (Gristina & Myrvik, 1988; Arciola *et al.*, 2018). Yet, these studies did not evaluate bacterial adhesion in the presence of eukaryotic cells, as stated by the “race to the surface” theory. A more recent study used a co-culture method in order to assess the impact of eukaryotic cells on the pathogenesis of PJI. It was found that clinical isolates adhered to the material surface at lower concentrations, in comparison to collection strains. Moreover, a destructive effect of bacteria on preosteoblastic cells was also detected, especially with higher concentrations of bacteria (Martinez-Perez *et al.*, 2017).

Despite *in vitro* models providing an informative insight into how bacteria interact with host cells and biomaterial surfaces, they often lack more than one host cell type and only observe the phenomena for a short time (Arciola *et al.*, 2018). *In vivo* models are needed to gain more insight into symptomatic and delayed low-grade infections.

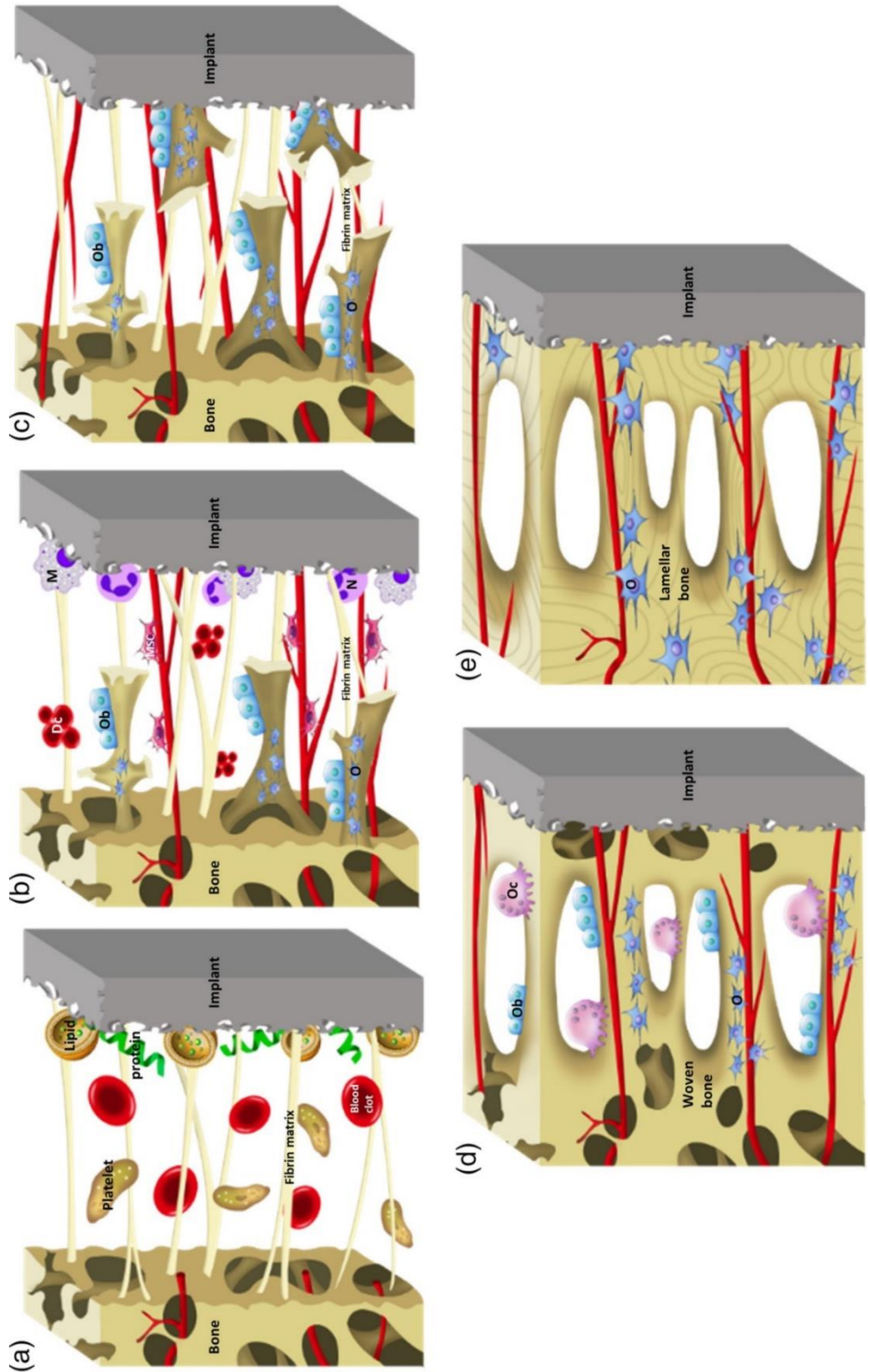


Figure 1.3 Schematic of Implant Osseointegration. Initially, osseointegration of the implant begins with the formation of blood clots and the fibrin matrix **(a)**. Then angiogenesis (the growth of new blood vessels) and woven bone formation occurs **(b)**. The woven bone goes through two stages of growth: distance osteogenesis (where the bone grows between two segments of bone) and contact osteogenesis (where the bone grows at the site of the implant) **(c)**. New woven bone fills the gap and undergoes remodelling **(d)**. Finally woven bone transforms into a more mature type of bone called lamellar bone **(e)**. **DC:** Decomposed clot; **M:** Macrophage; **N:** Neutrophil; **O:** Osteocyte; **Ob:** Osteoblast; **Oc:** Osteoclast. Reproduced from Liu *et al.* (2019) (CC BY 4.0)

1.5.3.4 Role of Biofilm in PJI

Bacteria that contaminate prosthetics are generally not sparsely distributed, single adherent cells. Most often, they form biofilms, which are bacterial aggregates that tightly adhere to the biomaterial surface, encased in a matrix of extracellular polymeric substances (EPS) (Gristina & Costerton, 1985; Li *et al.*, 2018; Arciola *et al.*, 2018). The EPS of biofilms is comprised of polysaccharides, proteins, teichoic and lipoteichoic acids, and extracellular DNA. However, the composition and amount vary between organism types (Tande & Patel, 2014). The community within the biofilm may be polymicrobial or monomicrobial, however, even if the biofilm is monomicrobial, it may consist of subpopulations of the same organism with different phenotypic and genotypic attributes (Tande & Patel, 2014). The development of a biofilm is not a static process, it consists of several stages including microbial adhesion to a surface, initial growth on the biomaterial surface, formation of microcolonies from cellular aggregation, EPS formation, biofilm maturation and finally, dispersal (Fig. 1.4). When matured, biofilms occur in a multicellular, nonhomogeneous system which comprises of microbial cells that communicate with one another through chemical or electrical signalling in a process known as quorum sensing. These separate subpopulations within the biofilm may have different functions, which supports the biofilm as a whole, making biofilms akin to a multicellular organism (Tande & Patel, 2014). However, once a biofilm is established on the implant surface, it is very difficult to eradicate.

Biofilms are usually responsible for the persistence of PJI and are a source of bacterial spread into other sites of the body. When in a biofilm state, bacteria are protected from conventional antimicrobial therapies and the host immune system, making treatment of the infection difficult (Donlan & Costerton, 2002). In fact, the minimum biofilm eradication concentration (MBEC) can be up to 1000 times greater than the minimum inhibitory concentration (MIC) of their planktonic counterpart (Davidson *et al.*, 2019). A major factor that makes bacteria in a biofilm more resistant to antimicrobial agents is their slow growth rate and the presence of resistant subpopulations (referred to as persistors) (Costerton *et al.*, 1999; del Pozo & Patel, 2007). Moreover, the high cell density of a

biofilm aids in increased rates of horizontal gene transfer between organisms, which permits the sharing of virulence genes and antibiotic resistance genes (Sorensen *et al.*, 2005; Davidson *et al.*, 2019; McConoughey *et al.*, 2014).

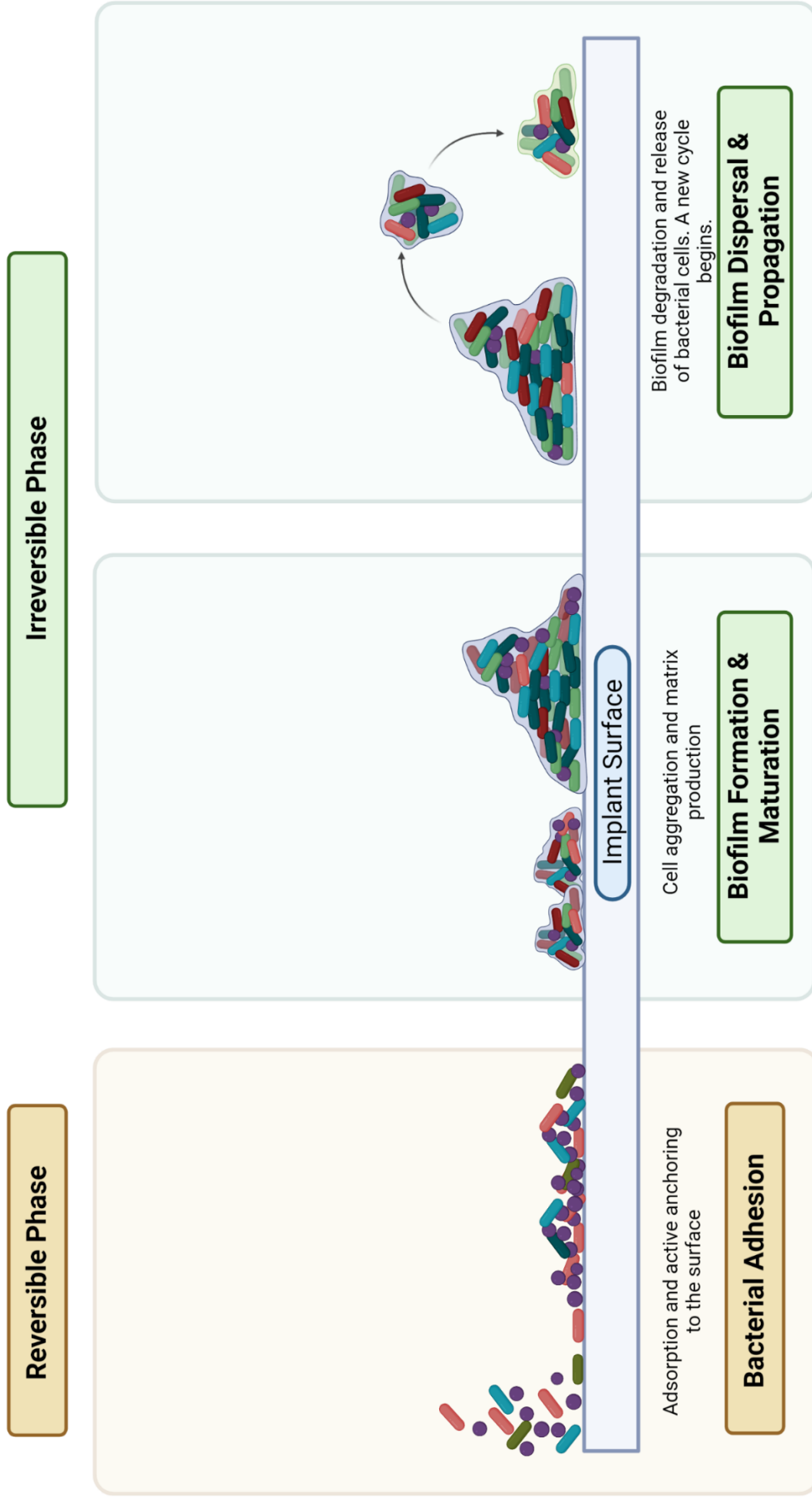


Figure 1.4 Stages of Biofilm Formation. Planktonic bacteria reversibly adsorb onto the implant surface. After a short period of time, the initial colonisers irreversibly attach to the surface and start to form EPS. The biofilm matrix progressively builds up and larger bacterial aggregates develop. Eventually, the mature biofilm is degraded and cells are dispersed. Created with Biorender.com

Biofilms are also proficient at inhibiting the host's immune response. The presence of a foreign body (in this case, the prosthesis) within the patient, along with postoperative scar tissue is already hard to access for the immune response, given the lack of blood supply to the area (Davidson *et al.*, 2019; McConoughey *et al.*, 2014). This compromises the immune cell's ability to reach the surface and clear the infection (McConoughey *et al.*, 2014). For instance, a study by Vaudaux *et al.* (1985) found that > 95% of the *S. aureus* that adhered to PMMA survived exposure to neutrophils, in comparison to < 10% planktonic *S. aureus* when exposed to the same conditions. It was also found that polymorphonuclear leucocytes failed to sufficiently phagocytose *S. aureus* cells within the EPS, despite the leucocytes penetrating into the biofilm (Leid *et al.*, 2002).

Interestingly, whilst biofilms have been implicated in PJI, some of the evidence is suggested to be anecdotal as a result of inconsistencies in culturing and clinical symptoms (Stoodley *et al.*, 2008). However, culturing and identification of biofilm bacteria is usually difficult, as they are in a metabolically dormant state, especially when trying to diagnose infection in delayed- and late-onset PJIs. Moreover, mixed population biofilms will not have their components in equal proportions, and subpopulations within the biofilm will have different reactions to antimicrobial agents and the host immune system, making it difficult to detect in a clinical setting (Tande & Patel, 2014). The success of identifying biofilm bacteria using classical culturing techniques can be a little as 30% (Hall-Stoodley *et al.*, 2006). However, viable bacteria from a biofilm have been identified using *ex vivo* techniques. By using fluorescent *in situ* hybridisation (FISH), confocal microscopy and polymerase chain reaction (PCR), Stoodley *et al.* (2008) were able to identify metabolically active *S. aureus* from explanted tissues and cement from a patient who underwent the removal of a total elbow arthroplasty. In addition, they also demonstrated the presence of live cocci on both the fibrous tissue and the prosthesis, indicating that an established biofilm can adhere to both the implant and the fibrous tissue that envelops the implant. Moreover, it was suggested that the tissue that envelops the prosthesis may also act as a source for pathogenic biofilms (Stoodley *et al.*, 2008). In the context of PJI, biofilm formation and

development are usually discussed in relation to growth that occurs on the prosthetic and not the surrounding tissue.

1.5.3.5 Aetiological agents of PJI

In order to choose the most appropriate antimicrobial treatment prior to culturing results, the common aetiological agents of PJI should be examined within the available literature. Tande & Patel (2014) examined 14 studies, which collectively looked at around 2,400 patients with hip or knee PJI. It was found that most infections were largely driven by *S. aureus* and coagulase-negative staphylococci, which accounts for around 50-60% of all PJIs, whilst streptococci and enterococci combined only account for approximately 10% of the knee and hip PJI cases.

1.5.3.5.1 *Staphylococcus aureus*

S. aureus is a significant pathogen in PJI due to its frequency and virulence. It is the leading aetiological agent of PJI in the US and the second-leading cause in Europe (Arciola *et al.*, 2018). Along with being one of the foremost aetiological agents in PJI it is also a major cause of severe invasive infections, such as nosocomial, community-acquired and healthcare-associated bloodstream infections (Wisplinghoff *et al.*, 2004; Kaasch *et al.*, 2014). These types of infection could lead to hematogenous PJI. In addition, implanted medical devices, obesity, diabetes and native colonisation of *S. aureus*, along with other co-morbidities can lead to an increased risk of invasive *S. aureus* infection (NJR 19th Annual Report, 2022; Jacobsson *et al.*, 2007). Treatment of *S. aureus* PJI is often difficult, mostly due to the organism's ability of forming small colony variants (SCV), which allow the bacteria to persist in a metabolically slowed state, biofilm formation and the emergence of antibiotic resistance (Riberio *et al.*, 2012). In particular, MRSA has emerged as a significant problem in implant-related infections and has subsequently received more attention than its methicillin sensitive counterpart (MSSA). MRSA are resistant to most β -lactam antibiotics, such as oxacillin, amoxicillin and penicillin. They are also resistant to tetracycline and other antibiotic classes such as third generation cephalosporins and upon exposure to vancomycin

(Vanc) and other glycopeptide antibiotics, MRSA strains can become less susceptible to these antibiotics (Riberio *et al.*, 2012; Teterycz *et al.*, 2010).

1.5.3.5.2 Coagulase-negative staphylococci

Coagulase negative staphylococci (CNS) comprise of a variety of microorganisms that are mostly ubiquitous members of the human microbiome. Historically, identifying specific species within this group has been challenging as much of the literature does not refer to one species, and the pathogenicity of these organisms remains uncertain (Tande & Patel, 2014). CNS species have been found to be the second most common cause of early-onset PJI as well as being one of the most frequent causes of delayed- and late-onset PJI (Tande & Patel, 2014). However, one particular species from this group, *Staphylococcus epidermidis* has become a prevalent issue within PJI. It is the most isolated member of CNS from implant-associated infections and are also associated with nosocomial and hospital-associated infections. In Europe, *S. epidermidis* is the leading cause of PJI, followed by *S. aureus* (Arciola *et al.*, 2018). Interestingly, some strains of *S. epidermidis* have been found to be more resistant to antibiotics than *S. aureus* (Riberio *et al.*, 2012; Harris *et al.*, 2010; Tande & Patel, 2014). Despite *S. epidermidis* being a ubiquitous member of the skin flora, if given the opportunity, it can become pathogenic and is known as an opportunistic pathogen. *S. epidermidis* often causes PJI through its ability to efficiently attach to the prosthetic surface and form a biofilm. In particular, *S. epidermidis* is known to produce polysaccharide intercellular adhesion (PIA), which is paramount for biofilm formation. In addition, the PIA is known to protect *S. epidermidis* from phagocytosis and from other host immune defence mechanisms (Riberio *et al.*, 2012; Tande & Patel, 2014; Fey & Olson, 2010). Other virulence mechanisms formed by *S. epidermidis*, such as phenol-soluble modulins and poly- γ -DL-glutamic acid have also been found to help mediate resistance to the innate immune system (Fey & Olson, 2010).

Other species from the CNS group that have been implicated in PJI include, *Staphylococcus simulans*, *Staphylococcus capitis*, *Staphylococcus caprae*, and *Staphylococcus lugdunensis* (Razonable *et al.*,

2001; Allignet *et al.*, 1999; Sampathkumar *et al.*, 2000; Lourtet-Hascoet *et al.*, 2018). Interestingly, whilst *S. capitis* has been shown to cause pneumonia, urinary tract infections (UTI), bloodstream infections and endocarditis, very few osteomyelitis infections have been reported in the literature (Lourtet-Hascoet *et al.*, 2018). However, in a study that looked into PJI cases, caused by CNS species, around 11% were caused by *S. capitis* (Lourtet-Hascoet *et al.*, 2018).

Another CNS species which is distinctive from the rest of the group, is *S. lugdunensis*. Unlike the other species which cannot produce coagulase, *S. lugdunensis* produces a bound coagulase, which can be misidentified as *S. aureus* when using a latex agglutination assay and other identification systems, such as biochemical strip tests (Mateo *et al.*, 2005; Tan *et al.*, 2008; Askar *et al.*, 2018). *S. lugdunensis* is capable of causing serious systemic infection, similar to that of *S. aureus* (Sampathkumar *et al.*, 2000; Tande & Patel, 2014). Interestingly, *S. lugdunensis* seems to infect knees arthroplasties rather than hip arthroplasties. A study by Askar *et al.* (2018) found that out of 84 PJIs, 58 (69.9%), 24 (28.6%) and 2 (2.4%) episodes were in knee, hips and other arthroplasty sites, respectively. Moreover, this observation was made by two other studies that looked into *S. lugdunensis* PJI (Shah *et al.*, 2010; Lourtet-Hascoet *et al.*, 2016).

1.5.3.5.3 Other Organisms

Enterococcus species, whilst a rare cause of PJI, have been implicated in around 12-15% of patients with early-onset PJI. Traditionally, *Enterococcus* species have been associated with UTI, bloodstream infections and endocarditis, however recently, it has been reported that *Enterococcus* species have been found in PJI with increasing frequency (El Helou *et al.*, 2008). For instance, a study conducted by Cobo *et al.* (2011) found that out of 139 early-onset-PJI cases, around 17 of them had isolated enterococci. Moreover, these enterococci are often found as part of a polymicrobial infection (Peel *et al.*, 2012). However, if found during late-onset PJI they are usually found in a monomicrobial state (El Helou *et al.*, 2008; Tande & Patel, 2014). Despite this, enterococci are the cause of only around 3% of PJIs and due to its rarity, it remains poorly understood.

Other organisms, such as aerobic Gram-negative bacilli has also been implicated in PJI over the years. Despite Gram-positive cocci being the most isolated organism from PJI, Gram-negative bacilli constitute around 10-23% of all PJI cases, most of them during early-onset PJI. Some studies have even found Gram-negative bacilli in up to 45% of PJI cases (Cobo *et al.*, 2011; Peel *et al.*, 2012; Rodriguez-Pardo *et al.*, 2014). Interestingly, a small study found that Gram-negative bacilli, specifically Enterobacteriaceae, were more likely to occur in hip, rather than knee implants, however this could be due to the hip joints closer proximity to the gastrointestinal tract (Tande & Patel, 2014; Aboltins *et al.*, 2011). Anaerobic bacteria have also been isolated from PJIs including, *Cutibacterium acnes*, *Clostridium* species, *Peptostreptococcus* species and *Bacteroides fragilis* (Tande & Patel, 2014; Marculescu & Cantey, 2008). However, most anaerobic bacteria implicated in PJI are normally found in polymicrobial PJI.

Polymicrobial PJI can account for 6 to 37% of all PJI (Li *et al.*, 2021). In early-onset infections around 35% of PJI are polymicrobial, whereas < 20% of PJI are polymicrobial at any time after prosthesis implantation (Bozhkova *et al.*, 2016; Tande & Patel, 2014). In one instance, it was found 56% of all polymicrobial infections occurred 90-days post implantation, whereas only 29% of the monomicrobial infections occurred during this timeframe (Marculescu & Cantey, 2008). Some studies have suggested that patients with polymicrobial PJI have a reduced recovery rate in comparison to monomicrobial PJI (Li *et al.*, 2021; Marculescu & Cantey, 2008; Tan *et al.*, 2016). In addition, the management of polymicrobial PJI is difficult and can result in repeated revisions and long-term administration of broad-spectrum antibiotics to help combat polymicrobial PJI. However, studies on polymicrobial PJI remain limited due to the low occurrence of polymicrobial PJI and there are still uncertainties regarding the risk factors of polymicrobial PJI (Li *et al.*, 2021; Bozhkova *et al.*, 2016).

1.5.3.6 Diagnosis and Treatment of PJI

Diagnosis of PJI is determined by a variety of clinical findings, such as results from peripheral blood, synovial fluid, histological analysis of periprosthetic tissue and microbiological analysis. In some cases,

radiography may be used if the infection has already caused damage to bone, however, radiography is very limited in its ability to diagnose PJI (McConoughey *et al.*, 2014; Tande & Patel, 2014). Early diagnosis of PJI is an important factor to save the prosthesis and function of the joint. The progression of PJI is often accompanied by signs such as, fever, swelling and purulent discharge. However, in the absence of physical signs of infection, it can be difficult to ascertain if the failure is due to aseptic loosening or infection (McConoughey *et al.*, 2014). Moreover, determining whether the aetiological agent is growing in a planktonic or biofilm state is especially challenging. Even if the aetiological agent can be isolated from the infected site and identified through *in vitro* culturing methods, this technique does not necessarily represent the *in vivo* growth state, as most bacteria can occur in both planktonic and biofilm states (McConoughey *et al.*, 2014). Traditionally, acute infections have been defined as having “signs and symptoms lasting < 14-28 days” and are considered to be caused by rapidly growing planktonic bacteria. As a result, they are usually present in periprosthetic tissue and fluids in high concentrations and can be diagnosed clearly using histopathological and microbiological techniques (McConoughey *et al.*, 2014; Widmer, 2001). However, delayed- and late-onset infections are harder to diagnose and is most likely attributed to the bacteria being in a biofilm state. This makes them difficult to treat for two main reasons, biofilms are difficult to remove from the implant surface, especially when in a mature state, and the reduced growth rate of biofilm bacteria makes it difficult to culture (Arciola *et al.*, 2018; McConoughey *et al.*, 2014; Tande & Patel, 2014).

In addition, the diagnosis of PJI has been proven difficult due to the lack of standardised clinical techniques and has resulted in the formation of organisations known as the Musculoskeletal Infection Society and European Bone and Joint Infection Society, which aimed to define specific guidelines for diagnostic purposes which could be utilised by physicians, surveillance authorities (such as the Centre for Disease Control) and all others involved in the management of PJI. The guidelines outline three major criteria that aid in the diagnosis of PJI and include:

- A sinus tract communicating with the implant

- Pathogen(s) are isolated by culture from at least two separate tissue or fluid samples obtained from the affected prosthetic joint
- That four of the following sub-criteria are met:
 - Elevated serum erythrocyte and serum C-reactive protein
 - Elevated synovium leucocyte count and neutrophil percentage
 - Presence of pus in the affected joint
 - Isolation of an organism from periprosthetic tissue or synovial fluid
 - Greater than five neutrophils per high power field when observing histological samples of periprosthetic tissue at x 400 magnification.

However, PJI may also be present even if fewer than four of these sub criteria are met (McConoughey *et al.*, 2014; Parvizi *et al.*, 2011).

When a patient develops a PJI that cannot be cleared by conventional antibiotic therapy, surgical intervention and medical therapy are the best options in a majority of cases. One way of retaining the implant whilst trying to clear the infection is by performing a debridement, taking antibiotics and implementing an implant retention procedure (DAIR). To reduce the risk of re-infection, the debridement must be thorough and complete. Prosthesis stability is assessed during surgery and usually followed by the replacement of exchangeable components such as the polyethylene liner or adjustable femoral head. The prosthesis and the periprosthetic tissue are then aggressively irrigated and closed over a drain (Koyonos *et al.*, 2011; Byren *et al.*, 2009; Tande & Patel, 2014). However, this treatment is often advised against due to the difficulty of controlling the infection, even when treating acute infections. One study found that out of 138 patients who underwent the DAIR procedure, infection control failed in 90 (65%) joints (Koyonos *et al.*, 2011). Moreover, the risk of failure using this strategy rises after stopping oral antibiotics and lengthening the antimicrobial therapy may only postpone the risk of failure, rather than preventing it (Byren *et al.*, 2009). Therefore, revision surgery for PJI seems to be the most suitable option.

Prosthesis removal in PJI cases is performed by using either a one-stage or two-stage revision procedure. One-stage revision involves removal of the original prosthesis and replacement with a new implant in a single surgical procedure. This involves the debridement of the surrounding tissue to clear the area of infection and secondary damage. Typically, the new implant is put in place with antimicrobial loaded PMMA. The antimicrobial loaded into the PMMA will depend on which causative agent is identified preoperatively. After surgery, the patient is treated with IV antibiotics for 4-6 weeks, followed by a course of oral antibiotics for 3-12 months (Tande & Patel, 2014; McConoughey *et al.*, 2014; Callaghan *et al.*, 1999).

A two-stage arthroplasty is considered the best option to preserve joint function and ensure eradication of the infection and involves two surgeries. During the first surgery, infected tissue is debrided and all prosthesis components, including the PMMA is removed, and cultures are taken away for clinical analysis. An antimicrobial PMMA spacer is usually placed into the joint after debridement in order to provide local antimicrobial treatment and maintain the joint space, and subsequently closed up. The period between the first and second stages allows for sufficient antimicrobial therapy and surveillance prior to going forward with the final phase. A second prosthesis is then implanted after completion of antimicrobial therapy (Tande & Patel, 2014; McConoughey *et al.*, 2014; Zimmerli & Ochsner, 2003).

However, despite the high success rate of a two-stage revision procedure, revision arthroplasty can increase the risk of reinfection, prosthetic complications, other revisions and high costs (Kunutsor *et al.*, 2016; Orapiriyakul *et al.*, 2018). With an increase in primary arthroplasties being undertaken, life expectancy and a growing healthcare burden due to OA, there is a need to find solutions that improve the longevity of primary TJAs (Patel *et al.*, 2015; Kunutsor *et al.*, 2016). This issue, which is addressed in this thesis could be realised by biologically modifying the biomaterials used in prosthetics.

1.5 Current Research to Prevent PJI

1.5.1 Overview

Surface modification of the implanted prosthesis is an effective means of reducing the risk of PJI. Altering biomaterial surface topography to deter bacterial attachment and the design of coatings that elute antimicrobial agents (AMAs) into the surrounding area have been explored (Thakur, 2017; Green *et al.*, 2011; Singha *et al.*, 2017). Steps to permanently immobilise bioactive molecules on the implant surface to prevent long-term bacterial adhesion have also been considered. Current research has primarily focused on controlled-release systems with the aim of eluting antibiotics and other AMAs from the surface itself to reduce the need of a two-stage revision procedure (Hickok & Shapiro, 2012). Porous materials like collagen sponges and bone cement have been loaded with antibiotics, aiming to keep the implant sterile, whilst eliminating bacterial contamination of the surrounding tissue. Biodegradable coatings and multilayer films have been developed for implants to further control antibacterial release (Buttaro *et al.*, 2005; Billon *et al.*, 2005; Ambrose *et al.*, 2004; Guan *et al.*, 2016). Although these systems are effective at preventing contamination of the implant, they do have limitations. For instance, high antibiotic concentrations are only sustained for a short amount of time. Gimeno *et al.* (2015) found that when fixation pins were loaded with cefazolin and linezolid, > 75% of the loaded antibiotic elutes within 120 hours. Whilst these antibiotics may reach therapeutic levels initially, the antibiotic concentrations could drop to sub-therapeutic levels over time, leaving the implant surface susceptible to re-attachment by surviving bacteria. Silver-coated fixation pins have also been explored and are successful in reducing the number of bacteria from the implant surface and surrounding medium (Furkert *et al.*, 2011). However, research is yet to address the cytotoxicity of eluted silver ions, implant efficacy and acquisition of silver resistance. Despite the overall potential of controlled-release systems, the limitations of these surfaces have stimulated research towards the design of coatings that are antimicrobial over the lifetime of the implant.

The development of immobilised antimicrobial implant coatings is an ongoing theme to address the lack of longevity found with controlled-release systems and to prevent bacterial attachment over the lifetime of the implant. A variety of AMAs have been successfully immobilised including, antiseptics (i.e., chlorhexidine, quaternary ammonium compounds), antibiotics, antimicrobial peptides (AMPs) and other AMAs (i.e., antifungals, enzymes).

1.5.2 Immobilisation Strategies

Various techniques have been developed in order to functionalise the biomaterial surface for AMA attachment. In particular, four main surface modification strategies have attracted considerable attention in recent years to immobilise AMAs and are described in the sections below.

1.5.2.1 Surface Grafting

Grafting-to is an indirect chemical grafting process that anchors molecules such as silanes, and polydopamine (PDA) (which possess desirable functional groups) onto the surface, allowing for further modification with various molecules (Chourifa *et al.*, 2019). In addition, the reaction is often specific, and the bond-effect is stable (Ivanova & Crawford, 2015). Silanisation is commonly used when immobilising AMAs as it is a low-cost and effective covalent coating technique and is rich in hydroxyl groups. Silanes have been used to functionalise a variety of biomaterials such as HA, titanium (Ti), bioglass and other metal oxides (Chourifa *et al.*, 2019; Ivanova & Crawford, 2015). Often, the newly hydroxylated surface requires a reaction with a cross-linking agent such as glutaraldehyde, or carbodiimide to ensure chemical reactivity and stability with the desired AMA (Chourifa *et al.*, 2019). Binoy *et al.* (2005) employed this technique to attach Vanc, a glycopeptide antibiotic, to the surface of titanium. These surfaces were functionalised with 3-aminopropyltriethoxysilane (APTES), followed by a reaction with aminoethoxyethoxyacetate (AEEA), a flexible linker, to yield an aminopropyl-functionalised surface. They purportedly attached Vanc using this technique by taking advantage of the antibiotic's carboxylic acid group as it has been shown that it was not required for antimicrobial

activity (Binoy *et al.*, 2005). More recently, Armenia *et al.* (2018), combined a silanisation technique with N'-ethylcarbodiimide hydrochloride (EDC)-N-hydroxysuccinimide (NHS) chemistry to attach teicoplanin, a lipoglycopeptide antibiotic, to the surface of iron oxide nanoparticles (IONPs). However, despite their efficacy there are issues pertaining to the use of silanes. Silanisation requires the use of noxious substances and often involves time-consuming functionalisation steps. In addition, silanes can suffer from hydrolytic instability under physiological conditions (Chouirfa *et al.*, 2019; Ivanova & Crawford, 2015).

A different and more recent strategy for grafting molecules onto the surface of biomaterials is through the application of PDA. The modification of surfaces using PDA has become increasingly attractive as it can avidly bind to virtually all inorganic and organic substrates through oxidation and self-polymerisation of dopamine hydrochloride (DHC) under mildly alkaline conditions (Wang *et al.*, 2017; Lee *et al.*, 2007). Deposited PDA platforms are highly versatile in that they can react with a diverse array of molecules by virtue of PDA reactive catechol, quinone, amine and imine groups. For instance, He *et al.* (2014) used this simple method to covalently attach the antibiotic cefotaxime sodium, to the surface of Ti. The quinone/catechol groups of PDA-modified Ti purportedly reacted with the amino groups on cefotaxime via Michael addition and Schiff base reactions in order to successfully immobilise the antibiotic to the surface. Other groups have also used this polymer functionalisation technique to immobilise other antimicrobials such as chlorhexidine and AMPs (Mohd Daud *et al.*, 2016, Browne *et al.*, 2022, Trzcinska *et al.*, 2020).

1.5.2.2 Surface-Initiated

The surface-initiated (also known as “graft-from”) approach, is another chemical technique used to modify surfaces and allows for polymer generation *in situ* by either chain growth polymerisation or surface-initiated polymerisation (Thakur, 2017). Interestingly, the immobilised AMA is essentially synthesised from the initiator groups on the surface (Green *et al.*, 2011). Indeed, AMAs can also be incorporated into these polymer coatings to further increase antibacterial efficacy. Recently, the

polymer brush coating technique has gained significant interest due to its mechanical stability and controllable brush thickness (Tang *et al.*, 2016). Furthermore, when compared to silanisation, polymer brush technologies can increase the spatial density of various functional groups, therefore increasing the number of AMAs that can covalently attach to the surface (Godoy-Gallardo *et al.*, 2014). For example, Godoy-Gallardo *et al.* (2014), used a copolymer brush technique to immobilise the AMP hLf1-11. Atom transfer radical polymerisation (ATRP) initiator (an emerging technique used in the preparation of polymer brushes) was used to prepare the surface for copolymerisation with N, N-dimethylacrylamide (DMA) and N-(3-aminopropyl) methacrylamide hydrochloride. This reaction was followed by the functionalisation of a cross-linker which was used to attach the AMP to the surface. More recently, zwitterionic polymers have been gaining traction in polymer brush coating technologies for their intrinsic antifouling properties and improved biocompatibility (Tang *et al.*, 2016; Zhao *et al.*, 2014; Hsiao *et al.*, 2014). Tang *et al.* (2016) took advantage of this and created a zwitterionic poly-(sulphobetaine methacrylate) brush coating functionalised with Triclosan, a broad-spectrum antiseptic. The polymer brush was also surface initiated using ATRP, and triclosan was subsequently attached to the polymer coating using a sulphonic ester.

Chemical vapour deposition (CVD) is another graft-from method that can be used to immobilise AMAs whereby vaporised solid material can be deposited onto a heated substrate to form a stable solid film (Chouirfa *et al.*, 2019; Park & Sudarshan, 2001). Xiao *et al.* (2018) used this approach to coat glass slides with a polymer (dibromomaleimide) in order to immobilise a cecropin-melittin hybrid AMP and Ozkan *et al.* (2016) used a two-step aerosol-assisted CVD process to immobilise copper nanoparticles. However, the CVD technique has limitations such as high costs and the use of elevated temperatures that can compromise the biomaterial (Creighton & Ho, 2001; Affatato, 2012).

1.5.2.3 Antimicrobial Inclusion

Unlike the previous methods, the antimicrobial inclusion (also known as “as-formed”) modification involves incorporating the AMA into the coating itself, with the AMA either cross-linked or entangled

within the coating substrate (Green *et al.*, 2011; Mendez-vilas, 2011; Singha *et al.*, 2017). Otari *et al.* (2013) created a silver-alginate biohydrogel using the as-formed method that was not only cost-effective, but environmentally friendly. Hydroxyapatite/gold nanoparticle/ argon nanocomposites have also been designed using this method aiming to improve the overall biocompatibility and antimicrobial properties of biomaterials (Vukomanovic *et al.*, 2014). However, most as-formed methods to date are mostly utilised to create controlled-release systems of AMAs (i.e., gentamicin, Vanc and AMPs) from as-formed nanostructures such as titanium dioxide and HA (Feng *et al.*, 2016; Zhu *et al.*, 2017; Ionita *et al.*, 2017).

1.5.2.4 Physical Modification

Physical modification is a well-known immobilisation technique that coats the biomaterial surface through physical adsorption (i.e., van der Waals and electrostatic interactions). In comparison to chemical grafting techniques such as silanisation, physical modification is a more fitting and practical technique to use in clinical settings due to its rapid application (Chen *et al.*, 2017). One of the simplest means of creating an antimicrobial surface using this technique is by attaching the AMA to the biomaterial itself without the need of a carrying system. For instance, Aykut *et al.* (2010) employed this method in order to attach the antibiotics teicoplanin and clindamycin to the surface of Ti. The titanium rods were sandblasted using mesh silica to increase the surface area and teicoplanin or clindamycin was subsequently attached by spraying the antibiotic onto the titanium surface. A more recent study also utilised this immobilisation technique to attach AMPs to various biomaterials such as titanium, HA and PMMA. Chen *et al.* (2017), created an “Anchor-AMP” based on the surface binding peptide SKHKGGKHKGGKHKHG and AMP KRWWKWWRRRC (Tet213), by using the N-terminus of the AMP to bind to the surface peptide. They immersed the biomaterial in the AMP solution to functionalise the surface with the Anchor-AMP and demonstrated strong affinity and stability of this peptide on various biomaterial surfaces using this simple physical method.

Other physical modification methods such as self-assembled monolayers (SAM) have also been used to develop immobilised AMA coatings and these reviews go into more detail about these techniques (Chouirfa *et al.*, 2019; Xiao *et al.*, 2018; Wronska *et al.*, 2016). However, there are limitations to using physical adsorption in AMA immobilisation. As physical adsorption relies on non-covalent interactions, issues such as poor stability and elution can occur, resulting in loss-of-functionality of the biomaterial surface over time (Chen *et al.*, 2017; Wronska *et al.*, 2016). In addition, the adsorption and activity of the AMA can vary between hydrophobic and hydrophilic surfaces (Wronska *et al.*, 2016).

Despite the success of immobilising a variety of AMAs onto the surface of biomaterials, such as AMPs, silver-ions, antiseptics like Triclosan and antimicrobial enzymes, these modifications can have adverse effects on the host cells. Ideally, the AMA needs to retain biological functionality when covalently grafted to a surface and demonstrate bactericidal activity at the level of the cell wall. In addition, stability to γ -irradiation, which is typically used to sterilise biomedical devices, is a desirable trait. Most importantly, the AMA should display minimal cytotoxicity and demonstrate compatibility with the host cells to ensure sufficient osseointegration of the implant (Chen *et al.*, 2023; Alves *et al.*, 2018). In realising this, inspiration has been taken from research towards the successful development of commercial chromatography media in which teicoplanin is covalently tethered to silica for enantiomeric separations (Armstrong *et al.*, 1995).

1.6 Teicoplanin

1.6.1 Structure of Teicoplanin and Mode of Action

Teicoplanin (Teic) is a lipoglycopeptide antibiotic produced by *Actinoplanes teichomyceticus* and is most commonly used against Gram-positive bacteria including methicillin-resistant *S. aureus* (MRSA). It was first described in the literature in 1978 and introduced clinically in 1988 in Italy under the name Targocid (Parenti *et al.*, 2000). Teic is comprised of 6 major components (A2-1 to A2-5 and A3-1) and 4 minor components (RS-1 to RS-4) with the most prevalent major component A2-2, having two available functional groups, an amine (juxtaposed to a carbonyl group) and a carboxylic acid moiety

(Fig. 1.5). All Teic components are glycopeptide analogs which have the same core aglycone basket composed of a linear heptapeptide scaffold with aromatic amino acids that have undergone extensive oxidative cross-linking, an α -D-mannose and an acetyl- β -D-glucosamine (European Medicines Agency, 2013; Jovetic *et al.*, 2010; Kahne *et al.*, 2005). In addition, the aromatic rings contain a chlorine substituent which confers a lipophilic nature to the glycopeptide which might contribute to its affinity for the bacterial cell membrane (Jovetic *et al.*, 2010). The A3-1 component of Teic is the core glycopeptide that is common to all Teic-like components; the five components of the A2 group also contain an additional N-acyl- β -D-glucosamine, with one of the glucosamine residues tethered to a fatty N-acyl chain extension (European Medicines Agency, 2013; Vimberg, 2021).

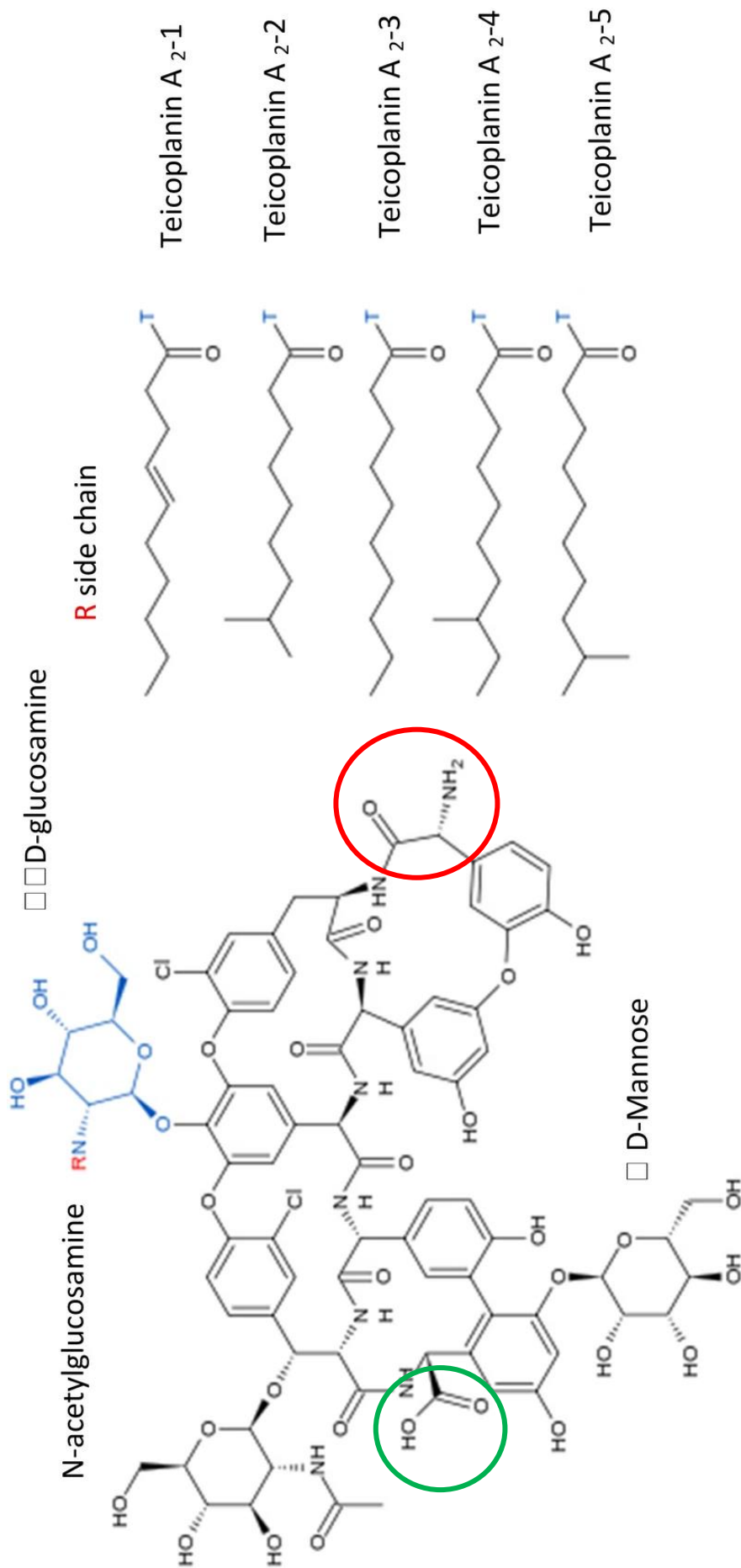


Figure 1.5 Chemical Structure of Teic. The amide juxtaposed to a carbonyl group is circled in red and the carboxylic acid group is circled in green. Reproduced from Britton et al. (2022) (CC BY 4.0)

The mode of action of Teic is similar to that of Vanc and mediates its antibacterial activity by binding to the D-alanyl-D-alanine component and sequestration of the lipid II substrate, which results in the inhibition of bacterial peptidoglycan synthesis (Zeng *et al.*, 2016). Importantly the antibiotic is acting at the level of the cell wall to kill the bacteria. This is unlike other antibiotics that need to penetrate bacteria to bring about their demise. Unlike Vanc, Teic does not dimerize in solution and the dimerization of Vanc has been correlated with the antibacterial potency of the antibiotic (Beauregard *et al.*, 1995; Jovetic *et al.*, 2010; Zeng *et al.*, 2016). However, Teic displays enhanced antibacterial activity in comparison to Vanc, despite the lack of dimerization. This could be explained by the lipophilic tail attached to one of the carbohydrate units which localises (anchors) the antibiotic in proximity to the lipid II substrate (Zeng *et al.*, 2016; Jovetic *et al.*, 2010; Economou *et al.*, 2013). Moreover, it has many advantages over Vanc such as a longer serum half-life, lower ototoxicity, nephrotoxicity and hypersensitivity and better stability *in vivo* (Binda *et al.*, 2014). Nevertheless, Teic is hypothesised to recognise its target in the same manner as Vanc via five hydrogen bonds (Economou *et al.*, 2013).

1.6.2 Use of Teic in Chromatography Applications

Recently, Teic been utilised as a tool in developing novel chiral stationary phases (CSP) for amino acid enantiomeric separation because of its excellent structural properties, multiple stereogenic centres and various functional groups (Armstrong *et al.*, 1995; Wang *et al.*, 2017; Taujenis *et al.*, 2014). Armstrong *et al.* (1995) were the first to take advantage of the available functional groups by tethering Teic to silica particles using the primary amino group and found that immobilised Teic had very good stability and enantioselectivity as a CSP for amino acids, peptides and α -hydroxycarboxylic acids. This product has become commercialised and is known as TeicoShell from AZYP LLC (Arlington, Texas). Other research has utilised Teic by immobilising it onto silica particles to optimise chiral separations in super/subcritical fluid chromatography (SFC) (Barhate *et al.*, 2015). It was shown that Teic performs

efficiently in all types of reverse phase, normal phase, polar organic mode and SFC applications without any performance degradation while interchangeably using one mode or another (Barhate *et al.*, 2015). It is therefore possible that the same functional group could be utilised in developing novel antibacterial bone biomaterial technologies.

The discovery that Teic could retain function whilst immobilised to a surface is crucial in realising the development of antibacterial bone biomaterials for reducing the incidence of PJI. There are issues regarding glycopeptide resistance however, Teic displays an increased potency towards some clinical isolates belonging to *Staphylococcus*, *Streptococcus* and *Enterococcus* genera when compared to Vanc (Van Bambeke, 2006). Moreover, Teic is active against resistant enterococci with the VanB phenotype (Armenia *et al.*, 2018; Binda *et al.*, 2014; Van Bambeke, 2006). However, Teic does have reduced potency against VanA phenotypes. Interestingly, there have been some recent developments regarding the biochemistry of Teic. Pathak & Miller (2013) found that by using peptide-based additives they were able to develop brominated analogues of Teic which exhibited enhanced antibacterial properties and were particularly effective against Vanc- and Teic-resistant strains. There is also evidence to suggest that Teic can still retain its biological activity after exposure to 25 kGy of γ -irradiation (Aykut *et al.*, 2010), which as mentioned above, is the preferred sterilisation route for medical implant devices. Overall, these features place Teic as a choice antimicrobial for immobilisation onto a biomaterial surface.

The aim of this thesis is to explore the potential of immobilising Teic to the surface of Ti, a widely used material for TJA, to minimize the risk of PJI. The fabrication of this novel surface finish will commence with a simple two-step process; coating the surface with PDA, followed by PDA-Ti exposure to Teic.

1.7 Objectives

1. To develop and optimise a Teic-PDA coating for Ti discs and to validate the stability of the antimicrobial coating.

2. Validation of a stable Teic-PDA-Ti coating using physicochemical and microbiological assessments.
3. Compatibility of Teic-PDA-Ti to human osteoblasts (hOBs) and human mesenchymal stem cells (hMSCs).
4. Assessment of coating survival to sterilisation and storage

Chapter 2 Polydopamine-modified Titanium for the Immobilisation of Teic

2.1 Introduction

The various routes taken to covalently attach molecules to solid materials usually requires the use of dangerous substances such as cyanogen bromide, aldehydes and silanes, often involving time-consuming functionalisation steps (Wang *et al.*, 2017; Kavran & Leahy, 2014). Other functionalisation processes may require specialist equipment which would place further constraints on product development. Therefore, it would be beneficial to find a more facile, cost-effective route in developing antibacterial technologies. One potential solution is the application of a polydopamine (PDA) thin film, an adaptable, cheap and simple capturing platform for biomaterial functionalisations. The spontaneous deposition of PDA onto a variety of surfaces creates a thin, confluent film which is amenable to secondary reactions via covalent and non-covalent interactions (Zhou *et al.*, 2014). In addition, it was the first single-step, material-independent surface modification method when it was first reported by Lee *et al.* (2007).

2.2 Origin and Basic Characteristics of PDA

The discovery of PDA was informed by the adhesive biomolecules produced by the edible blue mussel (*Mytilus edulis*) for attachment to wet surfaces. Mussels are promiscuous fouling organisms that have demonstrated the capability of attaching to virtually all types of inorganic and organic surfaces (Waite, 1987). The mussel's adhesion mechanism can be found on the byssus, the "foot" of the mussel. The byssus is comprised of a bundle of filaments, with the ends consisting of a flat, sticky plaque that allows the molluscs to attach to the surface (Andrea, 2019). It is at the plaque-substrate interface where two major adhesive proteins, known as the *Mytilus* foot proteins – 3 and -5 (Mfp-3 and -5) display two key characteristics that inspired the use of PDA: a high catechol content due to the

presence of 3, 4-dihydroxy-L-phenylalanine (DOPA) and a high amount of primary and secondary amines as a result of lysine and histidine residues (Ryu *et al.*, 2018; Lee *et al.*, 2007).

DOPA can form strong covalent and noncovalent interactions with a variety of substrates and along with other catechol compounds, can perform sufficiently as a binding agent for coating inorganic surfaces. However, the coating of organic substrates with DOPA alone proved difficult. The coexistence of catechol (DOPA) and the epsilon-amino group of lysine residues in Mfp3 and 5 was postulated to be responsible for mussel adhesion. Dopamine exhibits both catechol and amino functionalities (Lee *et al.*, 2007).

PDA coatings are formed by a simple method which involves immersing the chosen substrate in an aqueous solution of dopamine hydrochloride, buffered to a pH that is common in marine environments (~pH 8.5) and left to incubate for a set amount of time. This results in a spontaneous deposition of a thin, adherent polymer film (Fig. 2.1), which alters the physiochemical properties of the substrate. This primary coating can be used without further modification or can be utilised as a base through which secondary reactions can occur (Ryu *et al.*, 2018). The chemical composition of PDA affords reactions with a diverse range of agents including noble metals, oligonucleotides, peptides and proteins. This has resulted in PDA coatings being utilised in a broad range of applications such as, photonic materials (Razmjou *et al.*, 2017), chromatography (Wang *et al.*, 2017), biosensors (Li *et al.*, 2022), antifouling platforms (Kim *et al.*, 2018) and antimicrobial immobilisation (Mohd Daud *et al.*, 2018; Ryu *et al.*, 2018). Since dopamine hydrochloride is readily available and inexpensive, the fabrication of PDA-functionalised materials is an expanding area in contemporary biomaterial design.

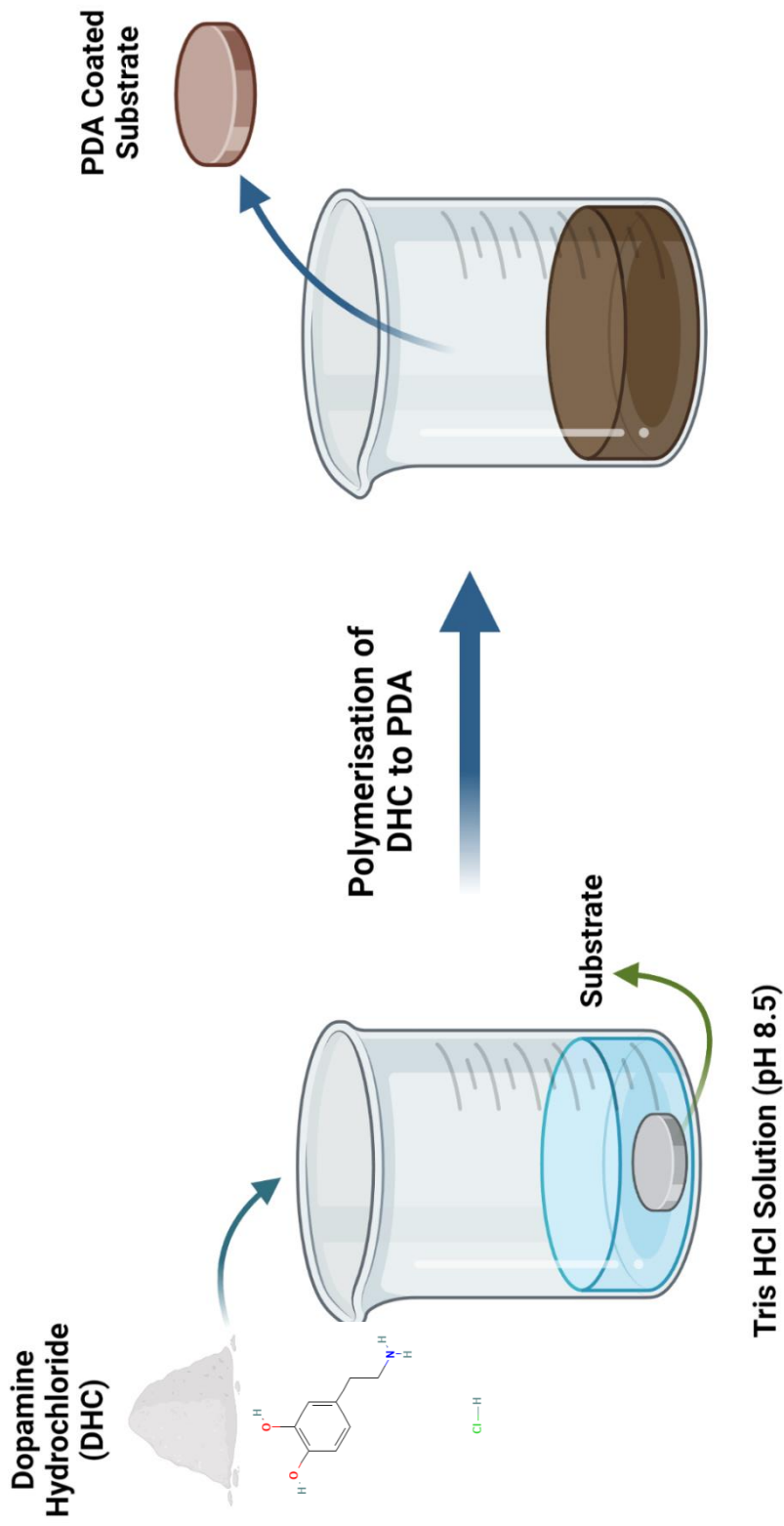


Figure 2.1 Polydopamine Film Formation. The chosen substrate is immersed in a solution of DHC in Tris-HCl (pH 8.5; left) and is left to polymerise via self-oxidation over a period of time. The substrate is subsequently coated in a PDA film (right).

Although PDA coatings have been utilised for a long period of time and great effort has been put into understanding PDA formation and structure, there is still a lack of consensus regarding the biochemical process of PDA formation. There is little doubt that PDA formation is initiated by the oxidation of dopamine by dissolved oxygen at an alkaline pH, as elimination of oxygen from the DHC solution either slows or eradicates PDA deposition. This process results in the oxidation product, dopamine-quinone. Subsequently, dopamine-quinone undergoes a nucleophilic intramolecular cyclisation reaction which eventually leads to the formation of 5, 6-dihydroxyindole (DHI). In most theories regarding the formation of PDA, the two compounds, dopamine-quinone and DHI are the key building blocks for PDA, albeit through various proposed pathways. For instance, it has been suggested that PDA is completely composed of noncovalent assemblies of dopamine, dopamine-quinone and DHI, whereas other studies have postulated that these molecules polymerise to form a heteropolymer, composed of catecholamine, quinone and indole repeat units (Ryu *et al.*, 2018). It is possible that both noncovalent and covalent pathways contribute towards PDA formation and that these pathways should not be viewed as mutually exclusive. However, there is no general agreement on the deposition kinetics of PDA. Nevertheless, it is apparent that the PDA deposition process is influenced by a variety of factors, such as the substrate properties, surface wettability, dopamine concentration, immersion time, solution pH, buffer type and temperature, among other factors (Klosterman *et al.*, 2015; Ball *et al.*, 2012; Lee *et al.*, 2007; Zhou *et al.*, 2014; Wang *et al.*, 2017).

The resulting PDA film can then interact covalently with various compounds such as amine-containing molecules, which interact with the PDA surface via Schiff-base reactions or Michael addition-type reactions for amine- or thiol-containing molecules (Lee *et al.*, 2007; Lee *et al.*, 2006; Lee *et al.*, 2009). Most biomacromolecules, including proteins, peptides, DNA and antimicrobials have been found to anchor onto various surfaces via the PDA coatings (Jia *et al.*, 2019). Moreover, PDA coatings have displayed great biocompatibility and have been reported to aid in modulating cellular responses, including cell migration, proliferation and differentiation. Overall, these features have made PDA

coatings highly desirable towards the development of novel orthopaedic devices which could include antibacterial implants.

The initial phase of research conducted for this chapter examined the potential of PDA-Ti to capture Teic in generating an antibacterial coating. The only study reporting on the interaction between PDA and Teic is that of Wang and colleagues (2017) who described the development of a chiral stationary phase in which Teic was tethered to PDA-iron oxide microparticles. The mechanism by which the antibiotic bound to PDA was not presented but it is possible that the NH₂ moiety of Teic is involved. To ascertain if immobilised Teic could retain antimicrobial activity, initial investigations utilised Cyanogen bromide (CNBr)-activated Sepharose to capture Teic. Research also focused on optimising the PDA deposition and monitoring the polymer using the Bicinchoninic Acid (BCA) as detailed previously (Andrea & Mansell, 2018). An examination of buffer type, incubation time and temperature, and how these parameters affect Teic attachment to PDA were also explored. The compatibility of Teic on the maturation of bone-forming osteoblasts was also conducted together with an assessment of the antibacterial efficacy of Teic-functionalised Ti.

2.3 Materials and Methods

2.3.1 Bacterial Strains and Culture Preparation

The organism used was a *Staphylococcus aureus* strain (NCTC 12981) obtained from Public Health England, Salisbury, UK. Stock cultures were maintained on beads at -80 °C. Working cultures were maintained on Brain-Heart Infusion agar plates (Oxoid; BHIA) and sub-cultured weekly for a maximum of four weeks to maintain viability and colony characteristics. For broth inoculum preparation, 2-3 colonies of a similar size were taken from a BHIA plate into 10 ml Brain-Heart Infusion broth (Oxoid; BHIB) and incubated for 16-18 h at 37 °C with gentle shaking (120 RPM). Obtaining more than one colony for the broth inoculum preparation was done in order to avoid an atypical variant. BHIB was used as the growth medium as it is a good, rich, general-purpose medium that permits good growth of a variety of bacteria (Britton *et al.*, 2022). Standards were made by adjusting overnight cultures in either phosphate buffered saline (PBS) or BHIB to an OD_{625nm} of 0.08 – 0.12 (0.5 McFarland standard; approx. 1.5 x 10⁷ cfu/ml) and further diluted to a final density of approx. 1.5 x 10⁵ cfu/ml in either BHIB or 1% peptone/PBS. This was used in all microbiological assays unless specified.

2.3.2 Maintenance and Treatment of Human (MG63) Osteoblasts

Osteosarcoma-derived MG63 cells display features that are preferred over primary human osteoblasts as the cells proliferate faster and display features in common with human osteoblast precursors or poorly differentiated osteoblasts. These cells produce type I collagen with no or low basal osteocalcin (OC) and alkaline phosphatase (ALP). However, when treated with 1,25 dihydroxyvitamin D (1,25D), OC expression increases (Czekanska *et al.*, 2012; Clover *et al.*, 1994). Moreover, when the same cells are treated with 1,25D and specific growth factors such as lysophosphatidic acid (LPA) or LPA analogues, the levels of ALP increase greatly, a notable feature that is observed in mature osteoblasts (Lancaster *et al.*, 2014; Gidley *et al.*, 2006; Mansell *et al.*, 2016). This places the MG63 as a suitable cell line to assess the pro-maturation response of biomaterial coatings.

MG63 cells (CRL -1427) were cultured in conventional tissue culture flasks (250 ml; Corning, Wiesbaden, Germany) in a humidified atmosphere at 37 °C and 5% CO₂. Cells were grown to confluence in Dulbecco's modified Eagle medium (DMEM)/F12 nutrient mix (Gibco, Paisley, Scotland) supplemented with sodium pyruvate (1 mM final concentration), L-glutamine (4 mM), streptomycin (100 ng/ml), penicillin (0.1 units/ml) and 10% foetal calf serum (Gibco, Paisley, Scotland). The growth media (500 ml final volume) was also supplemented with 1% v/v of a 100 x stock of non-essential amino acids. Once confluent, MG63's were ready for the experiments detailed in this chapter.

2.3.3 Reagents and Ti Disk Preparation

Orthopaedic-grade Ti discs (10 mm diameter; 1.5 mm thickness) were kindly provided by OsteoCare (Slough, UK). Unless stated otherwise all reagents were of analytical grade from either Fisher Scientific (Loughborough, UK) or Sigma-Aldrich (Poole, UK). Ti discs were washed with sterile distilled water 2-3 times in a conical flask, followed by concentrated nitric acid for 2-3 minutes with gentle swirling. After the acid wash, discs were washed thoroughly with sterile distilled water and left to dry in a laminar flow hood. Once dried, discs were baked for 3 days at 180 °C to promote titanium dioxide formation. Discs were stored under ambient conditions until use. Prior to use, discs were sterilised with 70% ethanol and allowed to dry in a laminar flow hood.

2.3.4 Influence of Teic on Human Osteoblast Maturation

Mature osteoblasts express alkaline phosphatase (ALP), the activity which is assessed by conversion of the colourless substrate para-nitrophenyl phosphate (p-NPP) to yellow para-nitrophenol (p-NP) under alkaline conditions. This method was adapted from Mansell *et al.* (2016). Multiwell (24-well) plates, initially seeded with MG63's at a density of 2×10^4 cell/ml/well, were left to grow under conventional culturing conditions (37 °C and 5% CO₂) for 3 days. Cells were subsequently starved using a serum-free, phenol red-free DMEM/F12 (SFCM, 1ml/well) for 24 hours. Once starved, cells were treated with either 1,25D (100 nM final concentration), FHBP (250 nM), Teic (50 µg/ml) or in combination and left to incubate for 3 days under conventional culturing conditions. Following

incubation, the medium was removed, and the monolayers were lysed with 100 μ l/well 7 mM sodium carbonate, 3 mM sodium bicarbonate (pH 10.3) supplemented with 0.1% (v/v) Triton X- 100 to lyse the cells. After 2 min, each well was treated with 200 μ l of 15 mM p-NPP (di-Tris salt, Sigma, UK) in 70 mM sodium carbonate, 30 mM sodium bicarbonate (pH 10.3), supplemented with 1 mM MgCl₂. Lysates were then left under conventional cell culturing conditions for 50 min. After the incubation period, 100 μ l aliquots were transferred to a 96-well microtitre plate and the absorbance was measured at 405 nm using a microplate reader (BMG Labtech), alongside a standard series of p-NP concentrations (0-500 μ M) to extrapolate product formation.

2.3.5 Attachment and Growth of *S. aureus* on Teic-Sepharose

2.3.5.1 Standard Curve of Teic using Bicinchoninic Acid (BCA)

A series of Teic concentrations (0.03125- 5 mg/ml) were made in coupling buffer (0.1 M NaHCO₃ + 0.5 M NaCl) and 25 μ l of each concentration transferred to a new bijoux for reaction with BCA. A 500 μ l aliquot of the BCA reagent (prepared according to the manufacturer's instructions) was added to each bijoux and left to incubate for 30 min at 37 °C. A 100 μ l aliquot in triplicate, was transferred to a 96-well plate and absorbance read at OD_{540nm} using a microplate reader (TECAN Infinite F200 Pro). Coupling buffer only was used as a blank.

2.3.5.2 Coupling of Teic to CNBr-Activated Sepharose

CNBr-activated Sepharose beads (200 mg) were prepared according to the manufacturer's instructions. Briefly, beads were swelled in 1 mM HCl for 10 min on ice, centrifuged at 3,000 x G for 5 minutes and the supernatant carefully aspirated. This was repeated three times. The swelled Sepharose beads were washed in molecular grade water (MGW), followed by coupling buffer and 1ml of 5 mg/ml Teic (in coupling buffer) was added to the beads and incubated overnight on a rotator at 2-8°C. The unreacted Teic was removed and the remaining active groups on the beads were blocked using 0.2 M glycine buffer for 2 h at room temperature. The beads were then washed alternatively five times with 5 ml of basic buffer (coupling buffer) and 5 ml of acidic buffer (acetate buffer (0.1 M

CH₃CO₂H, 0.1 M C₂H₃NaO₂ + 0.5 M NaCl, pH 4)) to remove the glycine. The beads were stored in a 1 M solution of NaCl at 2-8 °C until use. Glycine-Sepharose (Gly-Sepharose) beads were processed in the same manner, without Teic and used as a control. When required, Teic- and Gly-Sepharose beads were washed in PBS three times by centrifugation and resuspended in 1 ml PBS. To assess the concentration of attached Teic, a 25 µl aliquot of the Teic- and Gly-Sepharose beads were transferred to glass bijoux treated with BCA reagent as mentioned previously and compared against a Teic standard curve (2.3.5.1).

2.3.5.3 *S. aureus* viability on Teic-Sepharose

An overnight culture of *S. aureus* was standardised in BHIB and dispensed into a 24-well plate, then exposed to various concentrations of Teic- and Gly-Sepharose beads (~25 and 50 µg/ml). BHIB with bacteria was used as a positive control whilst the negative control wells contained BHIB only. This was incubated for 24 h at 37 °C. Aliquots of the positive control wells were diluted in PBS and dispensed on BHIA prior to incubation to determine cell density. After incubation aliquots from the treated wells were carefully taken, diluted in PBS and dispensed onto BHIA plates and incubated for 24 h at 37 °C.

2.3.6 PDA Optimisation

The experiments described below have been adapted from Andrea & Mansell (2018) and Ayre *et al.* (2016).

2.3.6.1 Standard Curve of DHC

A series of DHC concentrations (0.195 – 25 µg/ml) were made in MGW and 250 µl of each concentration transferred to a new bijoux. A 125 µl aliquot of the BCA reagent was added to each bijoux and incubated for 90 min at room temp. After incubation, 100 µl aliquots were added to a 96-well plate and absorbance read at OD_{540nm} using a microplate reader. Water only served as the control.

2.3.6.2 Effect of Incubation Time on PDA Formation at Tissue Culture Plastic (TCP)

TCP wells (24-well plate) were immersed in a 1 ml solution of 2 mg/ml DHC in 10 mM Tris-HCl (pH 8.5) and incubated for 24, 48 and 72 h. Control wells were immersed in 10 mM Tris-HCl (pH 8.5). Once incubated, wells were washed five times with molecular grade water (MGW) to dislodge loosely bound PDA. The final wash (250 μ l) was treated with 125 μ l BCA reagent to ensure the wash was efficient. A separate plate treated in the same manner was used to assess Teic functionalisation. Once washed, 250 μ l of MGW followed by 125 μ l of freshly prepared BCA reagent were added to treated and control wells. These were incubated under ambient conditions for 90 min. Samples (100 μ l) were transferred to a 96-well plate and the absorbances measured at OD_{540nm} using a microplate reader.

To determine if the incubation time affects the functionalisation of Teic on PDA films, PDA-treated TCP wells were immersed in a 5 mg/ml Teic and 10 mM Tris HCl solution (pH 8.5) and incubated for 24 h under ambient conditions. After incubation, wells were washed and seeded with a 10⁷ CFU/ml suspension of *S. aureus* in PBS and incubated for 4 h at 37 °C. The wells were washed with 0.85% saline after incubation to remove loosely adherent bacteria and a 20 μ l aliquot of BacLight™ LIVE/DEAD solution was added to the wells and incubated in the dark for 15 min. This was to allow sufficient uptake of the stains. Two images from random parts of the well were taken on a Nikon Eclipse TE300 fluorescence microscope using 200 X magnification at emission/excitation wavelengths of 485/530-630 nm respectively.

2.3.6.3 Effect of Buffer type on PDA Formation at Ti

Ti discs were immersed in a 1 ml solution of 2 mg/ml DHC solubilised in either 10 mM Tris HCl (pH 8.5), 10 mM NaHCO₃ (pH 8.3) or 10 mM HEPES (pH 7.4) and incubated under ambient conditions for 72 h. Discs in buffer only were used as a control. After incubation, discs were transferred to a new multwell plate and washed twice with MGW to remove unbound PDA and allowed to dry. Once dried, discs were assessed in the same manner as per 2.3.6.2. To determine if the buffer type affects the tethering of Teic on PDA films, PDA-treated Ti discs were steeped in a 5 mg/ml Teic and 10 mM Tris HCl solution

(pH 8.5) and incubated for 24 h under ambient conditions. After incubation, discs were transferred to a new multiwell plate and washed twice with MGW to remove loosely bound Teic and allowed to dry. Once dried, discs were transferred to a new well plate and inoculated with a 10^5 CFU/ml suspension of *S. aureus* in 0.1% Peptone/PBS and incubated at 37 °C for 4 h with gentle shaking (100 RPM). At each time point, discs were transferred to a new well plate and washed twice with 0.85 % saline to remove non-adherent bacteria. A 20 μ L aliquot of BacLight LIVE/DEAD™ were added to coverslips in a 6-well viewing chamber and the discs flipped (bacterial side down) onto the stain. These were incubated and imaged in the same manner as per 2.3.6.2.

2.3.6.4 Effect of Temperature on PDA Formation

Ti discs were immersed in a 1 ml solution of 2 mg/ml DHC in 10mM Tris (pH 8.5) and incubated at various temperatures (ambient, 35 and 50 °C) for 24 h. Discs in buffer only were used as a control. After incubation, discs were prepared and assessed with BCA as described in 2.3.6.2.

2.3.7 Attachment of *S. aureus* on PDA-modified Ti

Ti discs were immersed in a 1 ml solution of 2 mg/ml DHC in 10 mM Tris (pH 8.5) and incubated for 24, 48 and 72 h. Blank Ti discs were immersed in 10 mM Tris-HCl (pH 8.5) buffer and used as a control. After incubation, discs were washed and prepared as described in 2.3.6.3. Once dried, wells were inoculated with a 10^5 CFU/ml suspension of *S. aureus* in 0.1% Peptone/PBS and incubated at 37 °C for 4, 8 and 24 h with gentle shaking (100 RPM). At each time point, discs were transferred to a new well plate and washed twice with 0.85 % saline to remove non-adherent bacteria. A set of discs were transferred to a plastic universal containing 1 ml PBS and vortexed for 5 min to remove adherent bacteria. This was serially diluted and dispensed onto BHIA plates and incubated for 24 h at 37 °C. If no growth was present after 24 h incubation, plates were incubated for a further 24 h to confirm the absence of growth. The other set of discs were used for fluorescence microscopy as described in 2.3.6.3.

2.3.8 Attachment of *S. aureus* on Teic-PDA-modified Ti

Ti discs were immersed in a 1 ml solution of 2 mg/ml DHC in 10 mM Tris (pH 8.5) and incubated 72 h. PDA-Ti and blank Ti discs were immersed in 10 mM Tris-HCl (pH 8.5) buffer and used as a control. After incubation, discs were washed and prepared as described in 2.3.6.3. Once dried, a set of PDA and blank Ti discs were steeped in a 500 µg/ml Teic and 10 mM Tris (pH 8.5) solution and incubated for 24 h under ambient conditions. These were transferred to a new well plate and washed as described in 2.3.6.3. Discs were assessed in the same manner as 2.3.7.

2.3.9 Statistical Analysis

Unless stated otherwise, all experiments above were repeated three times in triplicate. All data were subject to a normality test to ensure data were normally distributed. A one- or two-way analysis of variance (ANOVA) or Kruskal-Wallis test was used, where appropriate, to test for statistical significance using Graphpad Prism (Version 8; San Diego, CA, USA) with $p < 0.05$ regarded as being statistically significant. When $p \leq 0.05$ was found, a Tukey or Sidak's multiple comparisons post-test was used between all groups. All data are expressed as the mean together with the standard deviation.

2.4 Results

2.4.1 Influence of Teic on a Model of Human Osteoblast Maturation

As anticipated the co-treatment of MG63 cells with 1,25D and FHBP led to a significant ($p < 0.0001$) increase in ALP activity compared to the agents used alone (Fig. 2.2). Interestingly the inclusion of Teic modestly enhanced the maturation of MG63's to 1,25D and FHBP.

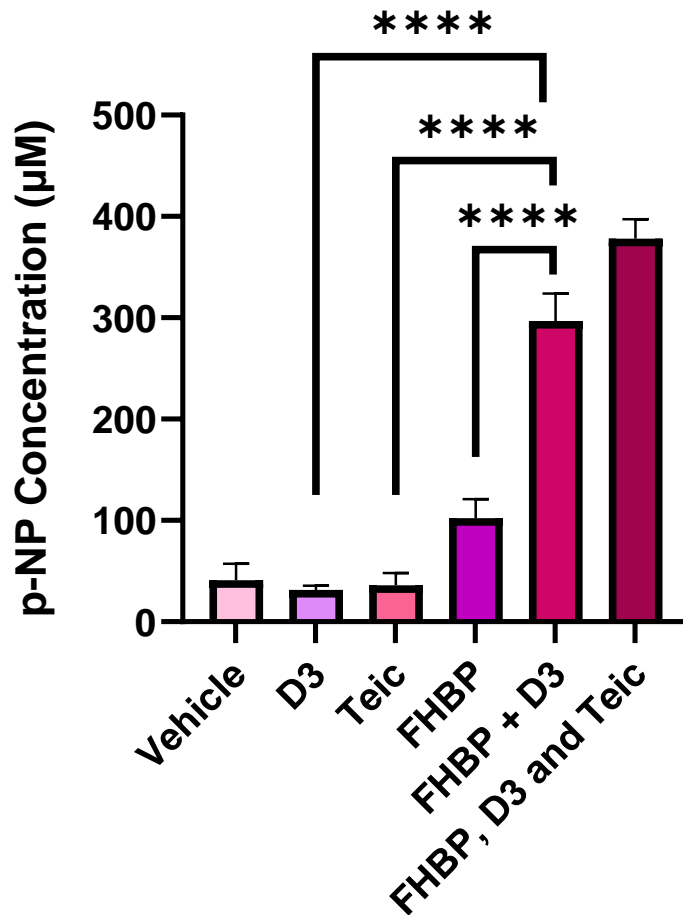


Figure 2.2 Influence of Teic on a Model of Human Osteoblast Maturation. MG63s in the presence of either 1,25D (100 nM), FHBP (250 nM), teicoplanin (50 µg/mL) or in combination were assessed for ALP activity using a p-nitrophenyl phosphate assay. Teic, in combination with 1,25D and FHBP displayed greater ALP formation than 1,25D and FHBP alone. All data (mean ± SD; N = 12) represent pooled quadruplicate runs from 3 independent experiments (**** = p < 0.0001).

2.4.2 *S. aureus* viability on Teic-Sepharose

Antibacterial activity of Teic- modified Sepharose beads was assessed by exposing *S. aureus* to various densities of Teic- and Gly-Sepharose beads (~25 & 50 µg/ml) for 24 hours at 37°C. Qualitatively, Teic Sepharose provided complete growth inhibition at both concentrations tested in comparison to the Gly-Sepharose beads (Fig. 2.3). The result of this assessment concurs with the viable counts. There was significant bactericidal activity from the Teic-Sepharose when compared to the Gly-Sepharose beads ($p < 0.0001$) which resulted in ≥ 3 -log reduction from the initial inoculum density (Fig. 2.4). There was also significance between the two Teic concentrations tested ($p < 0.001$) indicating that an increase in Teic-Sepharose allows for greater bactericidal activity. This demonstrates that not only was Teic immobilisation successful; it also retains significant antibacterial activity when tethered on this surface.

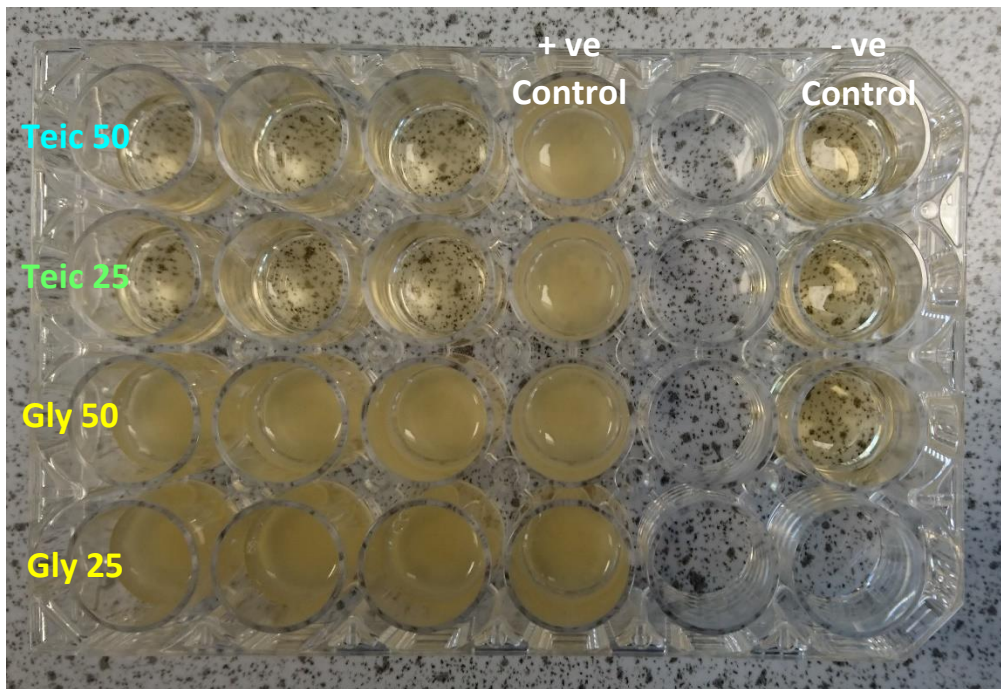


Figure 2.3 Antimicrobial assessment of Teic-Sepharose beads on *S. aureus*. Antibacterial activity of modified Sepharose beads was assessed by exposing *S. aureus* (1.5×10^5 CFU/ml) to various densities of Teic- and Gly-Sepharose beads (~25 & 50 $\mu\text{g/ml}$) for 24 hours at 37°C. Teic-Sepharose shows clear evidence of antimicrobial activity when compared to the Gly-Sepharose (turbid wells), indicating successful conjugation of Teic. The image depicted is a representative of 3 independent experiments.

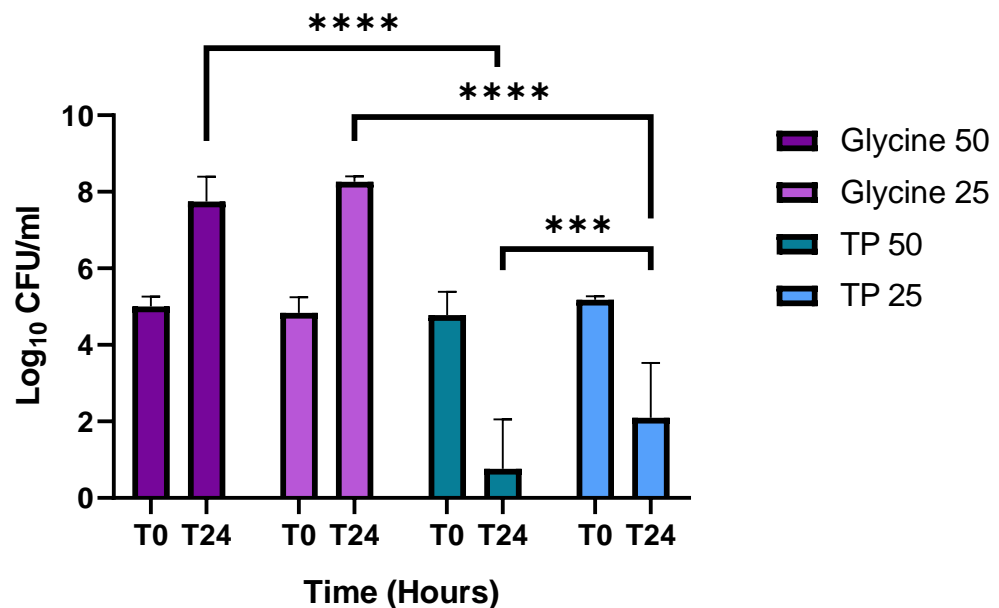


Figure 2.4 Bactericidal activity of Teic-Sepharose beads on *S. aureus*. Antibacterial activity of modified Sepharose beads was assessed by exposing *S. aureus* (1.5×10^5 CFU/ml) to various densities of Teic- and Gly-Sepharose beads (~25 & 50 $\mu\text{g/ml}$) for 24 hours at 37°C. Teic-Sepharose showed significant ($p < 0.0001$) bactericidal activity in comparison to the Gly-Sepharose. All data (mean \pm SD; N = 27) represent pooled triplicate runs from 3 independent experiments. Statistical significance was determined by two-way ANOVA and Tukey comparisons (** = $p < 0.001$; **** = $p < 0.0001$)

2.4.3 PDA Optimisation

To ensure there are optimal functional groups for Teic immobilisation, some factors influencing PDA formation were investigated, which include buffer type, reaction time and temperature. PDA film stability in long-term storage was also assessed.

2.4.3.1 Effect of Incubation Time on PDA Formation using TCP

TCP wells were immersed in a DHC (2mg/ml) and Tris HCl (10 mM; pH 8.5) solution for 24, 48 and 72 h, washed and assessed using BCA. The data from the DHC standard curve (2.3.6.1; data not shown) was used to extrapolate PDA from the TCP surfaces. From the information presented in Fig. 2.5, it is clear that PDA formation is affected by the incubation time. There are significant differences between all the times tested ($p < 0.001$), indicating that longer incubation times leads to greater PDA film deposition.

PDA-TCP wells were exposed to a solution of Teic (5 mg/ml) in 10mM Tris HCl (pH 8.5), washed and seeded with *S. aureus* in order to assess the efficiency of Teic modification on PDA-TCP using fluorescent microscopy. Bacterial survival on the surface of PDA- and control TCP wells appears greater in comparison to the Teic-PDA-TCP wells (Fig. 2.6). Teic functionalisation, however, seems to be dependent on the amount of PDA on the Ti surface as more dead bacteria were observed on Teic functionalised at 72 h compared to other time points. A TCP well was immersed in Teic (5mg/ml) for the same time as the PDA-TCP wells and used as an adsorption control. Interestingly, Teic-TCP retains antimicrobial activity when compared to the Teic-PDA-TCP (Fig. 2.6E). This would suggest that Teic can adsorb onto the surface of TCP without an intermediate cross linker.

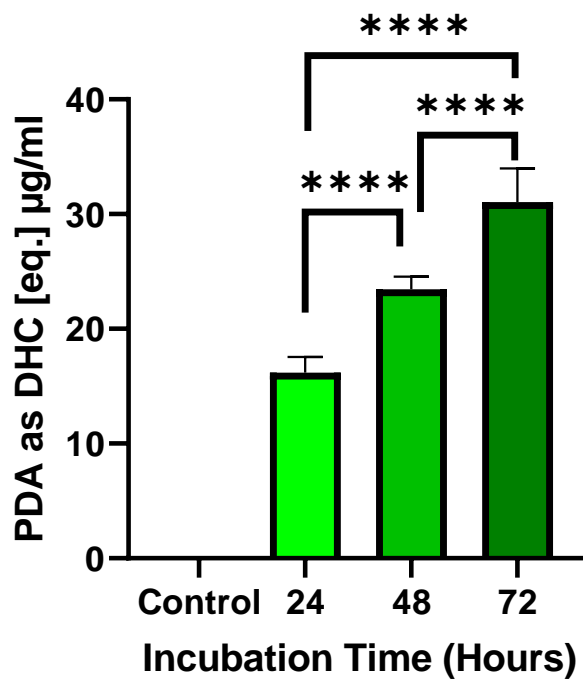


Figure 2.5 Effect of Incubation Time on PDA Formation. TCP wells were immersed in a DHC (2 mg/ml) and Tris HCl (10 mM; pH 8.5) solution for 24, 48 and 72 h, washed and assessed using BCA. It is evident that PDA deposition is a function of time. There are significant differences between the times tested ($p < 0.0001$) indicating that longer incubation times leads to greater PDA deposition. All data (mean \pm SD; N = 18) represent pooled triplicate runs from 3 independent experiments. Statistical significance was determined by one-way ANOVA and Tukey comparisons (** = $p < 0.001$; **** = $p < 0.0001$).

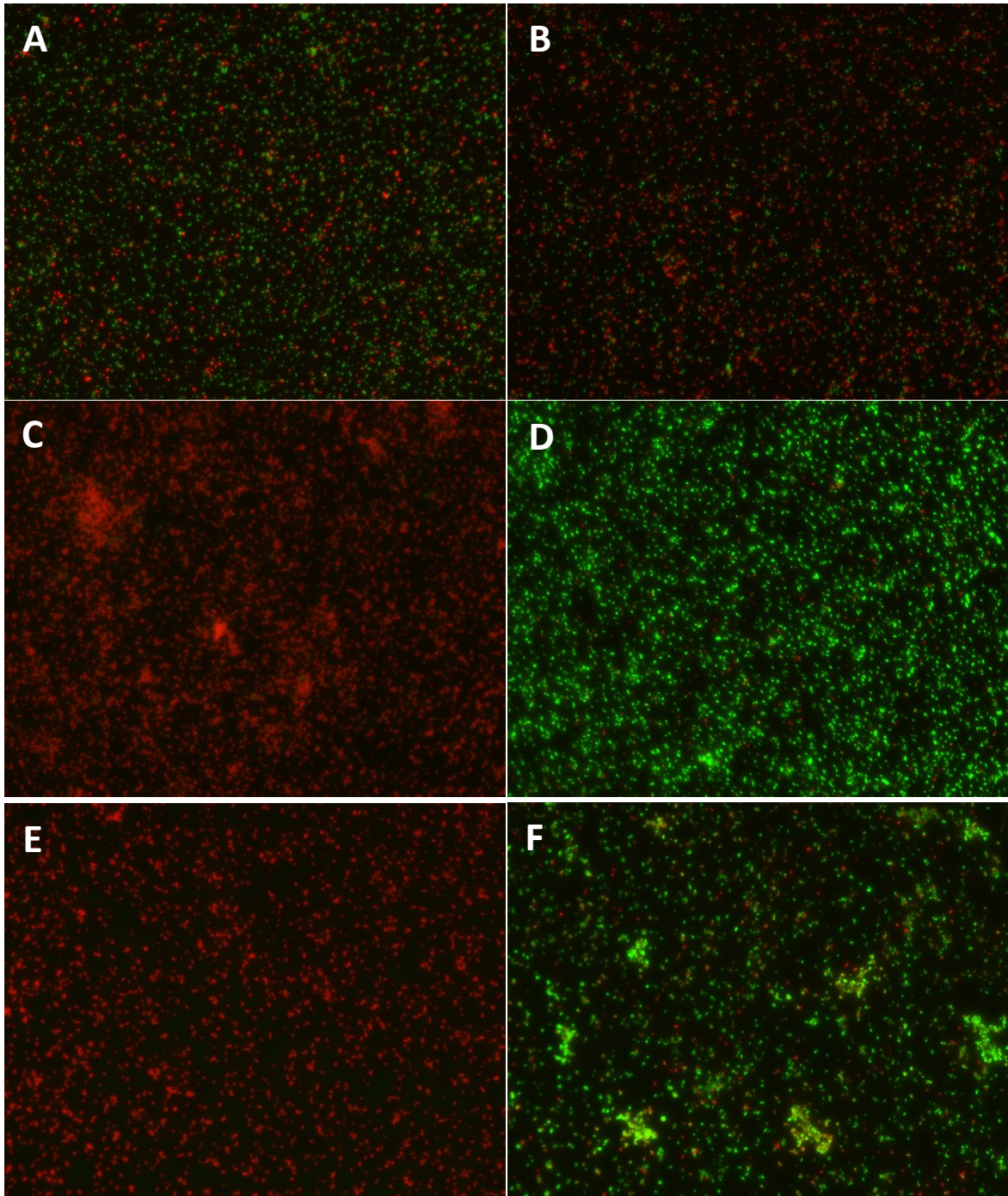


Figure 2.6 LIVE/DEAD assessment of *S. aureus* attachment on PDA-modified TCP. PDA-TCP wells were exposed to a solution of Teic (5 mg/ml) in 10mM Tris HCl (pH 8.5), washed and seeded with *S. aureus* in order to assess the efficiency of Teic modification on PDA-TCP using fluorescence microscopy. After 4 h incubation, two images from random parts of the well were taken on a fluorescence microscope using 200 X magnification at emission/excitation wavelengths of 485/530-630 nm respectively. A. 24h; B. 48h; C. 72h, D. PDA Control, E. Teic Only, F. Tris-HCl Only. This is a representation of 3 independent runs.

2.4.3.2 Effect of Buffer type on PDA Formation

Individual Ti discs were immersed in a 1 ml solution of 2 mg/ml DHC solubilised in either 10 mM Tris HCl (pH 8.5), 10 mM NaHCO₃ (pH 8.3) or 10 mM HEPES (pH 7.4), incubated for 72 h, washed and assessed for PDA deposition using BCA. From the information provided in Fig. 2.7, it is evident that buffer choice affects PDA film formation. There are significant differences between DHC immersed in sodium bicarbonate in comparison to Tris HCl and HEPES ($p < 0.0001$). Despite a small quantitative difference between Tris HCl and HEPES, there is no statistical significance.

PDA-Ti discs were modified with Teic and seeded with *S. aureus* in order to assess the effect of buffer choice on Teic attachment using fluorescence microscopy. It seems that buffer choice has no effect on the functionalisation of Teic on PDA-Ti surfaces (Fig. 2.8) as there were no significant differences in bacterial viability between all the buffer types tested.

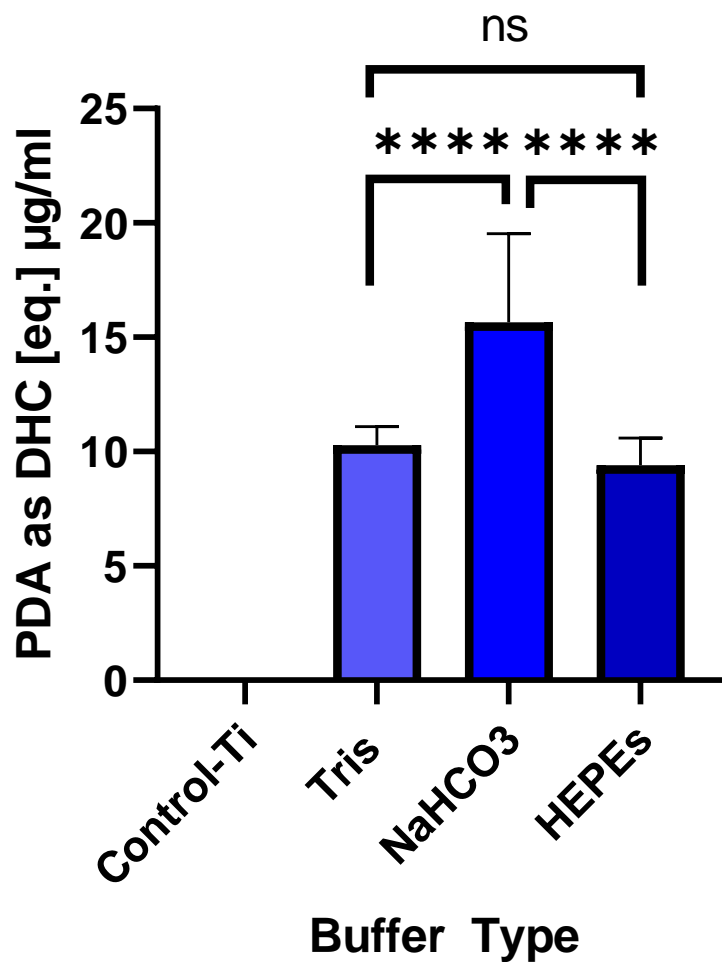


Figure 2.7 Influence of Buffer Type on PDA Formation. Individual Ti discs were immersed in a 1ml solution of 2 mg/ml DHC solubilised in either 10mM Tris HCl (pH 8.5), 10mM NaHCO₃ (pH 8.3) or 10mM HEPES (pH 7.4), incubated for 72 h, washed and assessed for PDA deposition using BCA. There is clear evidence that buffer choice affects PDA film formation. All data (mean ± SD; N=9) represent pooled triplicate runs from 3 independent experiments. Statistical significance was determined by one-way ANOVA and Tukey comparisons (**** = $p < 0.0001$).

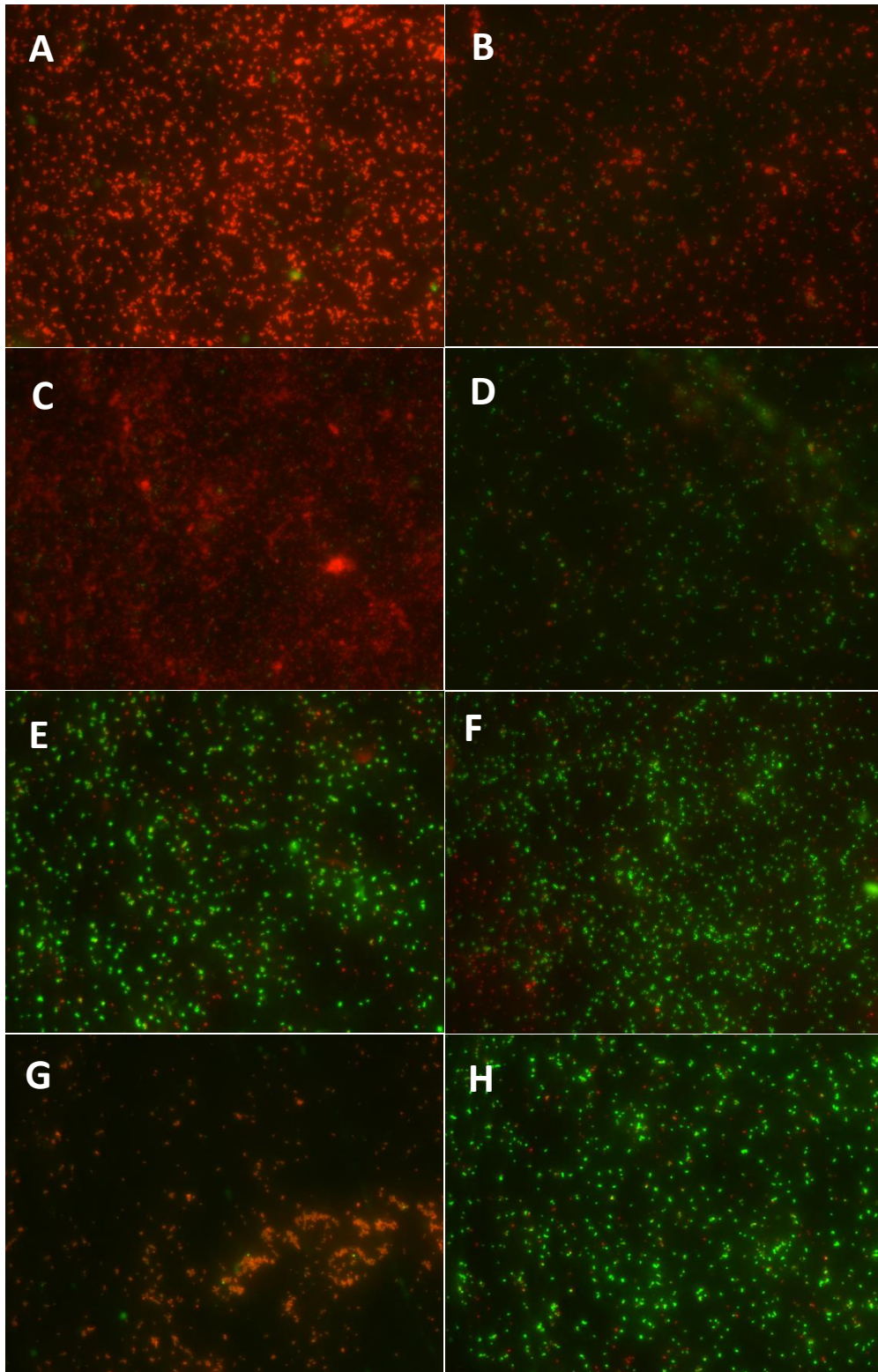


Figure 2.8 LIVE/DEAD assessment of buffer choice on attachment of *S. aureus* to Teic-PDA-Ti. PDA-Ti discs were modified with Teic and seeded with *S. aureus* in order to assess the effect of buffer choice on Teic attachment using fluorescence microscopy. After 4h incubation, two images from random parts of the disk were taken on a fluorescence microscope using 200X magnification at emission/excitation wavelengths of 485/530-630 nm respectively. **A.** Teic-PDA (Tris); **B.** Teic-PDA (NaHCO₃); **C.** Teic-PDA (HEPEs); **D.** Tris-HCl Only, **E.** HEPEs Only, **F.** NaHCO₃ Only, **G.** Teic Only, **H.** PDA Only. This is a representation of 3 independent runs.

2.4.3.3. Effect of Temperature on PDA Formation

Ti discs were immersed in DHC (2 mg/ml in 10 mM Tris, pH 8.5) and incubated at different temperatures (ambient, 35 and 50°C) for 24 h, washed and assessed with BCA reagent. It is clear that PDA formation is a function of temperature as there are significant increases in PDA film thickness when incubated at higher temperatures (Fig. 2.9) ($p < 0.0001$). This suggests that temperature could be a means of reducing the current incubation time.

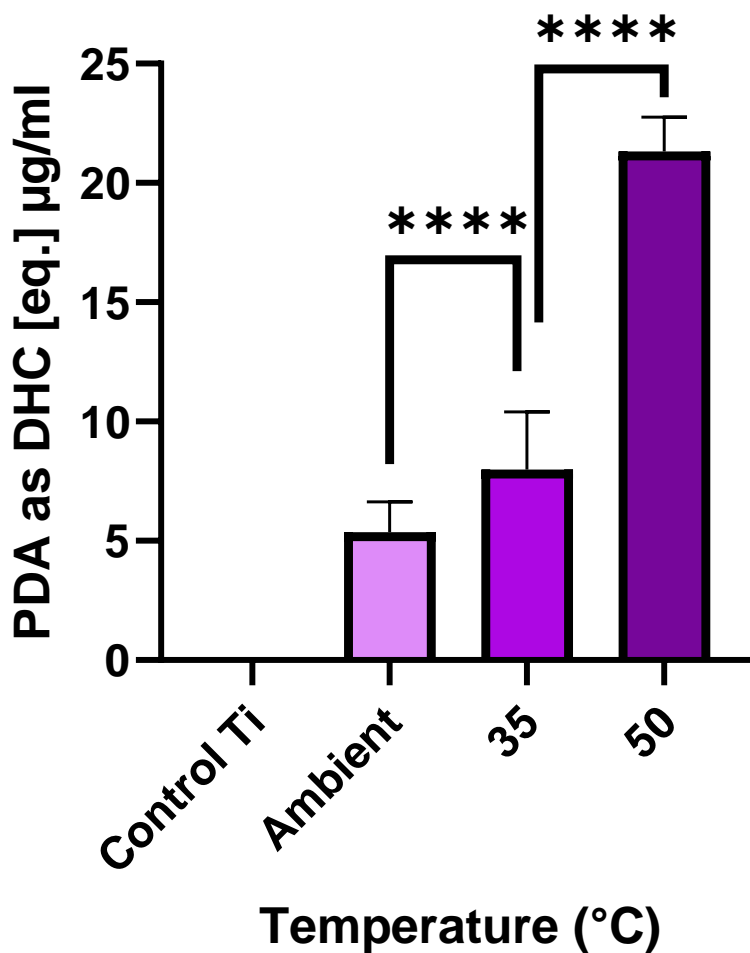


Figure 2.9 Effect of temperature on PDA Formation. Ti discs were immersed in DHC (2 mg/ml in 10 mM Tris, pH 8.5) and incubated at different temperatures (ambient, 35 and 50°C) for 24 h, washed and assessed with BCA reagent. It is clear that PDA formation is a function of temperature as there are significant increases in PDA film thickness when incubated at higher temperatures. All data (mean ± SD; N = 27) represent pooled triplicate runs from 3 independent experiments. Statistical significance was determined by one-way ANOVA and Tukey comparisons (**** = $p < 0.0001$).

2.4.4. Attachment of *S. aureus* to PDA-modified Ti

Ti discs were immersed in a DHC (2 mg/ml) and Tris HCl (10 mM; pH 8.5) solution for 24, 48 and 72 h, washed and inoculated with a 10^5 CFU/ml suspension of *S. aureus*. Bacterial attachment to PDA-modified and control Ti discs was assessed using fluorescence microscopy and viable counts. As indicated in Fig. 2.10, all PDA incubation times had no significant effect on bacterial attachment. Although there was a significant difference in attachment after 8 hours on the 72 h PDA film ($p < 0.05$), bacterial attachment was relatively consistent across all time points observed. The images depicted in Fig. 2.11 concur with the viability counts. This demonstrates that bacterial attachment is not affected by the introduction of a PDA film in comparison to bare-Ti.

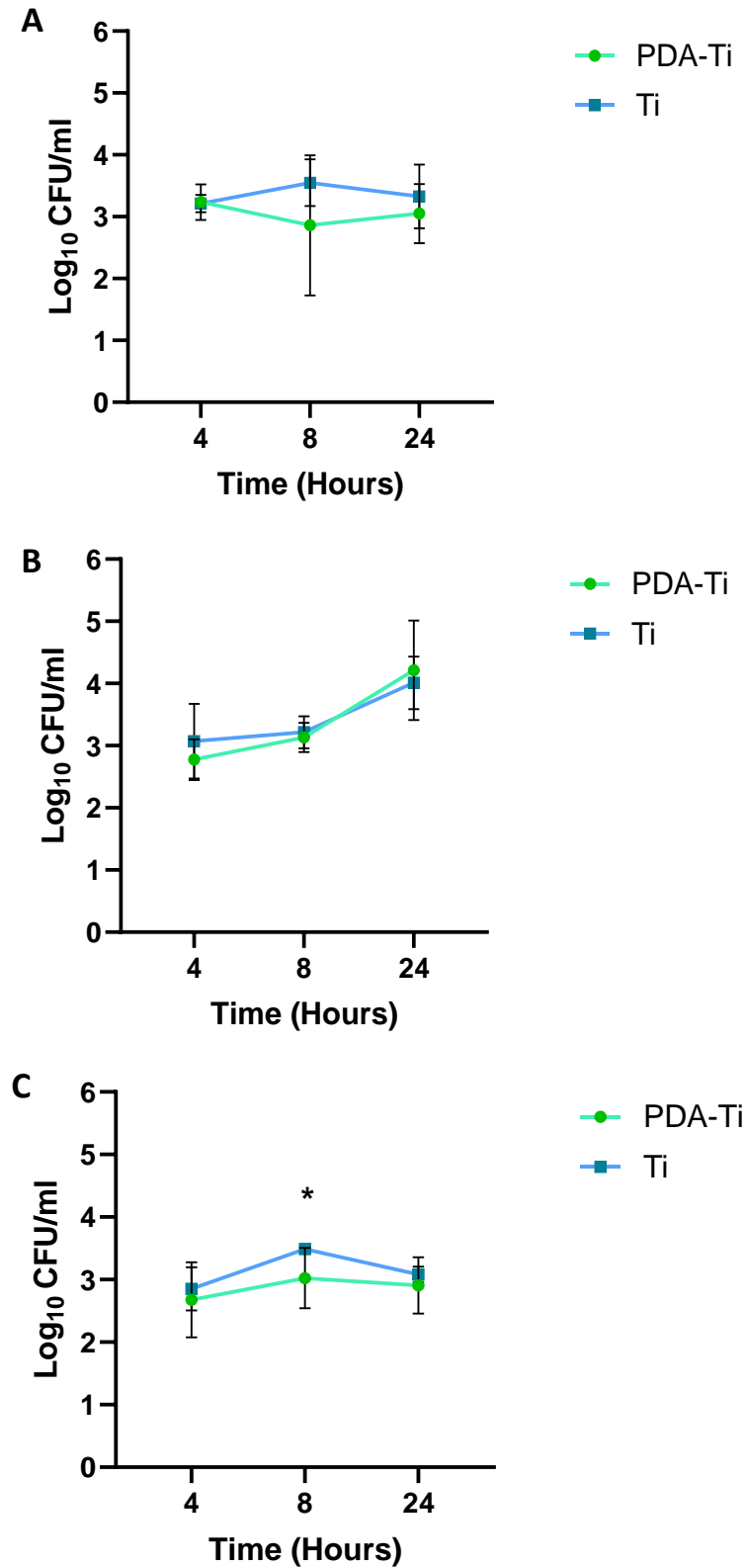


Figure 2.10 Attachment of *S. aureus* on PDA-modified Ti. Ti discs were immersed in a DHC (2 mg/ml) and Tris HCl (10 mM; pH 8.5) solution for 24, 48 and 72 h, washed and inoculated with a 10⁵ cfu/ml suspension of *S. aureus*. Bacterial attachment to PDA-modified and control Ti discs was assessed using viable counts. All data (mean ± SD; N=9) represent pooled triplicate runs from 3 independent experiments. **A.** 24 h, **B.** 48 h and **C.** 72 h. $p < 0.05$ (*).

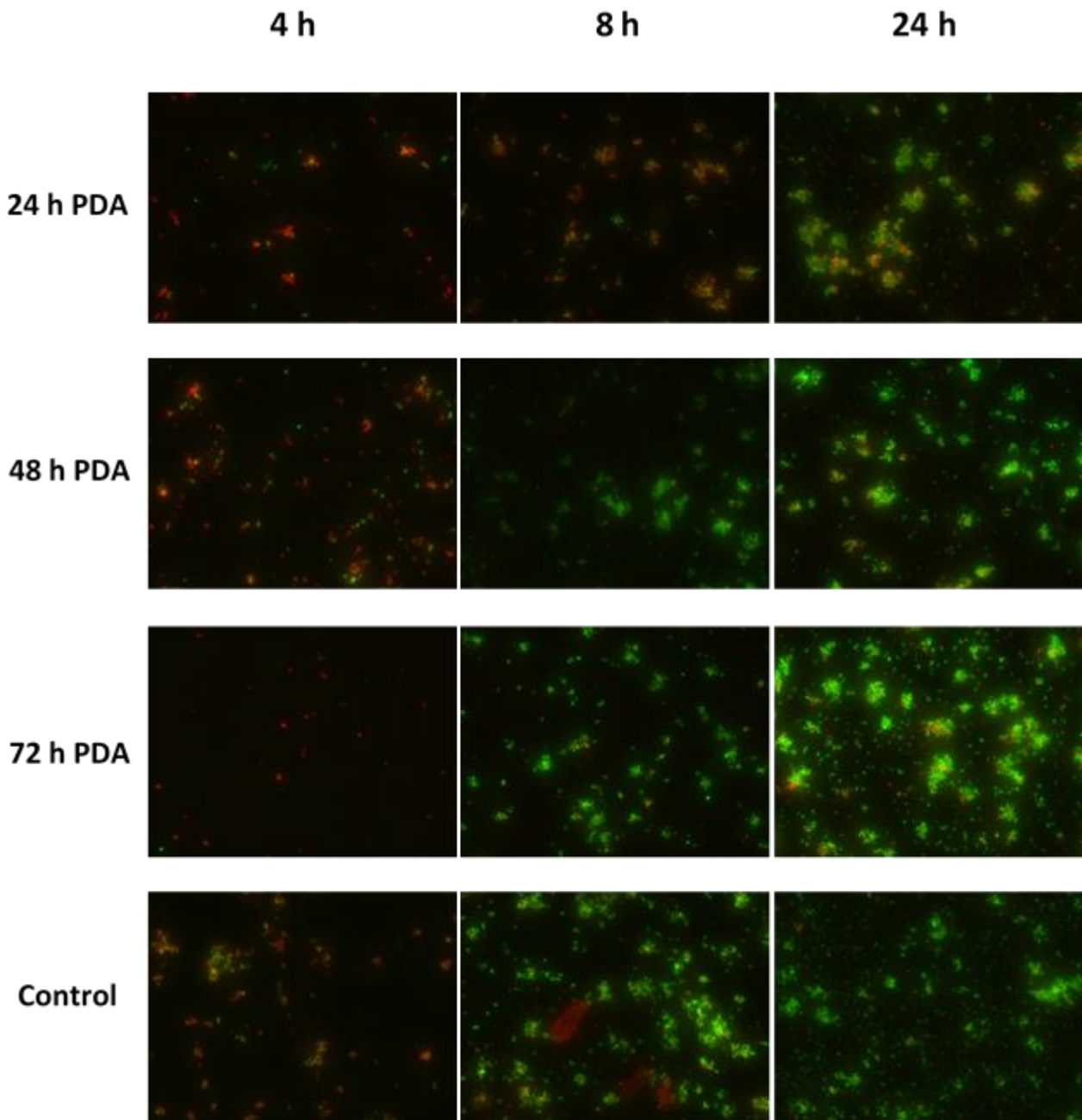


Figure 2.11 LIVE/DEAD assessment of *S. aureus* attachment on PDA-modified Ti. Ti discs were immersed in a DHC (2 mg/ml) and Tris HCl (10 mM; pH 8.5) solution for 24, 48 and 72 h, washed and inoculated with a 10^5 cfu/ml suspension of *S. aureus*. Bacterial attachment to PDA-modified and control Ti discs was assessed using fluorescence microscopy. After 4, 8 and 24 h incubation, two images from random parts of the disk were taken on a fluorescence microscope using 20X magnification at emission/excitation wavelengths of 485/530-630 nm respectively. This is a representation of three independent runs.

2.4.5. Attachment of *S. aureus* to Teic-PDA-modified Ti

Bacterial attachment to Teic-PDA-modified and control Ti discs was assessed using viable counts. At all time points tested, there was a significant reduction in bacterial attachment on the Teic-PDA-Ti when compared to the PDA-Ti and Ti control discs (Fig. 2.12; $p < 0.0001$). Interestingly, Teic-Ti also deterred significant bacterial attachment compared to the control discs and ($p < 0.0001$). The Teic-Ti results are comparable to the Teic-PDA-Ti discs.

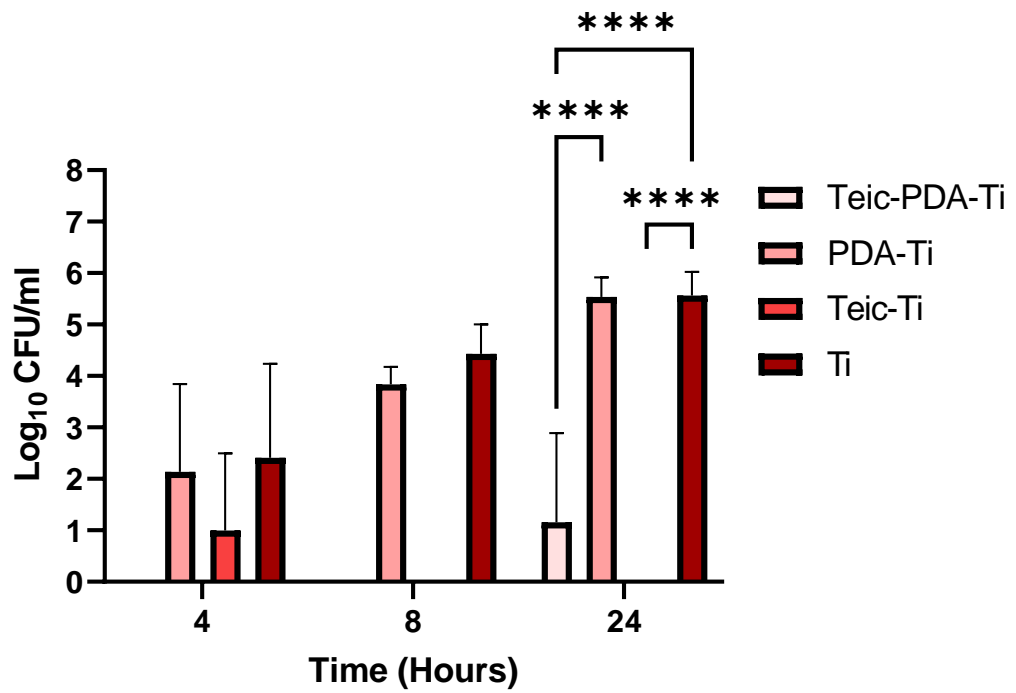


Figure 2.12 Attachment of *S. aureus* on Teic-PDA-modified Ti. PDA-Ti discs were immersed in a Teic (500 µg/ml) and Tris HCl (10 mM; pH 8.5) solution for 24 h, washed and inoculated with a 10⁵ cfu/ml suspension of *S. aureus*. Bacterial attachment to Teic-PDA-modified and control Ti discs was assessed using viable counts. There is a significant reduction in bacterial attachment on Teic-PDA-Ti in comparison to the other discs tested during the first run. In addition, Teic-Ti alone is also deterring significant bacterial attachment. All data (mean ± SD; N = 9) represent pooled triplicate runs from 3 independent experiments. p < 0.0001 (****)

2.5 Discussion

PJI's pose immense challenges to the medical community and are a significant economic burden on society. The ability of microorganisms to colonise implant surfaces and form biofilms is a critical step in the formation of PJI. Once enveloped in a biofilm, bacteria become recalcitrant to the host immune response and antibiotic intervention is of limited use. Herein, this chapter aimed to address this problem by subjecting *S. aureus* to Teic, tethered to the surface of PDA-modified Ti. Teic is a lipoglycopeptide antibiotic that is used to treat severe Gram-positive infections, including MRSA and has a similar antimicrobial spectrum to Vanc. Importantly, Teic acts at the level of the cell wall and is therefore ideal agent for surface presentation. It has many advantages over Vanc such as a longer half-life and lower ototoxicity and nephrotoxicity (Binda *et al.*, 2014). Yet, even with these advantages, a thorough search of the literature yielded only one report that used Teic to functionalise a surface for biomedical applications (Armenia *et al.*, 2018).

There were three main objectives to this initial investigation; assess the compatibility of Teic on a model of human (MG63) osteoblast maturation, ascertain if Teic could retain biological activity whilst immobilised, optimise the PDA coating and monitor the bacterial viability to Teic-PDA-functionalised surfaces. Initial investigations looked into the compatibility of Teic with MG63 osteoblasts to ensure Teic did not impact the maturation response. A mechanically robust mineralised bone matrix is the product of mature osteoblasts (Blair *et al.*, 2017). The transition of immature cells to more differentiated, mature osteoblasts is important for the process of the prosthesis osseointegration. It is important to therefore assess the compatibility of any implant coating on the process of osteoblast maturation. ALP is expressed by mature cells and is essential for bone collagen calcification (Whyte, 2010). The activity of this enzyme is reliably monitored using a chromogenic assay with p-NPP as the substrate. Teic did not appear to be toxic towards MG63 cells when using therapeutic levels of the antibiotic (Fig 2.2; 20-60 µg/ml; NHS, 2021). Interestingly, Teic modestly enhanced the maturation of MG63 cells in response to 1,25D and FHBP. This demonstrates that Teic may not only contribute to

the antibacterial activity of the modified surface, but it could also increase the biocompatibility of the coating. This phenomenon was also noted by Lancaster *et al.* (2015), who assessed the cytotoxicity of gentamicin and Teic against osteoblasts. Currently, no published research has examined this specific interaction. However, a study by Ashouri *et al.* (2016) does provide evidence that Teic enhances cell growth and proliferation in a breast tumor cell line. Despite this, the mechanism by which Teic promotes cell proliferation remains unknown.

To ascertain if immobilised Teic could retain antimicrobial activity, CNBr-activated Sepharose was utilised to capture Teic. The Teic complex has an available NH_2 group that was used to covalently bind to the CNBr-activated Sepharose. The concentration of bound Teic was confirmed with BCA reagent and found that ~ 1 mg/ml of Teic was retained after immersion of 200 mg Sepharose in a 5mg/ml solution of Teic. The antimicrobial activity was comparable to the MBC of free Teic for this particular strain (32 $\mu\text{g}/\text{ml}$; data not shown). Yet, there was still significant bactericidal activity when using ~ 25 $\mu\text{g}/\text{ml}$ Teic-Sepharose compared to the Gly-Sepharose beads, resulting in a 3-log reduction from the starting inoculum (10^5 CFU/ml (Fig. 2.4). This is the first report that has utilised CNBr-Activated Sepharose for conjugation of Teic. However, Armenia *et al.* (2018) managed to functionalise IONPs with Teic using APTES and found that nanoconjugated Teic still retained significant bactericidal activity, albeit slightly reduced, when compared to Teic in solution. This suggests that a small amount of antimicrobial activity could be lost when covalently attached, however all A2 subcomponents of Teic contribute to the overall antimicrobial activity of the molecule and display similar MIC's when the subcomponents are assessed separately (Boix-Montañes & Garcia-Arieta, 2013) indicating that the loss of antimicrobial activity solely due to immobilisation is negligible. Furthermore, the route of attachment on IONPs utilised the carboxyl group of Teic whereas, in this thesis Teic was attached to PDA using the NH_2 group, suggesting that the immobilisation method does not affect the antimicrobial activity of Teic. This is demonstrated when the Teic-Sepharose beads are compared to the Teic-modified IONPs. The Teic Sepharose was able to retain up to ~ 1 mg per ml of Sepharose beads and the APTES-modified IONPs only retained ~ 100 $\mu\text{g}/\text{ml}$. This difference could be due to the surface area

available for modification. Another issue pertaining to the use of CNBr and APTES-activated films is the toxicity of the chemicals used and the time it takes to functionalise a surface (Wang *et al.*, 2017). Thus, an alternative functionalisation method that is facile, environmentally friendly and economic was explored.

PDA recently celebrated a “decade of discovery”, following the first report that PDA could be used as a facile means of functionalising a surface. There have been many studies since detailing the fabrication of diverse and novel technologies such as: photonic materials (Razmjou *et al.*, 2017), chromatography media (Wang *et al.*, 2017), biosensors (Li *et al.*, 2022), antifouling platforms (Kim *et al.*, 2018) and antimicrobial immobilisation (Mohd Daud *et al.*, 2018). This is one of the few reports that utilises PDA to capture Teic to a surface for biomaterial applications. Evidence of successful PDA film deposition and optimisation of PDA formation was quantified using a BCA-based assay adapted from Andrea & Mansell (2018). Parameters such as temperature (ambient, 35 and 55°C), buffer choice (Tris HCl, NaHCO₃ and HEPES) and incubation time (24, 48 and 72 h) were assessed. It was found that longer incubation times led to greater PDA-film formation (Fig. 2.5), resulting in greater functional group availability as evidenced by the LIVE/DEAD images (Fig. 2.6). This supports the results found by Lee *et al.* (2007) whereby polymer film thickness was a function of immersion time. In their work, Atomic Force Microscopy (AFM) analysis was used and found that after 24 h the coating thickness reached a value of at least 50 nm. However, the current methods used in this report use a 72 h incubation time. From a manufacturing perspective, long immersion times could be a problem so temperature was assessed as it was found that the reaction temperature can accelerate the polymerisation process (Zhou *et al.*, 2014; Wang *et al.*, 2017). It was found that significant PDA was deposited onto the Ti surface within 24 h when incubated at 35 and 50 °C in comparison to ambient conditions, indicating that temperature does have a significant impact on dopamine-polymerisation and subsequent PDA deposition. Based on the thermodynamic principle, higher temperatures should promote dopamine oxidation as well as the deposition process of PDA onto a substrate. This result is consistent with both investigations that looked into dopamine polymerisation under various

temperatures (Wang *et al.*, 2017; Zhou *et al.*, 2014). However, from a qualitative observation, an increase in temperature also results in a more uneven coating in comparison to ambient temperatures. This could be due to the PDA aggregates formed during polymerisation. In this study PDA is deposited under static conditions, allowing for insoluble aggregates to form on the Ti surface. These excess aggregates are not covalently attached to the Ti surface and could disrupt cellular functions and allow for Teic to elute into the medium. This variability of PDA thickness was also found by Zhou *et al.* (2014) when looking into the deposition kinetics of PDA as a function of temperature and stirring. PDA film deposition was more consistent and even when using a vigorous stirring method at 60°C in comparison to static incubation at ambient temperature, leading to an improved PDA surface for further modification. Furthermore, sufficient PDA coating was achieved in 30 minutes. This could drastically improve the consistency of the PDA coating and functionalisation and could be explored in future work.

Tris HCl at a pH of 8.5 is the most commonly used buffer for polymerisation of DHC onto various surfaces, however, studies have shown that buffer composition can also influence PDA particle aggregation and deposition (Della Vecchia *et al.*, 2014; Patel *et al.*, 2018). So, Tris was compared to NaHCO₃ and HEPES. As seen in Fig. 2.7, PDA formation was found to also be a function of buffer choice. Interestingly, these results differ from what has been found in the literature. After 72 h incubation, DHC that was solubilised in NaHCO₃ had significantly higher PDA deposition in comparison to Tris and HEPES which had similar PDA film thickness. Whereas Andrea and Mansell (2018) immersed TCP wells in the same buffers and found Tris allows for greater PDA deposition. However, the dissimilarity in results could be explained by the difference in incubation time as no studies to date incubate DHC for more than 24 h. Another contrast this report has with the literature is the antimicrobial activity of the PDA films. When qualitatively analysing the images in Fig. 2.8, there are no differences in the ratio of living/dead cells when comparing the buffers to the blank-Ti. This is further supported by the viable counts in Fig. 2.10 where there are no significant differences in bacterial attachment between the PDA- and blank-Ti when using Tris. Whereby, Patel *et al.* (2018) found that not only did the buffers

affect the antimicrobial activity of the PDA coating; discs steeped in Tris had the lowest attachment in comparison to PBS, NaHCO₃ and sodium hydroxide. This difference could be due to the variations in material and surface roughness as a rougher surface allows for a larger surface area for bacterial colonisation. Moreover, different sizes of PDA aggregates are formed depending on the buffer used and can change the topography and surface morphology of the PDA film (Patel *et al.*, 2018).

The antimicrobial activity of functionalised Teic-PDA-Ti was assessed by immersing said modified discs in a suspension of *S. aureus* and quantitatively evaluated using a viable plate count after 24 h of incubation. When compared to the control discs, there was a significant difference in bacterial attachment on the Teic-PDA-Ti at 24 h as seen in Fig. 2.12, suggesting that the Teic-modified surface is preventing bacterial colonisation. Even when the concentration of Teic in the immersion solution was reduced (from 5 mg/ml to 500 µg/ml; data not shown), there was no change in the antibiotic efficacy of the Teic-modified Ti discs. These findings agree with studies that looked at immobilised Vanc on Ti (Antoci Jr. *et al.*, 2007; Antoci Jr. *et al.*, 2008). When Vanc was covalently attached to APTES-modified Ti, it was found that bacterial attachment was significantly reduced on the Vanc-Ti in comparison to the Ti control. Furthermore, it deterred biofilm formation and still retained activity when repeatedly challenged with bacteria, demonstrating that immobilised antimicrobials have potential in reducing the risk of PJI. Interestingly, the Teic-Ti discs also deterred significant bacterial attachment when compared to PDA-Ti and Ti only. Moreover, there was no significant difference found between Teic-PDA-Ti and Teic-Ti. This interaction was also observed when looking at Teic attachment to PDA-modified TCP (Fig. 2.6). This suggests that Teic might have a natural affinity for the oxide layer of Ti and Teic could attach to the biomaterial surface without the need of an intermediate crosslinker.

2.6 Conclusions

This chapter supports the potential of PDA as a facile, multifunctional platform for the functionalisation of biomaterial surfaces with Teic. In addition, the Teic-PDA-Ti surface demonstrates the ability to reduce bacterial colonisation when compared to unmodified Ti. Evidence of successful PDA film deposition and optimisation of PDA formation was quantified using a BCA-based assay and parameters such as temperature, buffer choice and incubation time were assessed. The PDA optimisation work has highlighted the need for further optimisation of the PDA deposition process and physiochemical analysis of the PDA-modified Ti in order to ensure a stable and consistent coating for future functionalisation strategies. Interestingly, it was found that Ti discs could be modified with Teic only and display similar antimicrobial activity as the Teic-modified PDA-Ti discs. These findings are particularly noteworthy as they suggest that a sufficient amount of Teic could attach to the surface of Ti without the need of an intermediate crosslinker. Cutting out PDA or indeed other capturing platforms, is an appealing option in keeping costs down. The natural surface finish of Ti is titanium dioxide (titania; TiO_2) and the interaction between this oxide and Teic is clearly warranted in going forward. These studies form the research detailed in the forthcoming chapter.

Chapter 3. Assessing the Interaction Between Teic and

TiO₂

The data presented in this chapter has been adapted from Britton *et al.* (2022) Scientific Reports [DOI: 10.1038/s41598-022-20310-8] (Appendix I). The physiochemical data presented in this chapter was collected and analysed by Dr. Wayne Nishio Ayre, Dr. Liana Azizova, Dr. Greg Shaw and Dr. Kyuei Lee.

3.1 Introduction

TiO₂ is the natural oxide layer that forms on the surface of titanium and is one of the most well studied oxides due to its wide range of industrial applications which include, cosmetics, sunscreens, paints and in the production of alloys (Peterson *et al.*, 2012; Nowack & Bucheli, 2007). TiO₂ is not only cost-effective but is mostly non-toxic and has been approved for use in food and drug-related products by the Food and Drug Administration (FDA)(Jafari *et al.*, 2020). The oxide consists of two crystalline forms, rutile and anatase, which have important industrial applications. The anatase form of TiO₂ is more active than the rutile form regarding photocatalytic and cytotoxic properties. Yet, mixed polymorphs of TiO₂ (i.e., anatase 80% and rutile 20%) are found to be more efficient in biomedical applications compared to the presence of one crystal (Jafari *et al.*, 2020). *In vitro* studies have demonstrated that both anatase and rutile phase are capable of forming bioactive hydroxyl apatite layers when in contact with bodily fluids and exhibit excellent biocompatibility (Sangeetha *et al.*, 2013). Consequently, rutile and anatase TiO₂ surfaces can function as substrates for cultivating various cell types (Zhao *et al.*, 2005; Buchloh *et al.*, 2003; Carballo-Vila *et al.*, 2008; Nakazawa *et al.*, 2006). For instance, TiO₂ film surfaces have been shown to support the survival of neurons from the mammalian central nervous system for up to 10 days in culture, with rutile surfaces demonstrating good adherence and axonal growth of culture rat cortical neurons (Carballo-Vila *et al.*, 2008). Furthermore, studies have reported that hepatocytes can proliferate and maintain their metabolic activity over a long-term period on rutile and anatase TiO₂ surfaces (Zhao *et al.*, 2005; Buchloh *et al.*, 2003; Nakazawa *et al.*, 2006). Titania

has also been utilised as a chromatography sorbent for the enrichment and purification of glycopeptides (Britton *et al.*, 2022; Mancera-Arteu *et al.*, 2020; Sheng *et al.*, 2013) and is more recently being explored as a potential sorbent for extracting antimicrobials out of natural water systems (Peterson *et al.*, 2012; Aljeboree & Alkaim, 2019; Fries *et al.*, 2016; Bayan *et al.*, 2021).

From the results in Chapter 2, it was found that Teic, the lipoglycopeptide antibiotic, was able to bind directly to titanium discs. It is hypothesised that Teic has a natural affinity for the oxide layer, retaining antibacterial activity without the need for an intermediate crosslinker. The aim of this chapter was to assess the interaction of Teic with TiO₂ and to determine if the attachment was affected by a change in parameters such as incubation time, temperature, and repeated washes. In addition, Teic-Ti discs were subjected to a mock bacterial culture to ascertain if the antibiotic was bound to the Ti surface or if it was eluting into the bacterial medium.

3.2 Materials and Methods

3.2.1 Bacterial Culture Preparation

Bacterial cultures and standards were prepared in the same manner as 2.3.1. The bacterial standards used in this chapter were diluted in 1% peptone/PBS and this was used in all microbiological assays unless specified. As Teic is active on the cell wall of proliferating cells, the bacteria must be metabolically active and so a minimal medium supplemented with 1% peptone was used.

3.2.2 Reagents and Ti Disc Preparation

Reagents and Ti disc preparation were prepared and processed in the same manner as 2.3.2. TiO₂-coated Ti/Au QCM sensors (14 mm; AT cut, resonant frequency of 5 MHz) were purchased from Microvacuum (Budapest, Hungary).

3.2.3 Bacterial Attachment to Teic-modified Ti

This method is similar to the one used in Chapter 2 (2.3.5.5) however, it was optimised to increase the efficiency of bacterial recovery (data not shown). Ti discs were immersed in a 1 ml solution of Teic (500 µg/ml) in 2-(N-Morpholino)ethanesulfonic acid (MES; 50 mM; pH 5.47) for 2 h, washed in MGW twice to remove weakly bound Teic and allowed to dry in a laminar flow hood. Once dried, Ti discs were exposed to a 10⁵ CFU/ml suspension of *S. aureus* for 24 h at 37 °C with gentle shaking (120 RPM). After incubation, discs were washed twice in 0.85% saline to remove loosely bound bacteria and transferred to a sterile universal with 1 ml of maximum recovery diluent (MRD; Oxoid). This was sonicated for 5 min to recover attached bacteria. The detached bacteria were transferred to a sterile universal tube and incubated for 30 min at 37 °C to achieve maximum recovery. MRD was used to recover the detached bacteria as it is an isotonic diluent that can ensure the recovery of bacteria from various sources which could be vulnerable in distilled water or aqueous suspensions. The low concentration of peptone present (0.1% w/v) does not cause replication of the bacteria when in the solution for 45 min (Patterson & Cassells, 1963; Straka & Stokes, 1957).

The recovered bacteria were diluted and dispensed onto BHIA using the Miles and Misra technique and incubated for 24 h at 37 °C and colonies were counted the following day (Miles *et al.*, 1938).

3.2.4 X-Ray Photoelectron Spectroscopy (XPS) of Teic-Ti

Ti discs were exposed to a 1 ml solution of Teic (500 µg/ml) in 50 mM MES (pH 5.47) and left under ambient conditions from 30 min up to 3 h. Elements on the surface of control and modified Ti samples were analysed using a NEXSA XPS system (Thermo Fisher, Waltham, US). A monochromatic X-ray source (Al-K α) beam was used for the data collection. The atomic percentages of the elements detected were calculated using Avantage Data System software (ThermoFisher, Waltham, MA, US).

3.2.5 Adsorption of Teic onto Ti

Orthopaedic-grade Ti discs and solid TiO₂ powder (mixture of rutile and anatase TiO₂; Sigma Aldrich 634662-25G) were used to assess Teic adsorption to the metal oxide. Teic standards used in the experiments below were made up in the same manner as 2.4.3.1 with slight modifications.

3.2.5.1 Effect of Incubation Time on Teic Adsorption to TiO₂

TiO₂ powder (50 mg) was dispensed into microcentrifuge tubes and immersed in 500 µl of Teic (500 µg/ml in 50 mM HEPES; pH 7.4) and left to incubate, for up to 30 min, under ambient conditions. TiO₂ with HEPES only was used as a control. At each time point, samples were centrifuged at 11,300 x g for 2 min and 25 µl of each supernatant was combined to 500 µl of a freshly prepared BCA reagent (as per the manufacturer's instructions) and incubated for 30 min at 60 °C. After incubation, sample aliquots (100 µl) were transferred to a 96-well plate and measured against a series of Teic standards (0.5 – 500 µg/ml) in HEPES (50 mM; pH 7.4) at 540 nm using a microplate reader.

To confirm Teic-TiO₂ attachment, the supernatant was decanted, and the titania samples were washed in HEPES twice by centrifugation and resuspended in 500 µl HEPES buffer. A 25 µl sample of each titania suspension was combined to 500 µl of BCA reagent and incubated for 30 min at 60 °C. After

incubation, samples were centrifuged and 100 μ l of the supernatant was transferred to a 96-well plate and assessed in the same manner as above.

3.2.5.2 Binding Durability of Teic Attachment to TiO₂

To ascertain how robust the adsorption of Teic was to the titania, TiO₂ powder (50 mg) was added to microcentrifuge tubes, followed by 500 μ l of Teic (500 μ g/ml in 50 mM HEPES; pH 7.4) and incubated under ambient conditions for 2 h. TiO₂ with HEPES only was used as a control. Once incubated, samples were centrifuged at 11,300 \times g for 2 min and the supernatants were discarded. The remaining titania pellets were washed up to 10 times with HEPES buffer (500 μ l per wash). After 1, 3, 5 and 10 washes, 25 μ l of each wash was combined with 500 μ l of freshly prepared BCA reagent and incubated for 30 min at 60 °C. After incubation, samples were transferred and measured in the same manner as 3.2.5.1.

To assess the efficacy of the Teic-TiO₂ attachment, the supernatant was decanted after each wash and the remaining pellets were resuspended in 500 μ l of HEPES. A 25 μ l sample of the resuspended pellet was combined with 500 μ l BCA reagent and incubated for 30 min at 60 °C. Once incubated, samples were processed and measured in the same manner as 3.2.5.1.

3.2.5.2.1 Thermal stability of Teic-TiO₂

Thermal Gravimetric Analysis (TGA) was performed to assess the thermal stability of Teic when bound to titania. TiO₂ powder (50 mg) was added to microcentrifuge tubes, followed by addition of either 500 μ l of Teic (500 μ g/ml) in HEPES (50 mM; pH 7.4) buffer or HEPES buffer alone as a control. The samples were incubated under ambient conditions for 2 h and then centrifuged at 11,300 \times g for 2 min. The supernatant was discarded, and the pellets were air dried at room temperature. Teic powder alone was also assessed as a reference sample. Teic-TiO₂ and control samples were run on a PerkinElmer Pyris 1 TGA instrument (Perkin Elmer, Beaconsfield, UK) under a nitrogen flow of 40 ml/min. The sample was stabilised at 30 °C for 20 min before heating to 800 °C at a rate of 5°C/min. Data was analysed using Pyris TGA software (Perkin Elmer, Beaconsfield, UK).

3.2.5.2 Short-term Stability of Teic-TiO₂ under Neutral Conditions

TiO₂ samples (50 mg) were added to microcentrifuge tubes, followed by 500 µl of Teic (500 µg/ml) in HEPES (50 mM; pH 7.4) buffer and incubated at room temperature for 2 h. TiO₂ with HEPES only was used as a control. All samples were washed once at 11,300 x g for 2 min, resuspended in HEPES and incubated for 4 h, 1, 2, 3 and 7 days at 37 °C. One sample was tested immediately (baseline) after Teic incubation to determine the initial Teic concentration on the TiO₂. At each time point, samples were centrifuged at 11,300 x g for 2 min and a 25 µl aliquot of the supernatant was added to 500 µl BCA reagent prior to washing and incubated for 30 min at 60 °C. This was measured in the same manner as 3.2.5.1.

To assess the Teic attachment to titania, the pellet was washed once and resuspended in 500 µl of HEPES. A 25 µl aliquot of each resuspended pellet was added to 500 µl of BCA reagent and incubated for 30 min at 60 °C. Once incubated, samples were centrifuged at 11,300 x g for 2 min and 100 µl aliquots were transferred to a 96-well plate and measured in the same manner as above.

3.2.6 Impact of Phosphate on the Binding of Teic to TiO₂

The influence of phosphate on the bonding between Teic and titania was assessed, as it has been found that the anion has a natural and strong affinity for the oxide (Yan *et al.*, 2010). TiO₂ powder (50 mg) was exposed to Teic (500 µg/ml) made up in either PBS (pH 7.3) with the concentration of phosphate being either 1 mM or 10 mM. The samples were left to incubate for 30 min at room temp. Teic (500 µg/ml)-TiO₂ in HEPES (50 mM; pH 7.4) and TiO₂ in HEPES only were used as controls. After incubation, samples were centrifuged (11,300 x g for 2 min) and 25 µl of the supernatant was combined with 500 µl of BCA reagent and incubated for 30 min at 60 °C. Once incubated, samples were measured in the same manner as 3.2.5.1.

To confirm Teic-TiO₂ attachment, the supernatant was decanted, and the powder samples were washed once by centrifugation and resuspended in 500 µl of buffer. A 25 µl aliquot of each

resuspended pellet was combined to 500 µl of BCA reagent and incubated for 30 mins at 60°C. Once incubated, samples were centrifuged at 11,300 x g for 2 min and 100 µl aliquots of the supernatant were transferred to a 96-well plate and measured in the same manner as 3.2.5.1.

3.2.7 The Effect of Phosphate on the Detachment of Teic from TiO₂

To determine the effect of phosphate on the detachment of Teic from titania, a quartz crystal microbalance (QCM) system with impedance measurement was used (QCM-I, MicroVacuum, Budapest, Hungary). TiO₂-coated QCM sensors (Ti-QCM) were put through HEPES buffer (50 mM; pH 7.4) at a flow rate of 100 µl/min using a peristaltic pump (Ismatec Reglo Digital, Wertheim, Germany) at a constant temperature of 21 °C using a built in Peltier driver to avoid temperature drifts (stability of ± 0.02 °C). After a stable baseline was obtained over a minimum of 10 min, 500 µg/ml of Teic in HEPES was injected using the Rheodyne MXP injection system with a semiautomatic switching valve (MXP9960-000, California, US) for a further 10 min. The Ti-QCM sensor was then subjected to a continuous flow of either HEPES or PBS with 1 mM, 2 mM, 5 mM or 10 mM phosphate concentrations for 10 min. Frequency at the 1st, 3rd and 5th overtones and dissipation measurements were collected. Sauerbrey mass was calculated using Biosense software (Microvacuum, Budapest, Hungary).

3.2.8 Elution Assessment of Teic from Ti

Ti discs were exposed to Teic (500 µg/ml in 50 mM MES, pH 5.4) and incubated for 2 h under ambient conditions. After incubation, discs were washed with distilled water to dislodge any loosely bound Teic and allowed to dry in a sterile environment. Control and functionalised Ti discs were then immersed in sterile 1% Peptone/PBS broth and left for 24 h at 37 °C with gentle shaking (120 RPM). After incubation, the recovered conditioned media (100 µl) was transferred to a sterile 96-well plate and inoculated with *S. aureus* (100 µl) at a final density 5 x 10⁵ CFU/ml. A positive growth control and a negative control (broth only) were also added to ensure sufficient growth of the organism and that

the broth is sterile. The samples left to incubate at 37 °C for 24 h. After incubation the OD at 595 nm (using a microplate reader) was taken to ascertain bacterial growth in the conditioned media.

To determine if the conditioned discs still retained any antibacterial activity the control and functionalised Ti discs were transferred to a new multiwell plate and washed in distilled water twice, allowed to dry and then exposed to a 10^5 CFU/mL suspension of *S. aureus* and incubated for a further 24 h at 37 °C with gentle shaking (120 RPM). After incubation, discs were recovered, washed twice with 0.85% saline and sonicated for 5 min in 1 ml of MRD to recover the attached bacteria. The detached bacteria were transferred to a new universal and incubated for 30 min at 37 °C in order to achieve maximum recovery. The recovered organisms were diluted and dispensed onto BHIA and incubated for 24 h at 37 °C.

3.2.9 Bacterial Viability and Elution studies of Teic-modified Iron Oxide Nanoparticles (IONPs)

Teic-modified IONPs (Teic-IONP; kindly provided by Giovanni Bernardini and colleagues, University of Insubria, Italy) were exposed to *S. aureus* to determine the antibacterial efficacy of the nanoconjugated antibiotics. These IONPs were prepared using (3-Aminopropyl)triethoxysilane (APTES) for the capture of Teic using EDC-NHS chemistry (Armenia *et al.*, 2018).

3.2.9.1 Viability of *S. aureus* against Teic-IONPs

An aliquot (150 μ l) of Teic-IONP (493 μ g/ml Teic; 4 mg/mL Fe₂O₃) in sodium borate (10 mM; pH 8.2) was combined to a 10^5 CFU/ml suspension of *S. aureus* (850 μ l) and incubated for 24 h at 37 °C. IONPs (4 mg/ml) and free Teic (~ 75 μ g/ml) were used as controls. To assess the antibacterial activity of the Teic-IONP storage buffer, 150 μ L of the Teic-IONP was exposed to a neodymium (Nd) magnet in a multiwell plate. This was done to separate the Teic-IONP from the storage buffer. After separation, the buffer was carefully aspirated and combined to 850 μ L of a 10^5 CFU/ml *S. aureus* suspension and

incubated for 24 h at 37 °C. After incubation, all samples were diluted in MRD, dispensed onto BHIA and incubated for a further 24 h at 37 °C.

3.2.9.2 Elution Assessment of Teic from IONPs

An aliquot (150 µl) of Teic-IONP (493 µg/ml Teic; 4 mg/ml Fe₂O₃) in sodium borate (10 mM; pH 8.2) was blended with 1% Peptone/PBS broth (850 µl) and incubated for 24 h at 37 °C. IONPs (4 mg/ml in water) treated in the same manner were used as a control. After incubation, samples were centrifuged at 11,300 x g for 2 min and the recovered conditioned media (100 µl) was transferred to a sterile 96-well plate and inoculated with *S. aureus* (100 µl) and left to incubate for 37 °C for 24 h under static conditions. At the desired time, the OD_{595nm} was taken to ascertain bacterial growth using a microplate reader (TECAN).

To determine if the modified-IONPs still retained any antimicrobial activity, the control and functionalised IONPs were washed twice in distilled water using centrifugation and the Teic-IONPs were resuspended in 150 µl of 10 mM sodium borate (pH 8.2) and subsequently exposed to 850 µl of a 10⁵ CFU/ml *S. aureus* suspension and incubated for 24 h at 37 °C. The bare IONPs were resuspended in water and treated in the same manner as the Teic IONPs. Free Teic (~ 75 µg/ml) was used as a control. After incubation, all samples were diluted in MRD, dispensed onto BHIA and incubated for 24 h at 37 °C.

3.2.10 The Binding of N-Acetyl-L-Lys-D-Ala-D-Ala to a Teic Stationary Phase (TSP)

A commercially available chiral stationary phase, consisting of covalently bound Teic to silica was sourced from AZYP, LLC (Arlington, Texas) in which approximately 68 mg of Teic is bound to 1 g of silica. The tripeptide N-Acetyl-L-Lys-D-Ala-D-Ala (Cambridge Bioscience, UK) was reconstituted to 200 µg/ml in 50 mM HEPES (pH 7.4). TSP (100 mg) was exposed to 500 µl of the tripeptide (200 µg/ml) and incubated under ambient conditions for 30 min. After incubation, the sample was centrifuged (11,300

x g) for 2 min and the supernatant was collected (500 μ l) and aspirated into a new microcentrifuge tube. The pH of the supernatant was adjusted to \sim 8.4 using 1 M NaOH and exposed to 5 μ L of genipin (250 mM in DMSO) and then left to react at 60°C for 2 h.

To assess the binding of the tripeptide, the remaining pellet was washed three times in HEPES (50 mM; pH 7.4) using centrifugation and resuspended in 500 μ l of buffer. The pH of the pellet was adjusted to \sim 8.4 and subsequently exposed to 5 μ l of genipin and left to react for 2 h at 60 °C. After incubation, OD_{595nm} of the samples were measured using a microplate reader. Plain silica shells (AZYP, LLC, Texas) were used as controls and assessed in the same manner.

3.2.11 Bacterial viability to TSP

To assess the antibacterial activity of the chiral stationary phase, aliquots (50 mg) were added to microcentrifuge tubes and immersed in a 70% ethanol solution for 10 min to sterilise the powder. This was washed three times in a 1% peptone/PBS solution using centrifugation (11,300 x g). After centrifugation, the washed pellets were resuspended in 1 ml of a 1% peptone/PBS solution containing 10⁵ CFU/mL of *S. aureus* and transferred to a sterile bijou. A further 4 ml of the bacterial suspension was added to the bijou to a final volume of 5 ml (final concentration of TSP suspension is 10 mg/mL, corresponding to 680 μ g/ml Teic). This was incubated for 24 h at 37 °C with gentle shaking (120 RPM). A final concentration of free Teic (600 μ g/ml) solution and untreated silica were used as controls. After incubation, samples were diluted in MRD, dispensed onto BHIA and incubated for a further 24 h at 37 °C.

3.3 Results

3.3.1 Bacterial viability to Teic-Ti

Bacterial attachment to Teic-modified Ti was assessed by exposing *S. aureus* to functionalised and control Ti for 24 h at 37 °C. Attachment of *S. aureus* to the modified Ti surface was found to be significantly less ($p < 0.0001$) when compared to Ti alone (Fig. 3.1) and resulted in a 5-log reduction from the initial seeding density (10^5 CFU/ml). Out of the 36 Teic-modified discs exposed to *S. aureus*, only 7 discs supported bacterial attachment ($\sim 10^2$ - 10^3 CFU/ml). However, they still had a significant reduction ($p < 0.01$) in attachment to the surface, leading to a 2- or 3-log reduction, in comparison to Ti alone.

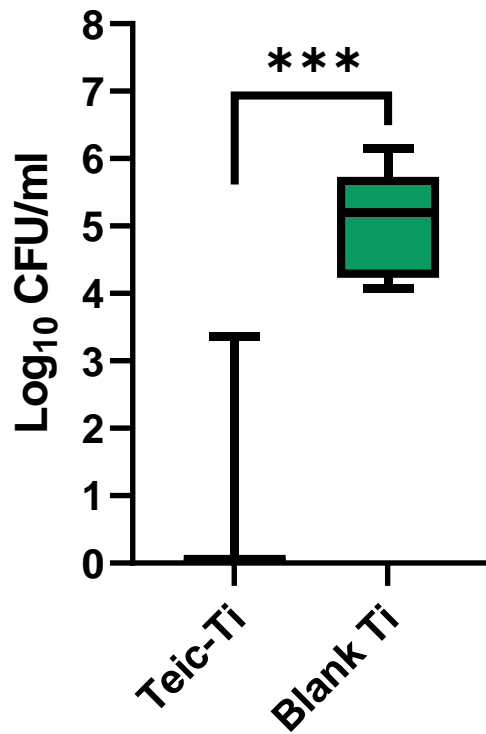


Figure 3.1 Antibacterial efficacy of Teic-modified Ti. Ti discs were immersed in 500 µg/ml Teic (50mM MES; pH 5.47) for 2 h under ambient conditions. After incubation, functional and control discs were transferred to a new well plate, washed twice in distilled water and subsequently exposed to a 10⁵ CFU/mL suspension of *S. aureus* in 1% Peptone/PBS for 24 h at 37 °C with gentle shaking (120 RPM). After incubation, discs were recovered, washed twice with 0.85% saline and sonicated for 5 min in 1 ml of MRD to recover attached bacteria. The detached bacteria were transferred to a new universal and incubated for 30 min at 37 °C in order to achieve maximum recovery. The recovered organisms were diluted and dispensed onto BHIA and incubated for 24 h at 37 °C. When Ti discs are steeped in a solution of Teic, the modified surfaces are capable of significantly reducing bacterial attachment in comparison to the control (blank) Ti (***) $p < 0.001$). All data (mean ± SD; N = 36) represent pooled triplicate runs from 12 independent experiments.

3.3.2 XPS of Teic-Ti

To analyse elements on the surface of control and functionalised Ti samples, physicochemical analysis using XPS was performed. It is clear that Teic adsorption occurs within 30 min of antibiotic exposure, as noted by the increase in the chlorine peaks (Cl_2) and a reduction in elemental oxygen (O) and titanium (Ti_2) over time (Fig. 3.2). In addition, as the incubation time of Teic increased, the atomic composition of the Ti surface changed, further confirming that Teic was adsorbing onto the Ti surface (Table 3.1).

Table 3.1 Elemental composition of control and Teic-functionalised Ti. Quantified atomic percentage (at.%) of the elements in each Ti specimen treated with Teic. The clear changes in elemental composition with increasing incubation time support Teic adsorption to the metal surface.

Time (h)	C1s (at.%)	N1s (at.%)	O1s (at.%)	Cl2p (at.%)	Ti2p (at.%)
-	41.9 ± 1.9	1.4 ± 0.1	45.0 ± 1.6	-	11.7 ± 0.4
0.5	45.0 ± 1.0	2.5 ± 0.2	43.2 ± 0.8	0.3 ± 0.1	9.1 ± 0.5
1	47 ± 0.6	2.6 ± 0.5	41.4 ± 0.9	0.3 ± 0.1	8.8 ± 0.1
3	62.3 ± 0.4	3.0 ± 0.1	30.1 ± 0.5	0.5 ± 0.1	4.0 ± 0.5

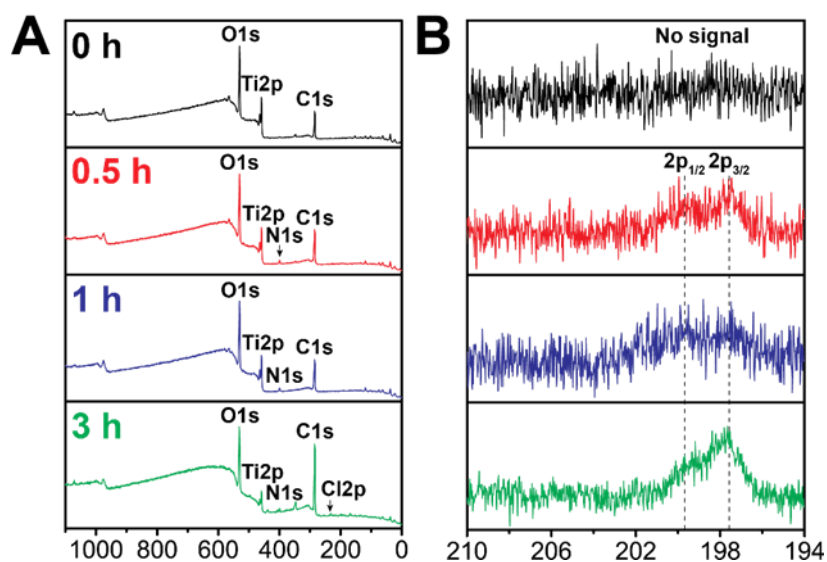


Figure 3.2 Detection of Teic coating on the Ti surface. X-Ray Photoelectron Spectroscopy (XPS) analysis of **A.** survey peaks and **B.** high-resolution Cl_{2p} peaks of Teic-treated Ti discs with different immersion times: 0, 0.5, 1, and 3 h. It is clear that Teic adsorption occurs within 30 min of Teic exposure.

3.3.3 Adsorption of Teic onto Ti

To observe the binding of Teic with titania, some factors that could affect the interaction were assessed such as, incubation time, repeated washing, thermal stability and the impact of phosphate. Short term stability under neutral conditions was also assessed.

3.3.3.1 Influence of incubation time on Teic Attachment to TiO₂

To observe the adsorption of Teic to the metal oxide, TiO₂ powder was used and the antibiotic monitored using BCA. From the information provided in Figure 3.3 it was found that Teic adsorption to TiO₂ was the same for all time points tested, with around 300-350 µg/ml being adsorbed by the titania. This would suggest that immersing the oxide in Teic for only 5 min would provide the Ti surface with sufficient antibacterial activity.

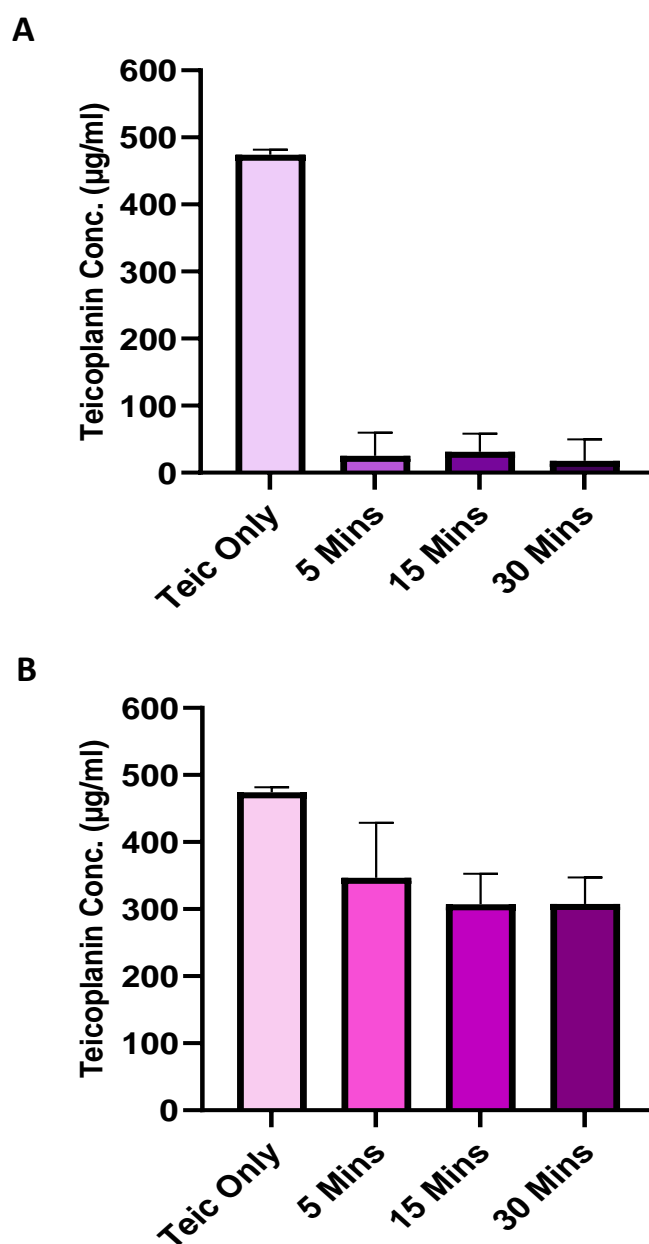


Figure 3.3 Influence of HEPES on Teic adsorption to TiO₂. TiO₂ samples (50 mg) were immersed in 500 µl of 500 µg/ml Teic solubilised in 50 mM HEPES (pH 7.4) and incubated at room temperature for 5, 15 and 30 min. TiO₂ with HEPES only was used as a control. At each time point, samples were centrifuged at 11,300 x g for 2 min and a 25 µl aliquot of each supernatant added to 500 µl of BCA reagent. This was incubated for 30 min at 60 °C. Once incubated, 100 µl aliquots were transferred to a 96-well plate and measured at 540 nm using a microplate reader. To confirm Teic-TiO₂ attachment, the supernatant was decanted, and samples were washed twice by centrifugation (11,300 x g) and resuspended in 500 µl HEPES buffer. A 25 µl aliquot of each sample was added to 500 µl of BCA reagent and incubated for 30 min at 60 °C. Once incubated, samples were centrifuged at 11,300 x g for 2 min and 100 µl aliquots were transferred to a 96-well plate and measured in the same manner as above. All data (mean ± SD; N = 20) represent pooled quadruplicate runs from 5 independent experiments. **A.** Teic concentration in supernatant post-incubation and **B.** Teic attachment on TiO₂

3.3.3.2 Durability of Teic-TiO₂ to washing

To determine the durability of Teic attachment to TiO₂ the modified oxide was subjected to repeated washing and assessed using BCA. Despite the small loss of Teic after the first wash (Fig. 3.4), with around 10% of the bound antibiotic eluting into the medium, the oxide still retained a large amount of the antibiotic, even after 10 washes, suggesting a robust attachment.

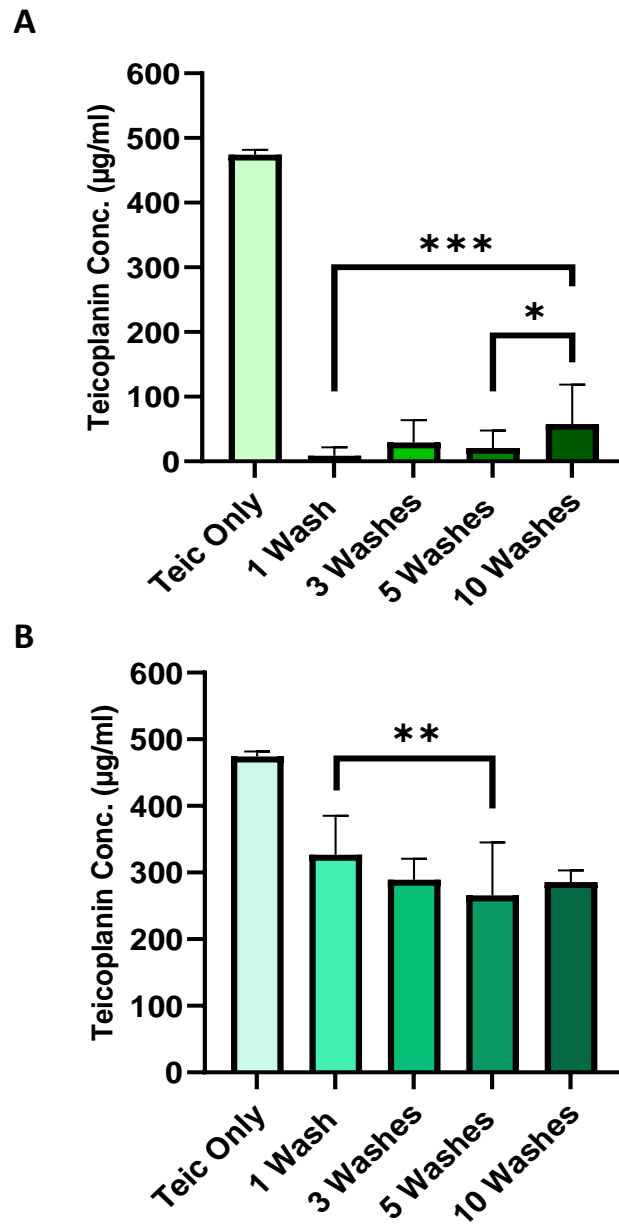


Figure 3.4 Durability of Teic-TiO₂ to Washing. TiO₂ samples (50 mg) were added to Eppendorf tubes, followed by 500 µl of Teic (500 µg/ml) in HEPES (50 mM; pH 7.4) buffer and incubated at room temperature for 2 h. TiO₂ with HEPES buffer only was used as a control. After incubation samples were centrifuged at 11,300 x g for 2 min and 25 µl aliquots of the supernatant was added to 500 µl BCA reagent prior to washing and incubated for 30 min at 60 °C. Once incubated, 100 µl aliquots were transferred to a 96-well plate and measured at 540 nm using a microplate reader (TECAN) (data not shown). After 1, 3, 5 and 10 washes, samples were centrifuged at 11,300 x g for 2 min and 25 µl aliquots of the supernatant was added to 500 µl BCA reagent prior to washing and incubated for 30 min at 60 °C. Once incubated, 100 µl aliquots were transferred to a 96-well plate and measured at 540 nm using a microplate reader. To assess the efficacy of the Teic-TiO₂ attachment, the supernatant was decanted, and pellets were resuspended in 500 µl of HEPES buffer. A 25 µl aliquot of each sample was added to 500 µl of BCA reagent and incubated for 30 min at 60 °C. Once incubated, samples were centrifuged at 11,300 x g for 2 min and 100 µl aliquots were transferred to a 96-well plate and measured in the same manner as above. All data (mean ± SD; N = 20) represent pooled quadruplicate runs from 5 independent experiments. **A.** Teic concentration in wash supernatant post-incubation and **B.** Teic attachment on TiO₂. p < 0.05 (*), p < 0.01 (**) and p < 0.001 (***).

3.3.3.3 Thermal stability of Teic-TiO₂

To further ascertain the durability of the Teic attachment to the metal oxide, TGA was performed on Teic bound to TiO₂, TiO₂ powder, and Teic alone. Percentage weight loss curves for Teic alone demonstrated an initial decrease at temperatures below 100 °C, as noted by the black line in Fig. 3.5A. This is most likely due to the residual moisture evaporation. Rapid thermal degradation of Teic was observed at temperatures greater than 250 °C, with three notable derivative peaks (red line) observed at approximately 270 °C, 357 °C and 402 °C and a total weight reduction of 53.14%. TiO₂ in HEPES only displayed a single weight loss peak between 250 °C and 400 °C. Interestingly, a similar percentage weight and derivative curve was observed for Teic-bound TiO₂, however a greater weight loss of 13.97% was observed between 250 °C and 400 °C with a notable peak at 365 °C (Fig. 3.5C), when compared with TiO₂ only. The greater weight loss is most likely attributed to the disassociation of Teic from TiO₂. However, it has been demonstrated that Teic, when bound to TiO₂ displays great thermal stability and can remain bound in temperatures up to 250 °C.

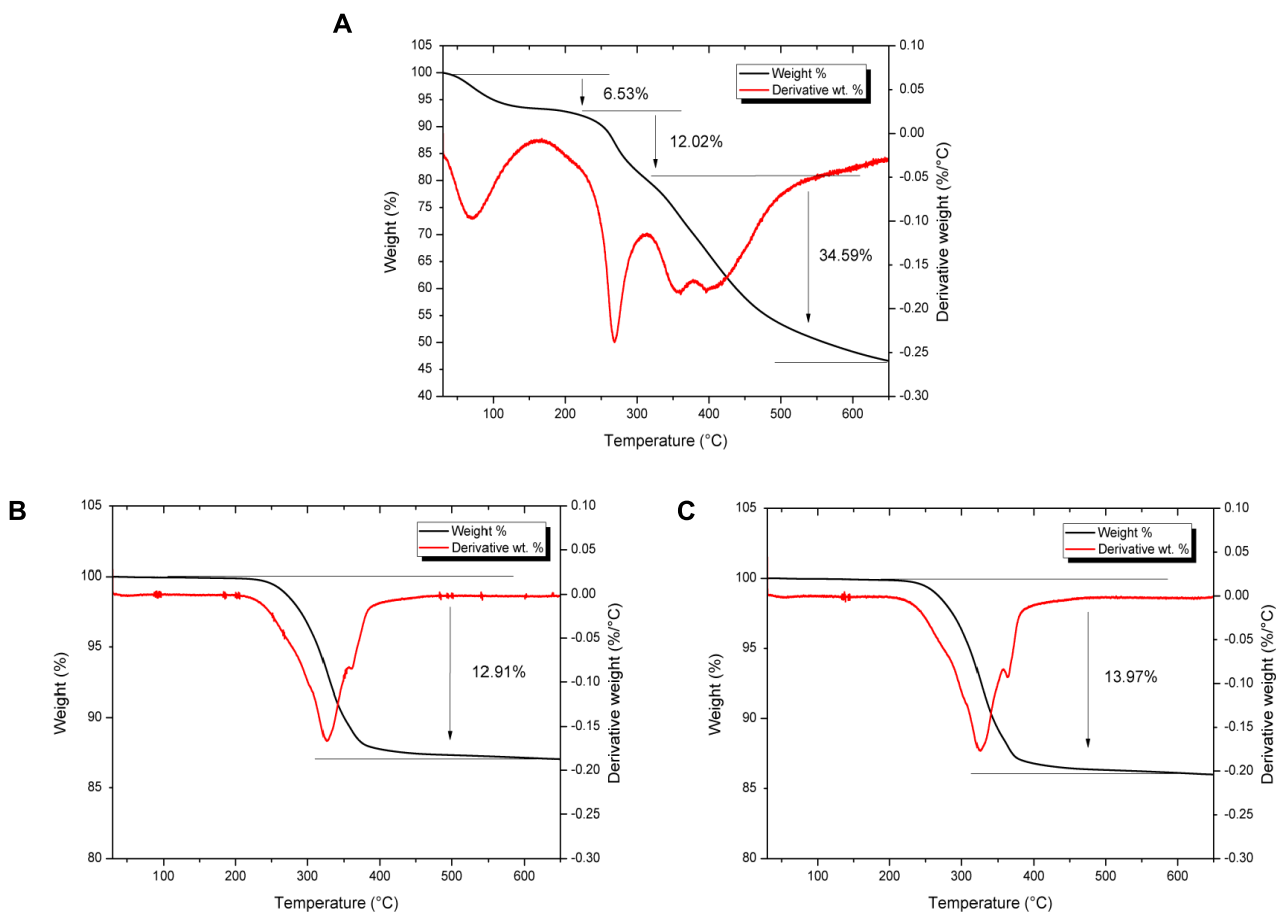


Figure 3.5 Thermal stability of Teic immobilised on the surface of TiO₂ using Thermal Gravimetric Analysis (TGA). TiO₂ powder (50 mg) was incubated with either 500 μ l of Teic (500 μ g/ml) in HEPES (50 mM; pH 7.4) buffer or HEPES buffer alone as a control for 2 h under ambient conditions and then centrifuged at 11,300 x g for 2 min. The centrifuged pellets were air dried at room temperature before undergoing TGA. **A.** Percentage weight curves for Teic alone shows an initial decrease at temperatures below 100 $^{\circ}$ C due to moisture evaporation. This was followed by rapid thermal degradation at temperatures greater than 250 $^{\circ}$ C. **B.** TiO₂ samples incubated in HEPES buffer showed a single dissociation step between 250 $^{\circ}$ C and 400 $^{\circ}$ C and a percentage weight change of 12.91%. **C.** Similar percentage weight and derivative weight curves were obtained for TiO₂ samples incubated with Teic, however a greater weight loss of 13.97% was observed between 250 $^{\circ}$ C and 400 $^{\circ}$ C indicating the additional dissociation of Teic from the surface of TiO₂ at high temperatures.

3.3.3.4 Short Term Stability of Teic-TiO₂ under Neutral Conditions

To determine the stability of Teic attachment to TiO₂ under neutral conditions, the modified oxide was immersed in HEPES and left to incubate at 37 °C for 7 days. At each time point TiO₂ samples are assessed with BCA. It is clear that a large amount of the antibiotic remained bound to the oxide over the course of 7 days, however a significant ($p < 0.0001$) amount was lost at the 7-day timepoint when compared to the baseline (Fig. 3.6B). Despite this, there was still enough antibiotic retained to elicit an antibacterial effect.

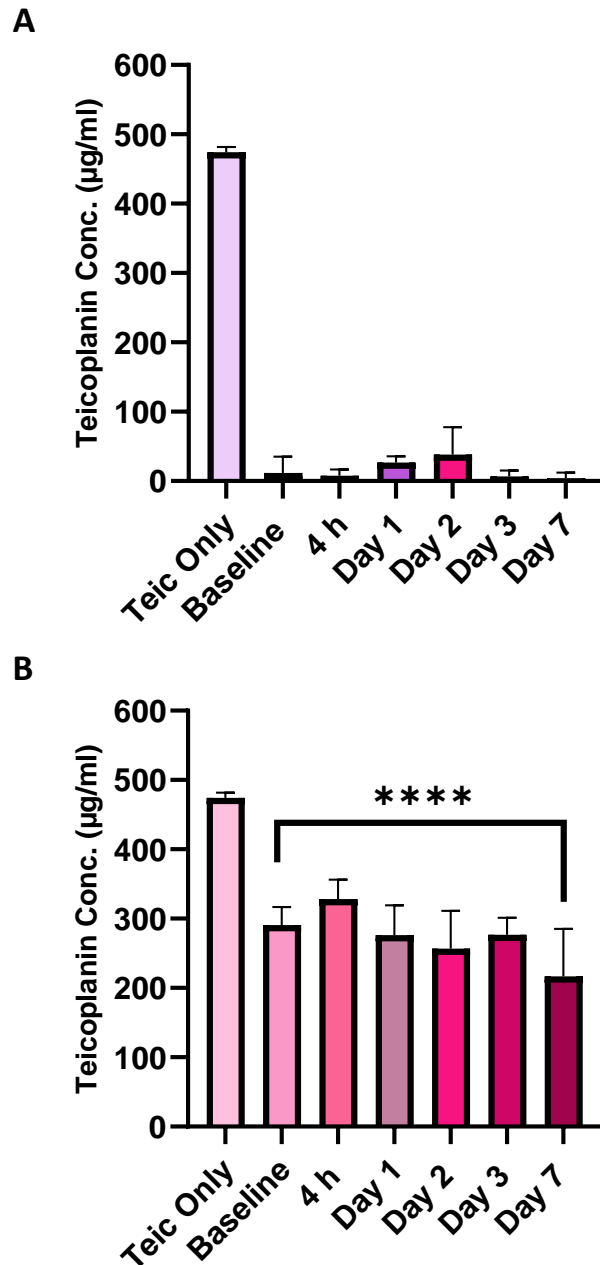


Figure 3.6 Short Term Stability of Teic-TiO₂ under Neutral Conditions. TiO₂ samples (50 mg) were added to Eppendorf tubes, followed by 500 µl of Teic (500 µg/ml) in HEPES (50 mM; pH 7.4) buffer and incubated at room temperature for 2 h. TiO₂ with HEPES only was used as a control. After incubation, samples were centrifuged at 11,300 x g for 2 min and 25 µl aliquots of the supernatant was added to 500 µl BCA reagent prior to washing and incubated for 30 min at 60 °C. Once incubated, 100 µl aliquots were transferred to a 96-well plate and measured at 540 nm using a microplate reader (TECAN) (data not shown). All samples were washed once, resuspended in HEPES and incubated for 4 h, 1, 2, 3 and 7 days at 37 °C. One sample was tested immediately (baseline) after Teic incubation to determine the initial Teic concentration on the TiO₂. At each time point, samples were centrifuged at 11,300 x g for 2 min and a 25 µl aliquot of the supernatant was added to 500 µl BCA reagent prior to washing and incubated for 30 min at 60 °C. This was measured in the same manner as above. To assess the stability of the Teic-TiO₂ attachment, the pellet was washed once and resuspended in 500 µl of HEPES. A 25 µl aliquot of each resuspended pellet was added to 500 µl of BCA reagent and incubated for 30 min at 60 °C. Once incubated, samples were centrifuged at 11,300 x g for 2 min and 100 µ aliquots were transferred to a 96-well plate and measured in the same manner as above. All data (mean ± SD; N = 20) represent pooled quadruplicate runs from 5 independent experiments. **A.** Teic concentration in wash supernatant post-incubation and **B.** Teic attachment on TiO₂

3.3.3.5 Impact of Phosphate on the Binding of Teic to TiO₂

The impact of phosphate on the bonding between Teic and TiO₂ was examined, as the anion is known to have an affinity for the oxide (Yan *et al.*, 2010). It was found that the phosphate could compromise the binding of Teic to the oxide in a concentration dependent manner (Fig. 3.7). Increasing the phosphate concentration in the Teic incubation buffer generated TiO₂ samples with less Teic attached. This most likely suggests that the anion has a greater affinity for the oxide than the antibiotic.

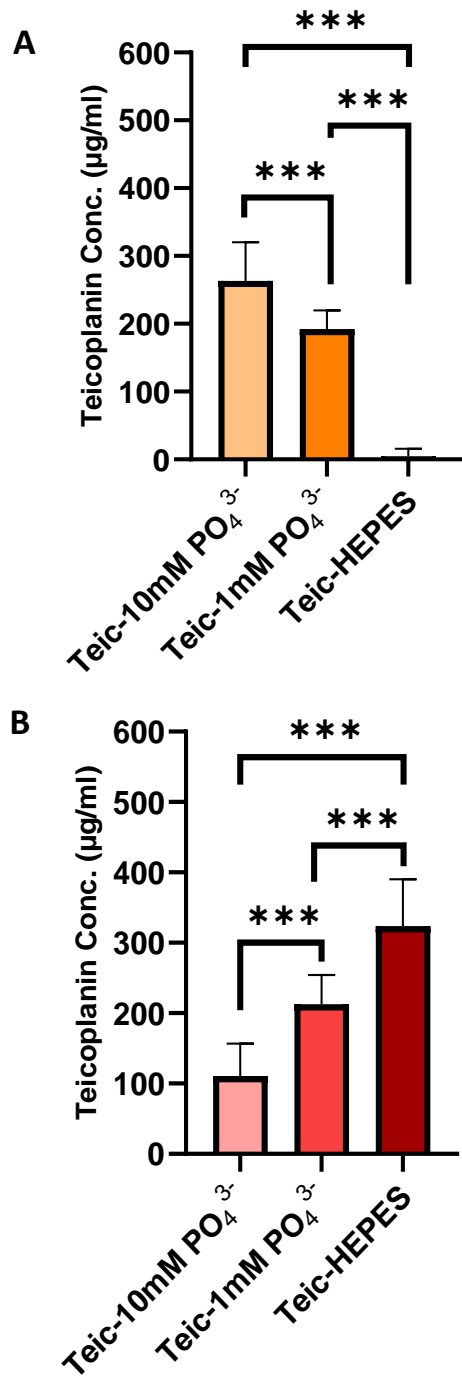


Figure 3.7 Influence of phosphate on Teic adsorption to TiO₂. **A.** TiO₂ samples (50 mg) were exposed to 500 µg/ml Teic in PBS where the phosphate concentration was either 1 mM or 10 mM and samples left to incubate at room temperature for 30 min. Teic-TiO₂ in HEPES served as a control. After incubation, samples were centrifuged at 11,300 x g for 2 min and 25 µl aliquots of the supernatant were combined to 500 µl BCA reagent and incubated for 30 mins at 60 °C. Once incubated, 100 µl aliquots were transferred to a 96-well plate and measured at 540 nm using a microplate reader. **B.** To confirm Teic-TiO₂ attachment, the supernatant was decanted, and samples were washed once by centrifugation (11,300 x g) and resuspended in 500 µl buffer. A 25 µl aliquot of each sample was added to 500 µl of BCA reagent and incubated for 30 min at 60 °C. Once incubated, samples were centrifuged and 100 µl aliquots were transferred to a 96-well plate and measured in the same manner as above. It is evident that phosphate reduces the extent of Teic binding to the metal oxide. All data (mean ± SD; N = 20) represent pooled quadruplicate runs from 5 independent experiments. p < 0.001 (***).

3.3.3.6 The Effect of Phosphate on the Displacement of Teic from TiO₂

From the information provided in Fig. (3.8) it is clear that phosphate compromises the binding of Teic to the metal oxide. The injection of Teic (500 µg/ml) in HEPES resulted in rapid adsorption of Teic to the surface of the Ti-QCM sensor which plateaued after approximately 5 min, resulting in a surface coverage of around 100-200 ng/cm² (according to the Sauerbrey mass calculations). This rapid adsorption of Teic concurs with the findings presented in Fig. 3.3. When washing the surface of the Teic-coated Ti-QCM sensor with HEPES, only loosely bound Teic was removed from the surface of the Ti-QCM sensor, and a majority of the antibiotic remained bound (Fig 3.8A). On the other hand, when washing the surface of the sensor with buffers containing phosphate, it resulted in rapid disassociation of Teic from the Ti-QCM sensor (Fig 3.8B-E).

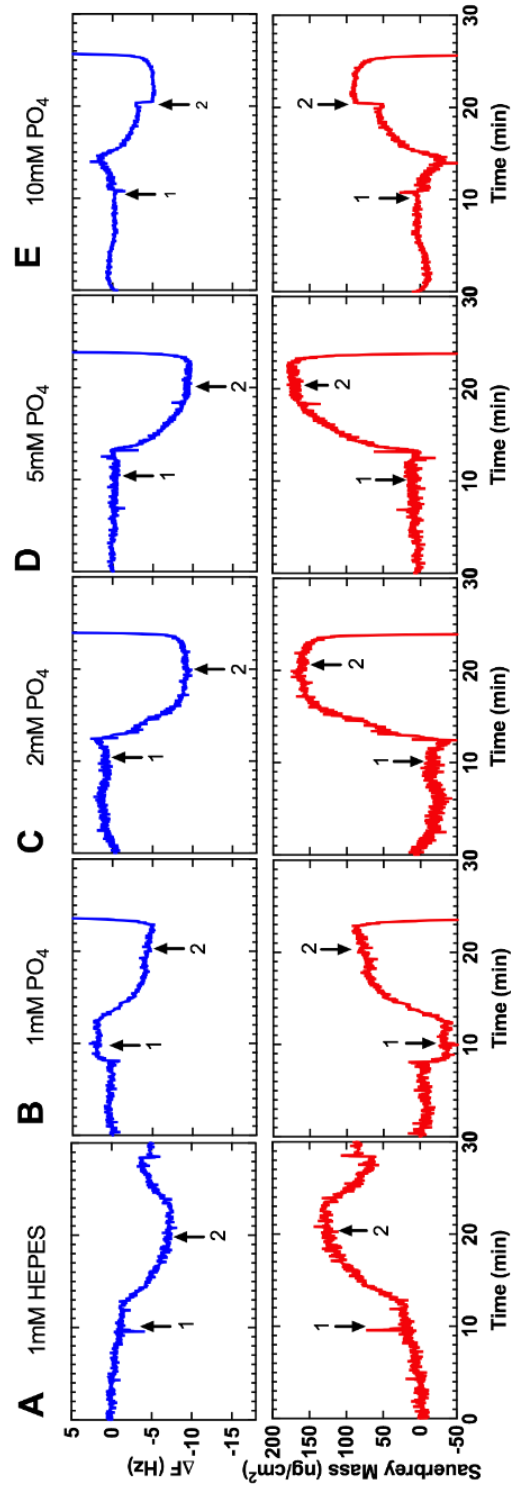


Figure 3.8 Influence of phosphate on Teic detachment from TiO_2 . Ti-QCM sensors were subjected to HEPES buffer (50 mM; pH 7.4) at a flow rate of $100 \mu\text{l}/\text{min}$ at 21°C for 10 min prior to $500 \mu\text{g}/\text{ml}$ Teic in HEPES for 10 min (arrow 1). Coated Ti-QCM sensors were then washed for a final 10 min with either A. HEPES or PBS with B. 1 mM, 2 mM, C. 5 mM or D, 10 mM phosphate concentrations (arrow 2). Representative plots from triplicate ($N = 3$) experiments showing change in fundamental frequency (upper panels) and calculated Sauerbrey mass (lower panels).

3.3.4 Elution Assessment of Teic from Ti Discs

To determine if the antibiotic was eluting from the Ti surface, functionalised and control Ti discs were conditioned in a 1% Peptone/PBS broth for 24 h. Qualitatively, the Ti control discs did not inhibit the growth of *S. aureus*, with the turbidity of the wells comparable to the positive control (data not shown). In comparison, the broth from the Teic-Ti discs provided complete inhibition of *S. aureus* growth (Fig. 3.9A) and was comparable to the negative controls, indicating that the antibiotic is eluting from the Ti surface.

To assess the bactericidal activity of the conditioned media recovered from Teic-Ti, samples were spot-inoculated on to BHIA and left to incubate for 24 h at 37 °C. This confirmed that the culture medium from the modified discs had a large amount of bactericidal activity as no growth occurred after incubation when compared to the broth recovered from the control Ti discs (data not shown). The conditioned discs were exposed to *S. aureus* to ascertain if some of the Teic was still bound to the discs, and it was found that a large amount of the antibacterial activity was lost, further confirming that the antibiotic elutes from the surface (Fig. 3.9B).

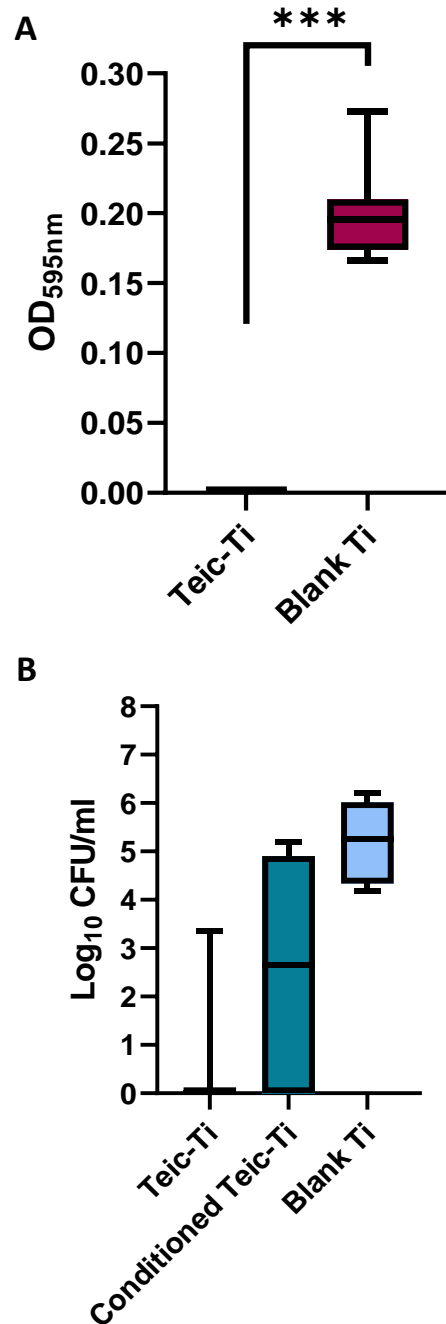


Figure 3.9 Antibacterial activity of Teic-Ti after culture conditioning. **A.** Ti discs were exposed to Teic (500 $\mu\text{g}/\text{ml}$ in 50 mM MES, pH 5.4) and incubated for 2 h under ambient conditions. After incubation, discs were washed with distilled water to dislodge any loosely bound Teic and allowed to dry in a sterile environment. Control and functionalised Ti discs were then immersed in 1% peptone/PBS and left for 24 h at 37 $^{\circ}\text{C}$ with gentle shaking (120 RPM). After incubation, the recovered conditioned media (100 μl) was transferred to a sterile 96-well plate and inoculated with *S. aureus* (100 μl) and left to incubate at 37 $^{\circ}\text{C}$ for 24 h. At the desired time the OD at 595 nm was measured to ascertain bacterial growth using a microplate reader. The significant reduction (***) in OD supports antibiotic leaching into the culture medium. **B.** To determine if the conditioned discs still retained any antimicrobial activity the control and functionalised Ti discs were transferred to a new multiwell plate and washed in distilled water twice, allowed to dry and then exposed to a 10^5 CFU/mL suspension of *S. aureus* and incubated for a further 24 h at 37 $^{\circ}\text{C}$ with gentle shaking (120 RPM). After incubation, discs were recovered, washed twice with 0.85% saline, and sonicated for 5 min in 1 ml of MRD to recover the attached bacteria. The detached bacteria were transferred to a new universal and incubated for 30 min at 37 $^{\circ}\text{C}$ in order to achieve maximum recovery. All data (mean \pm SD; N = 9) represent pooled triplicate runs from 3 independent experiments.

3.3.5 Bacterial Viability and Elution Studies of Teic-IONPs

3.3.5.1 Viability of *S. aureus* against Teic-IONPs

Teic-IONPs were exposed to *S. aureus* for 24 h at 37 °C to determine the antibacterial efficacy of the nanoconjugated antibiotics. As can be seen from Fig. 3.10, the modified oxide nanoparticles did exhibit significant bactericidal activity when compared to the bare IONPs ($p < 0.001$). It was also found that the IONPs alone did result in a 2-log reduction from the initial inoculum density. Interestingly, the Teic-IONP storage buffer exposed to *S. aureus* had very similar outcomes to that obtained for free Teic and Teic-IONP.

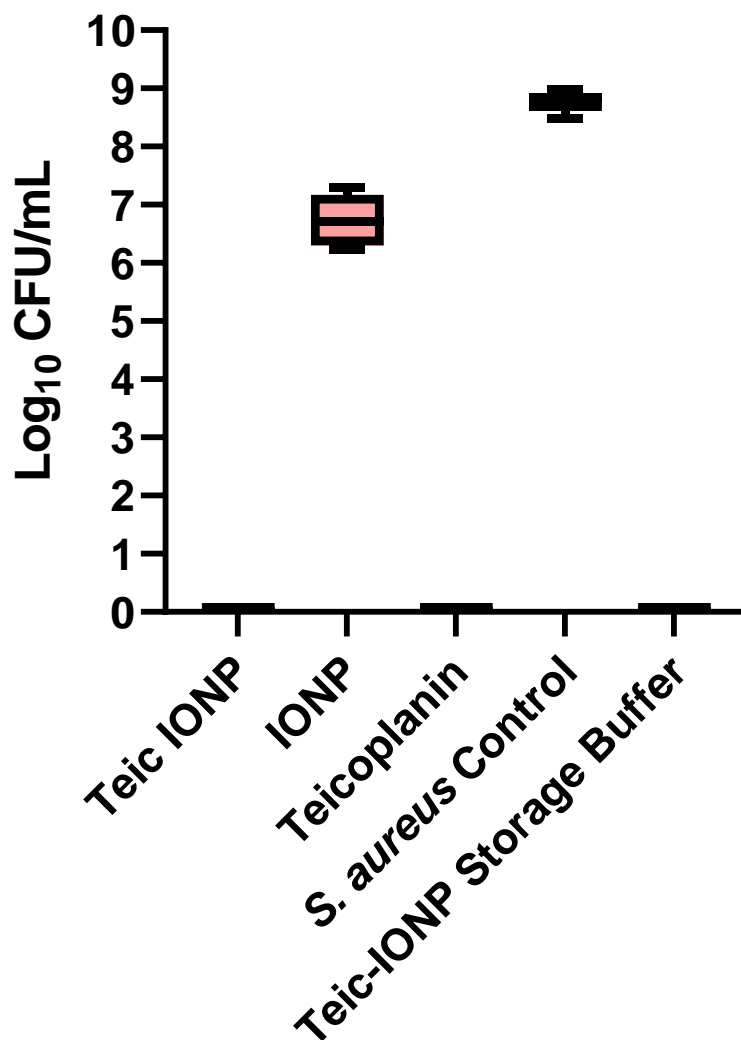


Figure 3.10 Antibacterial activity of Teic-IONP. An aliquot (150 μ l) of Teic-IONP (493 μ g/mL Teic; 4mg/mL Fe_2O_3) in sodium borate (10 mM; pH 8.2) was added to a 10^5 cfu/ml suspension of *S. aureus* (850 μ L) and incubated for 24 h at 37°C. IONPs (4mg/ml) and free teicoplanin (~ 75 μ g/mL) were used as controls. To assess the antibacterial activity of the Teic-IONP storage buffer, 150 μ L of the Teic-IONP was added to a Neodymium (Nd) magnet in a multiwell plate. This was done to separate the Teic-IONP from the storage buffer. After separation, the buffer was carefully aspirated and added to 850 μ L of a 10^5 cfu/mL *S. aureus* suspension and incubated for 24 h at 37°C. After incubation, all samples were diluted in MRD, dispensed onto BHIA and incubated for a further 24 h at 37°C. All data (mean \pm SD; N = 12) represent pooled sextuplicate runs from 2 independent experiments.

3.3.5.2 Elution Assessment of Teic-IONPs

To ascertain if the antibiotic is securely bound to the surface, the IONPs were conditioned in the bacterial culture medium for 24 hours. It was found that the culture media recovered from control IONPs supported bacterial growth with evidence of solution turbidity and OD₅₉₅ values ranging between 0.17-0.27 (Fig. 3.11A). In contrast, the conditioned media recovered from Teic-IONPs completely inhibited bacterial growth, as indicated by clear solutions and OD₅₉₅ values similar to the blanks. The conditioned IONPs were subsequently exposed to *S. aureus* to determine if they were still able to reduce the viability of *S. aureus*. The findings obtained for these conditioned samples indicated a moderate loss of antibacterial activity, further confirming that the antibiotic elutes from the oxide surface under the conditions described (Fig. 3.11B).

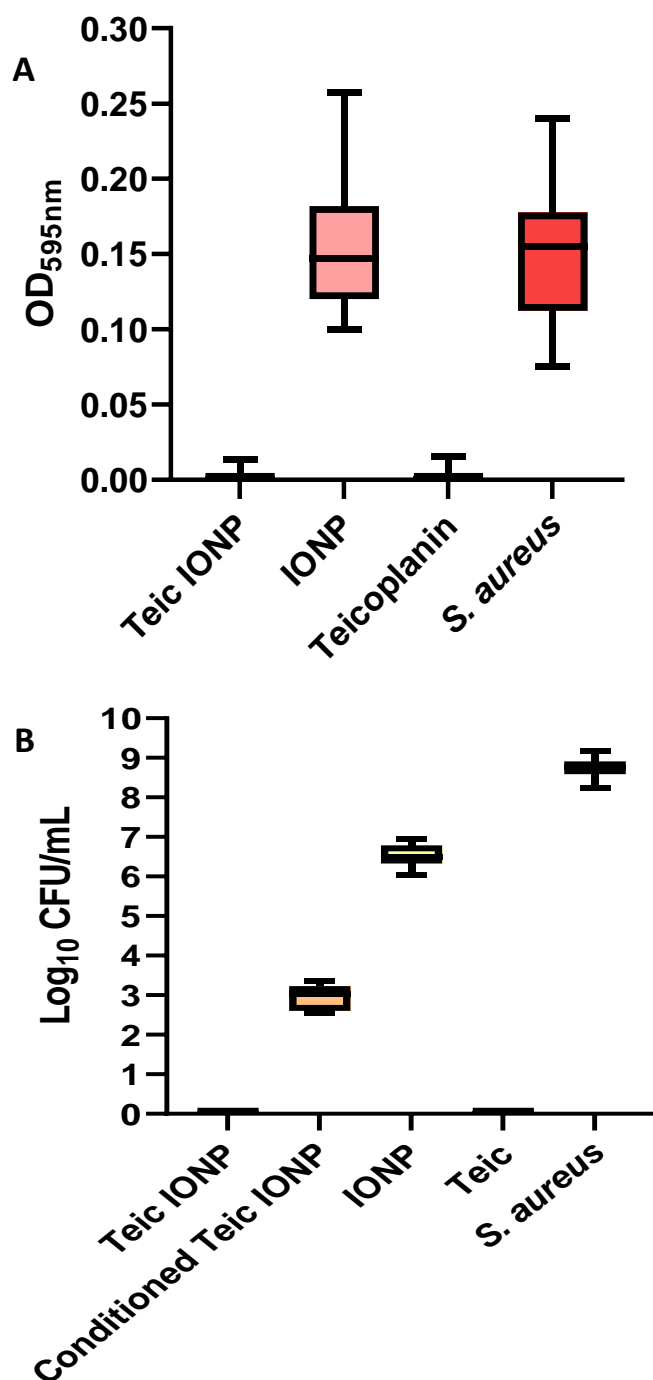


Figure 3.11 Antibacterial activity of Teic-IONP after culture conditioning. **A.** An aliquot (150 μ l) of Teic-IONP (493 μ g/mL Teic; 4 mg/ml Fe_2O_3) in sodium borate (10 mM; pH 8.2) was added to 1% peptone/PBS broth (850 μ l) and incubated for 24 h at 37 $^\circ\text{C}$. IONPs (4 mg/ml in water) treated in the same manner were used as a control. After incubation, samples were centrifuged at 11,300 \times g for 2 min and the recovered conditioned media (100 μ l) was transferred to a sterile 96-well plate and inoculated with *S. aureus* (100 μ l) and left to incubate for 37 $^\circ\text{C}$ for 24 h under static conditions. At the desired time the OD_{595nm} was taken to ascertain bacterial growth using a microplate reader (TECAN). **B.** To determine if the conditioned IONPs still retained any antimicrobial activity, the control and functionalised IONPs were washed twice in distilled water using centrifugation and the Teic-IONPs were resuspended in 150 μ l of 10 mM sodium borate (pH 8.2) and subsequently exposed to 850 μ l of a 10^5 cfu/ml *S. aureus* suspension and incubated for 24 h at 37 $^\circ\text{C}$. The bare IONPs were resuspended in water and treated in the same manner as the Teic IONPs. Free teicoplanin (\sim 75 μ g/ml) was used as a control. After incubation, all samples were diluted in MRD, dispensed onto BHIA and incubated for 24 h at 37 $^\circ\text{C}$. There is a moderate loss of activity from the conditioned Teic-IONPs. All data (mean \pm SD; N = 12) represent pooled sextuplicate runs from 2 independent experiments.

3.3.6 Binding of N-Acetyl-L-Lys-D-Ala-D-Ala to the TSP

The binding of the chiral stationary phase to the tripeptide was monitored using genipin, a natural product of Gardenia fruits (*Gardenia jasminoides*) that forms a blue chromogen when it reacts with amino groups (Riacci *et al.*, 2021). The results indicate that the tripeptide successfully bound to the stationary phase (Fig. 3.12). The OD of the tripeptide control and the silica particle control (SPC) supernatant had no significant difference, suggesting that none of the tripeptide bonded to the SPC. In contrast, the TSP supernatant had a significant decrease in OD (Fig. 3.12; $p < 0.001$), suggesting the tripeptide was able to bind well to the TSP. These findings suggest that the chiral stationary phase is functional.

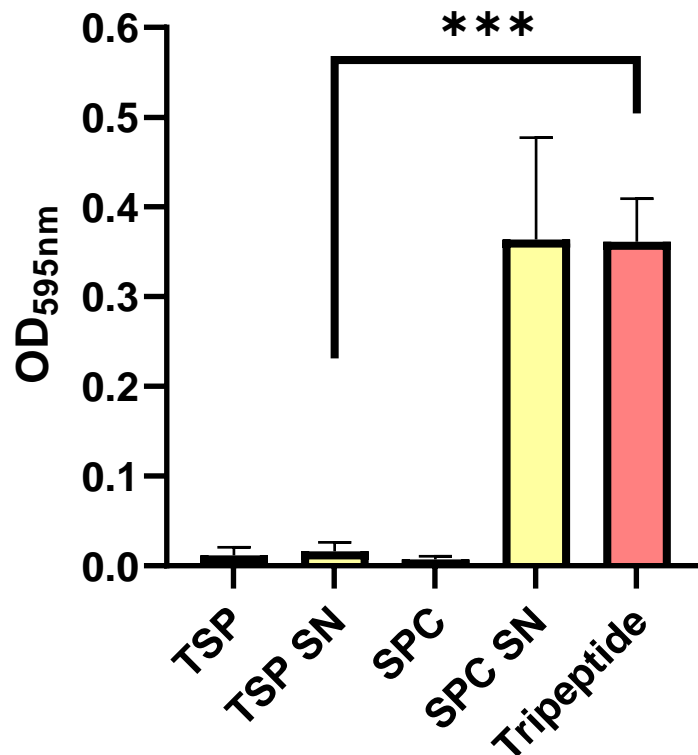


Figure 3.12 The tripeptide N-Acetyl-L-Lys-D-Ala-D-Ala binds avidly to a TSP. Aliquots (100 mg) of TSP and a silica particle control (SPC) were exposed to 500 μ l of the tripeptide (200 μ g/ml) prepared in 50mM HEPES (pH 7.4) and incubated at room temperature for 30 mins. After incubation, samples were centrifuged and the supernatants (SN) collected, the pH adjusted to 8.4 and 500 μ l treated with 5 μ L of genipin (250mM in DMSO). Samples were left to incubate at 60°C for 2 h. After incubation, the optical density (OD) of the samples were measured using a microplate reader. The OD for the tripeptide control and SPC SN were similar indicating no tripeptide binding to the SPC. In contrast the SN recovered from the TSP had a significantly reduced OD when compared to the tripeptide control, indicating good binding of the tripeptide with the TSP. All data (mean \pm SD; N = 9) represent pooled triplicate runs from 3 independent experiments. $p < 0.001$ (***)

3.3.7 Viability of *S. aureus* to the TSP

To determine if the immobilised Teic had the capacity to kill bacteria, the stationary phase and control silica were exposed to *S. aureus* for 24h. When *S. aureus* (10^5 CFU/ml) was exposed to free Teic (600 $\mu\text{g/ml}$), there was significant bactericidal activity when compared to the bacterial control ($p < 0.0001$) which resulted in a ≥ 7 -log reduction from the initial inoculum density (Fig. 3.13). However, when *S. aureus* was exposed to 10 mg of the TSP (with a Teic concentration equivalent to 680 $\mu\text{g/ml}$), there was no effect on bacterial viability when compared to the SPC and inoculum control, which would suggest that when Teic is covalently tethered to a surface, it does not retain its antibacterial function.

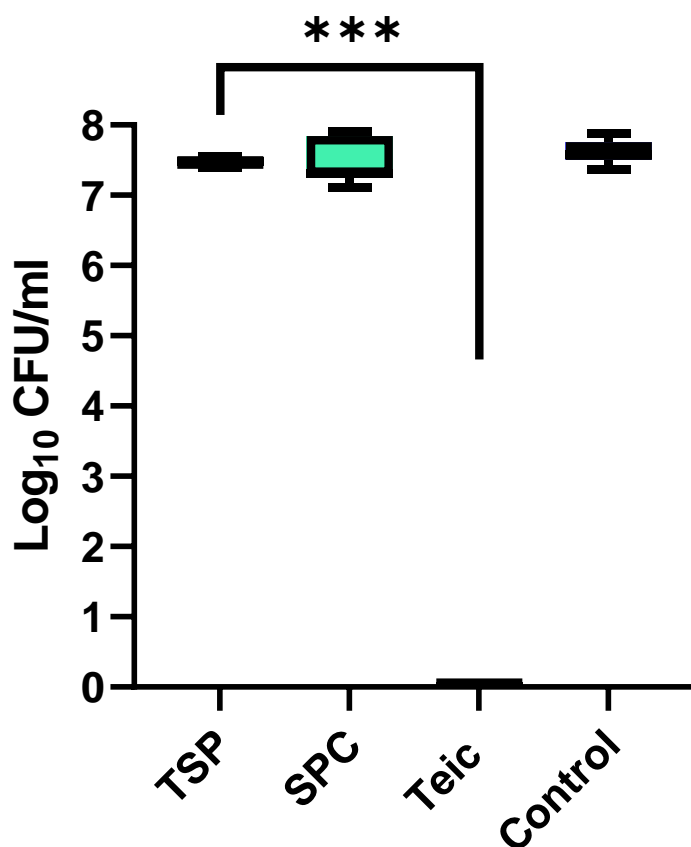


Figure 3.13 Immobilised Teic does not display any antibacterial activity towards *S. aureus*. Aliquots (50 mg) of TSP and a silica particle control (SPC; 50 mg) were exposed to a 10^5 CFU/ml suspension of *S. aureus* and incubated for 24 h at 37 °C. A bacterial culture alone and a culture spiked with free teicoplanin (600 µg/ml) served as controls. As anticipated, cultures treated with free Teic led to significant reduction in bacterial viability when compared to the growth control. In contrast, the TSP cultures exhibited similar bacterial numbers to SPC and bacterial controls. All data (mean ± SD; N = 9) represent pooled triplicate runs from 3 independent experiments. $p < 0.001$ (***)

3.4 Discussion

During the course of the studies conducted in Chapter 2, it was found that simply steeping medical-grade Ti discs in an aqueous solution of Teic led to a modified surface that displayed antibacterial activity against *S. aureus* which was comparable to the Teic-modified PDA-Ti discs. This suggested that Teic had a natural affinity for the oxide layer of Ti and that a sufficient amount of Teic could attach to the biomaterial surface without the need of a crosslinker. Therefore, the aim of this chapter was to investigate the interactions between Teic and TiO₂ by using a mixture of rutile and anatase titania alongside Ti discs and immersing samples in a solution of Teic. Parameters such as immersion time (5 min, 15 min and 30 min) attachment durability, short-term and thermal stability and impact of phosphate were assessed. The elution profile of Teic-modified Ti was also assessed.

The presence of Teic on the Ti surface was detected using XPS analysis. Confirmation of the presence of Teic was observed in the form of increasing Cl₂ peaks (Cl₂) over time, suggesting that Teic can adsorb to the surface within 30 min of antibiotic exposure. To confirm that Teic-modified Ti demonstrated antimicrobial activity, Ti discs were immersed in a solution of Teic for 2 h and exposed to *S. aureus* for 24 h. The Teic-Ti discs displayed significant antimicrobial activity ($p < 0.0001$) when compared to the initial inoculum density (1×10^5 CFU/ml) and control Ti discs as seen in Fig. 3.1, suggesting that the Teic-modified Ti is deterring bacterial attachment. These findings agree with studies that looked into Teic-modified Ti wires and screws (Aykut *et al.*, 2010; Catalbas *et al.*, 2020). For instance, Aykut *et al.* (2010) coated Ti wires with a methanolic solution of Teic and implanted the wires into an infected rabbit model. Out of the 10 rabbits that had a Teic-coated wire implanted, no bacterial growth was observed on any of the wires when extracted after 7 days. Moreover, there was no bacterial growth detected on the bone tissue in the group with Teic-coated wires and is a desirable outcome given that *S. aureus* has a high affinity for bone tissue and has been found to accelerate the induction of osteonecrosis and bone matrix resorption (Aykut *et al.*, 2010). The study conducted by Catalbas *et al.* (2020) had found that Teic bound to Ti screws did not impact the osseointegration process of the

screws, however they did not assess the antibacterial activity of the Teic-Ti screws, only the biomechanical and histomorphometric effects.

To support the theory that Teic is binding to the natural oxide layer of Ti, a mixture of rutile and anatase titania (50 mg) was exposed to an aqueous solution of Teic (500 μ l; 500 μ g/ml) and antibiotic binding monitored using a BCA reagent. Adsorption of Teic to TiO₂ was rapid, with around 90% of the antibiotic bound to the oxide after 5 min incubation (Fig. 3.3). This is further supported by the QCM measurements (Fig. 3.8). In addition, there was little change in the adsorption of Teic onto TiO₂ across all the time points tested and interestingly, the QCM measurements found that Teic adsorption plateaued after 5 min. Similar results have been observed by a group who used TiO₂ as a sorbent to remove Vanc, a glycopeptide antibiotic, from water. It was discovered that approximately 70-85% of the glycopeptide was removed from the water within 15 min (Lofrano *et al.*, 2018). However, it is not known how much was removed after 5 min. Despite this, it highlights the oxide's affinity for glycopeptides and that the attachment occurs rapidly. It was found that the Teic adsorption to TiO₂ was robust, when Teic-TiO₂ was subjected to repeated washing (up to 10 times) the majority of the antibiotic remained bound to the oxide (Fig. 3.4). The Teic-modified TiO₂ also demonstrated thermal stability. When looking at the TGA data, Teic was able to stay bound to the oxide when exposed to temperatures up to 250 °C (Fig. 3.5). Furthermore, Teic was able to remain bound to the titania when incubated in HEPES at 37 °C over the course of 7 days (Fig. 3.6), with only ~10% loss of the bound antibiotic. Despite a thorough search of the literature, this is the first time the durability of an antibiotic bound to bare titania has been assessed. Although the exact mechanism of Teic binding to TiO₂ remains unclear, there has been a study that looked into the retention mechanism of glycopeptides on TiO₂. It was found that both hydrophilic interactions and ligand-exchange retention mechanisms between TiO₂ and the saccharides were involved in the binding of glycopeptides to TiO₂ (Sheng *et al.*, 2013; Chen *et al.*, 2021). This could very well explain how Teic is binding to TiO₂ in this study.

To determine if the antibiotic is eluting or bound to the surface of Ti during bacterial culture, Teic-modified Ti discs were subjected to a mock bacterial culture for 24 h at 37 °C and the recovered medium exposed to *S. aureus*. When looking at Fig. 3.9A, the conditioned media provided complete growth inhibition of *S. aureus* when compared to the control suggesting that the antibiotic had eluted from the surface and is most likely responsible for the antibacterial activity observed in previous studies. The leaching of Teic from Ti wires was also observed by Aykut *et al.* (2010) as indicated by the disk diffusion assay. To determine if the Teic-modified Ti discs still retained any antibacterial activity, the conditioned discs were inoculated with *S. aureus* and incubated for 24 h at 37 °C. It was found that the conditioned discs did not retain antibacterial activity and bacterial attachment was significantly greater on the conditioned Teic-Ti discs, when compared to the unconditioned Teic-Ti (Fig. 3.9B). Attachment of *S. aureus* was similar to that of the control Ti, further suggesting that that antibiotic had eluted from the surface. During the course of this study, it was noted that phosphate has a strong natural affinity for titania (Yan *et al.*, 2010) and since the minimal medium used for the antibacterial assessments contains phosphate, the next study subsequently looked into the impact of phosphate on the binding of Teic to TiO₂.

When Teic was reconstituted in PBS and applied to titania, the amount of antibiotic bound to the oxide was markedly less compared to Teic applied to titania in HEPES alone (Fig. 3.7). Moreover, when reducing phosphate to a physiological concentration (1 mM), the phosphate was still preventing Teic from binding to the oxide, suggesting that phosphate has a greater affinity for the oxide than the glycopeptide. However, it did permit significantly more attachment when compared to the 10 mM phosphate, suggesting that the binding of Teic to titania when in the presence of phosphate, is concentration dependent. These results were also supported by the QCM data. When subjecting the Teic-Ti discs to solutions with varying concentrations of phosphate (1 mM, 2 mM, 5 mM and 10 mM), rapid disassociation of Teic from the Ti surface was observed. Zhao *et al.* (2008) has also observed this phenomenon when assessing the impact of phosphate on the photocatalytic activity of TiO₂. They found that modifying the surface with a phosphoric acid resulted in a surface-bound phosphate anion

that subsequently impacted the adsorption of most substrates, suppressing the oxides' ability to degrade organic pollutants. A more recent study found that phosphate can also impact the adsorption of proteins, such as albumin (Xu & Grassian, 2017). Under acidic conditions, phosphate was found to reduce albumin adsorption but no change at neutral pH. This contrasts with what was found for Teic adsorption to titania using neutral HEPES. This difference may be attributed to the great affinity albumin has for the hydroxyl (OH⁻) groups present on titania when hydrated at a neutral pH (Xu & Grassian, 2017).

Whilst the facile adsorption of Teic to Ti appears to be a favourable solution towards developing antibacterial implant technology, it was clear that this interaction will be compromised by physiological phosphate. Given that phosphate is a prevalent and essential electrolyte in the human body, this particular technology is not an ideal option in tackling the issue of periprosthetic joint infection. An alternative strategy is clearly required and so work focused back onto covalently grafting Teic onto Ti, in light of a recent technology that utilised iron oxide nanoparticles (IONPs) to immobilise Teic for local delivery of the antibiotic (Armenia *et al.*, 2018). Using APTES and EDC/NHS chemistry, this group anchored Teic onto the IONPs using the carboxyl functional group on Teic. The resultant material displayed excellent antibacterial activity against *S. aureus* and *Bacillus subtilis* and was able to retain 90% of the antibiotic on the surface after a month of storage. Armenia *et al.* (2018), very kindly provided these modified IONPs which were subjected to an elution assessment to determine if the antibiotic remained bound when conditioned with the culture medium. Initial experiments assessing the antibacterial activity of the Teic-IONPs found that the nanoconjugated antibiotics demonstrated significant antibacterial activity when compared to the bare IONPs (Fig. 3.10). In addition, the reduction in bacterial viability observed from the Teic-IONPs was similar to free Teic. However, the bare-IONPs did significantly reduce bacterial viability when compared to the growth control, with a 2-log reduction from the initial inoculum density. These findings are in agreement with Armenia *et al.* (2018). They found that the Teic-IONPs had significant antibacterial activity against *S. aureus* when compared to APTES-IONPs and bare-IONPs. Conversely, despite the bare IONPs

impacting the growth of *S. aureus*, they found that there was no difference in the viability of *S. aureus* in the presence of bare IONPs when compared to the growth control. Yet, this observation could be due to the difference in the type of *S. aureus* strain used. Interestingly, when assessing the storage buffer for antibacterial activity the reduction was comparable to that of the Teic-IONPs and free Teic, suggesting that the antibiotic is eluting into the buffer. The Teic-IONPs were then conditioned in the bacterial culture medium for 24 h at 37 °C to ascertain if the antibiotic was indeed eluting from the modified surface. Qualitatively, the culture media recovered from the control IONPs supported the growth of *S. aureus*. In contrast, the conditioned media recovered from the Teic-IONPs completely inhibited bacterial growth, supporting the observations found with the storage buffer in Fig. 3.11A and suggesting that Teic is eluting from the modified surface. The conditioned Teic-IONP and controls were subsequently exposed to *S. aureus* to see if the modified IONPs still retained any antibacterial activity. From the results obtained in Fig. 3.11B, it is clear that the conditioned Teic-IONPs demonstrate a moderate loss of antibacterial activity, further suggesting that the antibiotic is eluting from the surface, albeit at a slower rate than what was observed on the Teic-modified Ti discs. However, the bacterial viability on the Teic-IONPs is still significantly lower than bare IONPs and growth control.

Yet, there is a commercially available chiral stationary phase that successfully immobilised Teic to the surface of silica particles for the purpose of enantiomeric chromatography separations (TEICOSHELL, AZYP, LLC), demonstrating that it is indeed possible to immobilise the glycopeptide to a surface. However, despite its ability to work as a chiral selector, the antibacterial activity of the stationary phase has yet to be elucidated. Prior to subjecting the TSP to a bacterial assessment, it was worth investigating its binding capacity to the tripeptide N-acetyl-L-lys-D-ala-D-ala, as it shares similarity to the Lys-D-alanyl-D-alanine containing peptides in the cell wall precursors of *S. aureus*. Moreover, this specific tripeptide has been utilised by Economou *et al.* (2012) when detecting Teic via a direct fluorescence polarisation assay and so using this tripeptide seemed suitable to confirm the functionality of the TSP. It was possible to monitor the binding of the tripeptide to the TSP by using

genipin, a natural component extracted from *Gardenia jasminoides* which is able to readily react with primary amines, after exposure to oxygen, resulting in the production of a dark blue chromogen (Riacci *et al.*, 2021). The binding interactions between the tripeptide and TSP were apparent with the sample supernatants demonstrating undetectable levels of tripeptide after a 30 min exposure to TSP (Fig. 3.12). This is in contrast to the control silica particles exposed to the tripeptide. The supernatant of the controls reacted with the genipin resulting in deep blue solutions, suggesting that the tripeptide is not binding to the silica particles. However, despite being able to demonstrate TSP functionality the same material was without antibacterial activity against *S. aureus*. When the TSP and controls were exposed to a 10^5 CFU/ml culture of *S. aureus* the TSP permitted significant growth of *S. aureus* when compared to the free Teic control. Moreover, there were no differences in viability between the TSP, SPC and *S. aureus* control. Normally, bacterial viability is significantly reduced when in the presence of 50 $\mu\text{g/ml}$ Teic (Fig. 2.3), however despite the Teic concentration of the TSP being equivalent to 680 $\mu\text{g/ml}$, no reduction in bacterial viability was observed, suggesting that immobilised Teic does not display antibacterial activity (Fig. 3.13). These findings conflict with what has been reported in the literature regarding the successful, covalent functionalisation of Ti and IONPs with Teic/glycopeptide antibiotics (Armenia *et al.*, 2018; Berini *et al.*, 2021; Hickok & Shapiro, 2012). In each instance, APTES was used to coat the biomaterial surface with amines, followed by NHS-EDC chemistry in order to conjugate the carboxyl group of Teic to the amine-coated Ti surface. Even though they demonstrated good antibacterial activity against Gram-positive bacteria, the elution of the antibiotic from the surface was not investigated. Moreover, there was a distinct lack of physiochemical analysis (such as XPS, FTIR or QCM) which can aid in the confirmation of the presence/absence of the antibiotic on the modified surface. Given that glycopeptides have a great affinity for TiO_2 and other oxides, it is important to consider these factors (Sheng *et al.*, 2013; Haci Mehmet *et al.*, 2019; Mancera-Artu *et al.*, 2020).

It is possible that the studies mentioned above are looking at the natural and strong affinity of glycopeptide antibiotics to metal oxides and that the antibacterial activity being observed is due to

the antibiotic leaching from the surface. It would also seem that the phosphate present in the bacterial culture medium used in said studies is promoting the elution of the antibiotic from the metal surface. In contrast, a commercially available, covalently functionalised Teic-chiral stationary phase, displayed no antibacterial activity against *S. aureus*, despite it interacting well with N-acetyl-L-lys-D-ala-D-ala.

3.5 Conclusions

This chapter demonstrated the facile adsorption of Teic onto the surface of Ti. In addition, the interaction of Teic binding to the oxide was monitored using a BCA-based assay and parameters including immersion time, attachment robustness, short-term and thermal stability and the impact of phosphate were assessed. Whilst the interaction between Teic and titania was robust, it was found that phosphate resulted in the loss of the antibiotic from the oxide and could explain how the antibiotic is eluting from the Ti surface when culture conditioning the modified metal. Prior to moving back onto covalently attaching Teic to the Ti surface, Teic-modified IONPs and a commercially available Teic-chiral stationary phase were examined to determine if they displayed antibacterial activity whilst immobilised. It was found that the Teic-IONPs did demonstrate excellent antibacterial activity, however when conditioned in the culture medium, elution of Teic was observed. Furthermore, the the TSP was able to bind well to the tripeptide, N-acetyl-lys-D-ala-D-ala, yet despite this, when exposed to *S. aureus* the TSP was unable to display antibacterial activity. To conclude, covalently immobilising the glycopeptide antibiotic to biomaterial surface does not appear to be a viable option. However, the antibacterial activity of Teic against *S. aureus* is beneficial. Moreover, as reported in the previous chapter, Teic was found to enhance 1,25D-stimulated osteoblast maturation which places Teic as a valuable tool in minimising the infection of implanted biomaterials. Therefore, Chapter 4 will focus on controlling the release of Teic using hydrogel technology.

Chapter 4 A Teic-Chitosan-Gelatin Hydrogel Composite for Antibacterial Applications: Proof-of-Concept

In the previous chapter it was found that Teic avidly bound to Ti, however this interaction was reversed by phosphate resulting in antibiotic loss from the Ti surface. Whilst it was tempting to consider a more robust, covalent attachment of Teic to Ti, a commercially available Teic-CSP did not display any antibacterial activity towards *S. aureus*. However, Teic could still find an application in a bone regenerative setting; the antibiotic exhibits great antibacterial activity against *S. aureus* and it supports the maturation of human osteoblasts. Therefore, this chapter focusses on the controlled release of Teic using a hydrogel technology.

4.1 Overview

Hydrogels are water-swollen polymer networks that have exhibited great versatility in encapsulating and delivering therapeutics (Johnson *et al.*, 2018; Cheng *et al.*, 2022). They are defined as crosslinked polymers that possess hydrophilic properties, allowing them to absorb large quantities of water or biological fluids without losing their structure (Ottenbrite *et al.*, 2010; Rodriguez-Rodriguez *et al.*, 2020). These materials offer moderate-to-high, physical, chemical, and mechanical stability in their swollen state and possess a soft consistency similar to living tissues (Ottenbrite *et al.*, 2010; Rodriguez-Rodriguez *et al.*, 2020). Moreover, hydrogels with a three-dimensional crosslinked network display the capability of loading a large number of antimicrobial agents and releasing them locally and in a controlled manner, making them a promising candidate as antimicrobial coatings for the prevention of PJI (Fu *et al.*, 2021; Zhao *et al.*, 2015; Zhang & Huang, 2020; Wei *et al.*, 2019).

Antimicrobial hydrogels can usually be divided into two categories: antifouling hydrogels and bactericidal hydrogel coatings (Fu *et al.*, 2021; Wei *et al.*, 2019). Antifouling coatings are designed with the aim to prevent bacterial attachment and nonspecific protein adsorption, subsequently preventing the formation of a biofilm. These types of coatings are typically made of hydrophilic polymers such as

poly(ethylene glycol) (PEG), zwitterion polymers or poly(N-vinylpyrrolidone) (Wang *et al.*, 2022; Lee *et al.*, 2018; Ding *et al.*, 2012). However, there are currently no coatings that are completely resistant to bacterial attachment over time. Without any biocidal properties, the hydrogel will inevitably become contaminated with bacteria that “break-through” the antifouling polymer layer. Bactericidal hydrogel coatings can provide a more reliable and straightforward solution in preventing biofilm formation. These types of antimicrobial hydrogels are designed to prevent the formation of a biofilm by greatly reducing bacterial viability through either coming into contact with the material surface or by releasing the agents in the local vicinity (Campoccia *et al.*, 2013; Wei *et al.*, 2019). Contact-killing hydrogels utilise surface-attached biocidal agents ranging from natural biomolecules like AMPs and enzymes to synthetic compounds or polymers such as quaternary ammonium compounds (QAC) and various polycations (Jiao *et al.*, 2017; Jain *et al.*, 2014). Whereas release-killing hydrogels commonly use agents like antibiotics, metal nanoparticles and other biocidal agents that are loaded or encapsulated within the hydrogel.

4.2 Gelatin Hydrogels

An important aspect when making these hydrogels is that the material encapsulating the antimicrobial agent is biocompatible and contain no toxic or harmful substances (Lian *et al.*, 2021). Polyamino-acids, proteins and polysaccharides are among the biopolymers that are widely used in biomaterial fabrication. Amidst this, gelatin, a random-coil polypeptide derived from denatured collagen, has been used in studies looking into the controlled release of antimicrobials (Lian *et al.*, 2021; Fang *et al.*, 2020; Nagarajan *et al.*, 2016). Gelatin is a natural biopolymer that is obtained through the hydrolysis of collagen and is an abundant, cheap and non-toxic material approved by the FDA. It consists of -NH₂ and -COOH functionalities which can improve the polymer network structure (Sethi & Kaith, 2022). Moreover, it does not express antigenicity and is highly resorbable and biocompatible (Rodriguez-Rodriguez *et al.*, 2020; Nagarajan *et al.*, 2016; Xing *et al.*, 2014; Massoumi *et al.*, 2019; Rose *et al.*, 2014). One of the ways gelatin hydrogels can be fabricated is through physical crosslinking. Physical

crosslinking can be obtained through specific conditions such as concentration (~2% w/v) or temperature (below 30 °C). However, if the temperature exceeds 35 °C the gelation will be compromised, impacting the physical polymer network. Therefore, physical crosslinking of gelatin hydrogels can lead to poor stability, poor mechanical strength, and low elasticity, which can significantly limit their biological applications at physiological temperatures (37 °C). However, chemically crosslinking the hydrogels could be a solution in improving stability to body temperature and this will be covered in 4.5.

4.3 Chitosan Hydrogels

Chitosan (CS) is a naturally occurring polysaccharide commonly found in the shells of marine crustaceans, arthropod exoskeletons, and the cell walls of fungi (Thein-Han *et al.*, 2009; Di Martino *et al.*, 2005; Miranda *et al.*, 2011). It is obtained from the deacetylation of chitin and is available in various forms which differ in the degree of deacetylation and molecular weight (Seth & Kaith, 2022; Kurita, 2006; Kean & Thanou, 2010). CS has been recognised as having great biomaterial potential due to its biocompatibility, biodegradability, and non-toxicity, along with good mechanical properties, making it a great candidate in the field of tissue regeneration and repair (Fang *et al.*, 2020; Bano *et al.*, 2017; Muxika *et al.*, 2017; Lu *et al.*, 2017). CS is often used in the production of powders, beads, microspheres, microparticles, sponges and hydrogels and are either crosslinked through physical or chemical methods (Ikeda *et al.*, 2014; Rodriguez-Rodriguez *et al.*, 2020). As a natural polysaccharide, it also possesses antibacterial properties as a result of its cationic amino groups, which disrupts mass transport of proteins across the cell wall and interrupts the bacterial membrane (Di Martino *et al.*, 2005; Khor & Yong Lim, 2003). Moreover, CS and its derivatives have demonstrated synergistic activity with a variety of antibiotics (Tin *et al.*, 2010). However, the antibacterial efficacy of the CS-based hydrogel is dependent on the parameters of CS, such as the molecular weight, degree of deacetylation and the concentration of the CS solution (Chung & Chen, 2008; Song *et al.*, 2011; Zheng *et al.*, 2003;

Goy *et al.*, 2009). These factors can also affect biocompatibility of the hydrogel (Yang *et al.*, 2008; Rodrigues *et al.*, 2012).

CS is capable of forming a hydrogel without the need of any additives, yet as with gelatin, physical crosslinking of CS hydrogels comes with limitations such as, low mechanical strength, fragility and high degradation rates in acidic conditions (de Moura *et al.*, 2011). However, blending CS with a synthetic or natural biopolymer, such as gelatin, could provide a simple method for increasing the stability of biopolymer-based hydrogels and improve their mechanical properties (Rodriguez-Rodriguez *et al.*, 2020; Chiellini *et al.*, 2001). Moreover, crosslinking this hydrogel could impart superior mechanical properties and this will be covered in 4.5.

4.4 Composite Hydrogels

Despite the beneficial features the biopolymers exhibit on their own, they display several disadvantages to biomedical applications, such as rapid degradation, low chemical resistance and mechanical strength along with other factors, as mentioned above. One way to improve the stability of these polymers is by blending it with other biopolymers, which can drastically enhance their beneficial properties. Biopolymers that have been reinforced in this way are referred to as composite hydrogels.

The unique combination of CS antimicrobial properties and gelatin's cell adhesion ability has great potential to function as a scaffold for use in orthopaedic applications (Dhandayuthapani *et al.*, 2010). CS possesses primary and secondary hydroxyl groups, along with amino groups that permit the facile modification of the inter- and intramolecular hydrogen bonds. This ease of this modification allows the COOH groups in gelatin to react with the NH₂ groups in CS via Van der Waals or electrostatic interactions, enabling the crosslinking process. From this, CS-gelatin composite hydrogels can provide a good structure for cell growth and proliferation in comparison to their individual counterparts (Shahin *et al.*, 2020; Thein-Han *et al.*, 2009). Moreover, it aids in increasing mechanical strength, stability and the drug encapsulation capacity of CS and gelatin (Fischetti *et al.*, 2020; Naghizadeh *et*

al., 2018). For instance, Mathew & Arumainathan (2022) found that when crosslinking gelatin with CS for the delivery of dopamine hydrochloride, the solubility of CS and the stability of gelatin in aqueous solutions were improved. Moreover, X-Ray diffraction analysis confirmed that the dopamine was encapsulated and that an increase in crystallinity of the composite hydrogel led to an increase in pore size, subsequently enhancing the drug loading capability. However, 93% of the drug eluted within 30 h. Ideally, when using antibiotics in a controlled-release system, the agent should be eluting over the course of 7-14 days in order to prevent the formation of a biofilm. In addition, the concentration of the antibiotic during this time should be above the MBC (Pan *et al.*, 2018). One way to slow the elution rate when using biopolymer-based composite hydrogels is to use a chemical crosslinker to further strengthen the mechanical properties of the composite scaffold.

4.5 Chemical Crosslinkers

The covalent crosslinking of a hydrogel involves a chemical reaction that results in the formation of a strong, stable bond between the crosslinking agent and polymer chains. Compounds that contain at least two functional groups and are capable of eliciting a condensation reaction with the polymer can act as a covalent crosslinker. Chemically crosslinked hydrogels can result in a hydrogel with increased strength and can overcome dissolution in aqueous mediums, even under extreme pH conditions (Rodriguez-Rodriguez *et al.*, 2020; Sethi & Kaith, 2022). The most commonly used covalent crosslinkers for CS and gelatin include, glutaraldehyde, EDC, NHS, citric acid and genipin. Glutaraldehyde (Glut) is one of the most effective, inexpensive, and widely used chemical crosslinking agents (Rodriguez-Rodriguez *et al.*, 2020; Sethi & Kaith, 2022; Akhtar *et al.*, 2016; Baldino *et al.*, 2015). Biopolymers such as CS and gelatin can be crosslinked with Glut, and it can increase the strength of the composite hydrogel over a short period of time. Glut crosslinks the polymers by forming a bond between the amino or hydroxyl groups of the polymers and the aldehyde group in Glut via a Schiff's base reaction. A recent study utilised Glut as a crosslinker for tetracycline-loaded microspheres, integrated into a CS/alginate composite hydrogel. It was found that the cumulative release of tetracycline from the

crosslinked composite came out to ~66% after 14 days in contrast to the hydrogels and microspheres alone (Chen *et al.*, 2017). However, one of the major issues with using Glut as a crosslinker is that it displays cytotoxicity and elicits immunological responses, even when used at low concentrations. Moreover, Glut is not environmentally friendly and can lead to excessive crosslinking, potentially trapping the antimicrobial agent and preventing elution (Hennink & van Nostrum, 2002; Copello *et al.*, 2014; Kavya *et al.*, 2013). It is for this reason that interest has turned to naturally derived chemical crosslinkers that have low toxicity.

Genipin is a natural crosslinking agent extracted from geniposide, which is found in the fruits of *Genipa Americana* and *Gardenia jasminoides Eliis* (Fig. 4.1; Chiono *et al.*, 2008). This particular crosslinker has gained interest due to its low toxicity profile and its ability to react with the amino groups of polymers under mild conditions, resulting in a dark blue pigment (Andrade del Olmo *et al.*, 2022). This leads to a crosslinked structure with added strength and stability, allowing the hydrogel to retain its shape and composition even under physiological conditions. Fang *et al.* (2020) have utilised genipin as a means to crosslink a CS-gelatin composite, loaded with ciprofloxacin, in order to reduce the incidence of sea water immersion and bacterial infection. They found that not only did the crosslinked composite display good and prolonged antibacterial activity against *P. aeruginosa*, *E. coli* and *S. aureus*, it also displayed good biocompatibility and accelerated wound healing in an *in vivo* rat model. Another study found that genipin-crosslinked carboxymethyl (CM)-CS hydrogels, loaded with gentamicin, significantly reduced the growth of *S. aureus* and displayed strong biofilm inhibition (Wu *et al.*, 2014). In addition, the change in genipin concentration had little effect on the antibacterial efficacy of the composite. It was also noted that the CM-CS hydrogel promoted the adhesion, proliferation and differentiation of MC3T3-E1 osteoblast cells, further highlighting the benefits of using genipin as a crosslinker for hydrogel-based biomaterials.

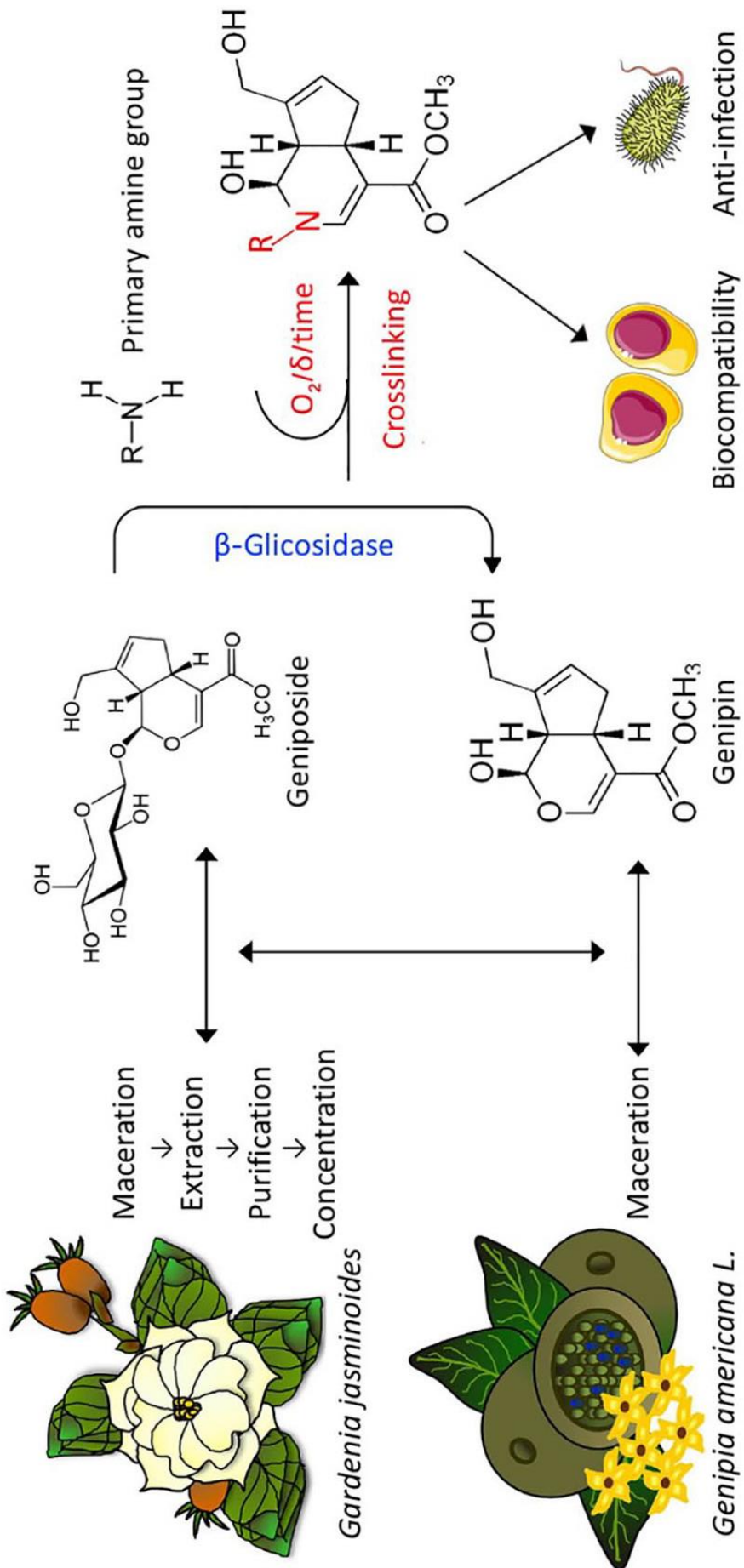


Figure 4.1 Origin of Genipin. Genipin is extracted from the fruits of *Genipia Americana* and *Gardenia jasminoides* Eliis. This natural crosslinker can react with amino groups in natural products. This image was reproduced from Wang et al. (2019) (CC BY 4.0)

This chapter explores the encapsulation of Teic in a gelatin-CS hydrogel composite using Glut and genipin crosslinkers. Initial studies looked at the release kinetics of Teic from a Glut or genipin crosslinked gelatin hydrogel using a disk diffusion assay and hydrogel trypsin digestion. Glut was used as it is a well-known crosslinking agent for gelatin. Moreover Vanc, a glycopeptide antibiotic, has exhibited a steady release from Glut-crosslinked gelatin microspheres (Nouri-Felekori *et al.*, 2019). Optimisation of the Glut or genipin concentration were also assessed to determine if the release of Teic is dependent on the concentration of the crosslinker. Composite hydrogel pucks were characterised by Fourier-Transform Infrared (FT-IR) spectroscopy, and the elution of the antibiotic from the composite scaffold was tracked using a disk diffusion assay and high performance liquid chromatography (HPLC). A mock trabecular bone model was filled with the Teic-loaded composite hydrogel and assessed in the same manner as the composite hydrogel pucks.

4.6 Materials and Methods

4.6.1 Bacterial Strains and Culture Preparation

Bacterial cultures and standards were prepared in the same manner as 2.3.1. The bacterial standards used in this chapter were either used as they were (0.5 McFarland standard; 1×10^7 CFU/ml) or diluted in 1% Peptone/PBS and this was used in all microbiological assays unless specified.

4.6.2 Reagents & Mock Bone Preparation

Gelatin (Gel; Type A, bloom gel strength 300), Teic, Gentamicin (Gent), Vanc, Glut (Grade II; 25% v/v in H₂O), Gen, Trypsin and 4-(2-Hydroxyethyl)piperazine-1-ethanesulfonic acid (HEPES) were purchased from Sigma Aldrich (Gillingham, UK). A 250 mM genipin stock was prepared in dimethyl sulfoxide (DMSO) and refrigerated until required. All other reagents were prepared fresh on the day. Ultrapure, medical-grade, water-soluble CS glutamate (Protosan UP G213) was purchased from Novamatrix (Sandvika, Norway). Mock cancellous bone (130 mm x 180 mm x 40 mm) was obtained from Sawbones™ (Malmo, Sweden). Mock bone was cut into 2 cm x 2 cm x 2 cm squares using a heated hack saw. The samples were sterilised in the laminar flow and sprayed with 70% EtOH and left to dry. Once dried, samples were aseptically transferred to a sterile container until ready for use.

4.6.3 Fabrication of Teic-Gel and Gel Hydrogels

All steps were performed in a laminar flow hood to ensure sterility of the hydrogel.

4.6.3.1 Teic-Glut-Gel and Glut-Gel Pucks

This preparation method has been adapted from Yang *et al.* (2018). A 20% (w/v) Gel stock was made up in 10 ml of deionised H₂O, heated up to 80 °C and allowed to dissolve. Once dissolved, the solution was kept at 60 °C in a water bath until needed. A series of Glut (2, 1, 0.5 and 0.25% v/v) concentrations were made up in 1 ml of HEPES (50 mM; pH 7.4) and 500 µl of each concentration was transferred into a sterile bijou. A 500 µl aliquot of the 20% Gel solution was added to the bijous containing Glut to give a final concentration of 10 % (w/v) Gel and 1, 0.5, 0.25 and 0.125% (v/v) of Glut. These hydrogels

were quickly mixed prior to gelation and left to incubate at room temperature for 2 h to allow for sufficient gelling. After incubation, the Glut-crosslinked hydrogels were immersed in 1 ml of a 0.1 M glycine solution and left to incubate for 2 h at room temperature. This was done to block the residual aldehyde groups on the Glut. The gels were washed with MGW twice and left at room temperature in sterile containers until use. For the Teic-Gel hydrogels, Gel (25% w/v) was reconstituted in 8 ml of deionised H₂O, heated up to 80 °C and allowed to dissolve. Once dissolved, the solution was cooled to 60 °C and 2 ml of a 10 mg/ml solution of Teic in 50 mM HEPES (pH 7.4) was added to the Gel solution, emulsified using a vortexer and left at 60 °C until needed. Crosslinking of the Teic-Gel hydrogel was the same as the process mentioned above (4.6.3.1.1).

4.6.3.2 Teic-Gen-Gel and Gen-Gel Pucks

A 20% (w/v) Gel stock was made up in 10 ml of deionised H₂O, heated up to 80 °C and allowed to dissolve. Once dissolved, the solution was kept at 60 °C in a water bath until needed. A series of Gen (10, 5, 2, and 1 mM) concentrations were made up in 500 µl of HEPES (50 mM; pH 7.4). A 500 µl aliquot of the 20% Gel solution was added to the bijoux containing Gen to give a final concentration of 10 % w/v Gel and 5, 2.5, 1 and 0.5 mM of Gen. The hydrogels were quickly emulsified prior to gelation and left to incubate at room temperature for 24 h to allow for sufficient gelling. After incubation, the Gen-Gel hydrogels were left at room temp in sterile containers until use. For the Teic-Gel hydrogels, Gel was reconstituted in 8 ml of deionised H₂O and allowed to dissolve. The solution was cooled to 60 °C and 2 ml of a 10 mg/ml solution of Teic in 50 mM HEPES (pH 7.4) was added to the Gel solution, emulsified using a vortexer and left at 60 °C until needed. Crosslinking of the Teic-Gel hydrogel was the same as the process mentioned above (4.6.3.1.2).

4.6.4 Effect of Crosslinker Concentration on Teic Elution

This method has been adapted from Fang *et al.* (2020) and Matuschek *et al.* (2013). Teic-Glut-Gel and Teic-Gen-Gel hydrogel pucks containing Teic were immersed in 1 ml of PBS from 2 h up to 7 days. At each time point 1 ml samples were taken and transferred to a sterile centrifuge tube, stored at -20 °C

and hydrogel samples were covered with 1 ml of fresh PBS. Once all the samples were collected, they were defrosted and assessed using a disk diffusion assay. Briefly, an overnight culture of *S. aureus* was standardised in PBS using the 0.5 McFarland Standard. BHIA plates were swabbed with the standardised culture and sterile paper disks (6 mm) were placed on the surface of the agar. A 20 µl aliquot of each sample was carefully placed on the paper disk and allowed to dry. Once dried, plates were inverted and incubated for 24 h at 37 °C. The zones of inhibition (ZOI) were measured the next day using Vernier callipers. Gent-Glut-Gel and Gent-Gen-Gel were used as controls and processed in the same manner as above.

4.6.5 Trypsin Digestion of Teic-Gel Hydrogels

This method was adapted from Lancaster *et al.* (2015). Prepared Teic-Glut-Gel hydrogels were immersed in 1 ml of PBS containing trypsin (750 U/mg) and incubated for 24 h at 37 °C with gentle shaking (100 RPM) to allow for sufficient digestion of the hydrogel. After incubation, the antimicrobial activity of the digested hydrogels was assessed using the disk diffusion assay as mentioned above (4.6.4).

4.6.6. Fabrication of Teic-CS-Gel and CS-Gel Composite Hydrogels

4.6.6.1 Teic-CS-Gel and CS-Gel Pucks

A 50% (w/v) Gel and 5% (w/v) CS stock were made up in 100 ml of deionised H₂O, heated up to 80 °C and allowed to dissolve. The composite hydrogel was made by combining 4 ml of CS (5% w/v) and 4 ml of Gel (50% w/v) to either 2 ml of MGW or 2 ml of a 10 mg/ml stock of Teic to a final volume of 10 ml. The control hydrogels were made in a similar manner by combining either 4 ml of CS or Gel to 4 ml of MGW with 2 ml of MGW or 2 ml of a 10 mg/ml stock of Teic to a final volume of 10 ml. These solutions were further diluted (1:2) in MGW to give a final concentration of 1 mg/ml Teic, 1% w/v of CS and 10% w/v Gel. A small aliquot of Gen was added to the composite solution to achieve a final concentration of 2.5 mM and 1 ml aliquots were quickly transferred to sterile bijous and allowed to gel overnight at room temp.

4.6.6.2 Injection of Teic-CS-Gel Hydrogel into a Mock Bone Model

The formation and crosslinking of the hydrogel were prepared in the same manner as 4.6.6.1. After the addition of the crosslinker, 5 ml of the hydrogel was taken up with a syringe and carefully injected into mock bone that had been wrapped in sterilised parafilm (see Appendix I). After the hydrogel was injected into the mock bone, the samples were transferred into 50 ml sterile centrifuge tubes and incubated for 24 h under ambient conditions, on a roller (60 RPM). Once the hydrogels in the mock bone had set, the parafilm was carefully taken off the mock bone using sterile forceps, as demonstrated in Appendix 1 and transferred to new 50 ml sterile centrifuge tubes.

4.6.7 Antibacterial Synergy Assessment of CS and Teic

Antibacterial synergy of Teic and CS were assessed using a checkerboard assay in a 96-well microtiter plate and was adapted from Bajaksouzian *et al.* (1997). Both CS and Teic were tested at final concentrations of 1-128 µg/ml. Double dilutions of both the antibiotic as well as the polysaccharide were used for the assay according to the EUCAST recommendations for MIC testing. Aliquots (50 µl) of 1% peptone/PBS were aseptically dispensed across all test wells prior to dilution. The polysaccharide was serially diluted along the abscissa (rows), whilst the antibiotic was diluted down the ordinate (columns). A series of Teic concentrations and a series of CS concentrations alone were used as controls. A standard of *S. aureus* (0.5 McFarland standard) was made and diluted 1:10 with 1% peptone/PBS. A 100 µl aliquot of the diluted standard was dispensed into test and control wells to give a final density of approx. 5×10^5 cfu/ml. The plates were incubated overnight for 24 h at 37 °C. Fractional inhibitory concentrations (FICs) were calculated as the MIC of drug A (Teic) or B (CS) in combination, divided by the MIC of drug A or B alone, and the FIC index was obtained by adding the FICs. FIC indices (FICI) were interpreted as synergistic when values were ≤ 0.5 , indifferent when values were > 0.5 to 4 and antagonistic when the values are > 4 (Bajaksouzian *et al.*, 1997).

4.6.8 Characterisation of the Crosslinked Composite Hydrogels loaded with Teic using FT-IR

This method was adapted from Cassimjee *et al.* (2022). The chemical structure of Teic-CS-Gen-Gel, Teic-CS-Gel, CS-Gen-Gel, CS-Gel hydrogels were assessed using FT-IR. Hydrogels were measured with a Spectrum Two FT-IR Spectrophotometer (PerkinElmer, Massachusetts, USA) by collecting 5 accumulative scans/second in the 4000-600 cm^{-1} region and using a lithium tantalate (LiTaO_3) MIR detector. The stage for the sample was cleaned with ethanol prior to analysis and a background spectrum was obtained. The FT-IR spectra was scanned at 4 cm^{-1} resolution and the signals were averaged. The spectra obtained were plotted using Origin statistical software (Massachusetts, US).

4.6.9 *In vitro* release of Teic from Composite Hydrogels – HPLC Analysis

4.6.9.1 Composite Hydrogel Pucks

This method was adapted from Tsai *et al.* (2009). Teic-CS-Gel and CS-Gel hydrogel pucks were immersed in 1 ml of PBS from 2 h up to 7 days. At each time point 1 ml samples were taken and transferred to a sterile centrifuge tube, stored at $-20\text{ }^\circ\text{C}$ and composite hydrogel samples were covered with 1 ml of fresh PBS. Once all the samples were collected, they were defrosted and assessed using HPLC. The concentration of Teic released from the composite hydrogels was determined using a ThermoFisher Vanquish HPLC system (ThermoFisher, Waltham, MA, US) coupled to a UV detector. The separation was performed using an Agilent Eclipse AAA column (150 mm x 4.6 mm; 5 μM), at a column temperature of $25\text{ }^\circ\text{C}$ and a flow rate of 1 ml/min in a mobile phase consisting of water (HPLC grade with 0.1% formic acid; mobile phase A) and acetonitrile (HPLC grade with 0.1% formic acid; mobile phase B). The detection wavelength for UV was at 220 nm. A calibration curve of total Teic concentrations in 95/5 % mobile phase A/B was constructed using twelve concentrations in the range of 0.1-100 $\mu\text{g/ml}$. The concentration of Teic in the hydrogel samples was extrapolated using the peak area of the Teic A2-2 component against the calibration curve.

4.6.9.2 Composite Hydrogel in a Mock Bone Model

This method was adapted from Fang *et al.* (2020). The mock bone samples were immersed in 20 ml of PBS from 2 h up to 7 days. At each time point, 1 ml samples were taken and stored at -20 °C and hydrogel samples were covered with 1 ml of fresh PBS. Once all the samples were collected, they were defrosted and assessed in the same manner as 4.6.9.1.

4.6.10 *In vitro* release of Teic from Composite Hydrogel – Disk Diffusion Assay

4.6.10.1 Composite Hydrogel Pucks

Teic-CS-Gel and CS-Gel hydrogel pucks were immersed in 1 ml of PBS from 2 h up to 7 days. At each time point 1 ml samples were taken and transferred to a sterile centrifuge tube, stored at -20 °C and composite hydrogel samples were covered with 1 ml of fresh PBS. Once all the samples were collected, they were defrosted and assessed in the same manner as 4.6.4.

4.6.10.2 Composite Hydrogel in a Mock Bone Model

The mock bone samples were immersed in 20 ml of PBS from 2 h up to 7 days. At each time point, 1 ml samples were taken and stored at -20 °C and hydrogel samples were covered with 1 ml of fresh PBS. Once all the samples were collected, they were defrosted and assessed in the same manner as 4.6.4.

4.6.11 Statistical Analysis

Unless stated otherwise, all experiments above were repeated three times in triplicate. All data were subject to a normality test to ensure data were normally distributed. A one- or two-way analysis of variance (ANOVA) or Kruskal-Wallis test was used, where appropriate, to test for statistical significance using Graphpad Prism (Version 8; San Diego, CA, USA) with $p < 0.05$ regarded as being statistically significant. When $p \leq 0.05$ was found, a Tukey or Sidak's multiple comparisons post-test was used between all groups. All data are expressed as the mean together with the standard deviation.

4.7 Results

4.7.1 Effect of the Crosslinker Concentration on Teic Elution from Gel Hydrogels

4.7.1.1 Glut Concentration

The impact of Glut concentration on the release of Teic from the Gel hydrogel was assessed using a disk diffusion assay. Interestingly, it appears that Glut significantly affects the release of Teic from the hydrogel when compared to the Teic-Gel control (Fig. 4.2; $p < 0.0001$) and it is clear that the release of Teic from the Glut-crosslinked Gel is not concentration dependent. Conversely, Gent was successfully released from the crosslinked Gel, and it was demonstrated that the release of Gent was dependent on the concentration of the crosslinker (data not shown).

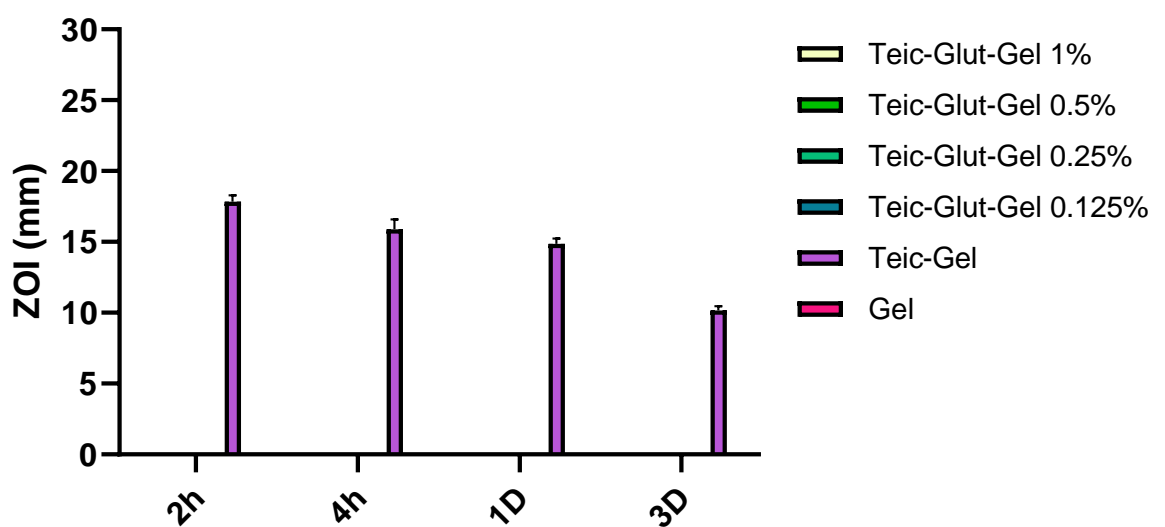


Figure 4.2 Effect of Glut Concentration of the Elution of Teic from Gel Hydrogels. A 500 μ l solution of Gel (20% w/v) and Teic (2 mg/ml) in HEPES (50 mM; pH 7.4) was mixed with 500 μ l of Glut (2, 1, 0.5 and 0.25 % v/v) and allowed to crosslink for 2 h. Once allowed to crosslink, the remaining aldehyde groups were blocked using a 1 ml solution of 0.1 M glycine and left to incubate at room temperature for 2 h. After incubation, hydrogels were washed twice with dH₂O and immersed in a 1 ml solution of PBS from 2 h up to 7 days. At each time point, 1 ml samples were taken and stored at -20 °C and hydrogels were covered with 1 ml of fresh PBS. Once all the samples were collected, samples were defrosted and used in a disc diffusion assay. Briefly, *S. aureus* was standardised in PBS using the 0.5 McFarland standard. BHA plates were swabbed with the standardised culture and sterile paper discs (6 mm) were placed on the surface of the agar. A 20 μ l aliquot of each sample were carefully placed on the paper disk and allowed to dry. Once dried, plates were inverted and incubated for 24 hours at 37 °C. The zones of inhibition (ZOI) were measured the next day using Vernier callipers. It is clear that the elution of Teic is not dependent on the concentration of Glut. All data (mean \pm SD; N = 18) represent pooled triplicate runs from 3 independent experiments. $p < 0.0001$ (****)

4.7.1.2 Trypsin Digestion of Teic-Glut-Gel Hydrogel

From the results provided in 4.7.1.1 it was theorised that the antibiotic was trapped within the hydrogel and so a trypsin digest was performed on the Teic-Glut-Gel pucks to determine if the antibiotic still remained active once the hydrogel was digested. It was found that the digested Teic-Glut-Gel did demonstrate antibacterial activity when compared to the undigested crosslinked Teic-Gel and Teic-Gel control (Fig. 4.3). However, there was a significant reduction in the ZOI when compared to the Teic-Gel control ($p < 0.0001$), suggesting that the crosslinker is impacting the antibacterial activity of the antibiotic.

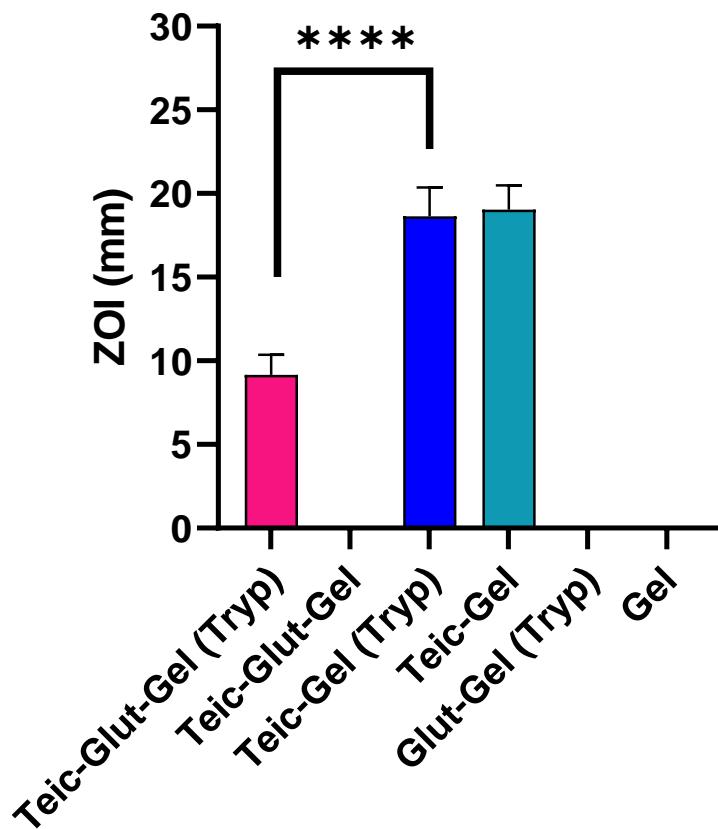
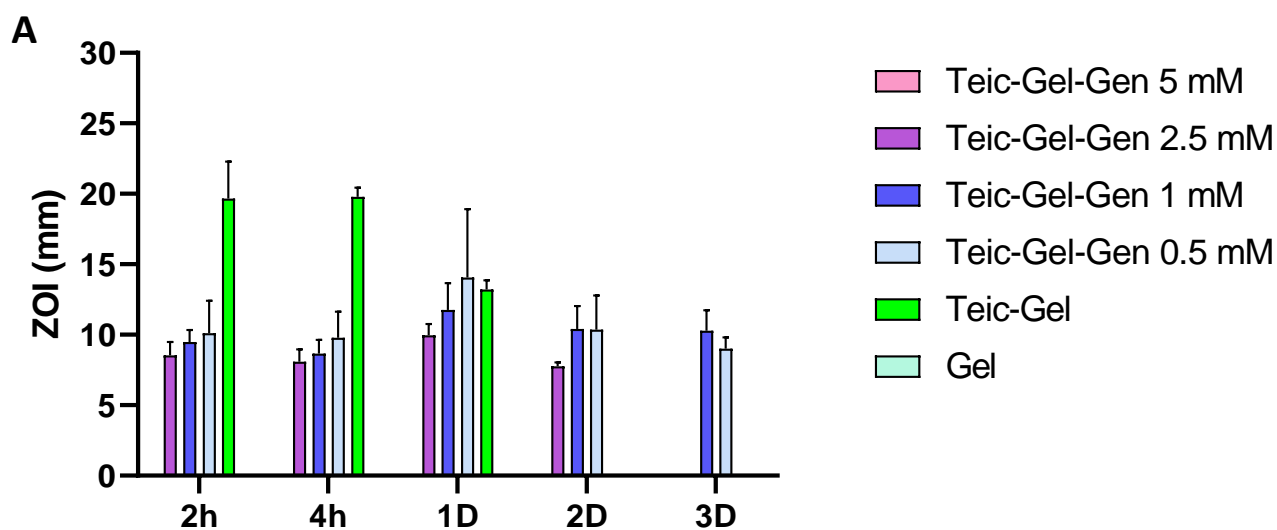


Figure 4.3 Evidence of Teic Recovery from Trypsinised Hydrogels. A 500 μ l solution of Gel (20% w/v) and Teic (2 mg/ml) in HEPES (50 mM; pH 7.4) was mixed with 500 μ l of Glut (0.5 % v/v) and allowed to crosslink for 2 h. Once crosslinked, the remaining aldehyde groups were blocked using a 1 ml solution of 0.1 M glycine and left to incubate at room temperature for 2 h. After incubation, hydrogels were washed twice with dH₂O and submerged in a 1ml solution of trypsin (750 U/mg) in PBS and incubated for 24 h at 37 °C with gentle shaking (100 RPM). After incubation, antimicrobial activity was assessed using the disc diffusion assay and was performed and zones measured in the same manner as Fig 4.2. It is clear that the antibiotic was trapped within the hydrogel. All data (mean \pm SD; N = 18) represent pooled triplicate runs from 3 independent experiments. $p < 0.0001$ (****)

4.7.1.3 Effect of the Gen Concentration on the Elution of Teic from Gel Hydrogels

The impact of Gen concentration on the release of Teic from the Gel hydrogel was assessed using a disk diffusion assay. From what can be seen in Fig. 4.4, it is clear that Teic is eluting from the Gen-crosslinked hydrogels and that the elution is a function of the Gen concentration. Using a Gen concentration of 5 mM seems to restrict the release of Teic as no ZOI was observed at any of the time points tested. The concentrations between 2.5 and 1 mM not only permitted the release of Teic, but it demonstrated a gradual release of the antibiotic. However, it does appear that the elution of the antibiotic can be inconsistent given the variation in the size of the error bars and is particularly notable with the lower concentrations of Gen. From the information provided in this assessment, future elution studies will use a Gen concentration of 2.5 mM.



B



Figure 4.4 Effect of Gen concentration on the elution of Teic from Gel Hydrogels. **A.** Gen-Gel hydrogels were formed by combining a 20% gelatin (w/v) and 2 mg/ml Teic solution (500 μ l) to various concentrations of Gen (5 – 0.5 mM) in HEPES (500 μ l). These were allowed to crosslink overnight. Once crosslinked, the hydrogels were immersed in a 1 ml solution of PBS from 2 h up to 3 days. At each time point 1 ml samples were taken and stored at -20 $^{\circ}$ C and hydrogels were covered with 1 ml of fresh PBS. Once all the samples were collected, samples were defrosted and used in a disc diffusion assay. Briefly, *S. aureus* was standardised in PBS using the 0.5 McFarland standard. BHIA plates were swabbed with the standardised culture and sterile paper discs (6 mm) were placed on the surface of the agar. A 20 μ l aliquot of each sample were carefully placed on the paper disc and allowed to dry. Once dried, plates were inverted and incubated for 24 hours at 37 $^{\circ}$ C. The zones of inhibition (ZOI) were measured the next day using Vernier callipers. Gel hydrogels with Gen only were used as controls (not shown here). **B.** Teic-Gen-Gel pucks casted in sterilised bijous (From the left: Teic-Gel, Teic-Gen-Gel (0.5 mM), Teic-Gen-Gel (1 mM), Teic-Gen-Gel (2.5 mM), Teic-Gen-Gel (5 mM), Gen-Gel (5mM), Gen-Gel (2.5 mM), Gen-Gel (1 mM), Gen-Gel (0.5 mM), Gel). The release of Teic from the hydrogel pucks is dependent on the concentration of Gen. All data (mean \pm SD; N = 18) represent pooled triplicate runs from 3 independent experiments

4.7.2 Antibacterial Synergy of CS and Teic

To determine if CS had any antibacterial synergy with Teic a checkerboard assay was performed in a microtiter plate and the MICs obtained after 24 h incubation at 37 °C. The checkerboard assay (Table 4.1) yielded indifferent indices (> 0.5) against all concentrations tested. Interestingly, the CS control presented growth at all concentrations tested, with no inhibition observed.

Table 4.1 Synergistic Activity of Teic and CS. Antibacterial synergy of Teic and CS were assessed using a checkerboard assay in a 96-well microtiter plate. Both Teic and CS were tested at final concentrations of 1-128 µg/ml. Double dilutions of both the antibiotic and the polysaccharide were used for the assay. Aliquots (50 µl) of 1% peptone/PBS were aseptically dispensed across all test wells prior to dilution. A series of Teic concentrations and a series of CS concentrations alone were used as controls. A standard of *S. aureus* (0.5 McFarland standard) was made and diluted to give a final density of approx. 5 x10⁵ CFU/ml. The plates were incubated overnight for 24 h at 37 °C. The FICI indicate an indifferent result, no synergistic or antagonistic activity was observed. All data represent pooled triplicate runs from 3 independent experiments.

	Agent	MIC (µg/ml)		FIC	FICI	Interpretation
		Alone	Combination			
<i>S. aureus</i>	Teic	1	1	1	1.007	Indifferent
	CS	> 128	1	0.007		

4.7.3 FT-IR Analysis of Composite Hydrogels

The recorded FT-IR spectra of the Teic-CS-Gen-Gel (TCGG) and CS-Gen-Gel (CGG) displayed the characteristic amine (NH) and hydroxyl (OH) stretching overlap at 3308 and 3298 cm^{-1} , respectively due to the presence of water. Bands observed at ~ 1080 and 1036 cm^{-1} (C-O stretching vibrations) are typical of the CS polysaccharide structure (Fernandes Queiroz *et al.*, 2014), whilst the band observed at 1552 cm^{-1} showed a characteristic band of Gel, represented by a bending vibration of NH and stretching vibrations of C-N groups (Das *et al.*, 2017) (data not shown). A carbonyl (C=O) stretch vibration at 1638 cm^{-1} and a slight increase in the OH bending vibrations at 1458 and 1464 cm^{-1} , respectively was observed for both crosslinked samples (CGG and TCGG) when compared to CS-Gel (CG) only (Fig. 4.5) which had a less intense band at 1640 cm^{-1} . However, there are little differences observed overall, between the uncrosslinked and crosslinked samples. In the Teic powder spectrum (Fig. 4.5A), the characteristic peaks of NH and OH stretching were present at 3262 cm^{-1} , 2926 and 2858 cm^{-1} demonstrated C-H stretching of aliphatic groups, 1648 cm^{-1} indicated C=O stretching and the bands at 1510 and 1428 cm^{-1} indicated aromatic C=C stretching (Amiri *et al.*, 2020). Yet, interestingly, no characteristic peaks of Teic were observed in modified hydrogel samples.

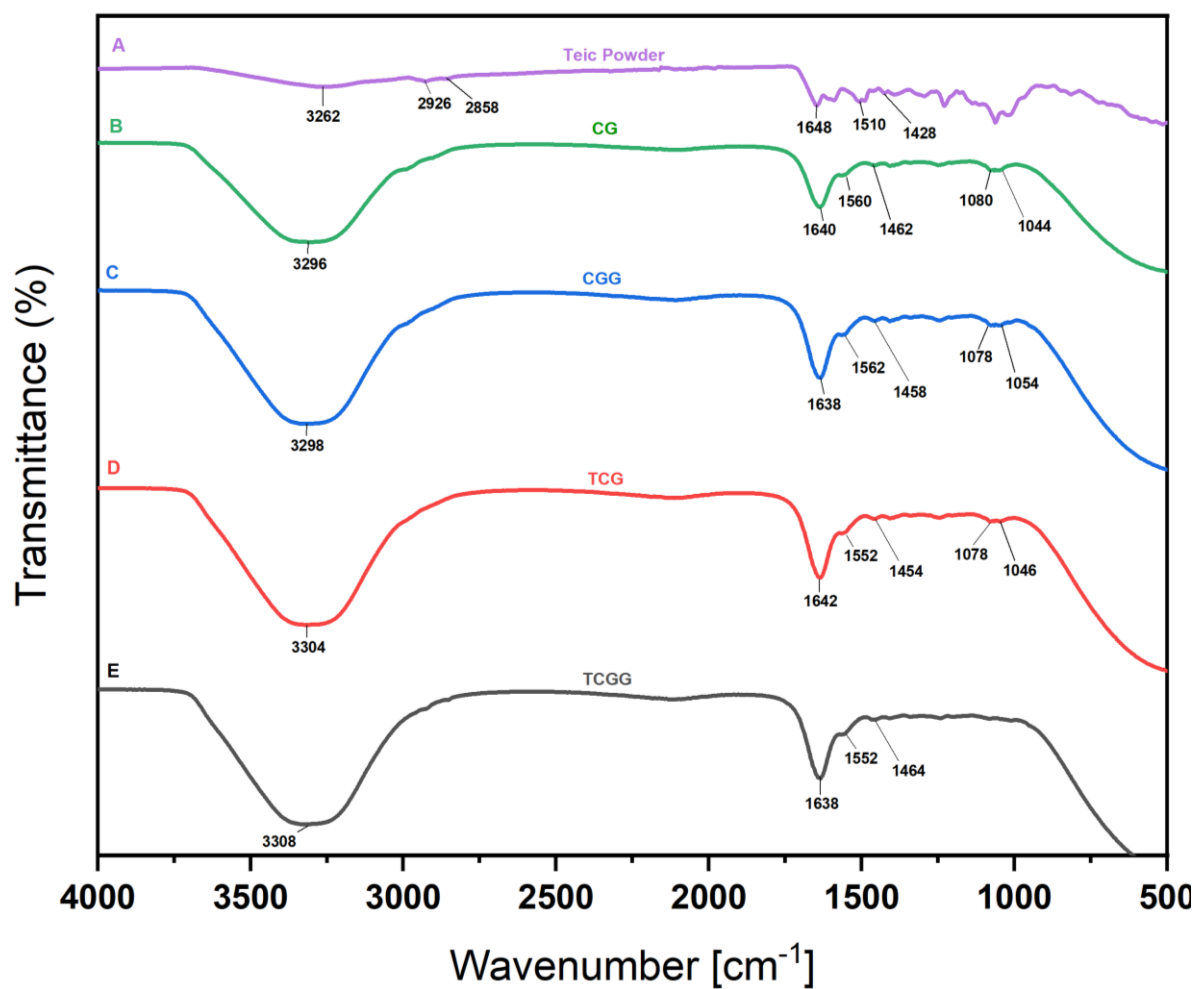


Figure 4.5 Characterisation of the composite hydrogels using FTIR. A. Teic Powder; B. CS-Gel (CG); C. CS-Gen-Gel (CGG); D. Teic-CS-Gel (TCG) and E. Teic-CS-Gen-Gel (TCGG). It is evident that the addition of Gen results in an increase in the intensity peaks at 1640 cm^{-1} and at 1458 and 1464 cm^{-1} .

4.7.4. *In vitro* release of Teic from Composite Hydrogel Pucks

4.7.6.1 Disk Diffusion Assay

To determine the antibacterial activity of the composite hydrogel a disk diffusion assay was used. Samples (20 μ l) were taken at pre-determined time points, plated onto BHIA inoculated with *S.aureus* and incubated for 24 h at 37 °C. As seen in Fig. 4.6 it is clear that all the Teic-modified hydrogels inhibited *S.aureus*. However, it appears that Teic-CS-Gen-Gel (Fig. 4.6A) had a lower ZOI at 2 h (12.7 ± 3.83 mm) when compared to Teic-CS-Gel (Fig 4.6B), Teic-Gen-CS (Fig. 4.6D) and Teic-Gel (Fig. 4.6E) which had ZOIs of 16.4 ± 3.69 , 16.9 ± 5.37 and 17 ± 0.82 mm, respectively. Teic-CS-Gen-Gel appears to have similar ZOIs across all time points tested, with only a moderate reduction in ZOI after 7 days (7.26 ± 0.30 mm) when compared to 2 h (12.7 ± 3.83 mm). Teic-Gen-Gel also had similar ZOIs over the course of 3 days, indicating a steady release of Teic. However, no ZOIs were observed after 5 and 7 days. As anticipated, the Teic-CS-Gel and Teic-Gel had a significant reduction in ZOI after 7 days (no ZOI detected) when compared to 2 h (16.4 ± 3.69 and 17 ± 0.82 mm; $p < 0.0001$). Interestingly, Teic-Gen-CS had a similar release pattern to the uncrosslinked samples, with a decrease in ZOI observed over time.

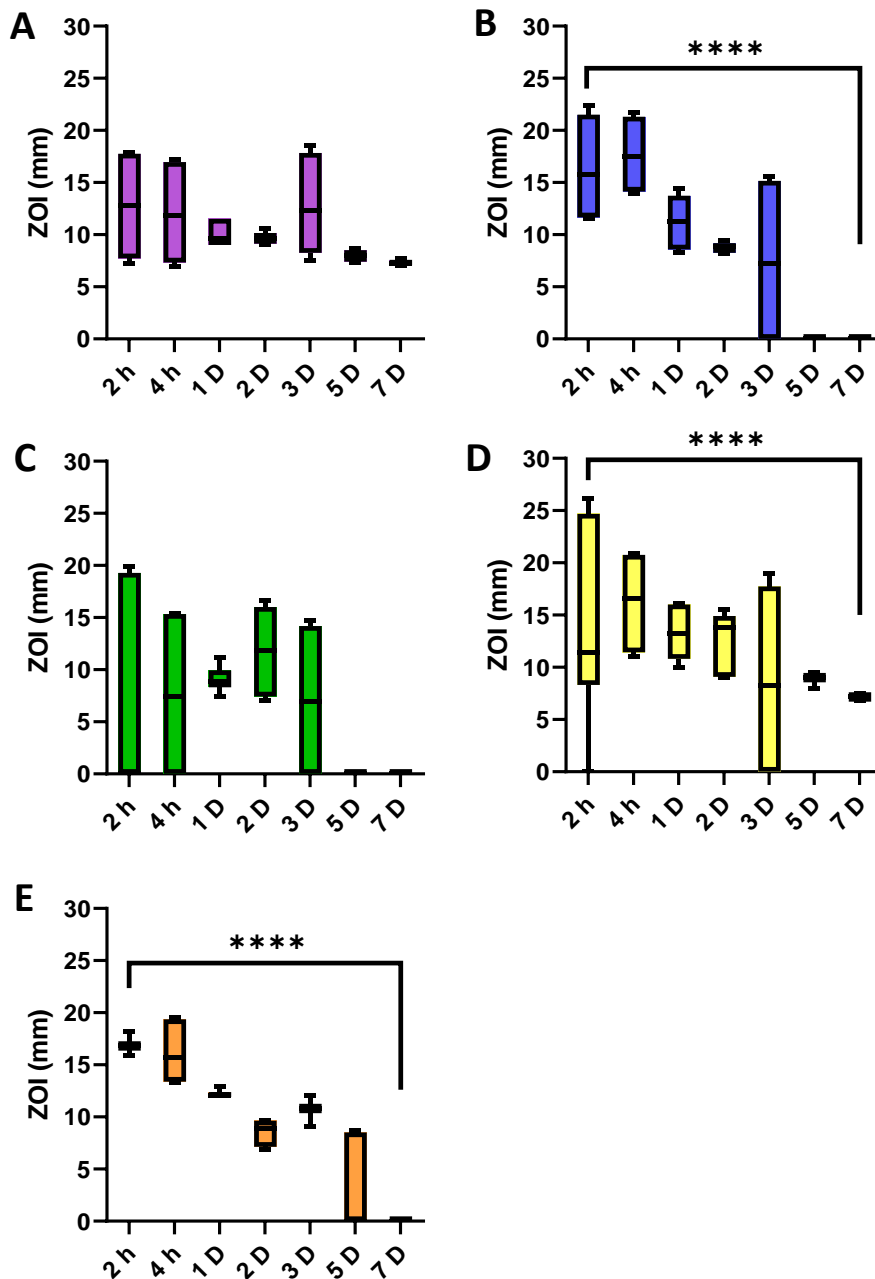


Figure 4.6 *In vitro* release of Teic from Composite Hydrogel Pucks – Disk Diffusion Assessment. CS-Gen-Gel hydrogels were formed by combining a 20% (w/v) Gel, 2% (w/v) CS and 2 mg/ml Teic solution (500 μ l) to 2.5 mM Gen in HEPES (500 μ l) giving a final concentration of 10% (w/v) Gel, 1% (w/v) CS and 1 mg/ml Teic. These were allowed to crosslink overnight. Once crosslinked, the hydrogels were immersed in a 1 ml solution of PBS from 2 h up to 7 days. At each time point 1 ml samples were taken and stored at -20 $^{\circ}$ C and hydrogels were covered with 1 ml of fresh PBS. Once all the samples were collected, samples were defrosted and used in a disc diffusion assay. Briefly, *S. aureus* was standardised in PBS using the 0.5 McFarland standard. BHIA plates were swabbed with the standardised culture and sterile paper discs (6 mm) were placed on the surface of the agar. A 20 μ l aliquot of each sample were carefully placed on the paper disk and allowed to dry. Once dried, plates were inverted and incubated for 24 hours at 37 $^{\circ}$ C. The zones of inhibition (ZOI) were measured the next day using Vernier callipers. Hydrogels with Gen only were used as controls (not shown here). **A.** Teic-CS-Gen-Gel; **B.** Teic-CS-Gel; **C.** Teic-Gen-Gel; **D.** Teic-Gen-CS; **E.** Teic-Gel. All data (mean \pm SD; N = 18) represent pooled triplicate runs from 3 independent experiments. $p < 0.0001$ (****)

4.7.6.2 HPLC Analysis

To further ascertain the antibiotic release ability of the hydrogels and to quantify the antibiotic concentration, Teic released from the composite hydrogels were assessed using HPLC. It is clear that the Teic-loaded composite (TCGG; Fig 4.7A) demonstrates a sustained release of the antibiotic when compared to the uncrosslinked samples, with only 85.1 μg (8.5%) of the antibiotic released from TCGG after 1 day. In contrast, TCG and TG had released 204.7 μg (20.4 %) and 202 μg (20.2%) of the antibiotic after 1 day, respectively, and is indicative of a burst release. TGG had a slightly lower release profile after 1 day, with only 61.3 μg (6.13%) released when compared to TCGG. After the incubation period, most of the antibiotic remained within the TCGG hydrogel scaffold, with around 830 μg (83%) of the antibiotic still present in the hydrogel after 7 days (Fig 4.7B). In addition, the TGG scaffold only released around 127.5 μg , in total, with around 868.4 μg (86.8%) still within the hydrogel scaffold after 7 days incubation. In contrast, TCG had 794 μg (76.4 %) and TG had 786 μg (78.6 %) remaining after 7 days. Interestingly, TGen-CS released more antibiotic than then uncrosslinked samples with only 675.3 μg (67.5%) remaining after a week.

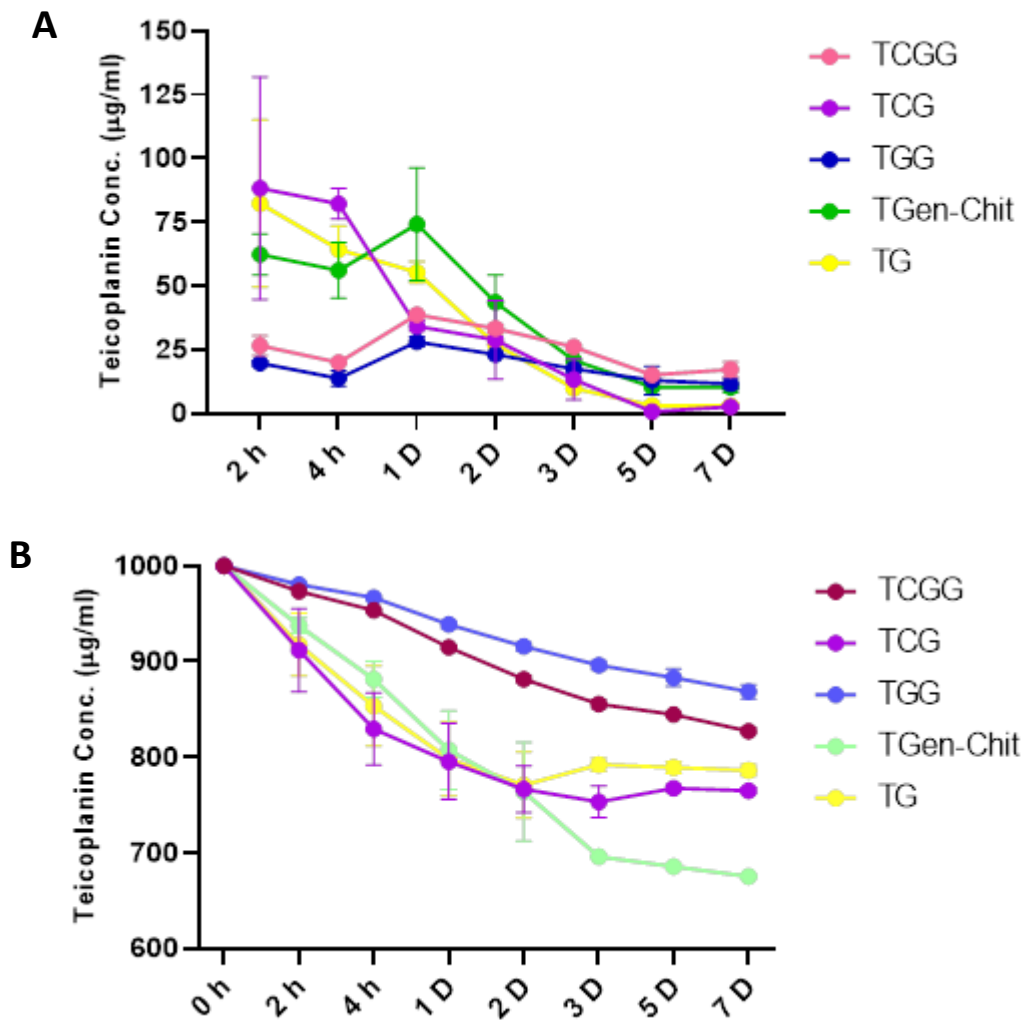


Figure 4.7 In vitro release of Teic from Composite Hydrogel Pucks – HPLC Analysis. CS-Gen-Gel hydrogels were formed by combining a 20% (w/v) Gel, 2% (w/v) CS and 2 mg/ml Teic solution (500 µl) to 2.5 mM Gen in HEPES (500 µl) giving a final concentration of 10% (w/v) Gel, 1% (w/v) CS and 1 mg/ml Teic. These were allowed to crosslink overnight. Once crosslinked, the hydrogels were immersed in a 1 ml solution of PBS from 2 h up to 7 days. At each time point 1 ml samples were taken and stored at -20 °C and hydrogels were covered with 1 ml of fresh PBS. Once all the samples were collected, samples were defrosted and the concentration of Teic was determined using HPLC. All data (mean ± SD; N = 9) represent pooled triplicate runs from 3 independent experiments. **A.** Average Teic release (µg/ml) **B.** Cumulative Teic release (µg/ml)

4.7.5. *In vitro* release of Teic from Composite Hydrogels in a Mock Bone

Model

4.7.7.1 Disk Diffusion Assay

Sawbones™ foams were utilised as a cancellous bone model, to assess how the hydrogel might release the antibiotic when injected within the cancellous bone surrounding the implant. Mock bone cubes (2 cm x 2 cm) injected with the Teic-loaded composite hydrogel were immersed in PBS for 7 days at 37 °C and samples (20 µl) were taken at pre-determined time points, plated on to BHIA inoculated with *S. aureus* and incubated for 24 h at 37 °C. It is evident that there is a difference in the initial release of Teic between the crosslinked and uncrosslinked samples (Fig. 4.8). No ZOI was observed for Teic-CS-Gen-Gel, Teic-Gen-Gel and Teic-Gen-CS after 2 h of incubation, whereas Teic-CS-Gel had a ZOI of 12 ± 0.83 mm and Teic-Gel had a ZOI of 17.7 ± 2 mm. However, it is interesting to note that after 4 h, no significant differences were observed between the ZOIs of the crosslinked and uncrosslinked samples, even up to 7 days.

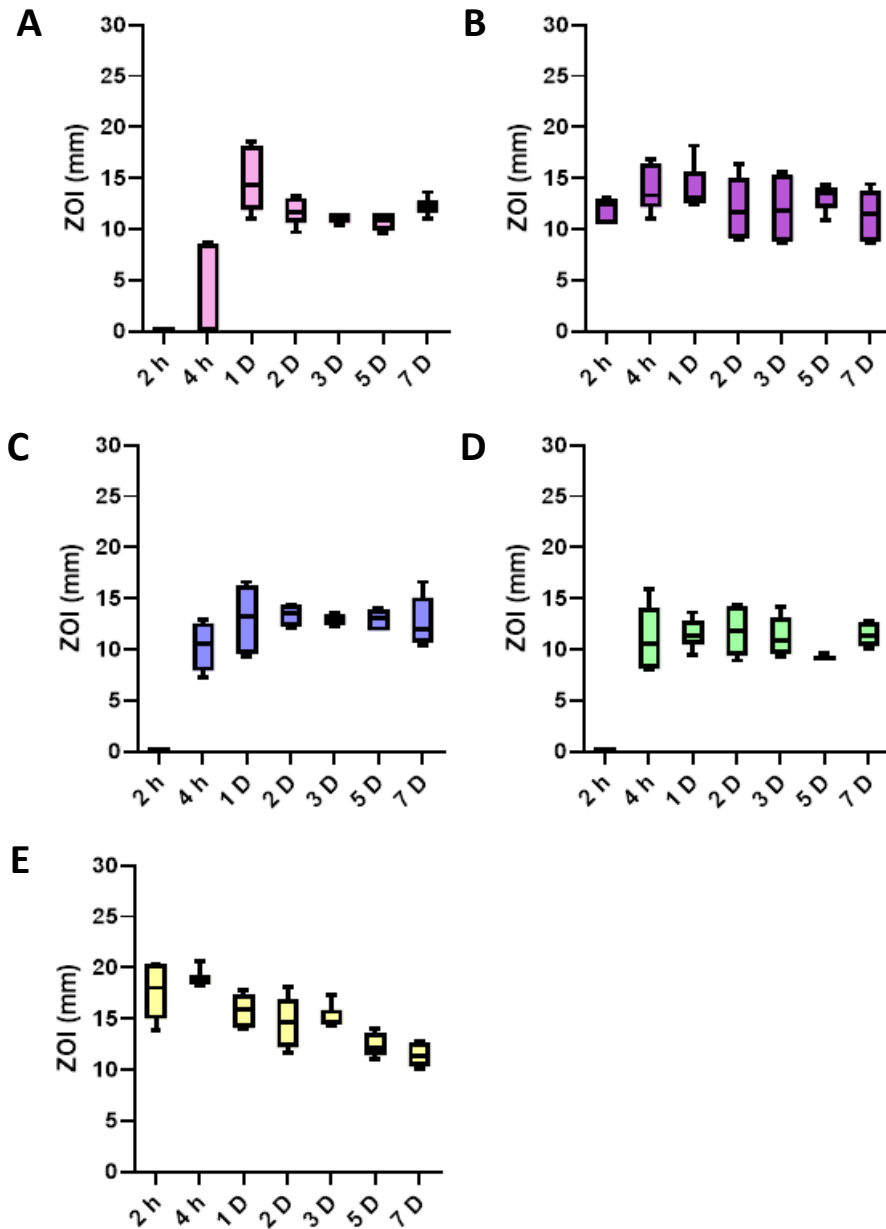


Figure 4.8 *In vitro* release of Teic from Composite Hydrogel in a Mock Bone Model – Disk Diffusion Assessment. CS-Gen-Gel hydrogels were formed by combining a 20% (w/v) Gel, 2% (w/v) CS and 2 mg/ml Teic solution (500 μ l) to 2.5 mM Gen in HEPES (500 μ l) giving a final concentration of 10% (w/v) Gel, 1% (w/v) CS and 1 mg/ml Teic. The hydrogel solution was injected into the mock bone and allowed to crosslink overnight. Once crosslinked, the hydrogels were immersed in a 1 ml solution of PBS from 2 h up to 7 days. At each time point 1 ml samples were taken and stored at -20 $^{\circ}$ C and hydrogels were covered with 1 ml of fresh PBS. Once all the samples were collected, samples were defrosted and used in a disc diffusion assay. Briefly, *S. aureus* was standardised in PBS using the 0.5 McFarland standard. BHA plates were swabbed with the standardised culture and sterile paper discs (6 mm) were placed on the surface of the agar. A 20 μ l aliquot of each sample were carefully placed on the paper disc and allowed to dry. Once dried, plates were inverted and incubated for 24 hours at 37 $^{\circ}$ C. The zones of inhibition (ZOI) were measured the next day using Vernier callipers. Hydrogels with Gen only were used as controls (not shown here). **A.** Teic-CS-Gen-Gel; **B.** Teic-CS-Gel; **C.** Teic-Gen-Gel; **D.** Teic-Gen-CS; **E.** Teic-Gel (mean \pm SD; N = 18) represent pooled triplicate runs from 3 independent experiments.

4.7.7.2 HPLC Analysis

To quantify the concentration of the antibiotic released from the hydrogel at the pre-determined time points, HPLC was employed. After 2 h TCGG, TGG and TGen-CS had only released 8.9 μg (0.89%), 8.46 μg (0.85%) and 11.12 μg (1.11%) respectively after 2 h incubation (Fig 4.9A). Whereas TCG and TG released 29.2 μg (2.92%) and 39.3 μg (3.93%), respectively during the first 2 h. This trend was still observed after 1 day of incubation with TCGG releasing 43.2 μg (4.32%), TGG releasing 37.6 μg (3.76%) and TGen-CS releasing 58.5 μg (5.85%). In contrast, the uncrosslinked samples released 75 μg (7.5%; TCG) and 117 μg (11.7%; TG) of Teic after 1 day and is indicative of a burst release (Fig. ?B). It is worth noting that after 1 day, no significant differences in the release of Teic were found between the crosslinked and uncrosslinked samples, even up to 7 days (Fig. 4.9A) and concurs with the results found in Fig. 4.8. However, there are differences between the crosslinked and uncrosslinked samples when looking at the overall reduction of Teic from the starting concentration (Fig. 4.9B). After 7 days most of the antibiotic remained within the crosslinked composite scaffolds, with TCGG having 856.6 μg (86%), TGG having 918.1 μg (92%) remaining and TGen-CS having 836 μg (84%) left. In contrast, the uncrosslinked samples had released more of the antibiotic over the course of 7 days with only 798.4 μg (79.8%) and 753.4 μg (75.3%) remaining for TCG and TG, respectively.

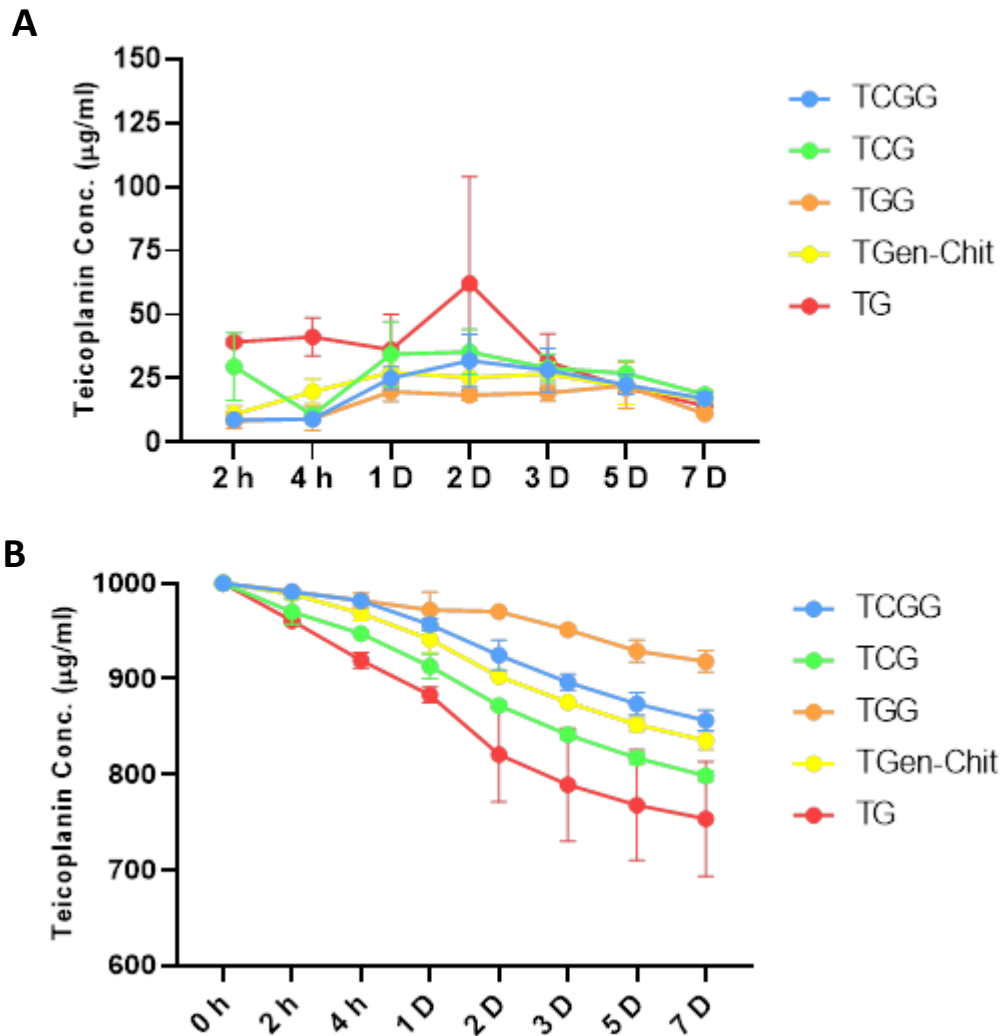


Figure 4.9 *In vitro* release of Teic from Composite Hydrogel in a Mock Bone Model – HPLC Analysis. CS-Gen-Gel hydrogels were formed by combining a 20% (w/v) Gel, 2% (w/v) CS and 2 mg/ml Teic solution (500 µl) to 2.5 mM Gen in HEPES (500 µl) giving a final concentration of 10% (w/v) Gel, 1% (w/v) CS and 1 mg/ml Teic. The hydrogel solution was injected into the mock bone and allowed to crosslink overnight. Once crosslinked, the hydrogels were immersed in a 1 ml solution of PBS from 2 h up to 7 days. At each time point 1 ml samples were taken and stored at -20 °C and hydrogels were covered with 1 ml of fresh PBS. Once all the samples were collected, samples were defrosted and the concentration of Teic was determined using HPLC. All data (mean ± SD; N = 9) represent pooled triplicate runs from 3 independent experiment. **A.** Average Teic release (µg/ml) **B.** Cumulative Teic release (µg/ml)

4.8 Discussion

Reducing the risk of infection due to contamination of implanted materials continues to be a research priority in contemporary material science research (Britton *et al.*, 2022). The covalent grafting of suitable antimicrobials was seen as a potential solution to minimise the risk of PJI. However, the work presented in Chapter 3 found that, immobilising the glycopeptide antibiotic Teic was not a feasible option at this time. Therefore, formulating ways to deliver the antibiotic either on or around the biomaterial might be a more suitable alternative and so further work examined the controlled release of Teic since it has not only displayed great antibacterial activity but also biocompatibility, as seen in Chapter 2. One of the ways this could be done is by entrapping Teic in a hydrogel matrix. Hydrogels can be very useful in engineering antibacterial surfaces for the prevention of PJI. They are a class of a highly hydrated biomaterials, produced by either natural or synthetic biopolymers with many being biocompatible. In addition, they can be designed to have mechanical properties similar to living tissue and have been used in a variety of applications including treatment of chronic and traumatic wounds, drug delivery and surface coatings for implants (Yu *et al.*, 2021; Rodriguez-Rodriguez *et al.*, 2020). The aim of this chapter was to encapsulate Teic in a CS-Gel hydrogel composite using Gen as a crosslinker for the controlled and steady release of the antibiotic.

Initial investigations were used to determine the release characteristics of Teic from a chemically crosslinked Gel and to optimise the concentration of the crosslinker. Glut was first used over the course of this work due to it being the most commonly used and inexpensive chemical crosslinker for the formation of Gel hydrogels and sponges (Yang *et al.*, 2018). It was found that no Teic was released from all Glut concentrations tested (1, 0.5, 0.25 and 0.125%), suggesting that the antibiotic was either trapped or bound to the crosslinker in some way. To confirm if Teic was trapped, Gent was used as a control antibiotic as it is known to release from Glut-crosslinked Gel hydrogels (Sivakumar & Panduranga, 2002; Chang *et al.*, 2003). In contrast to what was observed with the Teic-Glut-Gel, Gent was able to release at a steady rate from the Glut-Gel (data not shown) confirming that Teic was

indeed trapped in crosslinked hydrogel matrix. It is possible that Teic was trapped within the crosslinked hydrogel due to the physical and chemical properties of the hydrogel matrix. Despite chemical crosslinking being able to stabilise the hydrogel and prevent degradation, it also forms these small pores of spaces which act as a reservoir for the antibiotic molecules. It is possible the antibiotic size could impact the release of the antibiotic and given that Teic is a relatively large molecule (MW: 1879.7) when compared to Gent (MW: 477.6) it is likely that Teic is “trapped” in these small pores. It is also conceivable that the Teic has reacted in some way with the crosslinker, compromising either the release or the antibacterial activity of the antibiotic. So, to determine if the antibiotic was trapped within the matrix of the hydrogel, a trypsin digest was employed. After immersing the Teic-Glut-Gel hydrogel in a 0.05% Trypsin solution for 24 h at 37 °C, the digested samples were used in a disk diffusion assay. It was found that the digested Teic-Glut-Gel hydrogel did demonstrate antibacterial activity when compared to the Teic-Glut-Gel control, suggesting that the antibiotic was trapped within the hydrogel matrix (Fig. 4.2). However, when compared to the digested Teic-Gel there was a significant reduction in antibacterial activity, indicating that that Glut was interacting with the antibiotic in some way. While there is currently no literature available regarding the interaction between Teic and Glut, it has been hypothesized that the effect of Glut on biomolecules may vary depending on the concentration of the crosslinker. When Chui & Wan (1997) used Glut to crosslink trypsin they had found that the enzymatic activity was inversely proportional to the concentration of Glut used. At high Glut concentrations, a great extent of intramolecular crosslinking occurs and could lead to distortion of the enzyme structure. The distortion of the structure could reduce the biological activity of the enzyme (Chui & Wan, 1997; Migneault *et al.*, 2004). This could very well explain what has been observed with the trypsin digest of the Teic-Glut-Gel. However, more work would need to be done to greater understand this interaction.

Whilst Glut might be an inexpensive and rapid crosslinking agent, it is clear that the excessive crosslinking impacts on the release and biological activity of Teic and so work moved towards using Gen as a crosslinker. Gen is a naturally occurring crosslinker and has been used extensively in the

biomedical field due to its excellent biocompatibility, biodegradability and stable crosslinked attributes (Yu *et al.*, 2021; Mi *et al.*, 2002; Chang *et al.*, 2004). This is one of the few reports that utilises Gen as a means to control the release of Teic from a Gel-based hydrogel. Various concentrations of Gen (5, 2.5, 1,0.5 mM) were used to determine what concentration would be optimal for the steady and consistent release of Teic. As seen in Fig. 4.4, the bound antibiotics released more quickly from 0.5 mM Gen, with a bulk release observed after 1 day and the ZOI declining after 2 and 3 days incubation. However, when looking at the 1 and 2.5 mM concentrations there are only slight differences in release, with the 1 mM having a marginally larger ZOI on average in comparison to using 2.5 mM. It was noted that the release from the 1 mM genipin crosslinked Gel did appear to slightly increase after 1 day and then gradually decline. Yet, the 2.5 mM crosslinked gel appeared to have a consistent release cross 2 days. However, there was no release after the third day, this could be due to inconsistent elution as it was likely that some of the antibiotic was still within the hydrogel. Despite the last day not showing any elution, due to the consistency of the release shown within the first two days of incubation, the work moving forward used a 2.5 mM concentration of genipin and the incubation time of the hydrogel was increased to 7 days.

Despite the stability of the crosslinked Gel hydrogel, it has been noted within the literature that the hydrogels tend to be elastic and mechanically soft, making the polymeric scaffold difficult to handle (Saha & Tayalia, 2022). From a qualitative observation the crosslinked Gel scaffold was more pliable, however little pressure was needed to compromise the hydrogel structure, highlighting the need to further improve the mechanical strength and stability of the hydrogel. It has been reported that the combination of Gel with the natural polysaccharide, CS could enhance the overall performance of the hydrogel, leading to improved biocompatibility and stability (Georgopoulou *et al.*, 2018; Chiono *et al.*, 2008). Moreover, it could even improve the antibacterial activity characteristics of the hydrogel with CS and its derivatives demonstrating antibacterial synergy with a variety of antibiotics (Tin *et al.*, 2010). Therefore, this package of work looked into designing a composite hydrogel scaffold using Gel and CS.

Prior to assessing the composite hydrogel, it was important to determine if CS could impact the antibacterial activity of Teic, given that CS appears to have antibacterial properties and has demonstrated synergy with antibiotics (Tin *et al.*, 2010). A checkerboard assay was used to assess any synergy between the two components, the first time such an investigation has been performed. It was found that the FIC revealed indifferent indices, with no synergistic or antagonistic activity observed. Interestingly, CS displayed no antibacterial activity against *S. aureus* and was comparable to the growth control. Yet, within the literature it is strongly suggested that CS displayed antibacterial activity against *S. aureus*. However, this could very well be dependent on the type of CS used. Moreover, a couple of studies found that the antibacterial activity of CS glutamate is dependent on not only the deacetylation percentage and molecular weight, but it is also dependent on the CS concentration, pH of the medium and temperature (Roller & Covill, 1999; Roller & Covill, 2000). The activity can also be dependent on the type of organism and strain used. Despite the lack of antibacterial activity displayed from CS, it is beneficial to know that the polysaccharide does not impact on the antibacterial efficacy of Teic.

To observe the characteristics of the crosslinking mechanism of Gen with the CS-Gel hydrogel, FTIR was used. The FTIR spectra of non-crosslinked CS-Gel, Teic-loaded CS-Gel and the crosslinked counterparts are shown in Fig. 4.5. All samples had broad characteristic adsorption bands between 3260-3310 cm^{-1} due to the partial overlapping of amine and hydroxyl group stretching vibrations. The bands observed at ~ 1080 and ~ 1036 cm^{-1} (C-O stretching vibrations) for CS-Gel, CS-Gen-Gel and Teic-CS-Gel are typical of the CS polysaccharide structure, whereas the bands observed at 1550-1565 cm^{-1} for all hydrogel samples, are characteristic of Gel and are represented by a bending vibration of NH and stretching vibrations of C-N groups (Fernandes Queiroz *et al.*, 2014; Merina Paul Das *et al.*, 2017). It was noted that there was a slight increase in C=O stretch vibration found at 1638 cm^{-1} and in the OH bending vibrations at 1458 and 1464 cm^{-1} for the CS-Gen-Gel and Teic-CS-Gen-Gel samples, indicating the formation of a secondary amide. This could be due to the reaction between the primary amino groups in CS and Gel reacting with the ester group of Gen (Fig 4.5C & E), when compared to the CS-

Gel only (Fig 4.5B) which has a less intense band at 1640 cm^{-1} . However, there are little differences observed overall, between the crosslinked and non-crosslinked samples. This could be due to the concentration of the crosslinker. A similar observation was found by Chiono *et al.* (2008) who were using Gen to crosslink Gel/CS scaffolds for biomedical applications. When observing the functional group changes within the FTIR analysis, it was found that the detection of these changes in the band intensities was dependent on the concentration of the crosslinker, with higher concentrations demonstrating an increasing change in the band intensity and a slight shift in the bands typical position, whereas the hydrogels crosslinked with a low concentration of Gen had no noticeable changes in the band intensities, nor no noticeable shift when compared to the non-crosslinked samples. However, what was interesting to note was the absence of characteristic Teic peaks for the Teic-loaded hydrogel samples, when comparing against the Teic powder, nor was there any decrease or shifts in the typical absorption bands for the composite hydrogel. The lack of distinct Teic signals within the hydrogel spectra could be due to FTIR limitations in detecting well-dispersed Teic molecules or when using a low concentration of the antibiotic. This observation is in agreement with Vlasceanu *et al.* (2020) who encountered the same issue when attempting to detect graphene oxide (GO) in a CS-Gel hydrogel scaffold. It was found that even when increasing the concentration of GO, the addition of the oxide did not alter the spectra of the hydrogel. However, the lack of an adsorption shift, or increase in peaks could also support the idea that the antibiotic is well dispersed throughout the hydrogel matrix.

To determine the antibacterial activity of the Teic-loaded composite hydrogel, a disk diffusion assay was used. It is clear that the release profile of the antibiotic varied between the hydrogels (Fig.4.6). The hydrogels without genipin displayed a decreasing trend in ZOI, the longer the incubation period, whereas Teic-CS-Gen-Gel and Teic-Gen-Gel demonstrated a sustained release over the course of 7 days. However, it is interesting to note that the Teic-loaded CS hydrogel, crosslinked with Gen, displayed a decreasing trend in ZOI and was comparable to the non-crosslinked samples (Fig.4.6D). Moreover, this observation was seen when quantifying the Teic concentration in the hydrogel samples

using HPLC (Fig. 4.7). Unlike the other crosslinked samples, which had only released 170 μg (Teic-CS-Gen-Gel) and 127.5 μg (Teic-Gen-Gel), Teic-Gen-CS had released an average of 324.7 μg after 7 days of incubation. Interestingly, these results differ from what has been found in the literature. A study by Wu *et al.* (2014) had found that the release of Gent from the Gen-crosslinked CS hydrogels was sustained for up to 500 h. A more recent study has loaded Gen-crosslinked CS with a variety of antibiotics (tetracycline, amoxicillin, and cefuroxime) and assessed the elution of the antibiotics over the course of 200 h. It was found that all the antibiotics displayed a sustained elution over 8 days, moreover, tetracycline only had around 30% of the antibiotic remaining after 200 h (Andrade del Olmo *et al.*, 2022). However, the dissimilarity in the results could be explained by the concentration of Gen used to crosslink the CS hydrogel. Most studies tend to use around 2.5% (w/v), whereas in this particular study, the Gen concentration is equivalent to 0.00006% (w/v) and this could impact the crosslinking degree of the CS hydrogel. Yet, it was evident that using a high concentration of Gen could impact the release of Teic (Fig. 4.4) when used in the composite. Moreover, the type of CS used, and the temperature could affect the gelation kinetics and stability of the hydrogel (Mwale *et al.*, 2005; Szymanska & Winnicka, 2014). Another notable observation is that the Teic-Gen-Gel hydrogel, had a marginally slower release rate of Teic than the Teic-CS-Gen-Gel. It has been found in the literature that crosslinked Gel tends to be more mechanically stable than crosslinked CS (Chiono *et al.*, 2008). However, there appears to be a higher crosslinking degree in the Teic-Gen-Gel, resulting in not only a lower release rate of Teic, but also a release of Teic at an inconsistent rate as seen in Fig. 4.6B. This inconsistency in the rate of release could encourage the reattachment of bacteria onto the implant surface and so it is important that the diffusion of the antibiotic through the hydrogel is sustained. However, when the polymers are combined, the rate of release is not only steady but continuous and highlights the potential applications of composite hydrogels in controlling the release of antimicrobial agents.

Despite the previous chapters looking into creating a coating for the implants used in TJA, this chapter has focussed on creating a hydrogel that can be injected into an open porous scaffold which could

include trabecular bone, surrounding the implant, as the hydrogel coating might be impacted by the physical implantation of the prosthesis. Therefore, a cancellous bone model was used to assess the elution of Teic from the hydrogel scaffold. The mock cancellous bone (2 cm x 2 cm x 2 cm) was injected with 5 ml of the composite hydrogel containing 1 mg/ml of Teic and after gelation, was subsequently immersed in 20 ml of PBS for 7 days. It was found that the elution profile of Teic-CS-Gen-Gel and Teic-Gen-Gel was similar to that of the hydrogel pucks, with around (856 μ g) 86% and (918 μ g) 92% of the antibiotic remaining within the composite scaffolds, respectively, suggesting a slow and stable release (Fig.4.9B). Moreover, there was no significance between the ZOIs across all time points tested, further highlighting a stable release profile (Fig. 4.8A). In contrast, the uncrosslinked samples had released more of the antibiotic over the course of 7 days with only 798.4 μ g (79.8%) and 753.4 μ g (75.3%) remaining for Teic-CS-Gel and Teic-Gel, respectively (Fig. 4.9B). While this is one of the few studies that have examined the injection of an antibiotic-loaded hydrogel into cancellous bone, there are other studies that have applied antimicrobial coatings to bone, and their conclusions align with the results presented in this study. When netilmicin was impregnated onto cancellous bone only 30% of the adsorbed antibiotic was released after 24 h. Moreover, the antibiotic was still eluting from the bone for up to 6 weeks in PBS. However, the concentrations observed after 20 days were below the MIC for the antibiotic (Witso *et al.*, 2009). Whereas the composite hydrogel used in this study demonstrated a controlled-release of the antibiotic from the mock bone model, with the antibiotic releasing ~20x the MIC over 7 days. A more recent study designed a photo-crosslinkable hydrogel that incorporated quaternary ammonium compounds for use in femoral fractures (Liu *et al.*, 2023). It was found that the hydrogel demonstrated good antibacterial activity against *S. aureus* and MRSA *in vitro*. Moreover, the *in vivo* studies had found that the QAS-modified hydrogel scaffolds had almost completely vanquished *S. aureus* on day 42 in the infection model, further highlighting the potential of antimicrobial-loaded hydrogels in preventing PJI.

4.9 Conclusions

The findings presented support the potential of using an antibiotic-loaded composite hydrogel for the prevention of PJI. Initial studies looked into optimising the crosslinker and the concentration of the crosslinker using a Gel-based hydrogel scaffold. Through this, it was determined that using 2.5 mM of Gen would be optimal for use to crosslink the composite scaffold. Prior to assessing the composite hydrogel, an antimicrobial synergy assay was used to determine if CS would impact the antibacterial efficacy of Teic. Despite CS not having any notable antibacterial activity, it did not impede the antibacterial efficacy of Teic. The composite hydrogels were characterised using FTIR and composite scaffolds displayed antibacterial activity over the course of 7 days. Moreover, the release of the antibiotic was steady and consistent when looking at both the hydrogel pucks and cancellous bone model. To conclude, this proof-of-concept demonstrates the potential of a CS-Gel composite hydrogel scaffold loaded with Teic as a means to reduce the incidence of PJI.

Chapter 5 Discussion & Future Work

5.1 General Discussion

TJA is a highly effective procedure in relieving pain and disability associated with advanced joint disease. However, approximately 1-2% of arthroplasties fail due to periprosthetic joint infection (PJI) and require replacement. While revision arthroplasty has a high success rate, the procedure increases the risk of reinfection, prosthetic complications, further revisions, and high costs (Kunutsor et al., 2016; Orapiriyakul et al., 2018). With an increase in primary arthroplasties being performed, longer life expectancies, and an increasing healthcare burden due to OA, finding solutions that improve the longevity of TJAs is crucial. Therefore, the work presented in this thesis was focused on the development of an antibacterial Ti coating through either, the physical modification of Ti or by formulating an antibiotic-loaded hydrogel which could be applied around the implant.

First, the immobilisation of Teic, a glycopeptide antibiotic, onto a PDA-modified Ti disc was reported. Initial studies determined the osteocompatibility of Teic with MG63 osteoblasts by exposing the antibiotic to the cell line in combination with FHBP and 1,25D. It was noted that the antibiotic alone had no impact on MG63 ALP expression, yet when in combination with 1,25D and FHBP there was a significant increase in ALP activity, when compared to FHPB and 1,25D alone. How the combination of the antibiotic with the LPA analogue and 1,25D results in a synergistic response in ALP expression remains unclear and there is currently no published work that has observed this phenomenon. Evidence of Teic to remain biologically active whilst bound to a surface was assessed by using CNBR-activated Sepharose. The results demonstrated a significant reduction in *S. aureus* viability (≥ 3 -log reduction) at both concentrations tested (25 and 50 $\mu\text{g}/\text{ml}$), suggesting that Teic retains its biological activity when bound to a surface.

In realising the physical modification of Ti with Teic, the application of a PDA thin film following an earlier report by Wang and colleagues (2017) was considered. In their study, they developed a Teic-

CSP using PDA to capture the antibiotic onto iron oxide particles. In this thesis, the formation of a PDA film was carried out under static conditions using a mildly alkaline solution (10 mM Tris-HCl; pH 8.5) to start the polymerisation process of DHC into PDA. Different parameters were studied to optimise the PDA deposition process and it was confirmed that the deposition of a PDA film was a function of incubation time, buffer type and temperature. Despite this, the attachment of Teic onto the PDA-modified Ti was not impacted by these changes in parameters as confirmed by the LIVE/DEAD assays. Moreover, the growth and attachment of *S. aureus* was not impacted by the PDA-modified Ti when compared to bare-Ti, despite a couple of studies in the literature alluding to PDA films deterring the attachment of bacteria (Patel *et al.*, 2018; Su *et al.*, 2016). However, the difference in the antifouling activity could be due to a variety of factors such as the material used and the surface roughness, as discussed in Chapter 2. The PDA-modified Ti discs were functionalised with Teic and subsequently exposed to *S. aureus* for 4, 8 and 24 h at 37 °C. A significant reduction in bacterial attachment on the Teic-PDA-Ti discs, compared to the control discs (PDA-Ti and Ti) was observed and concurs with what has been found within the literature when assessing the antibacterial activity of Vanc covalently attached to Ti (Antoci *et al.*, 2007; Antoci *et al.*, 2008). Interestingly, the Ti discs with Teic adsorbed to the surface also displayed significant antibacterial activity and was comparable to the antibacterial activity observed with Teic attached to PDA-modified Ti, indicating that the antibiotic could readily adsorb onto the Ti surface without the need of an intermediate crosslinker.

The antibacterial activity observed from the control Teic-Ti discs in Chapter 2 was confirmed in Chapter 3 by steeping Ti discs in a solution of Teic (500 µg/ml) and exposing the Teic-modified discs to *S. aureus* for 24 h at 37 °C. As found in Chapter 2, the Ti discs steeped in Teic only exhibited significant antibacterial activity, when compared to bare Ti. The modified Teic-Ti surface was then chemically characterised by XPS analysis to determine if Teic is indeed present on the biomaterial. Accompanying changes in the atomic composition of the surface was noted; specifically, an increase in Cl- peaks and a decrease in Ti and O₂ peaks over time (Table 3.1; Chapter 3), indicative of Teic coating the surface of Ti. Furthermore, this suggested that Teic might be binding to the oxide layer, TiO₂, which naturally

forms on the surface of titanium. This naturally occurring surface finish has been found to have an affinity for glycopeptides (Sheng *et al.*, 2013) and given that Teic is a glycopeptide, this phenomenon most likely explains the affinity that the antibiotic displayed for the Ti surface. It was for this reason that the interactions of Teic with TiO₂ were assessed.

To corroborate that Teic could indeed bind to TiO₂, a mixture of rutile and anatase titania was exposed to an aqueous solution of Teic and antibiotic binding to TiO₂ monitored using a BCA reagent. Adsorption of the TiO₂ was rapid, with ~ 90% of the antibiotic bound to the oxide after only 5 min of incubation (Fig. 3.3). In addition, there was little change in the adsorption across all time points tested, which would suggest that adsorption of Teic plateaued around 5 min. This observation was supported by the QCM measurements. Furthermore, the Teic-TiO₂ interaction displayed great durability to washing and was able to remain bound to the oxide after 7 days incubation under neutral conditions. The attachment of the antibiotic to the oxide was also thermally stable, with disassociation of Teic from the Ti surface only occurring at temperatures greater than 250 °C. However, when the Teic-modified Ti discs were subjected to a mock bacterial culture, the conditioned media displayed antibacterial activity, indicating that the antibiotic was eluting into the medium. This was further confirmed by subjecting the conditioned Teic-Ti discs to *S. aureus* for 24 h at 37 °C. The conditioned Teic-Ti discs supported the growth of *S. aureus* and was comparable to the control Ti after 24 h incubation. This further confirmed that the antibiotic was eluting from the Ti surface and was the reason why the functionalised Ti surface was able to deter the attachment of *S. aureus* in previous experiments. Subsequently, it was found that phosphate could quickly displace Teic from the Ti discs and also compromise the binding of Teic to titania and is most likely due to the anions affinity to the oxide (Zhao *et al.*, 2008). Whilst the facile adsorption of Teic might be a convenient solution towards the development of antibacterial surfaces, it was evident that the Teic-TiO₂ interaction was compromised by physiological phosphate (~ 1 mM) and is therefore not an ideal option towards tackling this issue of PJI as there could be a burst release of the antibiotic into the surrounding area

and this would leave the implant surface susceptible to re-attachment by surviving bacteria. An alternative strategy was needed, and so the covalent grafting of Teic to Ti was reconsidered.

There was a recent technology developed that utilised IONPs to immobilise Teic for the local delivery of the antibiotic (Armenia et al., 2018). Using APTES and EDC/NHS chemistry, the group purportedly anchored Teic onto the IONPs using the carboxyl functional group on Teic, the result of which produced a material that displayed great antibacterial activity, as mentioned in Chapter 3. The group kindly provided the modified IONPs, and these were subjected to an antibacterial assessment to determine the efficacy of the Teic-modified IONPs. The nanoconjugated antibiotic demonstrated significant antibacterial activity when compared to bare IONPs and the *S. aureus* control (Fig. 3.10). In addition, the reduction in bacterial viability was similar to that of free Teic. Interestingly, when assessing the storage buffer for antibacterial activity, the reduction in bacterial viability was comparable to the Teic- modified IONPs, suggesting that the antibiotic was eluting into the buffer. This was confirmed by conditioning the Teic-IONPs in the bacterial culture medium and exposing the conditioned media to *S. aureus* after 24 h incubation. Qualitatively, it was found that the conditioned media recovered from the Teic-IONPs inhibited bacterial growth, supporting the observations made from the IONP storage buffer. Moreover, the conditioned Teic-IONP and controls were subsequently exposed to *S. aureus* to determine if the modified IONPS retained any antibacterial activity, and it was found that a moderate loss of antibacterial activity was observed (Fig. 3.11). Given the affinity of Teic for TiO₂ it is likely that the antibiotic will also bind to iron oxide. Based on the results outlined in Chapter 3 it is proposed that a significant proportion of Teic naturally binds to the IONPs regardless of the steps taken to target the carboxyl group of Teic using EDC/NHS chemistry. In doing so Armenia *et al.* (2018) could have inadvertently generated a passively modified IONP material. Perhaps the same is true for the Teic-modified magnetic nanoparticles developed by Wang and colleagues (2017).

It was clear that overriding the natural affinity of Teic to TiO₂ would be especially challenging in the development of a more robust antibacterial surface. Before considering any strategy aimed at

covalently grafting Teic to Ti it was important to ascertain if a commercially available Teic-CSP could exhibit antibacterial activity. Initial studies utilised genipin to monitor the interactions of the tripeptide, N-acetyl-L-lys-D-ala-D-ala and TSP and found that the tripeptide was able to bind with the Teic-CSP. As anticipated, the binding between the Teic-CSP and the tripeptide was compelling, with the sample supernatants having undetectable levels of the tripeptide within 30 min. In contrast, the control silica particles did not interact with the tripeptide and the recovered supernatants produced a deep blue pigment on exposure to genipin, thereby indicating that tripeptide was retained in the incubating solution. However, whilst being able to confirm the functionality of the TSP, the same material did not demonstrate antibacterial activity against *S. aureus*. The equivalent of approximately 680 µg/ml of Teic was bound to the silica and demonstrated no antibacterial activity when exposed to *S. aureus*. Normally, there is a significant reduction in bacterial viability when *S. aureus* is exposed to 50 µg/ml of free Teic (as seen in Chapter 2). The results obtained from the Teic-CSP experiment contradict those presented in Chapter 2 involving CNBr-activated Sepharose support. Antibacterial activity against *S. aureus* was observed when Teic was applied to the activated Sepharose. Unlike the impermeable silica shells of the Teic-CSP, Sepharose is a porous matrix that is commonly used for size exclusion chromatography. It is believed that Teic may have penetrated the pores of the Sepharose and subsequently released during the bacterial culture period.

Overall, the information gathered in Chapter 3 conflicts with other studies that report on the successful, covalent immobilisation of Teic and other glycopeptide antibiotics onto Ti and IONPs. As with the IONPs above, the techniques used to immobilise Teic to Ti used APTES, followed by NHS-EDC chemistry in order to bind the carboxyl group of Teic to the amine at the metal surface. However, many of these studies do not provide any physiochemical evidence, such as XPS, to confirm that the antibiotic was tethered to the metal surface through the proposed mechanism of binding. Moreover, none of those studies provided any evidence regarding the robustness of the interaction between the antibiotic and the substrate surface by performing mock bacterial cultures or leaching studies. It is clear that the antibacterial activity observed in Chapter 3 was coming from the antibiotic eluting into

the culture media. The phosphate present in the culture medium used in the experiment was most likely promoting the elution of the antibiotic from the metal surface. In contrast, the covalently bound Teic, used in chromatographic applications bound well to the tripeptide, yet displayed no antibacterial activity against *S. aureus*. Suggesting that direct immobilisation of the glycopeptide antibiotic to a biomaterial surface is not a viable option.

In light of the findings presented, an alternative solution to minimising PJI could include the controlled elution of Teic at or around the implanted device using a biocompatible, resorbable hydrogel system. Therefore, the research focus for Chapter 4 looked at creating a hydrogel scaffold to control the release of Teic. First, studies looked into the release profile of Teic from a chemically-crosslinked gelatin hydrogel and optimisation of the crosslinker concentration. Glutaraldehyde was initially used over the course of this study due to it being a commonly used and inexpensive crosslinker for the formation of gelatin hydrogels (Yang *et al.*, 2018). Despite Gent successfully releasing from the glut-crosslinked hydrogels (data not shown), no Teic was released from any of the Glut-crosslinked hydrogels tested, suggesting that the antibiotic was either trapped or bound to the chemical crosslinker. A trypsin digest performed on the Teic-loaded Glut-Gel hydrogels confirmed that the antibiotic was indeed trapped within the hydrogel, yet the antibacterial efficacy was reduced when compared to a digested Teic-Gel control. This reduction in efficacy could be due to intramolecular crosslinking of Glut (as discussed in Chapter 4), however more would need to be done to further understand this interaction. In realising the difficulty of using Glut as a crosslinker for the steady release of the glycopeptide antibiotic, genipin, a naturally derived crosslinking agent was used given its excellent biocompatibility, biodegradability and stable crosslinked attributes (Yu *et al.*, 2021; Mi *et al.*, 2002; Chen *et al.*, 2004). It was found that Teic release from the Gen-crosslinked hydrogels was a function of concentration and a concentration of 2.5 mM appeared to provide a consistent and steady release of Teic.

A hybrid hydrogel system was also considered for the controlled release of Teic. CS was paired with Gel following reports that it exhibited antibacterial activity and could even synergise with some antibiotics in reducing bacterial viability. Initial experiments examined the antibacterial efficacy of Teic in the presence of CS and so a checkerboard assay was performed to assess any antibacterial synergy between the two components. It was found that the FIC yielded indifferent indices across all concentrations tested, with no synergy occurring between the two components. This is the first time synergy between Teic and a CS derivative have been explored. Interestingly, no antibacterial activity was detected in CS and the growth present in the wells were comparable to the growth control. The findings in Chapter 4 conflicts with other studies that have reported on the synergistic activities of CS with other antibiotics. However, it is well known that the antibacterial activity of CS is dependent on a variety of factors including, the type of CS used, deacetylation percentage, molecular weight of CS, concentration of the polysaccharide and pH, among other factors (Roller & Anagnostopoulos, 1999; Roller and Covill, 2000) and could explain the differences found in Chapter 4. Despite the lack of antibacterial activity from CS it was beneficial to know that it would not impede on the antibacterial activity of the antibiotic.

To characterise the crosslinking mechanism of genipin with the CS-Gel composite FT-IR was used. Typical peaks of CS and Gel were observed, along with an increase in the C=O stretching vibration found at 1638 cm^{-1} and in the OH bending vibrations found at 1458 and 1464 cm^{-1} noted in the Teic-CS-Gen-Gel samples, suggesting the formation of an amide due to the reaction between gelatin and CS interacting with the crosslinker. However, no Teic peaks were detected in any of the samples which could be due to the low concentration of the antibiotic within the samples, as discussed in Chapter 4. The antibacterial activity of the hydrogel was then assessed by immersing the hydrogel pucks in PBS and subjecting the supernatant to a disk diffusion assay. The Teic-loaded composite hydrogel pucks, crosslinked with genipin displayed good and consistent inhibition of *S. aureus* over the course of 7-days in comparison to the uncrosslinked hydrogels which demonstrated a decrease in ZOI over the incubation period (Fig. 4.6). This observation was echoed in the HPLC analysis of the supernatants

whereby only ~170 µg (17%) of the antibiotic was released from the crosslinked-composite hydrogel after 7 days, whereas Teic-CS-Gel and Teic-Gel released ~206 (20.6%) and 214 µg (21.4%), respectively (Fig. 4.7B). Although Chapter 2 and 3 focused on creating a coating for the implants used in TJA, Chapter 4 focused on the potential of applying the hydrogel to the cancellous bone surrounding the implant, as one of the major concerns regarding implant coatings is their stability to the rigors of implantation. A mock cancellous bone model was injected with 5 ml of the composite hydrogel, left to set overnight, immersed in PBS once set and incubated for 7 days at 37 °C. As with the hydrogel pucks, the antibiotic that eluted from the crosslinked-composite hydrogels demonstrated a consistent ZOI over the course of 7 days (Fig. 4.8A) and when looking at Fig. 4.9B, it is clear that the Teic-CS-Gen-Gel had released significantly less Teic (144 µg) after 7 days in comparison to the uncrosslinked samples, highlighting the potential use of this composite hydrogel in reducing the incidence of PJI.

5.2 Concluding Remarks

In conclusion, this thesis has attempted to design a novel antibacterial biomaterial to reduce the risk of PJI. Chapter 2 focussed on immobilising Teic to a PDA-modified titanium surface and the PDA deposition kinetics were optimised in an attempt to improve the consistency and stability of the modified-Ti surface. When the Teic-modified PDA-Ti surface was exposed to *S. aureus* it was able to greatly reduce bacterial attachment when compared to the PDA-Ti and Ti controls, yet the Ti disc coated with Teic only displayed similar antibacterial activity as the Teic-PDA-Ti. From this, it was theorised that Teic was binding to the natural oxide layer of Ti and so Chapter 3 looked into the binding interactions of Teic with TiO₂. It was found that Teic was able to bind rapidly to the oxide surface and the interaction was able to withstand high heat and repeated washing. However, the presence of phosphate, even when at physiological concentrations, compromises the antibiotic's interaction with the oxide and could explain how the antibiotic elutes into the bacterial medium from the Ti surface. Prior to attempting to covalently attach the antibiotic to the surface, it was important to determine if the antibiotic would still retain its biological function whilst attached to the surface. Teic-modified

IONPs displayed great antibacterial activity when exposed to *S. aureus*, yet the antibiotic still eluted into the medium. Moreover, when a commercially available Teic-CSP was exposed to *S. aureus* no antibiomatic activity was observed, suggesting that covalent attachment of the glycopeptide antibiotic to a biomaterial surface does not result in the generation of an antibacterial surface. Yet, as expected, Teic has consistently displayed great antibacterial activity and was also able to enhance the maturation of osteoblasts. This places Teic as a valuable option for deterring bacterial attachment on biomaterial surfaces whilst potentially encouraging implant integration. Therefore, Chapter 4 focused on developing a composite hydrogel scaffold made from CS and Gel, crosslinked with genipin in order to control the release of Teic. The crosslinked composite hydrogel was characterised using FTIR and has demonstrated effective, consistent and prolonged antibacterial activity against *S. aureus* over the course of 7 days. Moreover, most of the antibiotic was still encased within the hydrogel and the release could potentially last beyond a week. This prolonged antibacterial activity was also observed when injecting the hydrogel into a cancellous bone model, demonstrating the potential of this composite scaffold in reducing the incidence of PJI. Overall, this thesis has demonstrated the potential of using Teic in orthopaedic applications but has also highlighted the difficulty in generating a stable, Teic-coated Ti surface finish.

5.3 Future Work

This thesis focused on the development of antibacterial technologies to reduce the incidence of PJI. Various strategies were investigated, although further studies can be carried out to gain a deeper understanding of how the materials interact with one another, optimisation of the biomaterials, as well as explore more of the antibacterial activity and cytocompatibility of the biomaterials developed in this thesis.

Due to the multidisciplinary nature of this research, the work could be taken in several directions in the future. For instance, although work moved beyond using PDA as a means to capture Teic, its potential in immobilising various compounds could still be used in future work. A recent study has

used PDA films as a means to enhance the binding capabilities of a gelatin hydrogel to a variety of PDA-coated implant materials (Dinh *et al.*, 2018) and this would be worth exploring as an alternative means of introducing the composite hydrogel during the TJA procedure. As both Gel and CS have been widely utilised for potential biomedical applications, it is important to further characterise how the polymers interact with one another and how the combination of the polymers change the physicochemical properties of the hydrogel. This can be obtained by performing a variety of physicochemical assessments such as contact angle measurements, swelling behaviour, and compressive modulus of elasticity, along with morphological assessments using techniques such as SEM. Although FT-IR was used as a means of monitoring the changes in the functional groups in the composite hydrogels, it was the only physicochemical assessment conducted in Chapter 4, moreover, it was not a very sensitive technique and the use of another surface characterisation technique such as XPS could aid in corroborating the results from the FTIR analysis.

It might also be worth exploring another type of CS. Although the water-soluble form used in this thesis allowed for a sufficient release of Teic when combined with gelatin, it might be more beneficial to use another type, as one of the more attractive features of CS is its proposed antibacterial capabilities. In addition, obtaining a water-soluble form of CS can be very expensive and from a manufacturing perspective, a potential antibacterial biomaterial would need to be cost-effective as not only would it make the biomaterial easier to produce on a mass scale, but it would also make it more accessible to patients and the providers. On that note, investigating alternative crosslinkers should be considered in future work; although genipin is biocompatible and can readily react with amino groups under mild conditions, it is a very expensive crosslinker. An alternative could be transglutaminase which has received increasing attention due to its ability to crosslink proteins. Moreover, transglutaminase extracted from microorganisms exhibits a high yield and is relatively inexpensive, highlighting its potential use as a crosslinking agent (Yang *et al.*, 2018).

Although the Teic-loaded composite hydrogel has displayed good inhibition against *S. aureus*, other microbial assessments should be used to further understand the antibacterial efficacy of the antibiotic-loaded hydrogel. One of the ways this could be approached is by immersing the hydrogel samples in a broth inoculated with *S. aureus*, sampling at predetermined time points over the course of a few days and plating the sample aliquots onto agar to ascertain the CFU/ml. Antibacterial efficacy assessments could move onto observing the interactions for a longer period of time, as this thesis has shown that the antibacterial activity can be retained at a steady rate for at least 7 days. Furthermore, a biocompatibility assessment can be conducted, such as evaluating the cytocompatibility of the hydrogel towards osteoblasts and monitoring growth and maturation.

In addition to injecting the composite hydrogel into the cancellous bone surrounding the implant, work could revisit coating the implant with the antibiotic-loaded composite hydrogel as mentioned earlier. Hydrogels are quite versatile and have been developed and tailored to meet the needs of a variety of applications (Ahmed, 2015). Given that hydrogels are able to swell when in contact with an aqueous solution it would be worth looking into grafting a hydrogel onto an orthopaedic biomaterial and either vacuum or freeze drying the hydrogel to form a film. It is possible that the hydrogel in this state might be able to withstand the rigors of implantation, especially if the hydrogel film is anchored to the Ti surface using an intermediate film such as PDA. One of the ways this could be explored, is by insertion of the hydrogel-coated Ti into a mock bone model, retrieving the sample after successful implantation and assessing the biological activity of the hydrogel-coated Ti post implantation. Along with using separate biological assays for the microbiological and cytocompatibility studies, a single model to assess both might be a good way to more accurately represent the situation seen from a clinical perspective. This could be done by exposing the antibiotic-loaded hydrogel to a mixed cell and bacterial inoculation in the presence of blood products and tissue fluids. This would replicate the “race for the surface” between the microorganisms and cells, which is thought to be critical to early healing and osseointegration processes that takes place around the implanted prosthesis (Shiels *et al.*, 2020; Liu *et al.*, 2020). If this coating was able to demonstrate excellent antibacterial and cytocompatibility

in vitro, the next step in evaluating its potential as a clinically useful product, would be their evaluation *in vivo*, using an animal model. This would initially be conducted with an appropriate microbial challenge, followed by immediate and short-term histological analysis of the surrounding tissue in order to ascertain the impact of the hydrogel coating on the rate and quality of osseointegration, as well as assessing the post-operative infection rate and long-term implant success.

And finally, if this coating is being developed with the aim of producing a commercial product, compliance with the relevant standards (such as the International Organisation for Standardisation, British Standards Institution) would be required in regard to the antimicrobial efficacy and cytocompatibility evaluations. In addition, industrial scaling of all aspects of the coating production would need to be considered (as briefly mentioned above) since it is an important logistical step when developing any biomaterial from a small-scale proof-of-concept study.

References

- Aboltins, C.A., Dowsey, M.M., Buising, K.L., Peel, T.N., Daffy, J.R., Choong, P.F.M. and Stanley, P.A. (2011) Gram-negative prosthetic joint infection treated with debridement, prosthesis retention and antibiotic regimens including a fluoroquinolone. *Clinical Microbiology and Infection*. 17 (6), pp.862–867.
- Achermann, Y., Vogt, M., Spormann, C., Kolling, C., Remschmidt, C., Wüst, J., Simmen, B. and Trampuz, A. (2011) Characteristics and outcome of 27 elbow periprosthetic joint infections: results from a 14-year cohort study of 358 elbow prostheses. *Clinical Microbiology and Infection*. 17 (3), pp.432–438.
- Affatato, S. (2012) Wear of orthopaedic implants and artificial joints. Cambridge, United Kingdom: Woodhead Publishing.
- Ahmed, E.M. (2015) Hydrogel: Preparation, characterization, and applications: A review. *Journal of Advanced Research*. 6 (2), pp.105–121.
- Akhtar, M.F., Hanif, M. and Ranjha, N.M. (2016) Methods of synthesis of hydrogels ... A review. *Saudi Pharmaceutical Journal*. 24 (5), pp. 554–559.
- Aljeboree, A.M. and Alkaim, A.F. (2019) Removal of Antibiotic Tetracycline (TCs) from aqueous solutions by using titanium dioxide (TiO₂) nanoparticles as an alternative material. *Journal of Physics: Conference Series*. 1294 (5), p. 052059.
- Allignet, J., Galdbart, J.-O., Morvan, A., Dyke, K.G.H., Vaudaux, P., Aubert, S., Desplaces, N. and Solh, N. El (1999) Tracking adhesion factors in *Staphylococcus caprae* strains responsible for human bone infections following implantation of orthopaedic material. *Microbiology*. 145 (8), pp.2033–2042.
- Alves, D.F., Magalhães, A.P., Neubauer, D., Bauer, M., Kamysz, W. and Pereira, M.O. (2018) Unveiling the fate of adhering bacteria to antimicrobial surfaces: expression of resistance-associated genes and macrophage-mediated phagocytosis. *Acta Biomaterialia*. 78, pp.189–197.

Ambrose, C.G., Clyburn, T.A., Louden, K., Joseph, J., Wright, J., Gulati, P., Gogola, G.R. and Mikos, A.G. (2004) Effective treatment of osteomyelitis with biodegradable microspheres in a rabbit model. *Clinical Orthopaedics & Related Research*. 421, pp.293–299.

Amiri, N., Ajami, S., Shahroodi, A., Jannatabadi, N., Amiri Darban, S., Fazly Bazzaz, B.S., Pishavar, E., Kalalinia, F. and Movaffagh, J. (2020) Teicoplanin-loaded chitosan-PEO nanofibers for local antibiotic delivery and wound healing. *International Journal of Biological Macromolecules*. 162, pp. 645–656.

Andrade del Olmo, J., Pérez-Álvarez, L., Sáez-Martínez, V., Benito-Cid, S., Ruiz-Rubio, L., Pérez-González, R., Vilas-Vilela, J.L. and Alonso, J.M. (2022) Wound healing and antibacterial chitosan-genipin hydrogels with controlled drug delivery for synergistic anti-inflammatory activity. *International Journal of Biological Macromolecules*. 203, pp. 679–694.

Andrea, A. (2019) Application of antimicrobial peptides for medical surfaces. PhD. Roskilde, Roskilde University.

Andrea, A. and Mansell, J.P. (2018) A facile and sensitive colorimetric approach to confirming the presence of polydopamine thin films on (bio)material surfaces. *Regenerative Medicine and Therapeutics*. 2 (1), pp. 30–36.

Antoci, V. et al. (2008) The inhibition of *Staphylococcus epidermidis* biofilm formation by vancomycin-modified titanium alloy and implications for the treatment of periprosthetic infection. *Biomaterials*. 29 (35), pp. 4684–4690.

Antoci, V., Adams, C.S., Hickok, N.J., Shapiro, I.M. and Parvizi, J. (2007) Vancomycin bound to Ti rods reduces periprosthetic infection: preliminary study. *Clinical Orthopaedics and Related Research*. (461), pp. 88–95.

Arciola, C.R., Campoccia, D. and Montanaro, L. (2018) Implant infections: adhesion, biofilm formation and immune evasion. *Nature Reviews Microbiology*. 16 (7), pp.397–409.

Armenia, I., Marcone, G.L., Berini, F., Orlandi, V.T., Pirrone, C., Martegani, E., Gornati, R., Bernardini, G. and Marinelli, F. (2018) Magnetic nanoconjugated teicoplanin: a novel tool for bacterial infection site targeting. *Frontiers in Microbiology*. 9 (2270), pp. 1-17.

Armstrong, D.W., Liu, Y. and Ekborgott, K.H. (1995) A covalently bonded teicoplanin chiral stationary phase for HPLC enantioseparations. *Chirality*. 7 (6), pp.474–497.

Askar, M., Bloch, B. and Bayston, R. (2018) Small-colony variant of *Staphylococcus lugdunensis* in prosthetic joint infection. *Arthroplasty Today*. 4 (3), pp.257–260.

Aykut, S., Öztürk, A., Özkan, Y., Yanik, K., İlman, A.A. and Özdemir, R.M. (2010) Evaluation and comparison of the antimicrobial efficacy of teicoplanin- and clindamycin-coated titanium implants. *The Journal of Bone and Joint Surgery*. 92-B (1), pp.159–163.

Ayre, W.N., Scott, T., Hallam, K., Blom, A.W., Denyer, S., Bone, H.K. and Mansell, J.P. (2016) Fluorophosphonate-functionalised titanium via a pre-adsorbed alkane phosphonic acid: a novel dual action surface finish for bone regenerative applications. *Journal of Materials Science: Materials in Medicine*. 27 (2), p. 36.

Bajaksouzian, S., Visalli, M.A., Jacobs, M.R. and Appelbaum, P.C. (1997) Activities of levofloxacin, ofloxacin, and ciprofloxacin, alone and in combination with amikacin, against acinetobacters as determined by checkerboard and time-kill studies. *Antimicrobial Agents and Chemotherapy*. 41 (5), pp. 1073–1076.

Baldino, L., Concilio, S., Cardea, S., De Marco, I. and Reverchon, E. (2015) Complete glutaraldehyde elimination during chitosan hydrogel drying by SC-CO₂ processing. *The Journal of Supercritical Fluids*. 103, pp. 70–76.

Ball, V., Frari, D. Del, Toniazzo, V. and Ruch, D. (2012) Kinetics of polydopamine film deposition as a function of pH and dopamine concentration: insights in the polydopamine deposition mechanism. *Journal of Colloid and Interface Science*. 386 (1), pp. 366–372.

Bano, I., Arshad, M., Yasin, T., Ghauri, M.A. and Younus, M. (2017) Chitosan: a potential biopolymer for wound management. *International Journal of Biological Macromolecules*. 102, pp. 380–383.

Barhate, C.L., Wahab, M.F., Breitbach, Z.S., Bell, D.S. and Armstrong, D.W. (2015) High efficiency, narrow particle size distribution, sub-2 μm based macrocyclic glycopeptide chiral stationary phases in HPLC and SFC. *Analytica Chimica Acta*. 898, pp. 128–137.

Bayan, E.M., Pustovaya, L.E. and Volkova, M.G. (2021) Recent advances in TiO_2 -based materials for photocatalytic degradation of antibiotics in aqueous systems. *Environmental Technology & Innovation*. 24, p. 101822.

Beauregard, D.A., Williams, D.H., Gwynn, M.N. and Knowles, D.J. (1995) Dimerization and membrane anchors in extracellular targeting of vancomycin group antibiotics. *Antimicrobial Agents and Chemotherapy*. 39 (3), pp.781–785.

Belmatoug, N., Cremieux, A. C., Bleton, R., Volk, A., Saleh-Mghir, A., Grossin, M., Garry, L. and Carbon, C. (1996) A new model of experimental prosthetic joint infection due to methicillin-resistant *Staphylococcus aureus*: a microbiologic, histopathologic, and magnetic resonance imaging characterization. *Journal of Infectious Diseases*. 174 (2), pp.414–417.

Berini, F., Orlandi, V.T., Gamberoni, F., Martegani, E., Armenia, I., Gornati, R., Bernardini, G. and Marinelli, F. (2021) Antimicrobial activity of nanoconjugated glycopeptide antibiotics and their effect on *Staphylococcus aureus* biofilm. *Frontiers in Microbiology*. 12.

Billon, A., Chabaud, L., Gouyette, A., Bouler, J.-M. and Merle, C. (2005) Vancomycin biodegradable poly(lactide-co-glycolide) microparticles for bone implantation. Influence of the formulation parameters on the size, morphology, drug loading and *in vitro* release. *Journal of Microencapsulation*. 22 (8), pp.841–852.

Binda, E., Marinelli, F. and Marcone, G. (2014) Old and new glycopeptide antibiotics: action and resistance. *Antibiotics*. 3 (4), pp.572–594.

- Black, J. (2005) *Biological performance of materials*. 4th edition. CRC Press.
- Blair, H.C. et al. (2017) Osteoblast differentiation and bone matrix formation in vivo and in vitro. *Tissue Engineering Part B: Reviews*. 23 (3), pp. 268–280.
- Bleb, H. and Kip, M. (2018) *White Paper on Joint Replacement* Bleß, H.-H. and Kip, M. (eds.) 1st edition. [online]. Berlin, Heidelberg. Springer.
- Blom, A.W., Hunt, L.P., Matharu, G.S., Reed, M.R. and Whitehouse, M.R. (2020) The effect of surgical approach in total hip replacement on outcomes: an analysis of 723,904 elective operations from the National Joint Registry for England, Wales, Northern Ireland and the Isle of Man. *BMC Medicine*. 18 (1), p.242.
- Boix-Montañes, A. and Garcia-Arieta, A. (2015) Composition specification of teicoplanin based on its estimated relative bioavailability. *Drug Development and Industrial Pharmacy*. 41 (2), pp. 218–223.
- Bozhkova, S., Tikhilov, R., Labutin, D., Denisov, A., Shubnyakov, I., Razorenov, V., Artyukh, V. and Rukina, A. (2016) Failure of the first step of two-stage revision due to polymicrobial prosthetic joint infection of the hip. *Journal of Orthopaedics and Traumatology*. 17 (4), pp.369–376.
- Branson, J.J. and Goldstein, W.M. (2003) Primary total hip arthroplasty. *AORN Journal*. 78 (6), pp.946–969.
- British Orthopaedic Association (2012) *Primary total hip replacement: a guide to good practice* [online]. Available from: https://britishhipociety.com/wp-content/uploads/2020/12/2012-Nov_BOA-Blue-Book.pdf
- Brittain, R. et al. (2022) NJR statistical analysis, support and associated services National Joint Registry. 19th Annual Report [online]. Available from: www.njrcentre.org.uk.

Britton, S., Lee, K., Azizova, L., Shaw, G., Ayre, W.N. and Mansell, J.P. (2022) Immobilised teicoplanin does not demonstrate antimicrobial activity against *Staphylococcus aureus*. *Scientific Reports*. 12 (1), p. 16661.

Browne, K., Kuppusamy, R., Chen, R., Willcox, M.D.P., Walsh, W.R., Black, D.StC. and Kumar, N. (2022) Bioinspired polydopamine coatings facilitate attachment of antimicrobial peptidomimetics with broad-spectrum antibacterial activity. *International Journal of Molecular Sciences*. 23 (6), p.2952.

Buchloh, S., Stieger, B., Meier, P.J. and Gaucklet, L. (2003) Hepatocyte performance on different crystallographic faces of rutile. *Biomaterials*. 24 (15), pp. 2605–2610.

Buttaro, M.A., Morandi, A., Rivello, H.G. and Piccaluga, F. (2005) Histology of vancomycin-supplemented impacted bone allografts in revision total hip arthroplasty. *The Journal of Bone and Joint Surgery. British volume*. 87-B (12), pp.1684–1687.

Byren, I., Bejon, P., Atkins, B.L., Angus, B., Masters, S., McLardy-Smith, P., Gundle, R. and Berendt, A. (2009) One hundred and twelve infected arthroplasties treated with 'DAIR' (debridement, antibiotics and implant retention: antibiotic duration and outcome. *Journal of Antimicrobial Chemotherapy*. 63 (6), pp.1264–1271.

Callaghan, J.J., Katz, R.P. and Johnston, R.C. (1999) One-stage revision surgery of the infected hip. *Clinical Orthopaedics and Related Research*. 369, pp.139–143.

Campoccia, D., Montanaro, L. and Arciola, C.R. (2013) A review of the biomaterial technologies for infection-resistant surfaces. *Biomaterials*. 34 (34), pp. 8533–8554.

Carballo-Vila, M., Moreno-Burriel, B., Chinarro, E., Jurado, J.R., Casañ-Pastor, N. and Collazos-Castro, J.E. (2009) Titanium oxide as substrate for neural cell growth. *Journal of Biomedical Materials Research Part A*. 90A (1), pp. 94–105.

Cassimjee, H., Kumar, P., Ubanako, P. and Choonara, Y.E. (2022) Genipin-crosslinked, proteosaccharide scaffolds for potential neural tissue engineering applications. *Pharmaceutics*. 14 (2), p. 441.

Catalbas, A., Akalin, Y., Şahin, İ.G., Cevik, N., Özkan, Y. and Öztürk, A. (2020) The effect of teicoplanin coating on osteointegration of titanium screws: a biomechanical and histomorphometric study in a rabbit model. *The European Research Journal*. 6 (5), pp. 401–408.

Chang, W.-H., Chang, Y., Lai, P.-H. and Sung, H.-W. (2003) A genipin-crosslinked gelatin membrane as wound-dressing material: *in vitro* and *in vivo* studies. *Journal of Biomaterials Science, Polymer Edition*. 14 (5), pp. 481–495.

Chen, A.F., Stewart, M.K., Heyl, A.E. and Klatt, B.A. (2012) Effect of immediate postoperative physical therapy on length of stay for total joint arthroplasty patients. *The Journal of Arthroplasty*. 27 (6), pp.851–856.

Chen, C., Zhang, X., Dong, X., Zhou, H., Li, X. and Liang, X. (2021) TiO₂ simultaneous enrichment, on-line deglycosylation, and sequential analysis of glyco- and phosphopeptides. *Frontiers in Chemistry*. 9.

Chen, J. et al. (2017) Preparation of an antimicrobial surface by direct assembly of antimicrobial peptide with its surface binding activity. *Journal of Materials Chemistry B*. 5 (13), pp.2407–2415.

Chen, X., Zhou, J., Qian, Y. and Zhao, L. (2023) Antibacterial coatings on orthopedic implants. *Materials Today Bio*. 19, p.100586.

Cheng, W., Wu, X., Zhang, Y., Wu, D., Meng, L., Chen, Y. and Tang, X. (2022) Recent applications of hydrogels in food safety sensing: Role of hydrogels. *Trends in Food Science & Technology*. 129, pp. 244–257.

Chiellini, F., Bizzarri, R., Ober, C.K., Schmaljohann, D., Yu, T., Solaro, R. and Chiellini, E. (2001) Patterning of polymeric hydrogels for biomedical applications. *Macromolecular Rapid Communications*. 22 (15), p. 1284.

- Chiono, V., Pulieri, E., Vozzi, G., Ciardelli, G., Ahluwalia, A. and Giusti, P. (2008) Genipin-crosslinked chitosan/gelatin blends for biomedical applications. *Journal of Materials Science: Materials in Medicine*. 19 (2), pp. 889–898.
- Chouirfa, H., Bouloussa, H., Migonney, V. and Falentin-Daudré, C. (2019) Review of titanium surface modification techniques and coatings for antibacterial applications. *Acta Biomaterialia*. 83, pp.37–54.
- Chui, W.K. and Wan, L.S.C. (1997) Prolonged retention of cross-linked trypsin in calcium alginate microspheres. *Journal of Microencapsulation*. 14 (1), pp. 51–61.
- Chung, Y.C. and Chen, C.Y. (2008) Antibacterial characteristics and activity of acid-soluble chitosan. *Bioresource Technology*. 99 (8), pp. 2806–2814.
- Clover, J. and Gowen, M. (1994) Are MG-63 and HOS TE85 human osteosarcoma cell lines representative models of the osteoblastic phenotype? *Bone*. 15 (6), pp. 585–591.
- Cobo, J. and Del Pozo, J.L. (2011) Prosthetic joint infection: diagnosis and management. *Expert Review of Anti-infective Therapy*. 9 (9), pp.787–802.
- Copello, G.J., Villanueva, M.E., González, J.A., López Egües, S. and Diaz, L.E. (2014) TEOS as an improved alternative for chitosan beads cross-linking: a comparative adsorption study. *Journal of Applied Polymer Science*. 131 (21).
- Cremieux, A. and Carbon, C. (1997) Experimental Models of Bone and Prosthetic Joint Infections. *Clinical Infectious Diseases*. 25 (6), pp.1295–1302.
- Czekanska, E., Stoddart, M., Richards, R. and Hayes, J. (2012) In search of an osteoblast cell model for in vitro research. *European Cells and Materials*. 24, pp. 1–17.
- Dale, H., Hallan, G., Espehaug, B., Havelin, L.I. and Engesaeter, L.B. (2009) Increasing risk of revision due to deep infection after hip arthroplasty. *Acta Orthopaedica*. 80 (6), pp.639–645.

- Das, M.P., R., S.P., Prasad, K., Jv, V. and M, R. (2017) Extraction and characterization of gelatin: a functional biopolymer. *International Journal of Pharmacy and Pharmaceutical Sciences*. 9 (9), p. 239.
- Davidson, D.J., Spratt, D. and Liddle, A.D. (2019) Implant materials and prosthetic joint infection: the battle with the biofilm. *EFORT Open Reviews*. 4 (11), pp.633–639.
- del Pozo, J.L. and Patel, R. (2007) The challenge of treating biofilm-associated bacterial Infections. *Clinical Pharmacology & Therapeutics*. 82 (2), pp.204–209.
- Della Vecchia, N.F., Luchini, A., Napolitano, A., Derrico, G., Vitiello, G., Szekely, N., Dischia, M. and Paduano, L. (2014) Tris buffer modulates polydopamine growth, aggregation, and paramagnetic properties. *Langmuir*. 30 (32), pp. 9811–9818.
- Dhandayuthapani, B., Krishnan, U.M. and Sethuraman, S. (2010) Fabrication and characterization of chitosan-gelatin blend nanofibers for skin tissue engineering. *Journal of Biomedical Materials Research Part B: Applied Biomaterials*. 94B (1), pp. 264-272
- Di Martino, A., Sittinger, M. and Risbud, M. V. (2005) Chitosan: a versatile biopolymer for orthopaedic tissue-engineering. *Biomaterials*. 26 (30), pp. 5983–5990.
- Ding, X., Yang, C., Lim, T.P., Hsu, L.Y., Engler, A.C., Hedrick, J.L. and Yang, Y.-Y. (2012) Antibacterial and antifouling catheter coatings using surface grafted PEG-b-cationic polycarbonate diblock copolymers. *Biomaterials*. 33 (28), pp. 6593–6603.
- Donlan, R.M. and Costerton, J.W. (2002) Biofilms: Survival Mechanisms of Clinically Relevant Microorganisms. *Clinical Microbiology Reviews*. 15 (2), pp.167–193.
- Economou, N.J., Nahoum, V., Weeks, S.D., Grasty, K.C., Zentner, I.J., Townsend, T.M., Bhuiya, M.W., Cocklin, S. and Loll, P.J. (2012) A Carrier Protein Strategy Yields the Structure of Dalbavancin. *Journal of the American Chemical Society*. 134 (10), pp. 4637–4645.

Economou, N.J., Zentner, I.J., Lazo, E., Jakoncic, J., Stojanoff, V., Weeks, S.D., Grasty, K.C., Cocklin, S. and Loll, P.J. (2013) Structure of the complex between teicoplanin and a bacterial cell-wall peptide: Use of a carrier-protein approach. *Acta Crystallographica Section D: Biological Crystallography*. 69 (4), pp.520–533.

El Helou, O.C., Berbari, E.F., Marculescu, C.E., Atrouni, W.I.E., Razonable, R.R., Steckelberg, J.M., Hanssen, A.D. and Osmon, D.R. (2008) Outcome of Enterococcal Prosthetic Joint Infection: Is Combination Systemic Therapy Superior to Monotherapy? *Clinical Infectious Diseases*. 47 (7), pp.903–909.

European Centre for Disease Prevention and Control (2022) *Antimicrobial Surveillance in Europe 2022-2020 Data* [online] Sweden: European Centre for Disease Prevention and Control. Available from: <https://www.ecdc.europa.eu/en/publications-data/antimicrobial-resistance-surveillance-europe-2022-2020-data> [Accessed 20 December 2022]

Fang, Q., Yao, Z., Feng, L., Liu, T., Wei, S., Xu, P., Guo, R., Cheng, B. and Wang, X. (2020) Antibiotic-loaded chitosan-gelatin scaffolds for infected seawater immersion wound healing. *International Journal of Biological Macromolecules*. 159, pp. 1140–1155.

Feng, W., Geng, Z., Li, Z., Cui, Z., Zhu, S., Liang, Y., Liu, Y., Wang, R. and Yang, X. (2016) Controlled release behaviour and antibacterial effects of antibiotic-loaded titania nanotubes. *Materials Science and Engineering: C*. 62, pp.105–112.

Fernandes Queiroz, M., Melo, K., Sabry, D., Sasaki, G. and Rocha, H. (2014) Does the use of chitosan contribute to oxalate kidney stone formation? *Marine Drugs*. 13 (1), pp. 141–158.

Fey, P.D. and Olson, M.E. (2010) Current concepts in biofilm formation of *Staphylococcus epidermidis*. *Future Microbiology*. 5 (6), pp.917–933.

Finley, R.L. et al. (2013) The scourge of antibiotic resistance: The important role of the environment. *Clinical Infectious Diseases*. 57 (5), pp.704–710.

- Fischetti, T., Celikkin, N., Contessi Negrini, N., Farè, S. and Swieszkowski, W. (2020) Tripolyphosphate-crosslinked chitosan/gelatin biocomposite ink for 3D printing of uniaxial scaffolds. *Frontiers in Bioengineering and Biotechnology*. 8.
- Fries, E., Crouzet, C., Michel, C. and Togola, A. (2016) Interactions of ciprofloxacin (CIP), titanium dioxide (TiO₂) nanoparticles and natural organic matter (NOM) in aqueous suspensions. *Science of The Total Environment*. 563–564, pp. 971–976.
- Fu, M., Liang, Y., Lv, X., Li, C., Yang, Y.Y., Yuan, P. and Ding, X. (2021) Recent advances in hydrogel-based anti-infective coatings. *Journal of Materials Science & Technology*. 85, pp. 169–183.
- Furkert, F.H., Sørensen, J.H., Arnoldi, J., Robioneck, B. and Steckel, H. (2011) Antimicrobial efficacy of surface-coated external fixation pins. *Current Microbiology*. 62 (6), pp.1743–1751.
- Gademan, M.G.J., Hofstede, S.N., Vliet Vlieland, T.P.M., Nelissen, R.G.H.H. and Marang-van de Mheen, P.J. (2016) Indication criteria for total hip or knee arthroplasty in osteoarthritis: a state-of-the-science overview. *BMC Musculoskeletal Disorders*. 17 (1), p.463.
- Gatin, L., Saleh-Mghir, A., Massin, P. and Crémieux, A.C. (2015) Critical analysis of experimental models of periprosthetic joint infection. *Orthopaedics & Traumatology: Surgery & Research*. 101 (7), pp.851–855.
- Georgopoulou, A., Papadogiannis, F., Batsali, A., Marakis, J., Alpantaki, K., Eliopoulos, A.G., Pontikoglou, C. and Chatzinikolaidou, M. (2018) Chitosan/gelatin scaffolds support bone regeneration. *Journal of Materials Science: Materials in Medicine*. 29 (5), p. 59.
- Gibon, E., Córdova, L.A., Lu, L., Lin, T.-H., Yao, Z., Hamadouche, M. and Goodman, S.B. (2017) The biological response to orthopedic implants for joint replacement. II: Polyethylene, ceramics, PMMA, and the foreign body reaction. *Journal of Biomedical Materials Research Part B: Applied Biomaterials*. 105 (6), pp.1685–1691.

Gidley, J., Openshaw, S., Pring, E.T., Sale, S. and Mansell, J.P. (2006) Lysophosphatidic acid cooperates with $1\alpha,25(\text{OH})_2\text{D}_3$ in stimulating human MG63 osteoblast maturation. *Prostaglandins & Other Lipid Mediators*. 80 (1–2), pp. 46–61.

Gimeno, M., Pinczowski, P., Pérez, M., Giorello, A., Martínez, M.Á., Santamaría, J., Arruebo, M. and Luján, L. (2015) A controlled antibiotic release system to prevent orthopedic-implant associated infections: An *in vitro* study. *European Journal of Pharmaceutics and Biopharmaceutics*. 96, pp.264–271.

Godoy-Gallardo, M., Mas-Moruno, C., Yu, K., Manero, J.M., Gil, F.J., Kizhakkedathu, J.N. and Rodriguez, D. (2015) Antibacterial properties of hLf1–11 peptide onto titanium surfaces: a comparison study between silanization and surface initiated polymerization. *Biomacromolecules*. 16 (2), pp.483–496.

Goy, R.C., Britto, D. de and Assis, O.B.G. (2009) A review of the antimicrobial activity of chitosan. *Polímeros*. 19 (3), pp. 241–247.

Green, J.-B.D., Fulghum, T. and Nordhaus, M.A. (2011) A review of immobilized antimicrobial agents and methods for testing. *Biointerphases*. 6 (4), pp.MR13–MR28.

Gristina, A.G., Naylor, P. and Myrvik, Q. (1988) Infections from biomaterials and implants: a race for the surface. *Medical progress through technology*. 14 (3–4), pp.205–24.

Guan, B. et al. (2016) Establishing antibacterial multilayer films on the surface of direct metal laser sintered titanium primed with phase-transited lysozyme. *Scientific Reports*. 6 (1), p.36408.

Hacı Mehmet, K., İzzet, A. and Bekir, S. (2019) A new titania glyco-purification tip for the fast enrichment and efficient analysis of glycopeptides and glycans by MALDI-TOF-MS. *Journal of Pharmaceutical and Biomedical Analysis*. 174, pp. 191–197.

Hall-Stoodley, L. et al. (2006) Direct Detection of Bacterial Biofilms on the Middle-Ear Mucosa of Children with Chronic Otitis Media. *Journal of the American Medical Association*. 296 (2), p.202.

Harris, S.R. et al. (2010) Evolution of MRSA during hospital transmission and intercontinental spread. *Science*. 327 (5964), pp.469–474.

He, S., Zhou, P., Wang, L., Xiong, X., Zhang, Y., Deng, Y. and Wei, S. (2014) Antibiotic-decorated titanium with enhanced antibacterial activity through adhesive polydopamine for dental/bone implant. *Journal of The Royal Society Interface*. 11 (95), p.20140169.

Head, W.C., Bauk, D.J. and Emerson, R.H. (1995) Titanium as the material of choice for cementless femoral components in total hip arthroplasty. *Clinical Orthopaedics and Related Research*. (311), pp.85–90.

Hennink, W.E. and van Nostrum, C.F. (2002) Novel crosslinking methods to design hydrogels. *Advanced Drug Delivery Reviews*. 54 (1), pp. 13–36.

Hickok, N.J. and Shapiro, I.M. (2012) Immobilized antibiotics to prevent orthopaedic implant infections. *Advanced Drug Delivery Reviews*. 64 (12), Elsevier, pp.1165–1176.

Hsiao, S.-W., Venault, A., Yang, H.-S. and Chang, Y. (2014) Bacterial resistance of self-assembled surfaces using PPO -b-PSBMA zwitterionic copolymer – Concomitant effects of surface topography and surface chemistry on attachment of live bacteria. *Colloids and Surfaces B: Biointerfaces*. 118, pp.254–260.

Hu, C.Y. and Yoon, T.-R. (2018) Recent updates for biomaterials used in total hip arthroplasty. *Biomaterials Research*. 22 (1), p.33.

Hunter, D.J. and Lo, G.H. (2008) The management of osteoarthritis: an overview and call to appropriate conservative treatment. *Rheumatic Disease Clinics of North America*. 34 (3), pp.689–712.

Ikeda, T., Ikeda, K., Yamamoto, K., Ishizaki, H., Yoshizawa, Y., Yanagiguchi, K., Yamada, S. and Hayashi, Y. (2014) Fabrication and characteristics of chitosan sponge as a tissue engineering scaffold. *BioMed Research International*. 2014, pp. 1–8.

Ionita, D., Bajenaru-Georgescu, D., Totea, G., Mazare, A., Schmuki, P. and Demetrescu, I. (2017) Activity of vancomycin release from bioinspired coatings of hydroxyapatite or TiO₂ nanotubes. *International Journal of Pharmaceutics*. 517 (1–2), pp.296–302.

Ivanova, E. and Crawford, R.J. (2015) *Antibacterial Surfaces*. 1st edition. Cham, Springer International Publishing.

Jacobsson, G., Dashti, S., Wahlberg, T. and Andersson, R. (2007) The epidemiology of and risk factors for invasive *Staphylococcus aureus* infections in western Sweden. *Scandinavian Journal of Infectious Diseases*. [online]. 39 (1), pp.6–13.

Jafari, S., Mahyad, B., Hashemzadeh, H., Janfaza, S., Gholikhani, T. and Tayebi, L. (2020) Biomedical applications of TiO₂ nanostructures: recent advances. *International Journal of Nanomedicine*. Volume 15, pp. 3447–3470.

Jain, A., Duvvuri, L.S., Farah, S., Beyth, N., Domb, A.J. and Khan, W. (2014) Antimicrobial Polymers. *Advanced Healthcare Materials*. 3 (12), pp. 1969–1985.

Jia, L. et al. (2019) Polydopamine-assisted surface modification for orthopaedic implants. *Journal of Orthopaedic Translation*. 17, pp. 82–95.

Jiao, Y., Niu, L., Ma, S., Li, J., Tay, F.R. and Chen, J. (2017) Quaternary ammonium-based biomedical materials: State-of-the-art, toxicological aspects and antimicrobial resistance. *Progress in Polymer Science*. 71, pp. 53–90.

John Hopkins Medicine (2022) *Hip Replacement Surgery*. Available from: <https://www.hopkinsmedicine.org/health/treatment-tests-and-therapies/hip-replacement-surgery> [Accessed 16 December 2022]

John Hopkins Medicine (2022) *Knee Replacement Surgery Procedure*. Available from: <https://www.hopkinsmedicine.org/health/treatment-tests-and-therapies/knee-replacement-surgery-procedure> [Accessed 18 December 2022]

- Johnson, C.T., Wroe, J.A., Agarwal, R., Martin, K.E., Guldberg, R.E., Donlan, R.M., Westblade, L.F. and García, A.J. (2018) Hydrogel delivery of lysostaphin eliminates orthopedic implant infection by *Staphylococcus aureus* and supports fracture healing. *Proceedings of the National Academy of Sciences* 115 (22).
- Jose, B., Antoci, V., Zeiger, A.R., Wickstrom, E. and Hickok, N.J. (2005) Vancomycin Covalently Bonded to Titanium Beads Kills *Staphylococcus aureus*. *Chemistry & Biology*. 12 (9), pp.1041–1048.
- Jovetic, S., Zhu, Y., Marcone, G.L., Marinelli, F. and Tramper, J. (2010) β -Lactam and glycopeptide antibiotics: first and last line of defense? *Trends in Biotechnology*. 28 (12), pp.596–604.
- Kaasch, A.J. et al. (2014) *Staphylococcus aureus* bloodstream infection: A pooled analysis of five prospective, observational studies. *Journal of Infection*. 68 (3), pp.242–251.
- Kahne, D., Leimkuhler, C., Lu, W. and Walsh, C. (2005) Glycopeptide and lipoglycopeptide antibiotics. *Chemical Reviews*. 105 (2), pp.425–448.
- Kapadia, B.H., Berg, R.A., Daley, J.A., Fritz, J., Bhave, A. and Mont, M.A. (2016) Periprosthetic joint infection. *The Lancet*. 387 (10016), pp.386–394.
- Kapadia, B.H., McElroy, M.J., Issa, K., Johnson, A.J., Bozic, K.J. and Mont, M.A. (2014) The Economic Impact of Periprosthetic Infections Following Total Knee Arthroplasty at a Specialized Tertiary-Care Center. *The Journal of Arthroplasty*. 29 (5), pp.929–932.
- Katti, K.S. (2004) Biomaterials in total joint replacement. *Colloids and Surfaces B: Biointerfaces*. 39 (3), pp.133–142.
- Kavran, J.M. and Leahy, D.J. (2014) Coupling Antibody to Cyanogen Bromide-Activated Sepharose. *Methods in Enzymology*. 541, pp. 27–34.

- Kavya, K.C., Jayakumar, R., Nair, S. and Chennazhi, K.P. (2013) Fabrication and characterization of chitosan/gelatin/nSiO₂ composite scaffold for bone tissue engineering. *International Journal of Biological Macromolecules*. 59, pp. 255–263.
- Kean, T. and Thanou, M. (2010) Biodegradation, biodistribution and toxicity of chitosan. *Advanced Drug Delivery Reviews*. 62 (1), pp. 3–11.
- Khor, E. and Lim, L.Y. (2003) Implantable applications of chitin and chitosan. *Biomaterials*. 24 (13), pp. 2339–2349.
- Kim, J., Kim, K., Choi, Y.-S., Kang, H., Kim, D.M. and Lee, J.-C. (2018) Polysulfone based ultrafiltration membranes with dopamine and nisin moieties showing antifouling and antimicrobial properties. *Separation and Purification Technology*. 202, pp. 9–20.
- Kim, J.-K., Park, I.W., Ro, D.H., Mun, B.-S., Han, H.-S. and Lee, M.C. (2021) Is a titanium implant for total knee arthroplasty better? A randomized controlled study. *The Journal of Arthroplasty*. 36 (4), pp.1302–1309.
- Klosterman, L., Riley, J.K. and Bettinger, C.J. (2015) Control of heterogeneous nucleation and growth kinetics of dopamine-melanin by altering substrate chemistry. *Langmuir*. 31 (11), pp. 3451–3458.
- Koyonos, L., Zmistowski, B., Della Valle, C.J. and Parvizi, J. (2011) Infection control rate of irrigation and debridement for periprosthetic joint infection. *Clinical Orthopaedics & Related Research*. 469 (11), pp.3043–3048.
- Kunutsor, S.K., Whitehouse, M.R., Blom, A.W. and Beswick, A.D. (2016) Patient-related risk factors for periprosthetic joint infection after total joint arthroplasty: a systematic review and meta-analysis. *PLOS ONE*. 11 (3), pp. 1-18.
- Kurita, K. (2006) Chitin and chitosan: functional biopolymers from marine crustaceans. *Marine Biotechnology*. 8 (3), pp. 203–226.

Kurtz, S.M., Ong, K.L., Lau, E., Bozic, K.J., Berry, D. and Parvizi, J. (2010) Prosthetic joint infection risk after TKA in the medicare population. *Clinical Orthopaedics & Related Research*. 468 (1), pp.52–56.

Lancaster, S. (2015) Novel routes towards securing human osteoblast maturation for potential orthopaedic applications. Doctor of Medicine. Bristol, University of Bristol.

Lancaster, S.T., Blackburn, J., Blom, A., Makishima, M., Ishizawa, M. and Mansell, J.P. (2014) 24,25-dihydroxyvitamin D3 cooperates with a stable, fluoromethylene LPA receptor agonist to secure human (MG63) osteoblast maturation. *Steroids*. 83, pp. 52–61.

Landor, I., Vavrik, P., Sosna, A., Jahoda, D., Hahn, H. and Daniel, M. (2007) Hydroxyapatite porous coating and the osteointegration of the total hip replacement. *Archives of Orthopaedic and Trauma Surgery*. 127 (2), pp.81–89.

Lee, H., Dellatore, S.M., Miller, W.M. and Messersmith, P.B. (2007) Mussel-inspired surface chemistry for multifunctional coatings. *Science*. 318 (5849), pp.426–430.

Lee, H., Rho, J. and Messersmith, P.B. (2009) Facile conjugation of biomolecules onto surfaces via mussel adhesive protein inspired coatings. *Advanced Materials*. 21 (4), pp. 431–434.

Lee, H., Scherer, N.F. and Messersmith, P.B. (2006) Single-molecule mechanics of mussel adhesion. *Proceedings of the National Academy of Sciences*. 103 (35), pp. 12999–13003.

Lee, S.Y., Lee, Y., Le Thi, P., Oh, D.H. and Park, K.D. (2018) Sulfobetaine methacrylate hydrogel-coated anti-fouling surfaces for implantable biomedical devices. *Biomaterials Research*. 22 (1), p. 3.

Leid, J.G., Shirtliff, M.E., Costerton, J.W. and Stoodley, and P. (2002) Human leukocytes adhere to, penetrate, and respond to *Staphylococcus aureus* biofilms. *Infection and Immunity*. 70 (11), pp.6339–6345.

Li, C., Renz, N. and Trampuz, A. (2018) Management of periprosthetic joint infection. *Hip & Pelvis*. 30 (3), p.138.

Li, H., Fu, J., Niu, E., Chai, W., Xu, C., Hao, L.B. and Chen, J. (2021) The risk factors of polymicrobial periprosthetic joint infection: a single-center retrospective cohort study. *BMC Musculoskeletal Disorders*. 22 (1), p.780.

Li, Y., Luo, L., Nie, M., Davenport, A., Li, Y., Li, B. and Choy, K.-L. (2022) A graphene nanoplatelet-polydopamine molecularly imprinted biosensor for Ultratrace creatinine detection. *Biosensors and Bioelectronics*. 216, p. 114638.

Lian, R., Cao, J., Jiang, X. and Rogachev, A. V. (2021) Prolonged release of ciprofloxacin hydrochloride from chitosan/gelatin/poly (vinyl alcohol) composite films. *Materials Today Communications*. 27, p. 102219.

Liddle, A.D., Judge, A., Pandit, H. and Murray, D.W. (2014) Adverse outcomes after total and unicompartmental knee replacement in 101 330 matched patients: a study of data from the National Joint Registry for England and Wales. *The Lancet*. 384 (9952), pp.1437–1445.

Liebs, T.R., Herzberg, W., Rütger, W., Haasters, J., Russlies, M. and Hassenpflug, J. (2012) Multicenter randomized controlled trial comparing early versus late aquatic therapy after total hip or knee arthroplasty. *Archives of Physical Medicine and Rehabilitation*. 93 (2), pp.192–199.

Liu, H.-W., Gu, W.-D., Xu, N.-W. and Sun, J.-Y. (2014) Surgical approaches in total knee arthroplasty: a meta-analysis comparing the midvastus and subvastus to the medial peripatellar approach. *The Journal of Arthroplasty*. 29 (12), pp.2298–2304.

Liu, Y., Dong, T., Chen, Y., Sun, N., Liu, Q., Huang, Z., Yang, Y., Cheng, H. and Yue, K. (2023) Biodegradable and cytocompatible hydrogel coating with antibacterial activity for the prevention of implant-associated infection. *ACS Applied Materials & Interfaces*. 15 (9), pp. 11507–11519.

Liu, Y., Rath, B., Tingart, M. and Eschweiler, J. (2020) Role of implants surface modification in osseointegration: a systematic review. *Journal of Biomedical Materials Research Part A*. 108 (3), pp. 470–484.

Lofrano, G., Ozkal, C.B., Carotenuto, M. and Meric, S. (2018) Comparison of TiO₂ and ZnO catalysts for heterogenous photocatalytic removal of vancomycin B. *Advances in environmental research*. 7 (3), pp. 213–223.

Lourtet-Hascoët, J., Félicé, M.P., Bicart-See, A., Bouige, A., Giordano, G. and Bonnet, E. (2018) Species and antimicrobial susceptibility testing of coagulase-negative staphylococci in periprosthetic joint infections. *Epidemiology and Infection*. 146 (14), pp.1771–1776.

Lu, Z., Gao, J., He, Q., Wu, J., Liang, D., Yang, H. and Chen, R. (2017) Enhanced antibacterial and wound healing activities of microporous chitosan-Ag/ZnO composite dressing. *Carbohydrate Polymers*. 156, pp. 460–469.

Mancera-Arteu, M., Benavente, F., Sanz-Nebot, V. and Giménez, E. (2023) Sensitive analysis of recombinant human erythropoietin glycopeptides by on-line phenylboronic acid solid-phase extraction capillary electrophoresis mass spectrometry. *Journal of Proteome Research*. 22 (3), pp. 826–836.

Mansell, J.P., Cooke, M., Read, M., Rudd, H., Shiel, A.I., Wilkins, K. and Manso, M. (2016) Chitinase 3-like 1 expression by human (MG63) osteoblasts in response to lysophosphatidic acid and 1,25-dihydroxyvitamin D3. *Biochimie*. 128–129, pp. 193–200.

Marculescu, C.E. and Cantey, R.J. (2008) Polymicrobial prosthetic joint infections: risk factors and outcome. *Clinical Orthopaedics & Related Research*. 466 (6), pp.1397–1404.

Massoumi, H., Nourmohammadi, J., Marvi, M.S. and Moztarzadeh, F. (2019) Comparative study of the properties of sericin-gelatin nanofibrous wound dressing containing halloysite nanotubes loaded with zinc and copper ions. *International Journal of Polymeric Materials and Polymeric Biomaterials*. 68 (18), pp. 1142–1153.

Mateo, M., Maestre, J.-R., Aguilar, L., Cafini, F., Puente, P., Sánchez, P., Alou, L., Giménez, M.-J. and Prieto, J. (2005) Genotypic versus phenotypic characterization, with respect to susceptibility and

identification, of 17 clinical isolates of *Staphylococcus lugdunensis*. *Journal of Antimicrobial Chemotherapy*. 56 (2), pp.287–291.

Matharu, G., Culliford, D., Blom, A. and Judge, A. (2022) Projections for primary hip and knee replacement surgery up to the year 2060: an analysis based on data from The National Joint Registry for England, Wales, Northern Ireland and the Isle of Man. *The Annals of The Royal College of Surgeons of England*. 104 (6), pp.443–448.

Mathew, S.A. and Arumainathan, S. (2022) Crosslinked chitosan–gelatin biocompatible nanocomposite as a neuro drug carrier. *ACS Omega*. 7 (22), pp. 18732–18744.

Matuschek, E., Brown, D.F.J. and Kahlmeter, G. (2013) Development of the EUCAST disk diffusion antimicrobial susceptibility testing method and its implementation in routine microbiology laboratories. *Clinical Microbiology and Infection*. 20 (4), pp. O255–O266.

McConoughey, S.J., Howlin, R., Granger, J.F., Manring, M.M., Calhoun, J.H., Shirtliff, M., Kathju, S. and Stoodley, P. (2014) Biofilms in periprosthetic orthopedic infections. *Future Microbiology*. 9 (8), pp.987–1007.

Mendez-Vilas, A. (2011) *Science Against Microbial Pathogens: Communicating Current Research and Technological Advances*. Spain: Formatex Research Center.

Mi, F.-L., Tan, Y.-C., Liang, H.-F. and Sung, H.-W. (2002) *In vivo* biocompatibility and degradability of a novel injectable-chitosan-based implant. *Biomaterials*. 23 (1), pp. 181–191.

Migneault, I., Dartiguenave, C., Bertrand, M.J. and Waldron, K.C. (2004) Glutaraldehyde: behavior in aqueous solution, reaction with proteins, and application to enzyme crosslinking. *BioTechniques*. 37 (5), pp. 790–802.

Mindroiu, M., Pirvu, C., Galateanu, B. and Demetrescu (2014) Corrosion behaviour and cell viability of untreated and laser treated Ti6Al7Nb alloys. *Revista de Chimie*. 63 (3), pp.328–334.

- Miranda, S.C.C.C., Silva, G.A.B., Hell, R.C.R., Martins, M.D., Alves, J.B. and Goes, A.M. (2011) Three-dimensional culture of rat BMMSCs in a porous chitosan-gelatin scaffold: a promising association for bone tissue engineering in oral reconstruction. *Archives of Oral Biology*. 56 (1), pp. 1–15.
- Miura, K., Yamada, N., Hanada, S., Jung, T.-K. and Itoi, E. (2011) The bone tissue compatibility of a new Ti–Nb–Sn alloy with a low young's modulus. *Acta Biomaterialia*. 7 (5), pp.2320–2326.
- Mohd Daud, N., Saeful Bahri, I.F., Nik Malek, N.A.N., Hermawan, H. and Saidin, S. (2016) Immobilization of antibacterial chlorhexidine on stainless steel using crosslinking polydopamine film: towards infection resistant medical devices. *Colloids and Surfaces B: Biointerfaces*. 145, pp.130–139.
- Moura, C.M. de, Moura, J.M. de, Soares, N.M. and Pinto, L.A. de A. (2011) Evaluation of molar weight and deacetylation degree of chitosan during chitin deacetylation reaction: Used to produce biofilm. *Chemical Engineering and Processing: Process Intensification*. 50 (4), pp. 351–355.
- Muxika, A., Etxabide, A., Uranga, J., Guerrero, P. and de la Caba, K. (2017) Chitosan as a bioactive polymer: processing, properties and applications. *International Journal of Biological Macromolecules*. 105, pp. 1358–1368.
- Mwale, F., Iordanova, M., Demers, C.N., Steffen, T., Roughley, P. and Antoniou, J. (2005) Biological evaluation of chitosan salts cross-linked to genipin as a cell scaffold for disk tissue engineering. *Tissue Engineering*. 11 (1–2), pp. 130–140.
- Nagarajan, S., Soussan, L., Bechelany, M., Teyssier, C., Cavailles, V., Pochat-Bohatier, C., Miele, P., Kalkura, N., Janot, J. M. and Balme, S. (2016) Novel biocompatible electrospun gelatin fiber mats with antibiotic drug delivery properties. *Journal of Materials Chemistry B*. 4 (6), pp. 1134–1141.
- Naghizadeh, Z., Karkhaneh, A. and Khojasteh, A. (2018) Self-crosslinking effect of chitosan and gelatin on alginate based hydrogels: Injectable in situ forming scaffolds. *Materials Science and Engineering: C*. 89, pp. 256–264.

Nakazawa, K., Lee, S.-W., Fukuda, J., Yang, D.-H. and Kunitake, T. (2006) Hepatocyte spheroid formation on a titanium dioxide gel surface and hepatocyte long-term culture. *Journal of Materials Science: Materials in Medicine*. 17 (4), pp. 359–364.

National Health Service (2019) *Hip Replacement*. Available from: <https://www.nhs.uk/conditions/hip-replacement/> [Accessed 16 December 2022]

National Health Service (2022) *Knee Replacement*. Available from: <https://www.nhsinform.scot/tests-and-treatments/surgical-procedures/knee-replacement> [Accessed 18 December 2022]

NHS (2021) *Guidelines for use of Teicoplanin* [online]. Doncaster: NHS. Available from: <https://www.dbth.nhs.uk/wp-content/uploads/2021/02/GUIDELINES-FOR-USE-OF-TEICOPLANIN-2020-v4.pdf> [Accessed 12 January 2023]

Nouri-Felekori, M., Khakbiz, M., Nezafati, N., Mohammadi, J. and Eslaminejad, M.B. (2019) Comparative analysis and properties evaluation of gelatin microspheres crosslinked with glutaraldehyde and 3-glycidoxypropyltrimethoxysilane as drug delivery systems for the antibiotic vancomycin. *International Journal of Pharmaceutics*. 557, pp. 208–220.

Nowack, B. and Bucheli, T.D. (2007) Occurrence, behavior and effects of nanoparticles in the environment. *Environmental Pollution*. 150 (1), pp. 5–22.

Orapiriyakul, W., Young, P.S., Dammati, L. and Tsimbouri, P.M. (2018) Antibacterial surface modification of titanium implants in orthopaedics. *Journal of Tissue Engineering*. 9, p.204173141878983.

Otari, S. V., Patil, R.M., Waghmare, S.R., Ghosh, S.J. and Pawar, S.H. (2013) A novel microbial synthesis of catalytically active Ag–alginate biohydrogel and its antimicrobial activity. *Dalton Transactions*. 42 (27), p.9966.

Ottenbrite, R.M., Park, K. and Okano, T. (2010) *Biomedical applications of hydrogels handbook*. New York, NY, Springer New York.

Ozkan, E., Crick, C.C., Taylor, A., Allan, E. and Parkin, I.P. (2016) Copper-based water repellent and antibacterial coatings by aerosol assisted chemical vapour deposition. *Chemical Science*. 7 (8), pp.5126–5131.

Palan, J. and Manktelow, A. (2018) Surgical approaches for primary total hip replacement. *Orthopaedics and Trauma*. 32 (1), pp.1–12.

Parenti, F., Schito, G.C. and Courvalin, P. (2000) Teicoplanin Chemistry and Microbiology. *Journal of Chemotherapy*. 12 (sup5), pp.5–14.

Park, J. H., Sudarshan, T. S. (2001) *Chemical vapour deposition*. United States of America: ASM International

Parvizi, J. et al. (2011) New definition for periprosthetic joint infection: from the workgroup of the Musculoskeletal Infection Society. *Clinical Orthopaedics & Related Research*. 469 (11), pp.2992–2994.

Parvizi, J., Pawasarat, I.M., Azzam, K.A., Joshi, A., Hansen, E.N. and Bozic, K.J. (2010) Periprosthetic joint infection: the economic impact of methicillin-resistant infections. *The Journal of Arthroplasty*. 25 (6), pp.103–107.

Patel, K., Singh, N., Yadav, J., Nayak, J.M., Sahoo, S.K., Lata, J., Chand, D., Kumar, S. and Kumar, R. (2018) Polydopamine films change their physicochemical and antimicrobial properties with a change in reaction conditions. *Physical Chemistry Chemical Physics*. 20 (8), pp. 5744–5755.

Pathak, T.P. and Miller, S.J. (2013) Chemical tailoring of teicoplanin with site-selective reactions. *Journal of the American Chemical Society*. 135 (22), pp. 8415–22.

Patterson, J.T. and Cassells, J.A. (1963) An examination of the value of adding peptone to diluents used in the bacteriological testing of bacon curing brines. *Journal of Applied Bacteriology*. 26 (3), pp. 493–497.

Peel, T.N., Cheng, A.C., Buising, K.L. and Choong, P.F.M. (2012) Microbiological aetiology, epidemiology, and clinical profile of prosthetic joint infections: are current antibiotic prophylaxis guidelines effective? *Antimicrobial Agents and Chemotherapy*. 56 (5), pp.2386–2391.

Peterson, J.W., Petrasky, L.J., Seymour, M.D., Burkhart, R.S. and Schuiling, A.B. (2012) Adsorption and breakdown of penicillin antibiotic in the presence of titanium oxide nanoparticles in water. *Chemosphere*. 87 (8), pp. 911–917.

Pivec, R., Johnson, A.J., Mears, S.C. and Mont, M.A. (2012) Hip arthroplasty. *The Lancet*. 380 (9855), pp.1768–1777.

Premkumar, A., Kolin, D.A., Farley, K.X., Wilson, J.M., McLawhorn, A.S., Cross, M.B. and Sculco, P.K. (2021) Projected economic burden of periprosthetic joint infection of the hip and knee in the United States. *The Journal of Arthroplasty*. 36 (5), pp.1484-1489.e3.

Rakow, A., Perka, C., Trampuz, A. and Renz, N. (2019) Origin and characteristics of haematogenous periprosthetic joint infection. *Clinical Microbiology and Infection*. 25 (7), pp.845–850.

Razmjou, A., Asadnia, M., Ghaebi, O., Yang, H.-C., Ebrahimi Warkiani, M., Hou, J. and Chen, V. (2017) Preparation of iridescent 2D photonic crystals by using a mussel-inspired spatial patterning of ZIF-8 with potential applications in optical switch and chemical sensor. *ACS Applied Materials & Interfaces*. 9 (43), pp. 38076–38080.

Razonable, R.R., Lewallen, D.G., Patel, R. and Osmon, D.R. (2001) Vertebral osteomyelitis and prosthetic joint infection due to *Staphylococcus simulans*. *Mayo Clinic Proceedings*. 76 (10), pp.1067–1070.

Riacci, L., Sorriento, A. and Ricotti, L. (2021) Genipin-based crosslinking of jellyfish collagen 3D hydrogels. *Gels*. 7 (4), p. 238.

Ribeiro, M., Monteiro, F.J. and Ferraz, M.P. (2012) Infection of orthopedic implants with emphasis on bacterial adhesion process and techniques used in studying bacterial-material interactions. *Biomatter*. 2 (4), pp.176–194.

Rodrigues, S., Dionísio, M., López, C.R. and Grenha, A. (2012) Biocompatibility of chitosan carriers with application in drug delivery. *Journal of Functional Biomaterials*. 3 (3), pp. 615–641.

Rodríguez-Pardo, D. *et al.* (2014) Gram-negative prosthetic joint infection: outcome of a debridement, antibiotics and implant retention approach. A large multicentre study. *Clinical Microbiology and Infection*. 20 (11), pp.0911–0919.

Rodríguez-Rodríguez, R., Espinosa-Andrews, H., Velasquillo-Martínez, C. and García-Carvajal, Z.Y. (2020) Composite hydrogels based on gelatin, chitosan and polyvinyl alcohol to biomedical applications: a review. *International Journal of Polymeric Materials and Polymeric Biomaterials*. 69 (1), pp. 1–20.

Roller, S. and Covill, N. (1999) The antifungal properties of chitosan in laboratory media and apple juice. *International Journal of Food Microbiology*. 47 (1–2), pp. 67–77.

Roller, S. and Covill, N. (2000) The antimicrobial properties of chitosan in mayonnaise and mayonnaise-based shrimp salads. *Journal of Food Protection*. 63 (2), pp. 202–209.

Rose, J., Pacelli, S., Haj, A., Dua, H., Hopkinson, A., White, L. and Rose, F. (2014) Gelatin-based materials in ocular tissue engineering. *Materials*. 7 (4), pp. 3106–3135.

Ryu, J.H., Messersmith, P.B. and Lee, H. (2018) Polydopamine surface chemistry: a decade of discovery. *ACS Applied Materials & Interfaces*. 10 (9), pp. 7523–7540.

Saha, R. and Tayalia, P. (2022) Clove oil-incorporated antibacterial gelatin–chitosan cryogels for tissue engineering: an *in vitro* study. *ACS Biomaterials Science & Engineering*. 8 (8), pp. 3557–3567.

Sampathkumar, P., Osmon, D.R. and Cockerill, F.R. (2000) Prosthetic joint infection due to *Staphylococcus lugdunensis*. *Mayo Clinic Proceedings*. 75 (5), pp.511–512.

Sangeetha, S., Kathyayini, S.R., Raj, P.D., Dhivya, P. and Sridharan, M. (2013) Biocompatibility studies on TiO₂ coated Ti surface. In: *International Conference on Advanced Nanomaterials & Emerging Engineering Technologies*. IEEE, pp. 404–408.

Seidlitz, C. and Kip, M. (2018) Introduction to the Indications and Procedures In: *White Paper on Joint Replacement*. 1st edition. Berlin, Heidelberg, Springer Berlin Heidelberg, 1–14.

Sendi, P., Banderet, F., Graber, P. and Zimmerli, W. (2011) Periprosthetic joint infection following *Staphylococcus aureus* bacteremia. *Journal of Infection*. 63 (1), pp.17–22.

Sethi, S., Medha and Kaith, B.S. (2022) A review on chitosan-gelatin nanocomposites: synthesis, characterization and biomedical applications. *Reactive and Functional Polymers*. 179, p. 105362.

Shah, N.B., Osmon, D.R., Fadel, H., Patel, R., Kohner, P.C., Steckelberg, J.M., Mabry, T. and Berbari, E.F. (2010) Laboratory and clinical characteristics of *Staphylococcus lugdunensis* prosthetic joint infections. *Journal of Clinical Microbiology*. 48 (5), pp.1600–1603.

Shahin, A., Ramazani S.A, A., Mehraji, S. and Eslami, H. (2022) Synthesis and characterization of a chitosan/gelatin transparent film crosslinked with a combination of EDC/NHS for corneal epithelial cell culture scaffold with potential application in cornea implantation. *International Journal of Polymeric Materials and Polymeric Biomaterials*. 71 (8), pp. 568–578.

Sheng, Q., Li, X., Yin, W., Yu, L., Ke, Y. and Liang, X. (2013) Retention mechanism and enrichment of glycopeptides on titanium dioxide. *Analytical Methods*. 5 (24), p. 7072.

Shiel, A.I., Ayre, W.N., Blom, A.W., Hallam, K.R., Heard, P.J., Payton, O., Picco, L. and Mansell, J.P. (2020) Development of a facile fluorophosphonate-functionalised titanium surface for potential orthopaedic applications. *Journal of Orthopaedic Translation*. 23, pp. 140–151.

Shiels, S., Mangum, L. and Wenke, J. (2020) Revisiting the “race for the surface” in a pre-clinical model of implant infection. *European Cells and Materials*. 39, pp. 77–95.

Simpson, A.H.R.W. (2022) Incidence, complications and novel treatment strategies: joint arthroplasty In: *Musculoskeletal Infection*. [online]. Cham, Springer International Publishing, 227–282.

Singha, P., Locklin, J. and Handa, H. (2017) A review of the recent advances in antimicrobial coatings for urinary catheters. *Acta Biomaterialia*. 50, pp.20–40.

Sivakumar, M. and Panduranga Rao, K. (2002) Preparation, characterization and *in vitro* release of gentamicin from coralline hydroxyapatite–gelatin composite microspheres. *Biomaterials*. 23 (15), pp. 3175–3181.

Smith, L.K., Garriga, C., Kingsbury, S.R., Pinedo-Villanueva, R., Delmestri, A., Arden, N.K., Stone, M., Conaghan, P.G. and Judge, A. (2022) UK poSt arthroplasty follow-up recommendations (UK SAFE): what does analysis of linked, routinely collected national data sets tell us about mid-late term revision risk after hip replacement? Retrospective cohort study. *BMJ Open*. 12 (3), p.e050877.

Song, L., Gan, L., Xiao, Y.-F., Wu, Y., Wu, F. and Gu, Z.-W. (2011) Antibacterial hydroxyapatite/chitosan complex coatings with superior osteoblastic cell response. *Materials Letters*. 65 (6), pp. 974–977.

Sørensen, S.J., Bailey, M., Hansen, L.H., Kroer, N. and Wuertz, S. (2005) Studying plasmid horizontal transfer in situ: a critical review. *Nature Reviews Microbiology*. 3 (9), pp.700–710.

Southwood, R., Rice, J., McDonald, P., Hakendorf, P. and Rozenbils, M. (1985) Infection in experimental hip arthroplasties. *The Journal of Bone and Joint Surgery. British volume*. 67-B (2), pp.229–231.

Stoodley, P., Nistico, L., Johnson, S., Lasko, L.-A., Baratz, M., Gahlot, V., Ehrlich, G.D. and Kathju, S. (2008) Direct Demonstration of viable *Staphylococcus aureus* biofilms in an infected total joint arthroplasty. *The Journal of Bone and Joint Surgery-American Volume*. 90 (8), pp.1751–1758.

- Straka, R.P. and Stokes, J.L. (1957) Rapid destruction of bacteria in commonly used diluents and its elimination. *Applied Microbiology*. 5 (1), pp. 21–25.
- Su, L., Yu, Y., Zhao, Y., Liang, F. and Zhang, X. (2016) Strong antibacterial polydopamine coatings prepared by a shaking-assisted method. *Scientific Reports*. 6 (1), p. 24420.
- Subbiahdoss, G., Kuijjer, R., Grijpma, D.W., van der Mei, H.C. and Busscher, H.J. (2009) Microbial biofilm growth vs. tissue integration: “The race for the surface” experimentally studied. *Acta Biomaterialia*. 5 (5), pp.1399–1404.
- Szymańska, E. and Winnicka, K. (2015) Stability of chitosan—a challenge for pharmaceutical and biomedical applications. *Marine Drugs*. 13 (4), pp. 1819–1846.
- Tan, T.Y., Ng, S.Y. and He, J. (2008) Microbiological characteristics, presumptive identification, and antibiotic susceptibilities of *Staphylococcus lugdunensis*. *Journal of Clinical Microbiology*. 46 (7), pp.2393–2395.
- Tande, A.J. and Patel, R. (2014) Prosthetic joint infection. *Clinical Microbiology Reviews*. 27 (2), pp.302–345.
- Tang, Z.-W., Ma, C.-Y., Wu, H.-X., Tan, L., Xiao, J.-Y., Zhuo, R.-X. and Liu, C.-J. (2016) Antiadhesive zwitterionic poly-(sulphobetaine methacrylate) brush coating functionalized with triclosan for high-efficiency antibacterial performance. *Progress in Organic Coatings*. 97, pp.277–287.
- Taujenis, L., Olšauskaitė, V. and Padaruskas, A. (2014) Enantioselective determination of protein amino acids in fertilizers by liquid chromatography–tandem mass spectrometry on chiral teicoplanin stationary phase. *Journal of Agricultural and Food Chemistry*. 62 (46), pp. 11099–11108.
- Teterycz, D., Ferry, T., Lew, D., Stern, R., Assal, M., Hoffmeyer, P., Bernard, L. and Uçkay, I. (2010) Outcome of orthopedic implant infections due to different staphylococci. *International Journal of Infectious Diseases*. 14 (10), pp.e913–e918.

Thakur, V. K. (2017) *Biopolymer Grafting: Applications*. 1st ed. Amsterdam: Elsevier

Thein-Han, W.W., Saikhun, J., Pholpramoo, C., Misra, R.D.K. and Kitiyanant, Y. (2009) Chitosan–gelatin scaffolds for tissue engineering: physico-chemical properties and biological response of buffalo embryonic stem cells and transfectant of GFP–buffalo embryonic stem cells. *Acta Biomaterialia*. 5 (9), pp. 3453–3466.

Tin, S., Lim, C., Sakharkar, M. and Sakharkar, K. (2010) Synergistic Combinations of Chitosans and Antibiotics in *Staphylococcus aureus*. *Letters in Drug Design & Discovery*. 7 (1), pp. 31–35.

Trzcińska, Z., Bruggeman, M., Ijakipour, H., Hodges, N.J., Bowen, J. and Stamboulis, A. (2020) Polydopamine linking substrate for AMPs: characterisation and stability on Ti6Al4V. *Materials*. 13 (17), p.3714.

Tsai, I., Wu, F., Gau, C. and Kuo, C. (2009) Method development for the determination of teicoplanin in patient serum by solid phase extraction and micellar electrokinetic chromatography. *Talanta*. 77 (3), pp. 1208–1216.

Uçkay, I. et al. (2009) Low incidence of haematogenous seeding to total hip and knee prostheses in patients with remote infections. *Journal of Infection*. 59 (5), pp.337–345.

Van Bambeke, F. (2006) Glycopeptides and glycodepsipeptides in clinical development: a comparative review of their antibacterial spectrum, pharmacokinetics and clinical efficacy. *Current opinion in investigational drugs* (London, England : 2000). 7 (8), pp. 740–9.

Vanhegan, I.S., Malik, A.K., Jayakumar, P., Ul Islam, S. and Haddad, F.S. (2012) A financial analysis of revision hip arthroplasty. *The Journal of Bone and Joint Surgery. British volume*. 94-B (5), pp.619–623.

Varacallo, M., Luo, T.D. and Johanson, N.A. (2023) *Total Knee Arthroplasty Techniques*. StatPearls [Online] Treasure Island, Florida. Statpearls Publishing. Available from: <https://www.ncbi.nlm.nih.gov/books/NBK499896/> [Accessed 23 December 2022]

Vaudaux, P.E., Zulian, G., Huggler, E. and Waldvogel, F.A. (1985) Attachment of *Staphylococcus aureus* to polymethylmethacrylate increases its resistance to phagocytosis in foreign body infection. *Infection and Immunity*. 50 (2), pp.472–477.

Vimberg, V. (2021) Teicoplanin—A New Use for an Old Drug in the COVID-19 Era? *Pharmaceuticals*. 14 (12), p.1227.

Vlasceanu, G.M., Şelaru, A., Dinescu, S., Balta, C., Herman, H., Gharbia, S., Hermenean, A., Ionita, M. and Costache, M. (2020) Comprehensive appraisal of graphene–oxide ratio in porous biopolymer hybrids targeting bone-tissue regeneration. *Nanomaterials*. 10 (8), p. 1444.

Vukomanović, M., Logar, M., Škapin, S.D. and Suvorov, D. (2014) Hydroxyapatite/gold/arginine: designing the structure to create antibacterial activity. *Journal of Material Chemistry B*. 2 (11), pp.1557–1564.

Waite, J.H. (1987) Nature's underwater adhesive specialist. *International Journal of Adhesion and Adhesives*. 7 (1), pp. 9–14.

Wang, H., An, X., Deng, X. and Ding, G. (2017) Facile synthesis and application of teicoplanin-modified magnetic microparticles for enantioseparation. *Electrophoresis*. 38 (9–10), pp.1374–1382.

Wang, X., Wang, J., Yu, Y., Yu, L., Wang, Y., Ren, K. and Ji, J. (2022) A polyzwitterion-based antifouling and flexible bilayer hydrogel coating. *Composites Part B: Engineering*. 244, p. 110164.

Wei, T., Yu, Q. and Chen, H. (2019) Responsive and synergistic antibacterial coatings: fighting against bacteria in a smart and effective way. *Advanced Healthcare Materials*. 8 (3), p. 1801381.

Widmer, A.F. (2001) New developments in diagnosis and treatment of infection in orthopedic implants. *Clinical Infectious Diseases*. 33 (s2), pp.S94–S106.

Williams, D., Garbuz, D. and Masri, B. (2010) Total knee arthroplasty: techniques and results. *BC Medical Journal*. 52 (9), pp.447–454.

Wisplinghoff, H., Bischoff, T., Tallent, S.M., Seifert, H., Wenzel, R.P. and Edmond, M.B. (2004) Nosocomial bloodstream infections in US hospitals: analysis of 24,179 cases from a prospective nationwide surveillance study. *Clinical Infectious Diseases*. 39 (3), pp.309–317.

Witsø, E., Persen, L., Benum, P. and Bergh, K. (2005) Cortical allograft as a vehicle for antibiotic delivery. *Acta Orthopaedica*. 76 (4), pp. 481–486.

Wronska, M.A., O'Connor, I.B., Tilbury, M.A., Srivastava, A. and Wall, J.G. (2016) Adding functions to biomaterial surfaces through protein incorporation. *Advanced Materials*. 28 (27), pp.5485–5508.

Wu, F., Meng, G., He, J., Wu, Y., Wu, F. and Gu, Z. (2014) Antibiotic-loaded chitosan hydrogel with superior dual functions: antibacterial efficacy and osteoblastic cell responses. *ACS Applied Materials & Interfaces*. 6 (13), pp. 10005–10013.

Xiao, M., Jasensky, J., Gerszberg, J., Chen, J., Tian, J., Lin, T., Lu, T., Lahann, J. and Chen, Z. (2018) Chemically immobilized antimicrobial peptide on polymer and self-assembled monolayer substrates. *Langmuir*. 34 (43), pp.12889–12896.

Xing, Q., Yates, K., Vogt, C., Qian, Z., Frost, M.C. and Zhao, F. (2014) Increasing mechanical strength of gelatin hydrogels by divalent metal ion removal. *Scientific Reports*. 4 (1), p. 4706.

Xu, Z. and Grassian, V.H. (2017) Bovine serum albumin adsorption on TiO₂ nanoparticle surfaces: effects of pH and coadsorption of phosphate on protein–surface interactions and protein structure. *The Journal of Physical Chemistry C*. 121 (39), pp. 21763–21771.

Yan, L., Xu, Y., Yu, H., Xin, X., Wei, Q. and Du, B. (2010) Adsorption of phosphate from aqueous solution by hydroxy-aluminum, hydroxy-iron and hydroxy-iron–aluminum pillared bentonites. *Journal of Hazardous Materials*. 179 (1–3), pp. 244–250.

Yang, G., Xiao, Z., Long, H., Ma, K., Zhang, J., Ren, X. and Zhang, J. (2018) Assessment of the characteristics and biocompatibility of gelatin sponge scaffolds prepared by various crosslinking methods. *Scientific Reports*. 8 (1), p. 1616.

Yang, J., Tian, F., Wang, Z., Wang, Q., Zeng, Y.-J. and Chen, S.-Q. (2008) Effect of chitosan molecular weight and deacetylation degree on hemostasis. *Journal of Biomedical Materials Research Part B: Applied Biomaterials*. 84B (1), pp. 131–137.

Yokoe, D.S., Avery, T.R., Platt, R. and Huang, S.S. (2013) Reporting surgical site infections following total hip and knee arthroplasty: impact of limiting surveillance to the operative hospital. *Clinical Infectious Diseases*. 57 (9), pp.1282–1288.

Yu, Y., Xu, S., Li, S. and Pan, H. (2021) Genipin-cross-linked hydrogels based on biomaterials for drug delivery: a review. *Biomaterials Science*. 9 (5), pp. 1583–1597.

Zeng, D., Debabov, D., Hartsell, T.L., Cano, R.J., Adams, S., Schuyler, J.A., McMillan, R. and Pace, J.L. (2016) Approved glycopeptide antibacterial drugs: mechanism of action and resistance. *Cold Spring Harbor Perspectives in Medicine*. 6 (12), p.a026989.

Zhang, Y. and Huang, Y. (2021) Rational design of smart hydrogels for biomedical applications. *Frontiers in Chemistry*. 8.

Zhao, D., Chen, C., Wang, Y., Ji, H., Ma, W., Zang, L. and Zhao, J. (2008) Surface modification of TiO₂ by phosphate: effect on photocatalytic activity and mechanism implication. *The Journal of Physical Chemistry C*. 112 (15), pp. 5993–6001.

Zhao, G., Schwartz, Z., Wieland, M., Rupp, F., Geis-Gerstorfer, J., Cochran, D.L. and Boyan, B.D. (2005) High surface energy enhances cell response to titanium substrate microstructure. *Journal of Biomedical Materials Research Part A*. 74A (1), pp. 49–58.

Zhao, W., Ye, Q., Hu, H., Wang, X. and Zhou, F. (2014) Grafting zwitterionic polymer brushes via electrochemical surface-initiated atomic-transfer radical polymerization for anti-fouling applications. *Journal of Materials Chemistry B*. 2 (33), pp.5352–5357.

Zhao, X., Li, P., Guo, B. and Ma, P.X. (2015) Antibacterial and conductive injectable hydrogels based on quaternized chitosan-graft-polyaniline/oxidized dextran for tissue engineering. *Acta Biomaterialia*. 26, pp. 236–248.

Zheng, L.-Y. and Zhu, J.-F. (2003) Study on antimicrobial activity of chitosan with different molecular weights. *Carbohydrate Polymers*. 54 (4), pp. 527–530.

Zhou, P., Deng, Y., Lyu, B., Zhang, R., Zhang, H., Ma, H., Lyu, Y. and Wei, S. (2014) Rapidly-deposited polydopamine coating via high temperature and vigorous stirring: formation, characterization and biofunctional evaluation. *PLoS ONE*. 9 (11), p. e113087.

Zhu, C., Zhang, W., Fang, S., Kong, R., Zou, G., Bao, N.-R., Zhao, J.-N. and Shang, X.-F. (2018) Antibiotic peptide-modified nanostructured titanium surface for enhancing bactericidal property. *Journal of Materials Science*. 53 (8), pp.5891–5908.

Zimmerli, W. and Ochsner, P.E. (2003) Management of infection associated with prosthetic joints. *Infection*. 31 (2), pp.99–108.



OPEN Immobilised teicoplanin does not demonstrate antimicrobial activity against *Staphylococcus aureus*

S. Britton¹, K. Lee², L. Azizova³, G. Shaw³, W. Nishio Ayre³ & J. P. Mansell^{1,2,3}

Antibacterial bone biomaterial coatings appeal to orthopaedics, dentistry and veterinary medicine. Achieving the successful, stable conjugation of suitable compounds to biomaterial surfaces is a major challenge. A pragmatic starting point is to make use of existing, approved antibiotics which are known to remain functional in a stationary, immobilised state. This includes the macrocyclic glycopeptide, teicoplanin, following the discovery, in the 1990's, that it could be used as a chiral selector in chromatographic enantiomeric separations. Importantly teicoplanin works at the level of the bacterial cell wall making it a potential candidate for biomaterial functionalisations. We initially sought to functionalise titanium (Ti) with polydopamine and use this platform to capture teicoplanin, however we were unable to avoid the natural affinity of the antibiotic to the oxide surface of the metal. Whilst the interaction between teicoplanin and Ti was robust, we found that phosphate resulted in antibiotic loss. Before contemplating the covalent attachment of teicoplanin to Ti we examined whether a commercial teicoplanin stationary phase could kill staphylococci. Whilst this commercially available material could bind N-Acetyl-L-Lys-D-Ala-D-Ala it was unable to kill bacteria. We therefore strongly discourage attempts at covalently immobilising teicoplanin and/or other glycopeptide antibiotics in the pursuit of novel antibacterial bone biomaterials.

Minimising infection risk of implantable bone biomaterials, e.g., titanium (Ti), continues to be a priority area in contemporary materials science research¹. Covalent grafting of suitable antibacterial agents to Ti could be a potential route but finding solutions to creating antibacterial surfaces is especially challenging; selected agents need to retain functionality when in a stationary, immobile state and need to demonstrate biocidal activity by acting at the level of the cell wall or membrane². Evidence of stability to γ -irradiation typically applied to medical devices is also highly desirable. Importantly the antimicrobial agent should display low or minimal toxicity, demonstrating compatibility with host cells to ensure osseointegration. In realising the development of an antibacterial Ti technology, we have taken inspiration from enantioselective chromatography using covalently immobilised glycopeptide antibiotics as the chiral selectors^{3–9}.

With regard to sourcing the appropriate antibacterial agent we have focused on teicoplanin (Teic), a macrocyclic glycopeptide antibiotic (Fig. 1) produced by *Actinoplanes teichomyceticus*¹⁰. Teic binds to the C-terminal of D-Ala-D-Ala motifs of non-crosslinked lipid II which forms during the biosynthesis of peptidoglycan, an essential component of the bacterial cell wall. This is especially important in realising the fabrication of a stably bound antibacterial Ti coating because Teic is acting at the level of the cell wall to eradicate bacteria. Both anaerobic and aerobic Gram-positive bacteria are susceptible to Teic, including MRSA which has particular significance in the context of total joint replacement infections¹. Compared to other glycopeptide antibiotics, e.g., ristocetin and vancomycin, Teic is markedly more surface active with multiple, unique, functional groups. Teic can be likened to a semi-rigid aglycone basket composed of four main ring systems that are fused. These in turn consist of seven aromatic rings, two of which have chlorine-substitutions and four of which exhibit ionisable phenolic moieties. Within the aglycone basket is an amine (cationic site) juxtaposed to a carbonyl group and a carboxylic acid group (anionic site). At the periphery are three monosaccharides; α -D-mannose, β -D-N-acetylglucosamine and β -D-N-acetylglucosamine of which one of the glucosamine residues is tethered to a fatty

¹Department of Applied Sciences, University of the West of England, Coldharbour Lane, Bristol BS16 1QY, UK. ²Department of Chemistry, Green-Nano Materials Research Center, Kyungpook National University, Daegu 41566, South Korea. ³School of Dentistry, Cardiff University, Cardiff CF14 4XY, UK. [✉]email: Jason.mansell@uwe.ac.uk

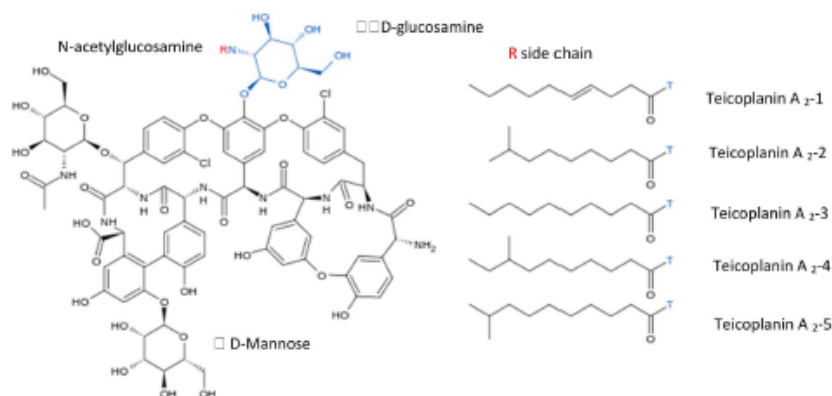


Figure 1. Structure of teicoplanin.

N-acyl chain extension. It is the presence of the hydrocarbon chain that is peculiar to Teic and a feature enabling the antibiotic to nestle within the lipid leaflet of bacteria¹¹.

During the early to mid-1990's Teic became a powerful tool in the development of novel chiral stationary phases for chromatographic enantiomeric separations¹². As a covalently-bound chiral selector, Teic performs well in the reversed phase, normal phase and "polar-organic" modes yielding highly efficacious multimodal chromatography media¹². In more recent times Teic bonded to silica is considered a "state of art" material for utilisation in super/subcritical liquid chromatography¹³. Specialised chromatography columns packed with silica covalently bonded to Teic for enantiomeric separations have been commercially available for many years, for example TeicoShell from Azyp LLC (Arlington, Texas).

The discovery that covalently tethered, immobilised Teic could retain biological function is key in developing antibacterial bone biomaterials that are capable of directly killing MRSA. Compared to vancomycin, Teic has a greater stability and exhibits lower nephro/ototoxicity and has reduced potential for causing red-man syndrome¹⁴. With regard to obvious concerns over antibiotic resistance there have been some noteworthy developments in Teic biochemistry. For example, Pathak and Miller¹⁵ have chemically modified the antibiotic to develop brominated variants to help combat the risk of resistance by providing a greater spectrum of antibacterial products. There is also evidence that Teic can withstand 25 kGy of γ -irradiation¹⁶, the preferred sterilisation route for implantable devices. Collectively these features place Teic as a choice candidate for Ti-functionalisation.

We initially sought to develop an antibacterial Ti surface by first coating the metal with polydopamine (PDA) following a report on the successful generation of a magnetic chiral stationary phase using Teic conjugated to PDA-coated iron oxide particles¹⁷. During the course of our work, we were unable to successfully graft Teic to PDA-Ti and found that the antibiotic simply bound well to the natural oxide finish of the metal. Some of the findings from this work are presented herein. We next turned our attention to covalently binding Teic to Ti following earlier claims that this might be a viable option for glycopeptide antibiotics^{18,19}. Before doing so we wanted to ascertain if a commercially available chiral stationary phase, consisting of Teic covalently tethered to silica shells, was capable of killing staphylococci.

Materials and methods

Reagents and Ti disc preparation. Unless stated otherwise all reagents were of analytical grade and purchased from Sigma-Aldrich (Poole, UK). Orthopaedic-grade Ti discs (10 mm diameter; 1.5 mm thickness) were kindly provided by OsteoCare (Slough, UK). On arrival the discs were thoroughly cleaned by extensive distilled water washing, exposure to acetone, water rinsing again, followed by concentrated nitric acid exposure, a further extensive water wash and then baking, in air, at 180 °C for 72 h. 14 mm TiO₂-coated AT cut QCM sensors (Ti-QCM, Ti/Au metallization with a TiO₂ coating and resonant frequency of 5 MHz) were purchased from Microvacuum (Budapest, Hungary).

Bacterial culture preparation. The organism used was a *Staphylococcus aureus* strain (NCTC 12981) obtained from Public Health England (Salisbury, UK). Stock cultures were maintained on beads at -80 °C. Working cultures were maintained on Brain-Heart Infusion agar plates (BHIA; Oxoid, Basingstoke, UK) and sub-cultured weekly for a maximum of four weeks to maintain viability and colony characteristics. For broth inoculum preparation, 2-3 colonies were taken from a BHIA plate into 10 ml Brain-Heart Infusion broth (BHIB; Oxoid, Basingstoke, UK) and incubated for 16-18 h at 37 °C with gentle shaking (120 RPM). The reason for using BHIB is that it is a good, rich, general-purpose medium that permits good growth of a variety of bacteria. Standards were made by adjusting overnight cultures in phosphate buffered saline (PBS) to an OD_{625nm} of 0.08-0.12 (0.5 McFarland standard; approx. 1.5 × 10⁷ CFU/ml) and further diluted in a 1% Petone/PBS broth to a

final density of 1.5×10^5 CFU/ml. This was used in all microbiological assays unless specified. Since Teic is active on the cell wall of proliferating cells, the bacteria need to be metabolically active, hence the rationale for using a minimal medium supplemented with 1% peptone.

Bacterial viability to Teic-Ti. This method was adapted from Ayre et al.²⁰ Ti discs were immersed in 500 µg/ml of Teic (1 ml) in 2-(N-Morpholino)ethanesulfonic acid (MES; 50 mM; pH 5.47) for 2 h, washed in distilled water twice to remove weakly bound Teic and allowed to dry. Once dried, Ti discs were exposed to a 10^5 CFU/ml suspension of *S. aureus* for 24 h at 37 °C with gentle shaking (120 RPM). After incubation, discs were recovered, washed twice with 0.85% saline and sonicated for 5 min in 1 ml of maximum recovery diluent (MRD; Oxoid, Basingstoke, UK) to recover attached bacteria. MRD is an isotonic diluent that combines a protective effect of peptone with the osmotic balance of physiological saline. The detached bacteria were transferred to a sterile universal tube and incubated for 30 min at 37 °C in order to achieve maximum recovery. The rationale for taking this approach is to reduce the risk of bacterial loss from sonication when using purely aqueous media. The recovered organisms were diluted and dispensed onto BHIA using the Miles and Misra technique²¹ and incubated for 24 h at 37 °C prior to colony counting. Over a period of approximately 2 months a total of 12 independent experiments were performed using 36 control and 36-functionalised Ti discs.

X-ray photoelectron spectroscopy (XPS) of Teic-Ti. In parallel with the studies conducted above, Ti discs were exposed to 500 µg/ml solution of Teic in 50 mM MES, pH 5.47 and left, under ambient conditions from 30 min up to 3 h. To analyse elements on the surface of Ti and functionalised samples, XPS spectra were taken by using NEXSA XPS system (ThermoFisher, Waltham, MA, US). A monochromatic X-ray source (Al-Kα) beam was used for the data collection. The calculation of the atomic percentages was performed using Avantage Data System software (ThermoFisher, Waltham, MA, US).

Teic-Ti adsorption studies. Orthopaedic-grade Ti discs and solid TiO₂ powder (mixture of rutile and anatase) were used to examine Teic adsorption to the metal oxide.

For the TiO₂ powder, 50 mg was dispensed into microcentrifuge tubes and immersed in 500 µl of Teic (500 µg/ml in 50 mM HEPES; pH 7.4) and left to incubate, for up to 30 min, under ambient conditions. TiO₂ with HEPES only was used as a control. At each time point, samples were centrifuged at $11,300 \times g$ for 2 min and 25 µl of each supernatant was added to 500 µl of freshly prepared bicinchoninic acid reagent (BCA; ThermoFisher, Waltham, MA, US) as per the manufacturer's instructions and incubated for 30 min at 60 °C. After incubation, sample aliquots (100 µl) were subsequently transferred to a 96-well plate and measured against a series of Teic standards at 540 nm using a microplate reader (TECAN, Männedorf, Switzerland). To confirm Teic-TiO₂ attachment, the supernatant was decanted and the powder samples were washed twice by centrifugation and resuspended in 500 µl HEPES buffer. A 25 µl sample of each powder suspension was added to 500 µl of BCA reagent, incubated and assessed in the same manner as above.

Assessment of binding robustness between Teic and TiO₂. To determine how robust the Teic adsorption was to the TiO₂, TiO₂ powder (50 mg) was added to microcentrifuge tubes, followed by 500 µl of Teic (500 µg/ml) in HEPES (50 mM; pH 7.4) buffer and incubated under ambient conditions for 2 h. TiO₂ with HEPES buffer only was used as a control. Once incubated, samples were centrifuged at $11,300 \times g$ for 2 min, the supernatants were discarded, and the pellets were washed up to 10 times with HEPES buffer (500 µl per wash). After 1, 3, 5 and 10 washes, 25 µl of each wash was combined with 500 µl of BCA and incubated for 30 min at 60 °C. Once incubated, 100 µl aliquots were transferred to a 96-well plate and measured at 540 nm using a microplate reader (TECAN, Männedorf, Switzerland). To assess the efficacy of the Teic-TiO₂ attachment, the supernatant was decanted after each wash and remaining pellets resuspended in 500 µl of HEPES buffer. A 25 µl sample of the resuspended pellet was combined to 500 µl of BCA reagent and incubated for 30 min at 60 °C. Once incubated, samples were centrifuged to pellet the powder and the supernatant was measured in the same manner as above.

Thermal Gravimetric Analysis (TGA) was performed in order to assess the thermal stability of immobilised Teic to the oxide of TiO₂. TiO₂ powder (50 mg) was added to microcentrifuge tubes, followed by addition of either 500 µl of Teic (500 µg/ml) in HEPES (50 mM; pH 7.4) buffer or HEPES buffer alone as a control. The samples were incubated under ambient conditions for 2 h and then centrifuged at $11,300 \times g$ for 2 min. The supernatant was discarded and the pellets air dried at room temperature. Teic powder was also analysed as a reference sample. Samples were run on a Pyris 1 TGA under a nitrogen flow of 40 ml/min (Perkin Elmer, Beaconsfield, UK). The sample was stabilised at 30 °C for 20 min before heating to 800 °C at a rate of 5 °C/min. Data was analysed using Pyris TGA software (Perkin Elmer, Beaconsfield, UK).

Influence of phosphate on Teic-TiO₂ binding. The impact of phosphate on the bonding between Teic-TiO₂ was also examined given the affinity of the anion to Ti²⁺. Briefly TiO₂ powder (50 mg) were exposed to 500 µg/ml Teic prepared in PBS (pH 7.3), where the phosphate concentration was either 1 mM or 10 mM and samples left to incubate at room temperature for 30 min. Teic (500 µg/ml)-TiO₂ in HEPES (50 mM; pH 7.4) and TiO₂ in HEPES only were used as controls. After incubation, samples were centrifuged and 25 µl of the supernatant was combined to 500 µl BCA reagent and incubated for 30 min at 60 °C. Once incubated, 100 µl aliquots were transferred to a 96-well plate and measured at 540 nm using a microplate reader. To confirm Teic-TiO₂ attachment, the supernatant was decanted, the powder samples were washed once by centrifugation ($11,300 \times g$) for 2 min and TiO₂ pellets resuspended in 500 µl buffer. A 25 µl aliquot of each powder suspension was added to

500 μ l of BCA reagent and incubated for 30 min at 60 °C. Once incubated, powder samples were centrifuged and 100 μ l of each supernatant were transferred to a 96-well plate and measured using a microplate reader.

Influence of phosphate on Teic detachment from TiO₂. To investigate the impact of phosphate on the detachment of Teic from TiO₂, a quartz crystal microbalance (QCM) system with impedance measurement was used (QCM-I, MicroVacuum, Budapest, Hungary). TiO₂-coated QCM sensors (Ti-QCM) were subjected to HEPES buffer (50 mM; pH 7.4) at a flow rate of 100 μ l/min using a peristaltic pump (Ismatec Reglo Digital, Wertheim, Germany) at a constant temperature of 21 °C using a high precision built in Peltier driver to avoid temperature drifts (stability of \pm 0.02 °C). After a stable baseline was obtained over a minimum of 10 min, 500 μ g/ml Teic in HEPES was injected using a Rheodyne MXP injection system with a semiautomatic switching valve (MXP9960-000, California, US) for another 10 min. The Ti-QCM sensor was then subjected to a final 10 min with either HEPES or PBS with 1 mM, 2 mM, 5 mM or 10 mM phosphate concentrations. Frequency at the 1st, 3rd and 5th overtones and dissipation measurements were collected. Sauerbrey mass was calculated using Biosense software (Microvacuum, Budapest, Hungary). Experiments were performed in triplicate.

Ti-Ti elution studies. Ti discs were exposed to Teic (500 μ g/ml in 50 mM MES, pH 5.4) and incubated for 2 h under ambient conditions. After incubation, discs were washed with distilled water to dislodge any loosely bound Teic and allowed to dry in a sterile environment. Control and functionalised Ti discs were then immersed in 1% Peptone/PBS and left for 24 h at 37 °C with gentle shaking (120 RPM). After incubation, the recovered conditioned media (100 μ l) was transferred to a sterile 96-well plate and inoculated with *S. aureus* (100 μ l) to achieve a final density of 10⁵ CFU/ml. The samples were then incubated at 37 °C for a further 24 h. At the desired time the optical density OD at 595 nm (using a microplate reader) was taken to ascertain bacterial growth in the conditioned media. To determine if the conditioned discs still retained any antimicrobial activity the control and functionalised Ti discs were transferred to a new multiwell plate and washed in distilled water twice, allowed to dry and then exposed to a 10⁵ CFU/ml suspension of *S. aureus* and incubated for a further 24 h at 37 °C with gentle shaking (120 RPM). After incubation, discs were recovered, washed twice with 0.85% saline and sonicated for 5 min in 1 ml of MRD to recover the attached bacteria. The detached bacteria were transferred to a new universal and incubated for 30 min at 37 °C in order to achieve maximum recovery. The recovered organisms were diluted and dispensed onto BHIA using the Miles and Misra technique²¹ and incubated for 24 h at 37 °C prior to colony counting.

Teico stationary phase (TSP)—N-Acetyl-L-Lys-D-Ala-D-Ala binding studies. A commercially available chiral stationary phase, consisting of covalently tethered Teic to silica shells (TSP) was sourced from AZYP (Arlington, Texas) in which approximately 68 mg of Teic is bound to 1 g of silica. The tripeptide N-Acetyl-L-Lys-D-Ala-D-Ala (Cambridge Bioscience, UK) was reconstituted to 200 μ g/ml in 50 mM HEPES (pH 7.4). Briefly, TSP (100 mg) was exposed to 500 μ l of the tripeptide.

(200 μ g/ml) and incubated under ambient conditions for 30 min. After incubation, the sample was centrifuged (11,300 \times g) for 2 min and the supernatant was collected (500 μ l) and transferred into a new microcentrifuge tube. The pH of the supernatant was adjusted to \sim 8.4 using NaOH and exposed to 5 μ l of genipin (250 mM in DMSO) and then left to react at 60 °C for 2 h. To assess the binding of the tripeptide to the TSP, the remaining pellet was washed three times in HEPES (50 mM; pH 7.4) using centrifugation and resuspended in 500 μ l of HEPES buffer. The pH of the pellet was adjusted to \sim 8.4 and subsequently exposed to 5 μ l of genipin and left to react for 2 h at 60 °C. After incubation, the OD₅₉₅ of the samples were measured using a microplate reader (TECAN, Männedorf Switzerland). Plain silica shells (AZYP, TX, US) was used as a control and assessed in the same manner.

Bacterial viability to TSP. To assess the antibacterial activity of the chiral stationary phase, aliquots (50 mg) were added to microcentrifuge tubes and immersed in a 70% ethanol solution for 10 min to sterilise the powder. This was washed three times in a 1% peptone/PBS solution using centrifugation (11,300 \times g). After centrifugation, the washed pellets were resuspended in 1 ml of a 1% peptone/PBS solution containing 10⁵ CFU/ml of *S. aureus* and transferred to a sterile bijou. A further 4 ml of the bacterial suspension was added to the bijou to a final volume of 5 ml (final concentration of TSP suspension was 10 mg/ml, corresponding to a final Teic concentration of 680 μ g/ml). This was incubated for 24 h at 37 °C with gentle shaking (120 RPM). A final concentration of free teicoplanin (600 μ g/ml) and untreated silica were used as controls. After incubation, samples were diluted in MRD, dispensed onto BHIA using the Miles & Misra technique²¹ and incubated for a further 24 h at 37 °C prior to colony counting.

Statistical analysis. Unless stated otherwise, all experiments above were repeated at least three times in triplicate. All data were subject to a normality test to ensure data were normally distributed. A one- or two-way analysis of variance (ANOVA) or Kruskal–Wallis test was used, where appropriate, to test for statistical significance using Graphpad Prism software (Version 8; San Diego, CA, USA) with $p < 0.05$ regarded as being statistically significant. When $p \leq 0.05$ was found, a Tukey or Sidak's multiple comparisons post-test was used between all groups. In some instances, an unpaired t -test (2-tailed) were used to compare the means of functionalised and control surfaces. All data are expressed as the mean together with the standard deviation.

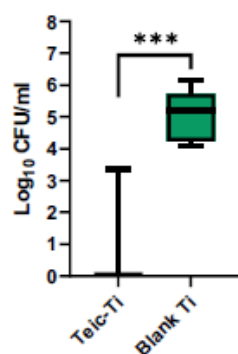


Figure 2. Antibacterial efficacy of Teic-modified Ti. Ti discs were immersed in 500 µg/ml Teic (50 mM MES; pH 5.47) for 2 h under ambient conditions. After incubation, functionalised and control discs were transferred to a new well plate, washed twice in distilled water and subsequently exposed to a 10^5 CFU/ml suspension of *S. aureus* in 1% Peptone/PBS for 24 h at 37 °C with gentle shaking (120 RPM). After incubation, discs were recovered, washed twice with 0.85% saline and sonicated for 5 min in 1 ml of MRD to recover attached bacteria. The detached bacteria were transferred to a new universal and incubated for 30 min at 37 °C in order to achieve maximum recovery. The recovered organisms were diluted and dispensed onto BHIA and incubated for 24 h at 37 °C. When Ti discs are steeped in a solution of Teic the modified surfaces are capable of significantly reducing bacterial attachment in comparison to the control (blank) Ti ($***p < 0.0001$). All data (mean ± SD; N=36) represent pooled triplicate runs from 12 independent experiments.

Results

Ti discs exposed to Teic exhibits antibacterial activity. Bacterial attachment to Teic-modified Ti was assessed by exposing *S. aureus* to functionalised and control Ti discs for 24 h at 37 °C. Attachment of *S. aureus* to the modified Ti surface was found to be significantly lower ($p < 0.0001$) when compared to Ti alone (Fig. 2) and resulted in a 5-log reduction from the initial seeding density (10^5 CFU/ml). Of the 36 Ti discs exposed to Teic, only 7 specimens were associated with modest bacterial growth ($\sim 10^2$ – 10^3 CFU/ml). Similar results were obtained for Ti discs exposed to Teic for as little as 5 min (data not shown).

Physicochemical evidence of Teic adsorption to Ti. To analyse elements on the surface of control and functionalised Ti samples, XPS was performed. Confirmation of the presence of Teic was observed in the form of increasing chlorine peaks (Cl_{2s}) over time, suggesting that Teic can adsorb to the surface within 30 min of exposure to the antibiotic (Fig. 3). As expected, a change in the atomic composition with increasing time supported adsorption of the antibiotic to Ti (Table 1).

Teic binds avidly to TiO₂. To observe the adsorption of Teic to the metal oxide, TiO₂ powder was used. Interestingly, it was found that Teic adsorption to TiO₂ was the same for all time points tested (Fig. 4A,B) and would suggest that immersing the oxide in Teic for as little as 5 min affords functionalisation. To determine the durability of Teic attachment to TiO₂ the modified oxide powder was subjected to repeated washings. Despite the small loss of Teic after the first wash (Fig. 4C,D) the oxide still retained a large amount of the antibiotic, even after 10 washes, suggesting a robust attachment.

To further elucidate the robustness of the Teic attachment to the oxide of TiO₂, TGA was performed on Teic alone, TiO₂ powder and TiO₂ powder functionalised with Teic. Percentage weight loss curves for Teic alone showed an initial decrease at temperatures below 100 °C due to residual moisture evaporation caused by the hydrophilic nature of Teic. Thermal decomposition of Teic was observed at temperatures greater than 250 °C with three distinct derivative peaks demonstrating maximum weight loss rates at approximately 270 °C, 357 °C and 402 °C (Fig. 5A). TiO₂ powder incubated in HEPES buffer showed a single weight loss step between 250 °C and 400 °C and a total percentage weight reduction of 12.91% (Fig. 5B). Similar percentage weight and derivative weight curves were obtained for TiO₂ samples incubated with Teic, however a greater weight loss of 13.97% was observed between 250 and 400 °C with a more distinct derivative peak at 365 °C (Fig. 5C). This greater weight loss indicates the dissociation of Teic from the surface of TiO₂ at high temperatures and thermal stability of immobilised Teic at temperatures up to 250 °C.

Phosphate compromises the binding of Teic to TiO₂. The impact of phosphate on the bonding between Teic and TiO₂ was examined as the anion is known to have a strong affinity for the oxide²². It was found that phosphate could compromise the binding of Teic to TiO₂ and that increasing the phosphate concentration from 1 to 10 mM resulted in less antibiotic binding to the oxide (Fig. 6). This likely suggests that the phosphate anion has a greater affinity for the oxide than the antibiotic. To control for the possible influence of sodium and/

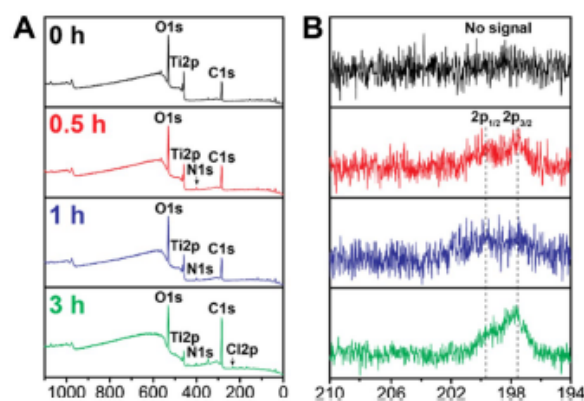


Figure 3. Detection of Teic coating on the Ti surface. X-Ray Photoelectron Spectroscopy (XPS) analysis of (A) survey peaks and (B) high-resolution Cl2p peaks of Teic-treated Ti discs with different immersion times: 0, 0.5, 1, and 3 h. It is clear that Teic adsorption occurs within 30 min of Teic exposure.

Time (h)	Cl1s (at.%)	N1s (at.%)	O1s (at.%)	Cl2p (at.%)	Ti2p (at.%)
–	41.9 ± 1.9	1.4 ± 0.1	45.0 ± 1.6	–	11.7 ± 0.4
0.5	45.0 ± 1.0	2.5 ± 0.2	43.2 ± 0.8	0.3 ± 0.1	9.1 ± 0.5
1	47 ± 0.6	2.6 ± 0.5	41.4 ± 0.9	0.3 ± 0.1	8.8 ± 0.1
3	42.3 ± 0.4	3.0 ± 0.1	30.1 ± 0.5	0.5 ± 0.1	4.0 ± 0.5

Table 1. Elemental composition of control and Teic-functionalised Ti. Quantified atomic percentage (at.%) of the elements in each Ti specimen treated with Teic. The clear changes in elemental composition with increasing incubation time support Teic adsorption to the metal surface.

or chloride ions we reconstituted Teic in 50 mM HEPES (pH 7.4) supplemented with NaCl up to 1 M and found this to be without impact on antibiotic binding to TiO₂ (data not shown).

Phosphate displaces Teic bound to TiO₂ rapidly. The ability of phosphate to readily detach Teic from the surface of TiO₂ is shown in Fig. 7. Injection of 500 µg/ml Teic in HEPES resulted in rapid adsorption of Teic to the surface of the Ti-QCM sensor which plateaued after approximately 5 min, resulting in a surface coverage of 100–200 ng/cm² (based on Sauerbrey mass calculations). Washing the surface of the coated Ti-QCM sensors with HEPES resulted in removal of loosely bound Teic (Fig. 7A) however the majority of Teic still remained on the surface of the Ti-QCM sensor. Conversely, washing the surface with phosphate containing buffers resulted in the immediate dissociation of Teic from the Ti-QCM sensor (Fig. 7B–E). Slight delays between injections and changes in resonant frequency were observed due to the length of tubing and time required for the injected sample to reach the surface of the Ti-QCM sensor.

Evidence of Teic loss following culture conditioning of Teic-functionalised Ti. To determine if the conditions of bacterial culture result in antibiotic elution from the Ti surface, functionalised and control Ti discs were subject to a mock bacterial culture for 24 h. As anticipated the culture media recovered from control Ti supported bacterial growth with evidence of solution turbidity and OD₂₉₅ values ranging between 0.17 and 0.27 (Fig. 8A). In contrast, the conditioned media recovered from Teic-functionalised Ti completely inhibited bacterial growth, as indicated by clear solutions and OD₂₉₅ values similar to the blanks. To assess the bactericidal activity, media recovered from Teic-Ti was spot inoculated on to BHIA and left to incubate for 24 h at 37 °C. This confirmed that the culture medium from the modified discs exhibited a large amount of bactericidal activity as no growth occurred after incubation when compared to the culture medium recovered from the control Ti discs (data not shown). The conditioned discs were subsequently exposed to *S. aureus* to determine if they were still able to kill bacteria. The findings obtained for these conditioned samples indicated a loss of antibacterial activity, further confirming that the antibiotic elutes from the metal surface under the conditions described (Fig. 8B).

A Teic chiral stationary phase (TSP) binds to the tripeptide N-Acetyl-L-Lys-D-Ala-D-Ala. The binding of the chiral stationary phase to the tripeptide was monitored using genipin, a natural chemical compo-

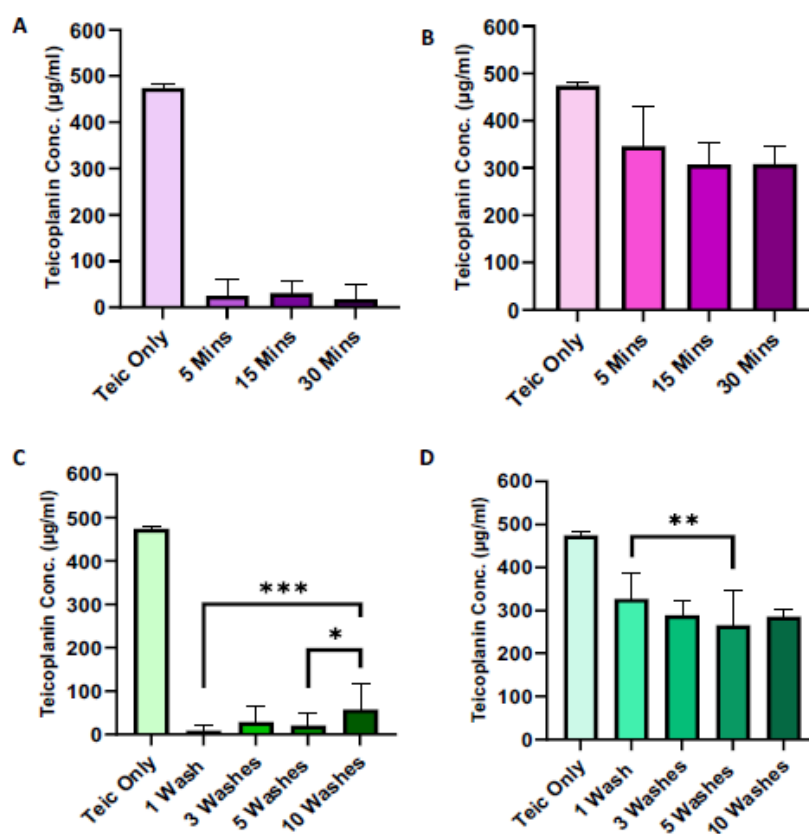


Figure 4. Evidence of a rapid and robust adsorption of Teic to TiO_2 . (A) TiO_2 powder (50 mg) was treated with 500 μl of 500 $\mu\text{g}/\text{ml}$ Teic in 50 mM HEPES (pH 7.4) and incubated at room temperature for 5, 15 and 30 min. At each time point, samples were centrifuged at $11,300 \times g$ for 2 min and 25 μl of each supernatant was combined to 500 μl of BCA reagent. Samples were incubated for 30 min at 60 $^\circ\text{C}$ and the absorbances read at 540 nm against an incubation control (Teic only). Within 5 min there is evidence of antibiotic adsorption to TiO_2 . (B) To confirm Teic- TiO_2 adsorption, the supernatant was decanted, and samples were washed twice by centrifugation and resuspended in 500 μl HEPES buffer. A 25 μl aliquot of each powder sample was added to 500 μl of BCA reagent and incubated for 30 min at 60 $^\circ\text{C}$. Once incubated, powder samples were centrifuged at $11,300 \times g$ for 2 min and 100 μl of each sample were transferred to a 96-well plate and measured in the same manner as above. (C) TiO_2 powder (50 mg) were similarly treated with 500 μl of Teic and incubated at room temperature for 2 h. Once incubated samples were centrifuged at $11,300 \times g$ for 2 min, the supernatants were discarded, and the pellets were washed up to 10 times with HEPES buffer (500 μl). Aliquots (25 μl) of each wash were subject to the BCA assay to ascertain antibiotic leaching. (D) After each set of washes the remaining TiO_2 pellets were resuspended in fresh buffer (500 μl) and samples containing the powder (25 μl) taken for the BCA assay. All data (mean \pm SD; N = 20) represent pooled quadruplicate runs from 5 independent experiments.

ment that forms a blue chromogen when it reacts with the ϵ -amino group of lysine²³. The results indicate that the tripeptide successfully bound to TSP (Fig. 9). The OD_{595} of the tripeptide control and the silica particle control (SPC) supernatants were essentially similar, suggesting that none of the tripeptide bonded to the SPC. In contrast, the TSP supernatant had a significant decrease in OD_{595} (Fig. 9), suggesting the tripeptide was able to bind well to the TSP. As expected, these findings provide evidence of a functional chiral stationary phase.

Immobilised Teic does not demonstrate biocidal activity against *S. aureus*. To determine if immobilised Teic, as a chiral stationary phase, had the capacity to kill bacteria, both the TSP and SPC were exposed to *S. aureus* for 24 h. When *S. aureus* (10^5 CFU/ml) was exposed to free Teic (600 $\mu\text{g}/\text{ml}$), there was the expected, stark bactericidal activity when compared to the bacterial control which resulted in a ≥ 7 -log reduc-

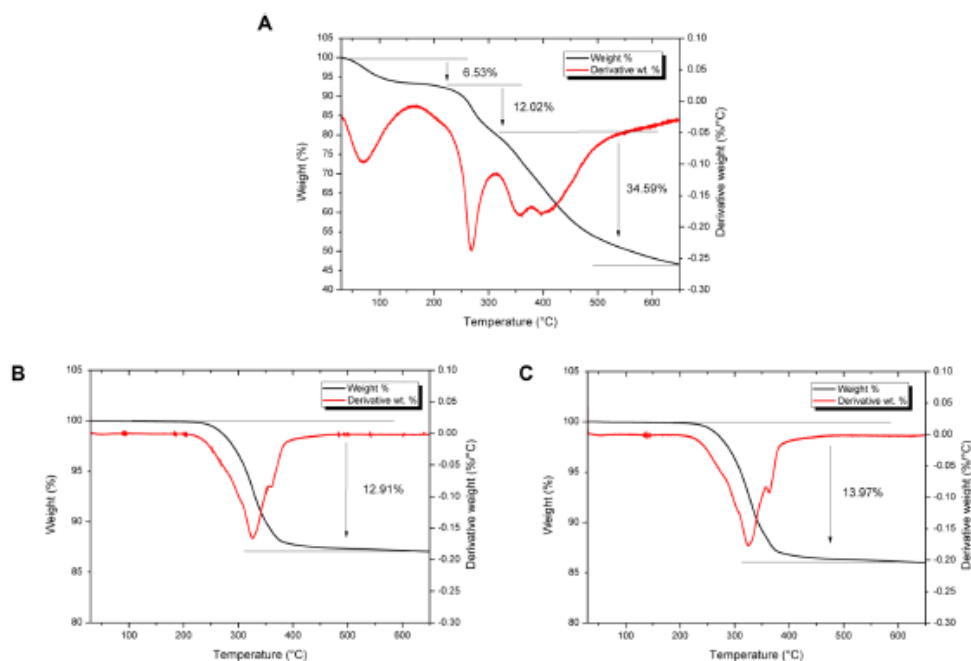


Figure 5. Thermal stability of Teic immobilised on the surface of TiO_2 using Thermal Gravimetric Analysis (TGA). TiO_2 powder (50 mg) was incubated with either 500 μl of Teic (500 $\mu\text{g}/\text{ml}$) in HEPES (50 mM; pH 7.4) buffer or HEPES buffer alone as a control for 2 h under ambient conditions and then centrifuged at $11,300 \times g$ for 2 min. The centrifuged pellets were air dried at room temperature before undergoing TGA. (A) Percentage weight curves for Teic alone shows an initial decrease at temperatures below 100 $^\circ\text{C}$ due to moisture evaporation. This was followed by rapid thermal degradation at temperatures greater than 250 $^\circ\text{C}$. (B) TiO_2 samples incubated in HEPES buffer showed a single dissociation step between 250 $^\circ\text{C}$ and 400 $^\circ\text{C}$ and a percentage weight change of 12.91%. (C) Similar percentage weight and derivative weight curves were obtained for TiO_2 samples incubated with Teic, however a greater weight loss of 13.97% was observed between 250 $^\circ\text{C}$ and 400 $^\circ\text{C}$ indicating the additional dissociation of Teic from the surface of TiO_2 at high temperatures.

tion from the initial inoculum density (Fig. 10). However, when *S. aureus* was exposed to 10 mg of TSP (with a Teic concentration equivalent to 680 $\mu\text{g}/\text{ml}$), there was no effect on bacterial viability when compared to the SPC and inoculum control. These findings indicate that when Teic is covalently tethered to a surface it is incapable of killing bacteria.

Discussion

The persistence of total joint replacement infections has a significant socioeconomic impact on both patient and healthcare providers and has incentivised the scientific community and industry to develop novel technologies to combat this problem. The covalent grafting of suitable antimicrobials could be a potential solution to minimising infection risk. In doing so the selected agent is firmly fixed to the implant surface thereby securing increased residence time and reducing the risk of antimicrobial leaching into the surrounding environment. Immobilised antimicrobials must therefore act at the level of the cell wall and/or membrane² and display evidence of functionality when tethered to a surface. One such candidate is Teic, a macrocyclic glycopeptide antibiotic, which has found widespread use as a chiral selector in enantiomeric chromatography^{3–9,12,13} and attacks Gram-positive bacteria at the level of the cell wall¹⁰.

During the course of our studies, we found that simply steeping medical-grade Ti discs in an aqueous solution of Teic generated a modified surface, as supported by XPS analysis and accompanying changes in the atomic composition of the metal surface. Importantly these Teic-functionalised discs demonstrated antimicrobial activity against *S. aureus*. This is in keeping with a report by Aykut and colleagues¹⁶ who treated Ti wires with a methanolic solution of Teic, the resultant material of which was capable of killing *S. aureus* and preventing Ti infection in a rabbit model. Titania (TiO_2) is the natural surface finish of the metal and a compound widely used as a chromatography sorbent for the enrichment and purification of glycopeptides^{24–26}.

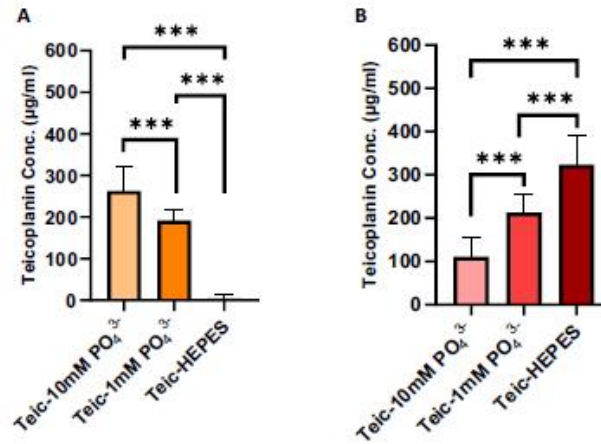


Figure 6. Influence of phosphate on Teic adsorption to TiO₂. (A) TiO₂ powder (50 mg) were exposed to 500 µg/ml Teic in PBS (500 µl) where the phosphate concentration was either 1 mM or 10 mM and samples left to incubate at room temperature for 30 min. Teic (500 µg/ml) reconstituted in 50 mM HEPES (pH 7.4) served as a positive control for TiO₂ binding. After incubation, 25 µl aliquots of the supernatant were combined to 500 µl BCA reagent and incubated for 30 min at 60 °C. Once incubated, 100 µl aliquots were transferred to a 96-well plate and measured at 540 nm using a microplate reader. It is evident that phosphate reduces the extent of Teic binding to the metal oxide ($***p < 0.0001$). (B) To confirm Teic attachment to TiO₂, the supernatant was decanted, and the powder samples were washed once by centrifugation (11,300 × g) and resuspended in 500 µl buffer. A 25 µl sample of each powder suspension was added to 500 µl of BCA reagent and incubated for 30 min at 60 °C. Once incubated, samples were centrifuged and 100 µl of the supernatant were transferred to a 96-well plate and measured in the same manner as above. Significantly less Teic ($***p < 0.0001$) is present on TiO₂ exposed to phosphate. All data (mean ± SD; N = 20) represent pooled quadruplicate runs from 5 independent experiments.

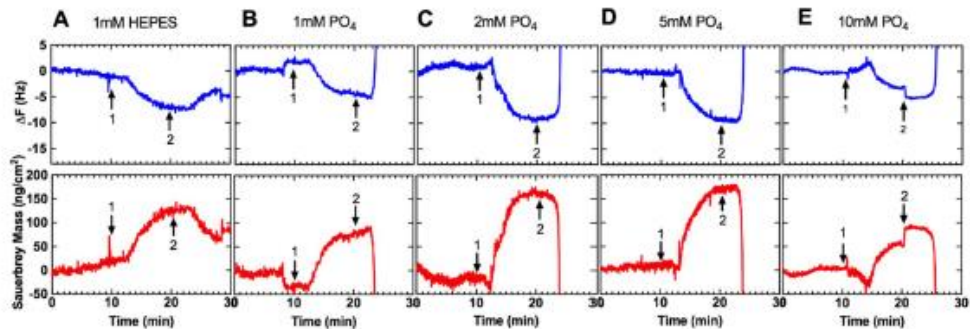


Figure 7. Influence of phosphate on Teic detachment from TiO₂. Ti-QCM sensors were subjected to HEPES buffer (50 mM; pH 7.4) at a flow rate of 100 µl/min at 21 °C for 10 min prior to 500 µg/ml Teic in HEPES for 10 min (arrow 1). Coated Ti-QCM sensors were then washed for a final 10 min with either (A). HEPES or PBS with (B). 1 mM, (C). 2 mM, (D). 5 mM or (E). 10 mM phosphate concentrations (arrow 2). Representative plots from triplicate (N = 3) experiments showing change in fundamental frequency (upper panels) and calculated Sauerbrey mass (lower panels).

To corroborate that Teic could bind to TiO₂, we exposed a mixture of rutile and anatase oxide (50 mg) to an aqueous solution of Teic (500 µl; 500 µg/ml) and monitored antibiotic binding using a BCA reagent. Adsorption of the glycopeptide antibiotic to TiO₂ was rapid; within 5 min approximately 90% was captured by the oxide. This was further demonstrated through QCM measurements. Furthermore, the interaction was robust, with the majority of the antibiotic remaining bound after multiple (up to 10) washings or continuous flow in HEPES

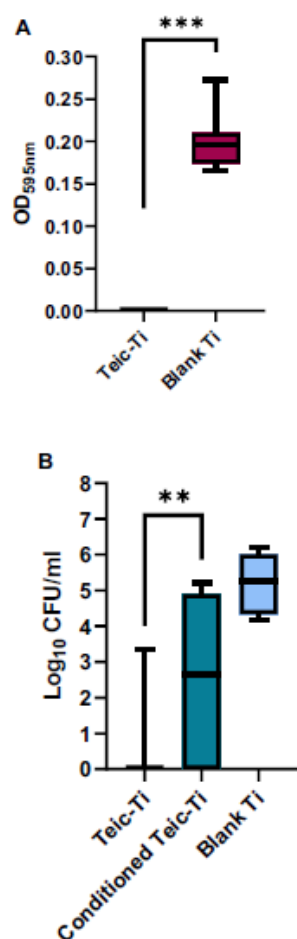


Figure 8. Antibacterial activity of Teic-Ti after culture conditioning. (A). Ti discs were exposed to Teic (500 µg/ml in 50 mM MES, pH 5.4) and incubated for 2 h under ambient conditions. After incubation, discs were washed with distilled water to dislodge any loosely bound Teic and allowed to dry in a sterile environment. Control and functionalised Ti discs were then immersed in 1% Peptone/PBS and left for 24 h at 37 °C with gentle shaking (120 RPM). After incubation, the recovered conditioned media (100 µl) was transferred to a sterile 96-well plate and inoculated with *S. aureus* (100 µl) and left to incubate at 37 °C for 24 h. At the desired time the OD at 595 nm was measured to ascertain bacterial growth using a microplate reader. The significant reduction (***) ($p < 0.0001$) in OD supports antibiotic leaching into the culture medium (B). To determine if the conditioned discs still retained any antimicrobial activity the control and functionalised Ti discs were transferred to a new multiwell plate and washed in distilled water twice, allowed to dry and then exposed to a 10^5 CFU/mL suspension of *S. aureus* and incubated for a further 24 h at 37 °C with gentle shaking (120 RPM). After incubation, discs were recovered, washed twice with 0.85% saline, and sonicated for 5 min in 1 ml of MRD to recover the attached bacteria. The detached bacteria were transferred to a new universal and incubated for 30 min at 37 °C in order to achieve maximum recovery. All data (mean ± SD; N = 9) represent pooled triplicate runs from 3 independent experiments.

buffer in the case of the QCM data. The attachment was also thermally stable as shown by the TGA data where dissociation of Teic from the TiO₂ surface was only observed at temperatures greater than 250 °C. We also found

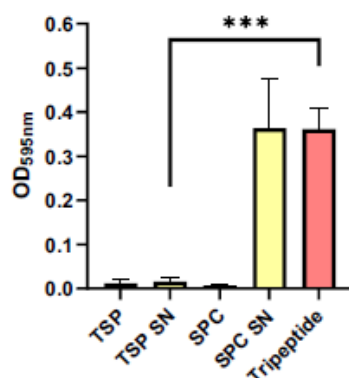


Figure 9. The tripeptide N-Acetyl-L-Lys-D-Ala-D-Ala binds avidly to a teicoplanin stationary phase (TSP). Aliquots (100 mg) of TSP and a silica particle control (SPC) were exposed to 500 μ l of the tripeptide (200 μ g/ml) prepared in 50 mM HEPES (pH 7.4) and incubated at room temperature for 30 min. After incubation, samples were centrifuged and the supernatants (SN) collected, the pH adjusted to 8.4 and 500 μ l treated with 5 μ l of gentipin (250 mM in DMSO). Samples were left to incubate at 60 $^{\circ}$ C for 2 h. After incubation, the optical density (OD) of the samples were measured using a microplate reader. The OD for the tripeptide control and SPC supernatants were similar indicating no tripeptide binding to the SPC. In contrast the supernatant recovered from the TSP had a significantly reduced OD ($***p < 0.0001$) when compared to the tripeptide control, indicating good binding of the tripeptide with the TSP. All data (mean \pm SD; N=9) represent pooled triplicate runs from 3 independent experiments.

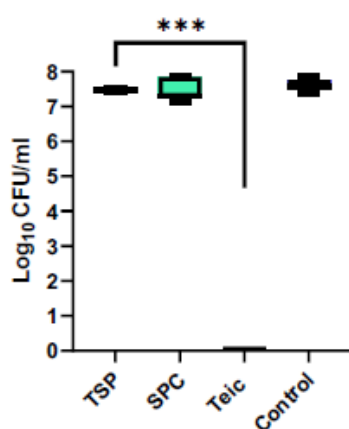


Figure 10. Immobilised Teic does not demonstrate biocidal activity against *S. aureus*. Aliquots (50 mg) of TSP and a silica particle control (SPC; 50 mg) were exposed to a 10^5 CFU/mL suspension of *S. aureus* and incubated for 24 h at 37 $^{\circ}$ C. A bacterial culture alone and a culture containing free Teic (600 μ g/ml) served as controls. As anticipated, cultures treated with free Teic led to complete bacterial demise ($***p < 0.0001$). In contrast, the TSP cultures exhibited similar bacterial numbers to SPC and bacterial controls. All data (mean \pm SD; N=9) represent pooled triplicate runs from 3 independent experiments.

that Teic remained bound to TiO₂ even when left incubated under neutral conditions for a week at 37 $^{\circ}$ C (data not shown). However, when Teic-functionalised Ti discs were subjected to a mock bacterial culture the conditioned media exhibited antibacterial activity. It was clear that the antibiotic was leaching from the metal surface, and this was the reason why the functionalised Ti was able to kill *S. aureus*. We subsequently found that phosphate

could displace Teic from Ti discs and that the anion could compromise the binding of Teic to TiO₂. This is most likely attributed to the fact that phosphate binds strongly to TiO₂²².

Whilst the facile adsorption of Teic to Ti might be a convenient solution towards the development of an anti-bacterial finish it was evident that this interaction was compromised by physiological phosphate (~1 mM) and therefore not an option towards tackling the issue of total joint replacement infections. Our findings echo those of Aykut and colleagues¹⁶ wherein Teic leaching was evident from treated Ti wires, as indicated from their agar diffusion assays. An alternative strategy was clearly needed, and we considered covalent grafting of the antibiotic to Ti given that immobilised Teic is able to function as a chiral selector in enantiomeric chromatography settings.

Herein we confirm that a commercially available teicoplanin chiral stationary phase (TSP), as expected, bound well to N-Acetyl-L-Lys-D-Ala-D-Ala, a peptide that shares similarity to the D-Ala-D-Ala motifs of non-crosslinked staphylococcal undecaprenyldiphospho-N-acetylmuramoyl-[N-acetylglucosamine]-L-alanyl-γ-D-glutamyl-L-lysyl-D-alanyl-D-alanine²⁷. The selection of N-Acetyl-L-Lys-D-Ala-D-Ala to confirm TSP functionality was informed from a study by Economou et al.²⁷ who successfully used this tripeptide for the detection of Teic via a direct fluorescence polarisation assay. We were able to monitor tripeptide binding to the TSP using genipin which reacted with the ε-amino group of the lysine residue producing a dark blue chromogen²³. The binding between the TSP and the tripeptide was compelling with sample supernatants having undetectable levels of the tripeptide within 30 min. This was in stark contrast to control silica particles exposed to the tripeptide wherein recovered supernatants reacted with genipin producing deep blue solutions. Whilst we were able to confirm TSP functionality, interestingly this same material did not demonstrate antimicrobial activity against *S. aureus*. Indeed, the equivalent of approximately 680 µg/ml Teic, as bound to silica, was without effect on bacterial viability. In our hands we typically find that the treatment of these bacteria with free Teic at a final concentration of 50 µg/ml results in the expected, complete bacterial demise within 24 h (data not shown). It is unlikely that the Teic of the TSP is unable to target bacterial D-Ala-D-Ala because spacers or linkers are used to couple the antibiotic to the silica shells; in the case of the TSP used in this study, the silica is initially functionalised with (3-aminopropyl) triethoxysilane (APTES) followed by 1,6 diisocyanatohexane to enable Teic-functionalisation of the pre-treated silica²⁸. Thus the antibiotic is away from the surface of this commercially available TSP.

Our findings conflict with other studies reporting on the successful, covalent, functionalisation of Ti and iron oxide nanoparticles (IONP's) with Teic/glycopeptide antibiotics^{18,19}. In each instance APTES was used to coat the surface with amines followed by NHS-EDC chemistry to conjugate the carboxyl of Teic to the amine at the metal surface. However, these reports did not provide any physicochemical evidence, e.g., using XPS to confirm that Teic was tethered to the metal surface through the proposed mechanism of binding. In addition, no studies were forthcoming to ascertain the robustness of the interaction between the surface and the antibiotic by performing mock bacterial cultures or leaching experiments. These considerations are particularly important given that glycopeptides bind avidly to TiO₂^{25,26,29}.

It is quite possible that the aforementioned studies^{18,19} are inadvertently reporting on the natural and strong affinity of Teic/glycopeptide antibiotics to the metal oxides and that these functional materials, as in our hands, are capable of demonstrating activity against *S. aureus* because of antibiotic leaching into the culture media. It would seem most likely that the phosphate present in the culture media used in these studies promotes antibiotic leaching from the metal surface. In contrast, a commercial, covalently functionalised Teic-chiral stationary phase, which interacted well with N-Acetyl-L-Lys-D-Ala-D-Ala, exhibited no antibacterial activity. To conclude we strongly advise against finding ways of covalently grafting glycopeptide antibiotics to Ti and, indeed, any (bio) material surface in the pursuit of novel antibacterial devices.

Data availability

The datasets used and/or analysed during the current study are available from the corresponding author (Jason.mansell@uwe.ac.uk) on reasonable request.

Received: 20 June 2022; Accepted: 12 September 2022

Published online: 05 October 2022

References

1. Lu, X. et al. Multifunctional coatings of titanium implants toward promoting osseointegration and preventing infection: Recent developments. *Front. Bioeng. Biotechnol.* **9**, 1–19 (2021).
2. Alves, D. F. et al. Unveiling the fate of adhering bacteria to antimicrobial surfaces: expression of resistance-associated genes and macrophage-mediated phagocytosis. *Acta Biomater.* **78**, 189–197 (2018).
3. Kučerová, G. et al. Enantioselective separation of unusual amino acids by high performance liquid chromatography. *Sep. Purif. Technol.* **119**, 123–128 (2013).
4. Patel, D. C., Breitbach, Z. S., Wahab, M. E., Barbate, C. L. & Armstrong, D. W. Gone in seconds: Praxis, performance, and peculiarities of ultrafast chiral liquid chromatography with superficially porous particles. *Anal. Chem.* **87**, 9137–9148 (2015).
5. Wimalasinghe, R. M., Breitbach, Z. S., Lee, J. T. & Armstrong, D. W. Separation of peptides on superficially porous particle based macrocyclic glycopeptide liquid chromatography stationary phases: Consideration of fast separations. *Anal. Bioanal. Chem.* **409**, 2437–2447 (2017).
6. Hellinghausen, G. et al. Effective methodologies for enantiomeric separations of 150 pharmacology and toxicology related 1° 2° and 3° amines with core-shell chiral stationary phases. *J. Pharm. Biomed. Anal.* **155**, 70–81 (2018).
7. Roy, D. & Armstrong, D. W. Fast super/subcritical fluid chromatographic enantioseparations on superficially porous particles bonded with broad selectivity chiral selectors relative to fully porous particles. *J. Chromatogr. A* **1605**, 360339 (2019).
8. Folprechtová, D. et al. Enantioselective potential of teicoplanin- and vancomycin-based superficially porous particles-packed columns for supercritical fluid chromatography. *J. Chromatogr. A* **1612**, 460687 (2020).
9. Taniács, D. et al. Enantioseparation of β₂-amino acids by liquid chromatography using core-shell chiral stationary phases based on teicoplanin and teicoplanin aglycone. *J. Chromatogr. A* **1653**, 462383 (2021).
10. Vimberg, V. Teicoplanin—A new use for an old drug in the covid-19 era?. *Pharmaceuticals* **14**, 1227 (2021).

11. Jovetic, S., Zhu, Y., Marcone, G. L., Marinelli, F. & Tramper, J. β -lactam and glycopeptide antibiotics: First and last line of defense? *Trends Biotechnol.* **28**, 596–604 (2010).
12. Armstrong, D. W., Liu, Y. & Ekborgott, K. H. A covalently bonded teicoplanin chiral stationary phase for HPLC enantioseparations. *Chirality* **7**, 474–497 (1995).
13. Barhate, C. L., Wahab, M. F., Breitbach, Z. S., Bell, D. S. & Armstrong, D. W. High efficiency, narrow particle size distribution, sub-2 μ m based macrocyclic glycopeptide chiral stationary phases in HPLC and SFC. *Anal. Chim. Acta* **898**, 128–137 (2015).
14. Rolston, K. V. L., Chow, A. W. & Bodey, G. P. Prospective, double-blind, randomized trial of teicoplanin versus vancomycin for the therapy of vascular access-associated bacteremia caused by gram-positive pathogens. *J. Infect. Chemother.* **5**, 208–212 (1999).
15. Pathak, T. P. & Miller, S. J. Chemical tailoring of teicoplanin with site-selective reactions. *J. Am. Chem. Soc.* **135**, 8415–8422 (2013).
16. Aykut, S. *et al.* Evaluation and comparison of the antimicrobial efficacy of teicoplanin- And clindamycin-coated titanium implants: An experimental study. *J. Bone Jt. Surg. Ser. B* **92**, 159–163 (2010).
17. Wang, H., An, X., Deng, X. & Ding, G. Facile synthesis and application of teicoplanin-modified magnetic microparticles for enantioseparation. *Electrophoresis* **38**, 1374–1382 (2017).
18. Hickok, N. J. & Shapiro, I. M. Immobilized antibiotics to prevent orthopaedic implant infections. *Adv. Drug Deliv. Rev.* **64**, 1165–1176 (2012).
19. Armenia, I. *et al.* Magnetic nanoconjugated teicoplanin: A novel tool for bacterial infection site targeting. *Front. Microbiol.* **9**, 2270 (2018).
20. Ayre, W. N. *et al.* Fluorophosphate-functionalised titanium via a pre-adsorbed alkane phosphonic acid: A novel dual action surface finish for bone regenerative applications. *J. Mater. Sci. Mater. Med.* **27**, 1–12 (2016).
21. Miles, A. A., Misra, S. S. & Irwin, J. O. The estimation of the bactericidal power of the blood. *J. Hyg. (Lond)* **38**, 732–749 (1938).
22. Yan, J. *et al.* Selective enrichment of glycopeptides/phosphopeptides using porous titania microspheres. *Chem. Commun.* **46**, 5488–5490 (2010).
23. Wang, Z. *et al.* Regeneration of skeletal system with genipin crosslinked biomaterials. *J. Tissue Eng.* **11**, 2041731420974861 (2020).
24. Sheng, Q. *et al.* Retention mechanism and enrichment of glycopeptides on titanium dioxide. *Anal. Methods* **5**, 7072–7080 (2013).
25. Haci Mehmet, K., Izzet, A. V. C. I. & Bekir, S. A. New titania glyco-purification tip for the fast enrichment and efficient analysis of glycopeptides and glycans by MALDI-TOF-MS. *J. Pharm. Biomed. Anal.* **174**, 191–197 (2019).
26. Mancera-Arteu, M., Lleshi, N., Sanz-Nebot, V., Giménez, E. & Benavente, F. Analysis of glycopeptide biomarkers by on-line TiO₂ solid-phase extraction capillary electrophoresis-mass spectrometry. *Talanta* **209**, 120563 (2020).
27. Economou, N. J. *et al.* Structure of the complex between teicoplanin and a bacterial cell-wall peptide: Use of a carrier-protein approach. *Acta Crystallogr. Sect. D Biol. Crystallogr.* **69**, 520–533 (2013).
28. Berthod, A. *et al.* Role of the carbohydrate moieties in chiral recognition on teicoplanin- based LC stationary phases. *Anal. Chem.* **72**, 1767–1780 (2000).
29. Stogios, P. J. & Savchenko, A. Molecular mechanisms of vancomycin resistance. *Protein Sci.* **29**, 654–669 (2020).

Acknowledgements

The research findings presented were generously supported by a Versus Arthritis PhD Scholarship (21895): “A novel antibacterial titanium implant technology for total joint arthroplasty.” The authors would also like to thank the University of The West of England, Bristol, for their research support and use of the laboratory facilities within the Centre for Research in Biosciences.

Author contributions

J.P.M. wrote the main manuscript text. SB prepared Figs. 2, 4, 6, 8, 9, 10. K.L. prepared Fig. 3 and W.A., L.A. and G.S. prepared Figs. 5 and 7. All authors reviewed the manuscript.

Funding

The research findings presented were generously supported by a Versus Arthritis PhD Scholarship (21895): “A novel antibacterial titanium implant technology for total joint arthroplasty.”

Competing interests


The authors declare no competing interests.

Additional information

Correspondence and requests for materials should be addressed to J.P.M.

Reprints and permissions information is available at www.nature.com/reprints.

Publisher's note Springer Nature remains neutral with regard to jurisdictional claims in published maps and institutional affiliations.

 **Open Access** This article is licensed under a Creative Commons Attribution 4.0 International License, which permits use, sharing, adaptation, distribution and reproduction in any medium or format, as long as you give appropriate credit to the original author(s) and the source, provide a link to the Creative Commons licence, and indicate if changes were made. The images or other third party material in this article are included in the article's Creative Commons licence, unless indicated otherwise in a credit line to the material. If material is not included in the article's Creative Commons licence and your intended use is not permitted by statutory regulation or exceeds the permitted use, you will need to obtain permission directly from the copyright holder. To view a copy of this licence, visit <http://creativecommons.org/licenses/by/4.0/>.

© The Author(s) 2022

Appendix II Supplementary Material

Injection of Composite Hydrogel into Mock Bone

All steps were performed in a laminar flow hood to ensure sterility. Samples were handled with ethanol sterilised forceps at all times.

Sawbones™ mock bone was cut into 2 x 2 cubes using a heated hacksaw and placed onto a sterilised surface in a laminar flow hood. Mock bone cubes were sprayed with 70% ethanol to sterilise the samples and allowed to dry (Fig. A1). Once dried, mock bone samples were wrapped twice in sterilised parafilm. This was to ensure that the hydrogel fills the mock bone samples well and reduce the risk of the hydrogel leaking during gelation (Fig. A2). The hydrogel was then carefully injected into the parafilm-wrapped mock bone samples (Fig. A3). After injection, the hydrogel mock bone samples were transferred to a sterile 50 ml falcon tube, placed on a roller (60 RPM) and incubated under ambient conditions for 24 h. After incubation, hydrogel filled mock bone samples were carefully unwrapped and transferred to a new sterile 50 ml falcon tube (Fig A4 & 5).

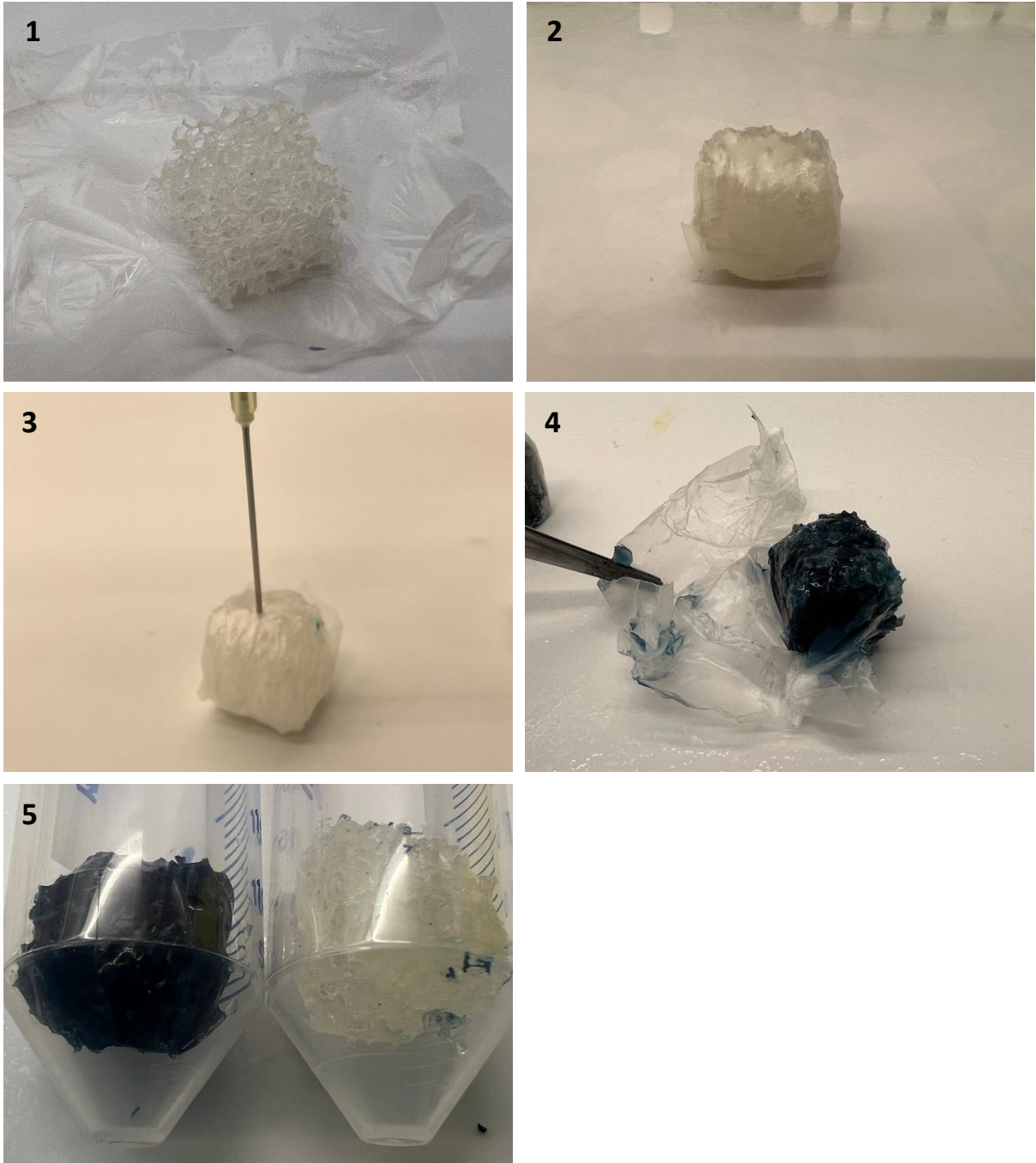


Figure A Injection of Hydrogel into Mock Bone Samples. 1. Samples were sterilised with 70% ethanol in a laminar flow hood. 2. After sterilisation, samples were wrapped in parafilm twice. 3. Hydrogel was carefully injected into the mock bone sample. 4. After gelation, samples were carefully unwrapped and transferred into sterile 50 ml falcon tubes (5).